POLITECNICO DI TORINO

Corso di Laurea Magistrale in

Ingegneria Aerospaziale

Tesi di Laurea Magistrale

Analysis of approximate solutions with Edelbaum's approximation for orbital maneuvers at periapsis/apoapsis

Relatore:

prof. Lorenzo Casalino

Candidato:

Giuseppe Romeo

257745

Anno Accademico 2021/2022

ABSTRACT

This paper proposes a series of estimated solutions with Electric Propulsion, based on Edelbaum's approximation, for the preliminary calculation of the propellant consumption and the required orbital changes in periapsis and apoapsis maneuvers during an interplanetary mission to Near-Earth Asteroids. A set of 75 asteroids is considered with a revolution period close to one year and small eccentricity and inclination, and the assumed time of flight for the mission is three years, so three burning arcs are performed. The estimation does not need numerical integration, but only the resolution of two three-variable algebraic systems is necessary to define the whole transfer; thus, the computational time and cost are significantly reduced. Various modifications have been made to the orbital elements of the arrival orbit to observe the trends of the parameters useful for the calculation of the algebraic systems: the inclination of the orbit is initially considered linearly proportional to the eccentricity, while in the following cases it is fixed at a certain number of values; the right ascension of ascending node in the first two cases is null, with the periapsis and the ascending node coinciding, then is assumed equal to $\pi/4$ and $\pi/2$, monitoring the changes due to the distancing of the line of nodes and the line of apsides. The results demonstrate a good accuracy of the method, especially in particular conditions. Both in periapsis and apoapsis maneuvers, the estimation is accurate for the furthest asteroids from Earth and quite inaccurate as regards the closest asteroids to Earth, hence a subgroup of asteroids whose distance does not allow to perform long burning arcs. When the inclination is set at slightly higher but still small values, together with an obvious increase in consumption, there is a very accurate response on almost the entire group of asteroids for maneuvers at both apsides, except for the very first asteroids which always have some oddities. Furthermore, also the RAAN variations, even with a small increase of fuel consumed, evidently contribute to raise the overall quality of the estimation; this can be seen especially in the results of the cases at low inclination, in which the precise solution tends to include a larger number of asteroids if the periapsis and the ascending node are not coincident, but in quadrature.
The analysis of the method in these different case studies has allowed to ascertain the goodness and relevance to reality of the results obtained, particularly in cases with a relatively high inclination (but always small to adhere to Edelbaum's approximation) and in cases with low to null inclination, but RAAN different from 0 (even if the latter increase more propellant consumption). New studies and analysis may be focused on improving the accuracy of this estimation method in the planar problem, i.e., with null inclination, in which the periapsis and the ascending node are coincident, that is, Ω equal to 0.

Table of Contents

INTRODUCTION

Electric Propulsion is now regularly used for space operations such as orbital and/or attitude adjustments, compensation of aerodynamic drag in the presence of an atmosphere and deep space missions. The low thrust values provided combined with the very high specific impulses [1] make it indeed possible to efficiently perform missions which do not involve overcoming high gravitational forces (i.e., launching a vehicle out of the atmosphere) and ending in strict times.

This paper proposes the use of an estimation method presented by L. Mascolo, A. De Iuliis, L. Casalino [2] and based on Edelbaum's approximation. The method, originally developed to analyze rendezvous transfer from Earth to the Near-Earth Asteroids, can be also employed to evaluate interplanetary transfers between two celestial bodies having similar and small value of semi-major axis, eccentricity, and inclination. The required changes of these orbital parameters throughout the transfer are also calculated algebraically, thus the method is not complex and computational time and cost are significantly reduced. The 75 asteroids, whose orbits are considered the arrival ones in this work, are actually fictitious and are needed to observe under what conditions and with which and how many orbital changes the parameters stably follow the predictions of the theory. The orbital elements that have been varied to monitor their influence on the method are the inclination (i) of the orbital plane, which in this work coincides with the Ecliptic plane, and the right ascension of ascending node (Ω, RAAN). Initially, the inclination is linearly linked to the eccentricity, gradually increasing, and therefore assumes variable values; subsequently, it is fixed four times to study and understand the effects of these changes. Furthermore, there is only one case with null inclination to also treat the planar problem. The RAAN can instead assume three possible values which basically reveal the orbital position of the ascending node with respect to the periapsis (or perihelion) and, as one can easily guess, heavily affects the costs and the overall accuracy of the preliminary estimation.

Therefore, the cases examined and dealt with hereinafter are sixteen.

NOMENCLATURE

a	Semi-major axis, AU
e	Eccentricity
e_x, e_y	Eccentricity vector components
i	Inclination, deg or rad
Ω	Right ascension of ascending node, deg or rad
ω	Argument of periapsis, deg or rad
m_p	Propellant mass, kg
m_i	Initial mass, kg
m_f	Final mass, kg
n	Number of revolutions
r	Radius, AU
r_p	Perihelion radius, AU
r_a	Aphelion radius, AU
T	Thrust, N
α	In-plane thrust angle, deg or rad
β	Out-of-plane thrust angle, deg or rad
ΔPA	Total propulsive effort at perihelion
ΔAP	Total propulsive effort at aphelion
ϑ_e	Reference right ascension, deg or rad
ϑ	Right ascension, deg or rad
Λ	Control law coefficient
$\Delta\vartheta$	Burn arc angular length, deg or rad
$\Delta \mathrm{V}$	Velocity increment, m/s
$\Delta i_{2\pi}$	1-rev. inclination change, deg or rad
K	Correction factor
k_0, k_1, k_2, k_3	Correction parameters

SUBSCRIPTS

E = Earth	T = Target
$iniz$ = Initial	fin = Final
PA = Perihelion maneuver	AP = Aphelion maneuver

1. SPACE PROPULSION – TRANSFER TO NEAs

1.1 Main differences between Chemical and Electric Propulsion

Space Propulsion is a field that deals with the realization and the development of engines or *thruster*, devices that through the third principle of dynamics set a spacecraft in motion with respect to a specific reference system. There are several applications related to this area: the exit from the Earth's atmosphere, orbital changes and adjustments, fly-by, interplanetary transfers, interstellar travels.

The exit from Earth's atmosphere is a maneuver that requires a huge thrust and velocity to defeat the atmospheric drag and the force of gravity of the planet. This kind of maneuver is well performed with Chemical Propulsion: propellants can be liquid, solid or hybrid and stored in tanks; the thrust is generated through their mixture and heating in the combustion chamber and the high-speed expulsion of the burnt gases. Chemical Propulsion is ideal when the performance is defined in terms of high thrust [1] and propellants can be stored in tanks with realistically acceptable volumes, which explains why *launchers* (engines specialized in exiting the atmosphere and placing vehicles into orbit) use mainly solid and liquid propellants. CP is therefore used when the mission goal is not to have high efficiency, but huge power in terms of thrust generated [1].

Nuclear Propulsion is studied and taken into consideration especially regarding longer lasting missions (such as a transfer to Mars), due to the enormous thrust produced which could shorten the duration of the mission. The amount of thrust generated is the highest of all the space thrusters, but there are still many doubts about the use of NP, starting with the safety of the eventual human presence in a spacecraft in which there is also a nuclear reactor, in terms of radiation shielding (for example with superconducting magnets) and protection of the reactor from external disturbances. To summarize, NP provides high thrust combined with high efficiency, but the technological complexity and the poor predictability of malfunctions make it still the subject of study today [1], with the main goal of reducing the effective time of a mission.

Electric Propulsion is now a serious alternative to Chemical Propulsion. EP does not require propellant tanks (less structural weight) and it is the most efficient among any types of Space Propulsion: it can be easily demonstrated, trough the definition of the *Specific Impulse*, that the gas outflow velocity and the fuel consumption are strictly related. In fact, with the same value of applied thrust, the lower the propellant consumption, the higher the gas outflow velocity is. This kind of propulsion is limited by the available electric power onboard the spacecraft [2], so the low thrust generated makes these thrusters unsuitable for aeronautical use or launching vehicles in orbit, but actually perfect for space applications as orbit transfers, alignment adjustments, aerodynamics drag compensation and, of course, interplanetary or deep space missions; namely operations in which the gravity of a planet must not be overcome, time is not a crucial factor and no excessive thrust is needed [3]. The large specific impulse of EP (particularly Ion Propulsion) enables low-thrust long-duration missions that would require huge amounts of propellant with CP and enormous tanks to contain it, making the mission unfeasible. One of the main reasons why EP has been utilized so far is the possibility of reaching some celestial bodies which are remnant debris of the solar system formation process. These asteroids have a perihelion distance of less than 1.3 AU, that's why they are known as NEAs, Near-Earth Asteroids [2]. These celestial bodies, given their proximity with the Earth, are easily accessible with low ΔV and propellant consumption and they have potentially unique scientific features such as their raw materials [4,5]. The purpose of this discussion is to find out if, through Edelbaum's approximation, the proposed estimation method always returns results relevant to theory even if certain orbital parameters are significantly varied.

1.2 Edelbaum's Approximation: the origin of the estimation method

The discussed estimation method is based on Edelbaum's approximation [6]. It is a considerable simplification to the general problem of interplanetary transfers, since if some parameters have similar small values both in the starting orbit and in the target orbit and their variations are also small, the ΔV and the propellant consumption inherent to the transfer can be minimized. This approach is suitable for the use of EP, since it is not based on the concept of thrust impulse given in an infinitesimal time, but on the concept of continuous thrust, with burning arcs and coasting arcs; so, it is possible to obtain the minimum-fuel trajectories to NEAs. It is therefore necessary to introduce the hypotheses related to Edelbaum's approximation, inherent to a trajectory performed with EP:

- *Almost-circular orbit ($e \approx 0$)*; this assumption has consequences regarding the semi-major axis, the spacecraft velocity and the shape of the orbit. The semi-major axis and the *semilatus rectum* can be confused at any moment with the radius of the circular trajectory ($a \approx p \approx r$); furthermore, the spacecraft velocity will be comparable to the circular velocity ($V^2 \approx \frac{\mu}{r}$) and the true, eccentric and mean anomalies can be confused with each other ($\nu \approx E \approx M$).
- *Small variations of inclination ($i \approx 0$)*; if the theory of small perturbations is considered and the plane of the orbit is taken as the reference plane, the following approximation can be utilized: $\cos i \approx 1, \sin i \approx i$.
- *Thrusts and acceleration are small ($\frac{T}{m} \ll \frac{\mu}{r^2}$).*
- *Thrust is analyzed through its components*; the in-plane thrust angle α and the out-of-plane thrust angle β are introduced to express a set of three perpendicular components:

1. $T_V = T \cos\alpha \cos\beta$ is the component along the velocity direction;
2. $T_R = T \sin\alpha \cos\beta$ is the component along the radial direction;
3. $T_W = T \sin\beta$ is the out-of-plane component [7].

The method generates two three-variable sets of algebraic equations which are numerically solved; thus, the problem due to the integration of the equations of motion does not occur and the computational complexity of the operation is significantly lowered. In addition to that, the computational time is drastically reduced, the preliminary evaluation of large groups of possible targets is quick and precise, and the overall accuracy is very high, even compared with other approaches with similar complexity, such as multiple-revolution Lambert's problem or three impulse transfers [2].

The proposed estimation method was originally conceived for dealing with rendezvous transfers from Earth to the most reachable NEAs. In this paper, it is shown that it can be also used with fairly accurate results for interplanetary transfers between two celestial bodies (such as the Earth and an asteroid of the NEAs or in the Main Belt) that have similar semi-major axis, eccentricity and inclination; the purpose of this work is indeed to determine and analyze what happens to the ΔV and to the propellant consumption if, in addition to varying more or less significantly one of these three parameters (*inclination*), other orbital parameters are also varied, for example the *right ascension of ascending node* Ω. It is important to notice that the method has been revised and improved from its initial version: some correction factors has been introduced to take the geometry of the transfer into account; so, the estimation accuracy is greatly improved compared to the previous work and the other existing methods with comparable computational cost [2].

1.3 Trajectories to NEAs

1.3.1 In-plane scenario

As reported by L. Mascolo, A. De Iuliis and L. Casalino [2], the trajectory to reach an asteroid can change according to the actual cost (in terms of ΔV and propellant consumption) required to make it; this cost is strongly related to changes in orbital parameters from the starting orbit to the target one. Generally, asteroids can be considered targets for science missions if the required changes of inclination and eccentricity are small with respect to Earth's reference orbit. Indeed, possible targets have semi-major axis close to 1 AU and small to null eccentricities and inclinations;

an asteroid with a semi-major axis larger than 1 AU and/or relevant changes in eccentricities and/or inclinations is selected as mission objective only if it has exceptional features that justify the cost of the transfer, such as (433) Eros reached by the NEAR spacecraft [8].

In this section, a transfer is analyzed in which the inclination of both the departure and arrival orbit is null (*planar problem*, treated in *case 0*), while the next paragraph deals with the plane change, and the final one is about RAAN variation.

The first assumption concerns the starting orbit, the Earth's one: a circular orbit with a radius of 1 AU ($e_E = 0, a_E = 1$). Intuitively, the simplest type of in-plane transfer to be performed consists of two impulsive maneuvers to raise the altitudes of perihelion and aphelion and obtain the semi-major axis of the target orbit [9]. Variations of eccentricity and semi-major axis Δe and Δa relative to the target orbit are closely related to each other. It is possible to notice this already from the calculation of the new altitudes of perihelion and aphelion: a perihelion impulse provides $r_a = a_T(1 + e_T)$, an aphelion impulse returns $r_p = a_T(1 - e_T)$. From these calculations it is easy to derive the variations Δe and Δa which modified the aphelion (with the perihelion maneuver, PA) and the perihelion (with the aphelion maneuver, AP):

$$\Delta a_{PA} = \Delta e_{PA} = [(a_T - 1) + e_T]/2$$

$$\Delta a_{AP} = -\Delta e_{AP} = [(a_T - 1) - e_T]/2$$

The assumption behind these two equations is that both the impulses are given at 1 AU from the Sun; in reality, the second impulse is affected from the effects of the first one, that modified the apsidal distance. These effects are neglected due to the complexity increase they would bring to the method compared to not too high improvements in terms of accuracy [2].

The two in-plane impulses applied to raise the apsidal distance can be easily performed with Chemical Propulsion. Electric Propulsion, given the low thrust provided, is not effective in terms of punctual impulses in which the engine fires for few fractions of a second, but is instead suitable for long thrusting arcs. However, a time-sustained thrusting arc, in which the thrust effect is spread among different orbital positions, is not as efficient in changing certain orbital parameters as a single high-trust impulse executed at a given point. In fact, a single burn may not even be able to produce the required changes. This is no longer a problem in missions where time is not an indispensable factor and these changes can be provided in many thrusting arcs, therefore multiple revolutions. Each maneuver is divided in smaller burns conveniently placed close to the apsides [2].

The 75 fictitious asteroids considered in this work each have a revolution period of about 1 year, thus a mission with an expected completion time of n years has n passages at the perihelion and n passages at the aphelion, allowing for n equal burns at each apside [9]. A single burn provides $1/n$ of the required changes of semi-major axis and eccentricity. In this case, the trip time is 3 years ($n = 3$), so it is expected to have 3 perihelion burns and 3 aphelion burns. Again, it is assumed that a burn is not affected by the previous one.

First, the components of eccentricity vector on the ecliptic plane are introduced to assure the proper alignment of the line of apsides [2]:

$$\Delta e_x = e_T \cos(\Omega_T + \omega_T) - e_E \cos(\Omega_E + \omega_E)$$

$$\Delta e_y = e_T \sin(\Omega_T + \omega_T) - e_E \sin(\Omega_E + \omega_E)$$

The variations Δe and Δa can be written as functions to these values:

$$\Delta e = \sqrt{{\Delta e_x}^2 + {\Delta e_y}^2} = e_T$$

$$\Delta a = a_T - a_E$$

Now it is possible to calculate the effective change in semi-major axis and eccentricity at each apside. With $n = 3$ burns, each perihelion maneuver (PA) has

$$\Delta a_{PA} = \frac{(\Delta a + \Delta e)}{2n} = \frac{a_T - a_E + e_T}{6}$$

$$\Delta e_{PAx} = \Delta a_{PA}\left(\frac{\Delta e_x}{\Delta e}\right) = \frac{a_T - a_E + e_T}{6}[\cos(\Omega_T + \omega_T)]$$

$$\Delta e_{PAy} = \Delta a_{PA}\left(\frac{\Delta e_y}{\Delta e}\right) = \frac{a_T - a_E + e_T}{6}[\sin(\Omega_T + \omega_T)]$$

Each aphelion maneuver (AP) has instead

$$\Delta a_{AP} = \frac{(\Delta a - \Delta e)}{2n} = \frac{a_T - a_E - e_T}{6}$$

$$\Delta e_{APx} = -\Delta a_{AP}\left(\frac{\Delta e_x}{\Delta e}\right) = \frac{a_E + e_T - a_T}{6}[\cos(\Omega_T + \omega_T)]$$

$$\Delta e_{APy} = -\Delta a_{AP}\left(\frac{\Delta e_y}{\Delta e}\right) = \frac{a_E + e_T - a_T}{6}[\sin(\Omega_T + \omega_T)]$$

As it has been mentioned earlier, the changes of a and e produced at each burn are linked, as to reach the right eccentricity value and assure the proper alignment of the line of apsides, the semi-major axis must be varied proportionally in the same orbital position (perihelion or aphelion) [2].

After describing the contributions of each burn to the changes of semi-major axis and eccentricity, the need is to have a thrust control law to assure the proper thrust direction and to monitor the evolution of the orbital parameters over time. The importance of the fact that thrust must always be oriented correctly is mainly related to the minimization of propellant consumption while proceeding to change the orbital elements. Gauss planetary equations accurately describe the temporal variation of the orbital parameters under the effect of thrusting. In a non-dimensional form, here are the related equations to a, e and i:

$$V\frac{da}{dt} = 2a\left(\frac{T}{m}\right)\cos\alpha\cos\beta$$

$$V\frac{de}{dt} = 2\left(\frac{T}{m}\right)(\cos\vartheta\cos\alpha\cos\beta + \sin\vartheta\sin\alpha\cos\beta)$$

$$V\frac{di}{dt} = \left(\frac{T}{m}\right)\cos\vartheta\sin\beta$$

In the *planar problem* ($i = 0$), only a and e are considered, and the thrust control law refers only to the thrust in-plane angle α. The optimal control law asserts that α can be expressed as a function of two parameters, ϑ_e and λ, related to the proximity of the line of apsides and to changes of eccentricity and semi-major axis. Thus, the in-plane angle is a function of the longitude ϑ with respect to ϑ_e for different values of λ, and for each orbital position there two possible solutions, from which the correct one is obtained through the boundary conditions of the problem [2]. The real issue with this control law is that numerical integration or elliptic integrals are necessary for the global resolution of the problem; for this reason, a linear control law that accurately approximates the solution is used instead of the optimal control law. In this case, the important parameters are ϑ_e and Λ: the first one is the same of the exact solution and $\vartheta = \vartheta_e$ represents the longitude where the thrust is perfectly horizontal, concurrent with the spacecraft velocity ($\Delta a > 0, \alpha = 0$) or opposite to the spacecraft velocity ($\Delta a < 0, \alpha = \pi$); Λ is a value between 0 and 1 which must be small to have thrust close to the velocity direction. Of course, large values of Λ mean a significant misalignment of thrust direction and a consumption increase. The linear control law can be written in two ways, depending on the sign of Δa:

$$\begin{cases} \alpha = \Lambda(\vartheta - \vartheta_e) & \Delta a > 0 \\ \alpha = \pi + \Lambda(\vartheta - \vartheta_e) & \Delta a < 0 \end{cases}$$

This linear control law allows for analytical integration and produces a set of three algebraic equations that relate the required changes of Δa, Δe_x and Δe_y to ϑ_e, Λ and the burn arc angular length Δϑ [2]. In the planar problem, these equations take into consideration the in-plane acceleration component, the main one, from with the mass of the spacecraft is therefore easily obtained; in the complete problem ($i \neq 0$), out-of-plane thrust angle β is equally important. The second algebraic system consists of three algebraic equations generated by the burn evaluation. It is easily solved with an iterative procedure in which tentative values are assumed for ϑ_e, Λ and Δϑ (in addition to β and using the initial mass) and Δa, Δe_x and Δe_y are analytically derived. After an initial correction given according to a Newton's scheme, the required orbital changes are achieved from the relations of Δa, Δe_x and Δe_y in perihelion and aphelion maneuvers.

1.3.2 Plane change

Variations of inclination are important since frequently a mission expects the target orbit to be out of phase by a few degrees with respect to the departure orbit. In this paper, a single case deals with the *planar problem* ($i = 0$, *case 0*) explained in the previous section; in three cases inclination of the arrival orbit is proportional to eccentricity and its variation ($i = (1/8)e$, *cases A*, *B*, *C*), while in six cases the inclination is set at a constant value, of which three with $i = 3°$ (*cases A3*, *B3* and *C3*) and three others with $i = 6°$ (*cases A6*, *B6* and *C6*).

The overall accuracy of the solution requires that out-of-plane thrust angle β has to be kept constant during each burn and then progressively adjusted as the iterations progress to obtain the desired plane change. More precisely, β has a constant positive value during the half revolution centered at the ascending node and the opposite negative value during the half revolution centered at the descending node [2]. Even regarding the Δi split, the optimal law is not chosen due to the complexity and the computational slowness; the adopted law considers the fact that maneuvers combination is advantageous especially when the ΔV of the different maneuvers are similar, because of the vector sum. Therefore, accurate results are expected if a large Δi is associated to with a large in-plane burn, because the inclination change is proportional to the changes of the in-plane orbital elements (ΔPA and ΔAP), which occurs with the burns to the two apsides. In this way, inclination change at each burn is easily derived [9]:

$$\Delta PA = |\Delta a_{PA}| + |\Delta e_{PA}| \quad \rightarrow \quad \Delta i_{PA} = \frac{\Delta PA}{(\Delta PA + \Delta AP)} \frac{\Delta i}{n}$$

$$\Delta AP = |\Delta a_{AP}| + |\Delta e_{AP}| \quad \rightarrow \quad \Delta i_{AP} = \frac{\Delta AP}{(\Delta PA + \Delta AP)} \frac{\Delta i}{n}$$

According to Edelbaum's approximation, is it possible to determine Δi starting from the differential equation that expresses the infinitesimal variation di with respect to the longitude (or angular position) ϑ:

$$di = \left(\frac{T}{m}\right) \sin\beta \cos\vartheta \, d\vartheta$$

It is important to observe that $\vartheta = 0, \pi$ are the corresponding positions for the ascending and the descending nodes respectively; hence it is evident, even mathematically, that thrusting at the nodes is more convenient ($di = (T/m) \sin\beta \, d\vartheta$). However, given the difficulty of prediction of the thrust effect for a generic burn that spans a $\Delta\vartheta$ angle, to determine the global Δi, it is necessary to go through a simple calculation of a specific inclination change along a single revolution $\Delta i_{2\pi}$, derived with $\beta = cost$ and $\Delta\vartheta = 2\pi$ [2]:

$$\Delta i_{2\pi} = 4\left(\frac{T}{m}\right) \sin\beta \quad \rightarrow \quad \Delta i = \frac{\Delta i_{2\pi}}{2\pi} = \frac{2}{\pi}\left(\frac{T}{m}\right) \sin\beta \, \Delta\vartheta$$

This relation seems decisive, but there is still a significant problem to be resolved: the average rate of inclination variation does not take into account the position of the burns with respect to the line of nodes. It is not a trivial issue since it considerably influences the propellant consumption. In detail, when the line of nodes is close to the line of apsides consumptions are underestimated, while they are overestimated when both lines are in quadrature or close to it (that is, when the two lines are separated by an angular difference close to or exactly 90°). As it is now clear, the assumption of a constant out-of-plane thrust angle β and the relative position of the line of nodes and the line of apsides are two indispensable and crucial factors for this estimation method accuracy [2]. Therefore, a correction factor K that strongly considers the geometry of the trip and accounts more considerably the effect of the out-of-plane thrust component T_W. Δi equation changes in the following way:

$$\Delta i = \frac{\frac{2}{\pi}\left(\frac{T}{m}\right) \sin\beta \, \Delta\vartheta}{K}$$

With

$$K = k_0 + k_1 k_2 k_3$$

This constituent parameters of the correction factor K, linked to some orbital elements, are now described:

- k_0 represents the cost of a plane change precisely at the node; a value of 0.6 is imposed, although the precise value would be $2/\pi = 0{,}6366..$, since the use of a linear approximate control law tends to overestimate the consumption, hence this lower value partially compensates this overestimation.
- $k_1 = 1 - \cos(2\Omega_T)$ is a parameter which considers the position of both line of apsides and line of nodes; in particular, the thrusting effect is maximum when they are coincident ($\Omega_T = 0, \pi, 2\pi$), while it is significantly penalized when they are in quadrature ($\Omega_T = \pi/2, 3\pi/2$).
- $k_2 = 1.5e_T$ takes into consideration one of the most important assumptions of Edelbaum's approximation: the eccentricity variation must be small, otherwise the cost of the maneuver highly increases. The reason why this is significant is that an orbit with small eccentricity, that is almost-circular, allows placing the burns to raise perihelion and/or aphelion close to the nodes instead of the apsides with a small extra cost to pay; in an eventual case with $e_T = 0$ these burns can be placed at any orbital longitude since the problem would deal with the transfer between two circular orbits. On the other hand, positioning the burns close to the apsides is essential to minimize the cost of the maneuver when the target orbit's eccentricity increases.
- $k_3 = [3 + \cos(\Delta\vartheta)]/4$ is related to the burn arc angular length, favoring long thrusting arcs; it is interesting to report that when the burn arc is longer than 90° it necessarily comprises both the lines of nodes and apsides. When this situation occurs, the value of β can be varied in the optimal solution to increase the out-of-plane thrust component $T_W = T \sin\beta$ at the nodes, where the plane change is more efficient, and the consumption is lower.

The evaluation of these four parameters leads K to assume the following range of values (with $e_T = 0.25$):

$$0.6 < K < 1.35$$

The minimum value 0.6 corresponds to a plane change maneuver precisely at the nodes, while the maximum value corresponds to a plane change maneuver executed about 60° away from the line of nodes [2].

1.3.3 RAAN variation

So far, the variations of some in-plane parameters (semi-major axis and eccentricity) and of the inclination with regard to the orbital plane change have been discussed. In this paragraph, the *right ascension of ascending node* (RAAN or Ω) change is presented, lately in the next chapters it is observed how it affects the consumption estimation, alone and together with the variations of the other elements. Ω is the orbital parameter that measures counterclockwise (as seen from north of the Ecliptic Plane) the angular distance between the First Point of Aries and the ascending node [10,11]. The set of 75 fictitious asteroids considered in this work assumes that the positions of periapsis and apoapsis are always maintained even while varying their altitudes, and so periapsis and apoapsis can be also called *perihelion* and *aphelion*, since the reference plane is the Ecliptic Plane; hence, it is possible to say that Ω represents in this work the angular difference from the line of apsides (starting from the perihelion) to the line of nodes (precisely, the ascending node).

Cases 0 and *A*, *A3* and *A6* presents for the target orbit $\Omega_T = 0$, meaning that the ascending node is coincident with the perihelion even when a plane change occurs (*cases A, A3* and *A6*). A different situation arises instead for *cases B*, *B3* and *B6*, which have $\Omega_T = 45°$, and for *cases C*, *C3* and *C6*, which present $\Omega_T = 90°$: in the first three *cases* the ascending node is 45° away from the perihelion, while in the other three ascending node and perihelion are in quadrature. As it has been seen in the previous section, a RAAN value significantly different from *0* especially penalizes the plane change maneuver (through k_1 factor of the correction factor K), but the *cases* with i changing proportionally to e (*cases B* and *C*) and the *cases* with a fixed i (particularly, the ones with relatively high i) show that, if eccentricity variation is small, the estimation of some important parameters such as Λ and ϑ_e improves considerably.

2. APPROXIMATE SOLUTIONS

This paper proposes approximate solutions based on Edelbaum's approximation of a 3-year mission using Electric Propulsion [9]. The mission, as already written in the first chapter, includes three passages at the periapsis and three passages at the apoapsis, in which the relative maneuvers necessary to raise the apsides' altitude and gradually change other orbital parameters are performed [2].

Initially, four *cases* have been studied; one of them treats the *planar problem* ($i = 0$), the remaining three have in common a plane change in which the inclination is proportional to the eccentricity and differ in the values of the RAAN. The initial *cases* are therefore presented below:

1. *Case 0*: the target orbit presents $a = 1$ at first, e progressively increasing, $i = 0$ and the other parameters are null;
2. *Case A*: the target orbit presents $a = 1$ at first, e progressively increasing, $i = (1/8)e$ and the other parameters are null;
3. *Case B*: the target orbit presents $a = 1$ at first, e progressively increasing, $i = (1/8)e,\ \Omega = \pi/4$ and the other parameters are null;
4. *Case C*: the target orbit presents $a = 1$ at first, e progressively increasing, $i = (1/8)e,\ \Omega = \pi/2$ and the other parameters are null.

Subsequently, some *cases* very similar to the initial ones, but with a fixed inclination, have been analyzed as a matter of comparison. The chosen inclinations with which the first four *cases* have been modified are $i = 1.5°$, $i = 3°$, $i = 4.5°$ and $i = 6°$ and do not depend on eccentricity. These cases are also reported here:

- *Case A1.5*: the target orbit presents $a = 1$ at first, e progressively increasing, $i = 1.5°$ and the other parameters are null;
- *Case A3*: the target orbit presents $a = 1$ at first, e progressively increasing, $i = 3°$ and the other parameters are null;
- *Case A4.5*: the target orbit presents $a = 1$ at first, e progressively increasing,

$i = 4.5°$ and the other parameters are null;

- *Case A6*: the target orbit presents $a = 1$ at first, e progressively increasing, $i = 6°$ and the other parameters are null;
- *Case B1.5*: the target orbit presents $a = 1$ at first, e progressively increasing, $i = 1.5°,\ \Omega = \pi/4$ and the other parameters are null;
- *Case B3*: the target orbit presents $a = 1$ at first, e progressively increasing, $i = 3°,\ \Omega = \pi/4$ and the other parameters are null;
- *Case B4.5*: the target orbit presents $a = 1$ at first, e progressively increasing, $i = 4.5°,\ \Omega = \pi/4$ and the other parameters are null;
- *Case B6*: the target orbit presents $a = 1$ at first, e progressively increasing, $i = 6°,\ \Omega = \pi/4$ and the other parameters are null;
- *Case C1.5*: the target orbit presents $a = 1$ at first, e progressively increasing, $i = 1.5°,\ \Omega = \pi/2$ and the other parameters are null;
- *Case C3*: the target orbit presents $a = 1$ at first, e progressively increasing, $i = 3°,\ \Omega = \pi/2$ and the other parameters are null;
- *Case C4.5*: the target orbit presents $a = 1$ at first, e progressively increasing, $i = 4.5°,\ \Omega = \pi/2$ and the other parameters are null;
- *Case C6*: the target orbit presents $a = 1$ at first, e progressively increasing, $i = 6°,\ \Omega = \pi/2$ and the other parameters are null.

The thrusting effects are therefore perceived and calculated through the burning arcs at perihelion and aphelion, always considering the relative proximity of the line of apsides and the line of nodes. In fact, the changes due to having a variable or fixed inclination and Ω variations are critical factors that determine the burn arc angular length and, in turn, the feasibility of the mission with respect to the number of burning arcs imposed and the different distances of the asteroids taken into account.

2.1 Perihelion maneuver

2.1.1 Planar Problem: *Case 0*

Speaking in terms of code used with Fortran programming language, the Earth is regarded as asteroid #1, so the considered group of 75 Near-Earth Asteroids goes from asteroid #2 to asteroid #76 (respectively, the closest and the farthest from Earth departure orbit). To avoid misunderstandings, it should also be taken into consideration that in each graph in this report the numbering does not reflect the one just reported but goes from asteroid #1 to asteroid #75 (only target asteroids are numbered).

The first analyzed case deals with the *planar problem*: the transfer consists only of the variations of the semi-major axis, made by changing the altitude of the apsides, and the eccentricity, having $i_E = i_T = 0$. The absence of an orbital plane change maneuver makes this case by far the simplest among all those studied in this work, and the least expensive in terms of propellant consumption. Asteroid #76, the farthest and the most expensive one, consumes indeed only $5{,}00281\ kg$ of the starting $20\ kg$, as it can be seen in the following joint graph of the propellant mass utilized and the final mass of the spacecraft (trivially, this last value is the difference between the starting mass and the propellant consumed).

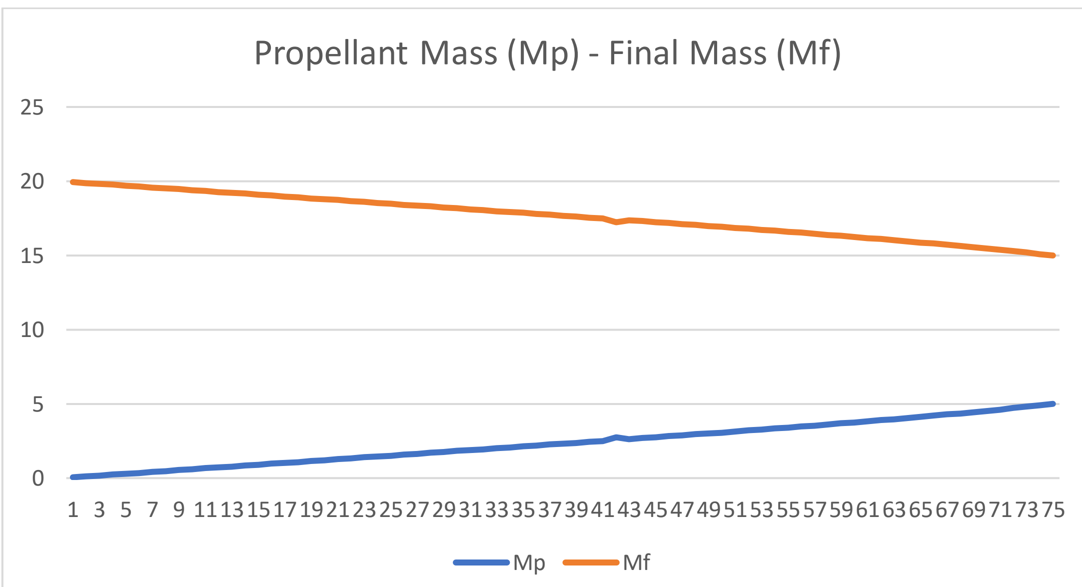

Figure 1. Trends of Propellant Mass and Final Mass

Although this initial feedback may seem encouraging, *case 0* is the one that globally presents the least accurate (but still acceptable) answer on the fundamental parameters calculated using this estimation method, that is, ϑ_e, Λ and the initial and final values of the in-plane thrust angle $\alpha_{iniz} - \alpha_{fin}$. ϑ_e is probably the most important of these parameters with regards to the accuracy of the solution, because when it is equal to 0 the thrust is practically horizontal [2] (there are no losses or errors due to misalignment) and the maneuver is perfectly centered at the perihelion (a crucial aspect especially for the plane change maneuvers in *cases* where the perihelion and the ascending node coincide, that is, $\Omega = 0$).

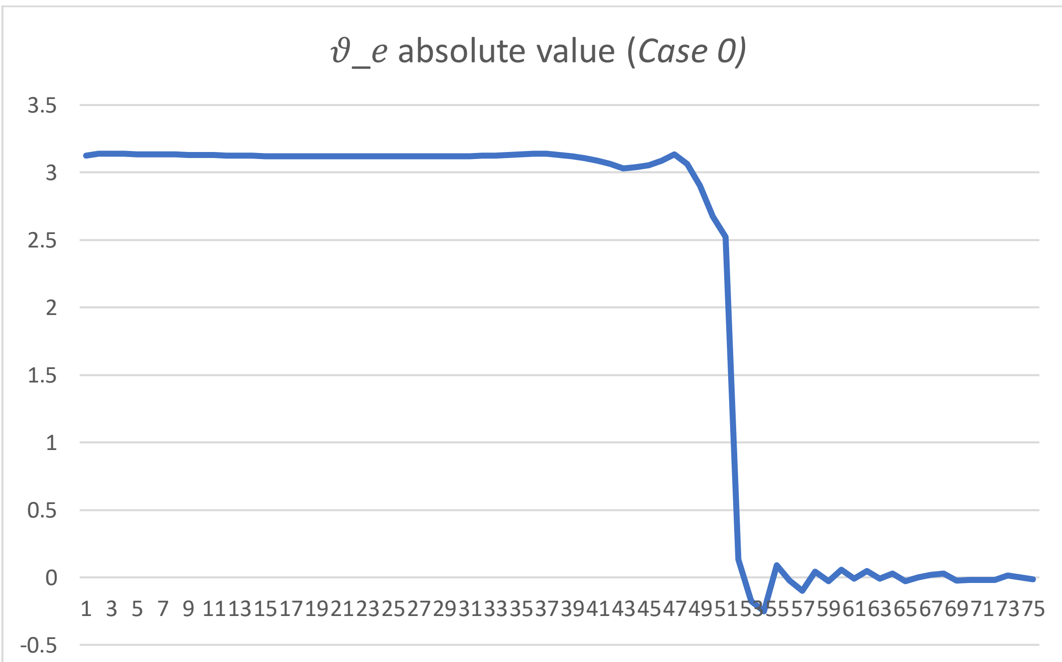

Figure 2. ϑ_e angle for Case 0 - Perihelion

In this graph, it is possible to notice that the first set of about 50 asteroids return an unexpected output. The original value of ϑ_e pulled out of the code seemed to fluctuate between π and $-\pi$, but these angular values represent the same orbital longitude, consequently it has been chosen to adopt the absolute value (in this range of about 50 asteroids) for greater clarity. However, as already written, $\vartheta_e \cong \pi$ may an issue for the accuracy of the method since, in essence, it estimates that the maneuver is performed not at the perihelion, but at the diametrically opposite point to it. At about asteroid #53, a transition takes place which brings the value in closest range of 0 and maintains it up to asteroid #76.

Λ assumes in *case 0* very acceptable values since they are very low, but it has a particular trend: it decreases starting from the first asteroid until it is almost equal to 0 at asteroid #51, and then begins to increase and maintains this trend until the final asteroids.

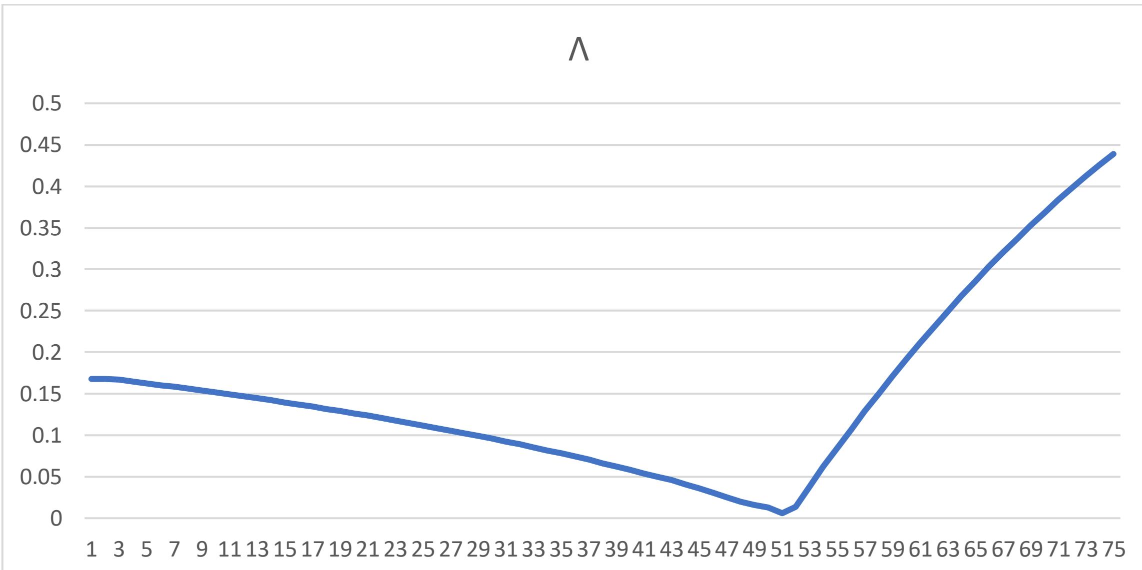

Figure 3. Λ value for Case 0 - Perihelion

It is particularly curious that for both ϑ_e and Λ the transition (of values for ϑ_e, of trend for Λ) takes place at a distance of very few asteroids. It has been observed that is not a random or isolated factor but is also found in subsequent *cases*, and it is even found in the trends of α_{iniz} and α_{fin}.

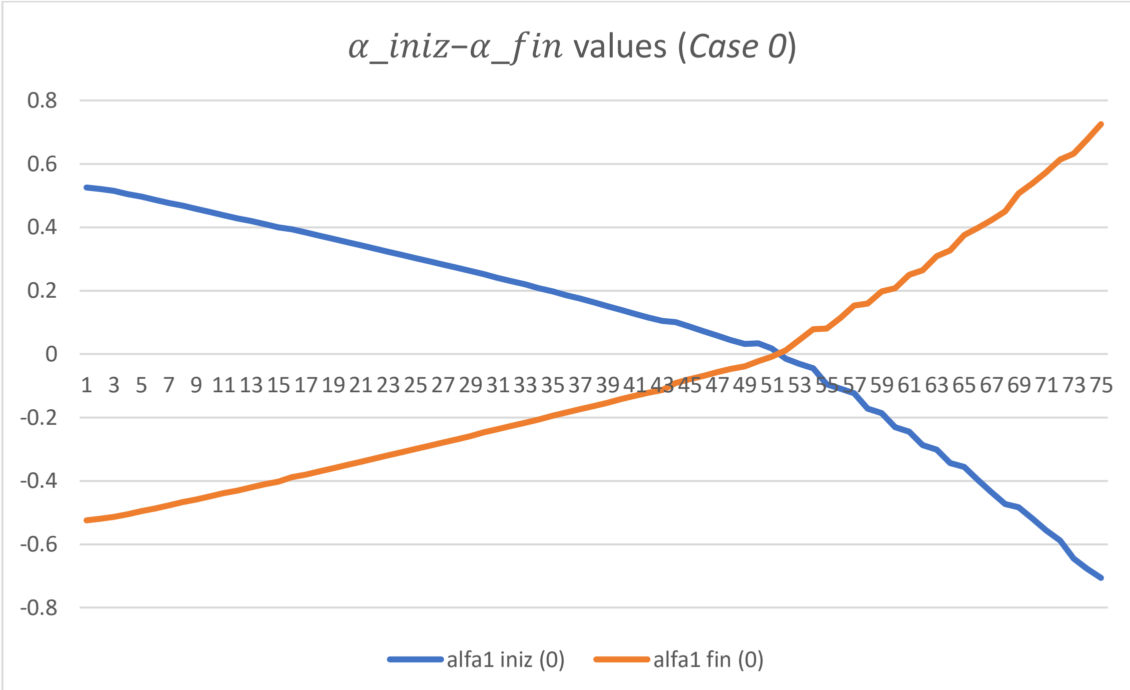

Figure 4. α_iniz–α_fin comparison for Case 0 - Perihelion

The estimation only makes sense if $\alpha_{fin} > \alpha_{iniz}$, and it is easy to note that the section of the graph for which the previous inequality is satisfied begins at the same asteroid where the Λ transition from decreasing to increasing occurs and a few asteroids away from the ϑ_e transition to 0. When $\alpha_{fin} < \alpha_{iniz}$, α is discontinuous since the burning arc is not centered at $\vartheta = \vartheta_e$, that is π in absolute value, but at $\vartheta = 0$, that is the perihelion [2]. It is also important to note that the adopted linear control law for the thrusting in-plane effect is valid when $-\pi < (\vartheta - \vartheta_e) < \pi$, hence the reason why having ϑ_e in a range of π could represent an inaccuracy of the method is easily understandable, although it is however acceptable as suboptimal solution and in the future it will be necessary to understand why the code choose these solutions instead of the responses expected.

Lastly, the graph of the burn arc angular length $\Delta\vartheta$ in perihelion for each asteroid is shown. This parameter, crucial for the veracity of the estimation, is calculated as the difference of the two orbital positions where the thrusting arc begins and ends: $\Delta\vartheta = \vartheta_{iniz,T} - \vartheta_{fin,T}$.

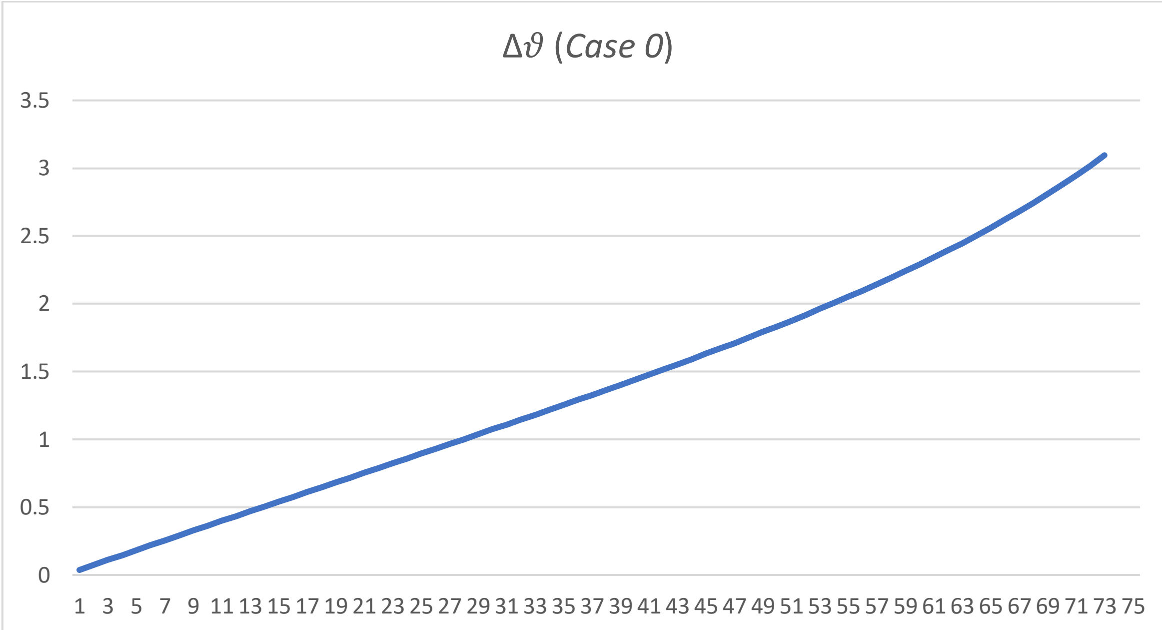

Figure 5. $\Delta\vartheta$ angle for Case 0 - Perihelion

As expected, the burning arcs are very small as far as the asteroids closest to Earth are concerned; then, the angular values increase significantly moving towards the most distant asteroids. This trend is practically identical to the trend of the propellant consumption, except for the last two asteroids which have $\Delta\vartheta$ values larger than π, an eventuality in disagreement with an assumption of reliability of the method that impose $\Delta\vartheta < \pi$ at each apside; hence, when $\Delta\vartheta > \pi$, in each *case* a correction is adopted by subtracting 2π and the taking the absolute value of the result: $\Delta\vartheta = |\Delta\vartheta_{iniz} - 2\pi|$. Trivially, $\Delta\vartheta$ values larger than π are always defined by subtracting 2π and their reported value is between 0 and 2π; therefore, the trend stops as soon as $\Delta\vartheta > \pi$, since the used relations are valid only if $\Delta\vartheta < \pi$.

This is interesting not only because $\Delta\vartheta$ and propellant consumption are actually connected, but also since the required orbital changes affect them both: the more orbital elements need to be varied, the larger $\Delta\vartheta$ and m_p are. This result is effectively shown and reported in the next section, in which *cases* with variable inclination (*A*, *B* and *C*) are treated.

2.2 Plane change with $i = (1/8)e$: *cases A, B and C*

Cases A, *B* and *C* share the linear dependence of inclination on eccentricity, and instead are distinguished due to the different positions that the ascending node assumes with respect to the line of apsides, hence for the different values of Ω. The rate of inclination change is described by the following equation:

$$i = (1/8)e$$

So, the inclination gradually increases as a fraction of the eccentricity, which also grows progressively. Due to this slow and in any case contained growth, the trends of the significant parameters as regards *cases A*, *B* and *C* can be compared with the results obtained with the *planar problem* in *case 0*.

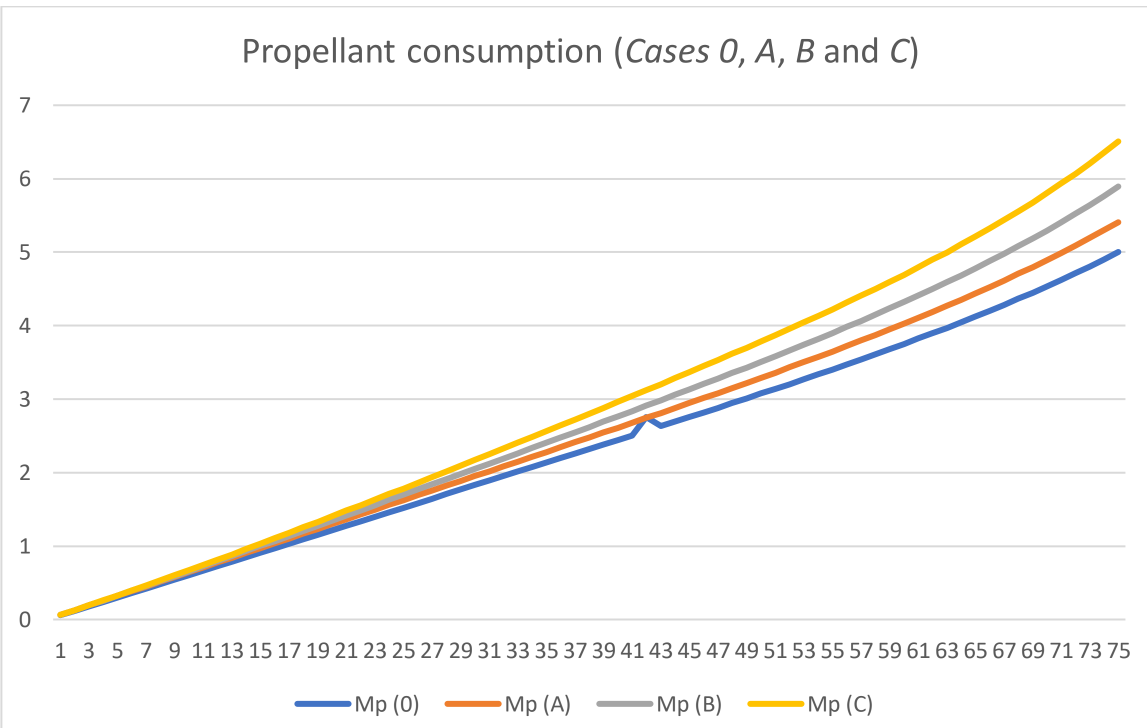

Figure 6. Propellant consumption comparison for Cases 0, A, B and C - Perihelion

The comparison of the propellant masses utilized in these first four *cases* provides a fairly predictable response: propellant consumption is strongly related to the required changes of orbital parameters from the departure orbit to the arrival orbit [2]; thus, *case C* is the one with the highest consumption since a lot of parameters are varied throughout the mission (a, e, i and Ω). On the contrary, the *case* in which the least propellant is used is trivially *case 0* as it performs a simpler mission, consisting only of the elevation of the apsides and the small increase of the eccentricity.

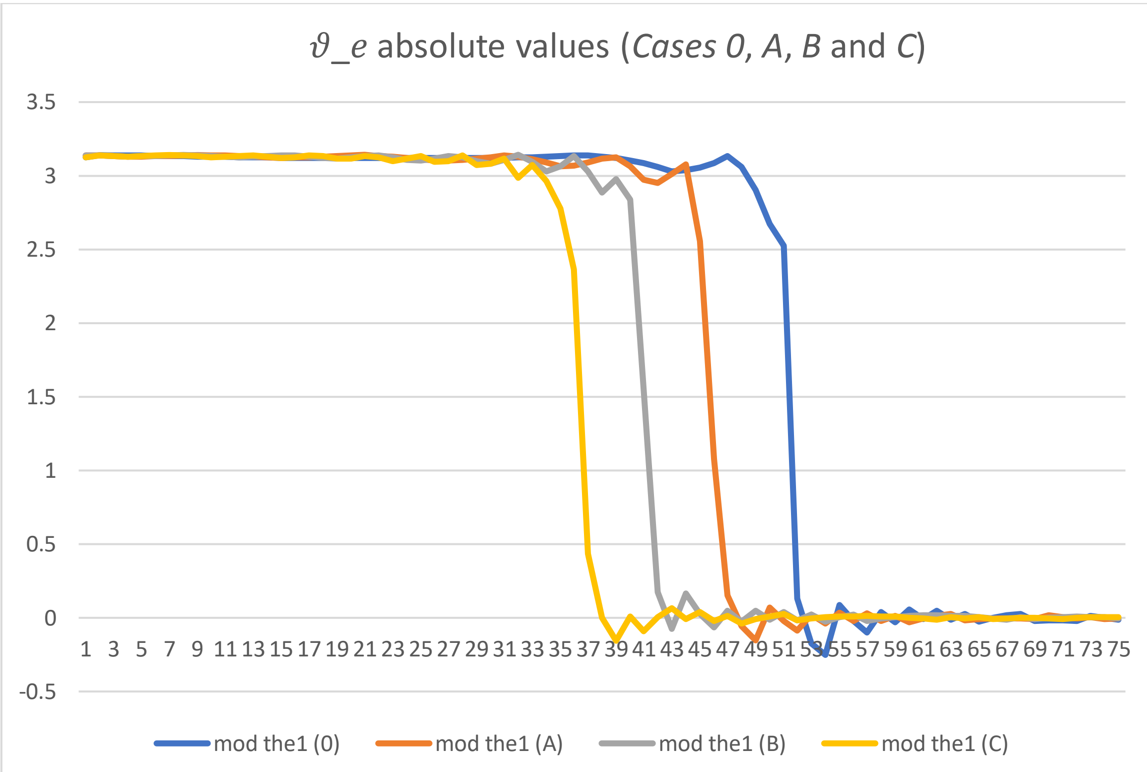

Figure 7. ϑ_e comparison for Cases 0, A, B and C - Perihelion

As it can be seen, the response of the estimation method regarding ϑ_e follows a similar path in all four *cases*. Also for the *cases* with variable inclination there is a first group of asteroids in which the answer is unexpected since $\vartheta_e \cong \pi$, and then, at a certain point, a transition to 0 occurs. It is easy to observe that the last group of asteroids, the one with an accurate answer in which $\vartheta_e \cong 0$, tends to grow going from *case 0* to *case C*, in fact the transition shifts to the left, i.e., towards a previous asteroid. And a similar, but slightly different situation occurs with Λ patterns.

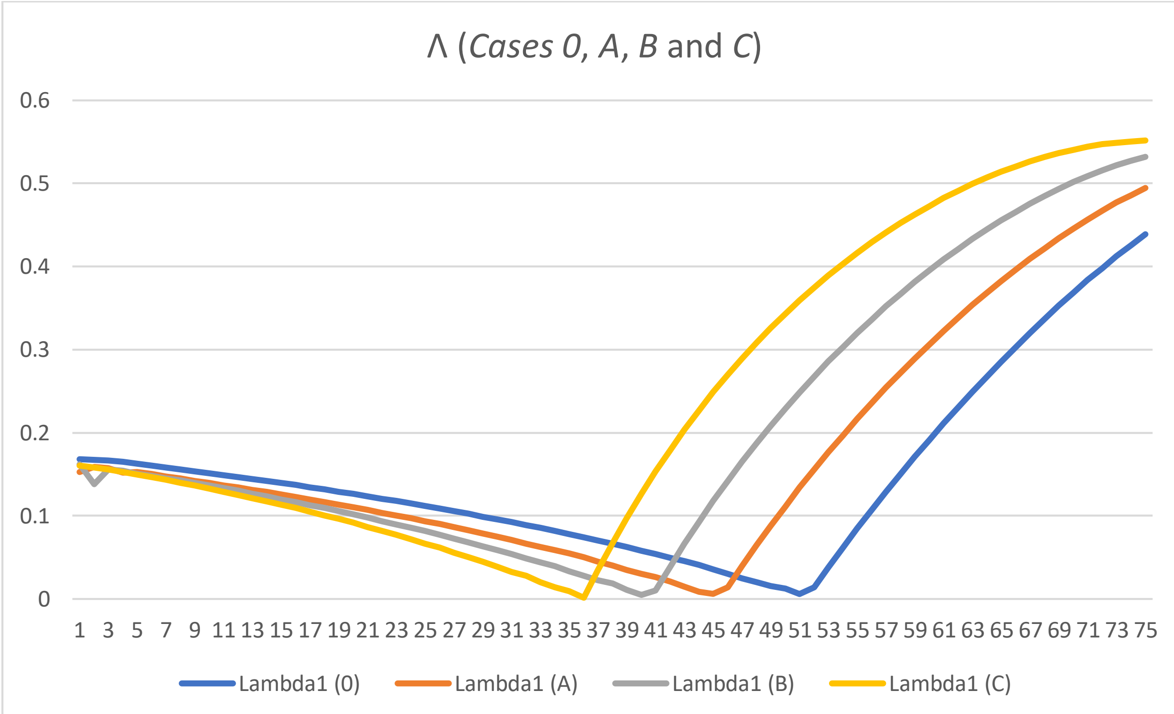

Figure 8. Λ comparison for Cases 0, A, B, C - Perihelion

It is no coincidence that the trends are practically identical, and the respective transitions occur a few asteroids before those of ϑ_e: these parameters are related, as well explained in chapter 1, section 1.3, and paragraph 1.3.1. In detail, it almost seems that these values offset each other, and any *case* can be taken to demonstrate this. *Case C* is taken as example. In this *case*, up to asteroid #37 ϑ_e response seems, as seen above, inaccurate, and the transition takes place at asteroid #39; Λ values in this first group of asteroids are instead very small, as theoretically they must be. This parameter is indeed in a range that goes from a value lower than 0,2 initially to an almost-null value at asteroid #37. Subsequently, when ϑ_e response becomes ideal and remains so until the last asteroid, Λ, which in the first part has a decreasing trend that brings it almost to 0, assumes an increasing logarithmic-like trend that leads it to have a value greater than 0,5 in the last asteroids, not irrelevant for a parameter between 0 and 1 [2].

The aspects described so far might suggest that there is no problem of an inaccurate answer if, somehow, ϑ_e and Λ tend to compensate each other more or less in the whole group of asteroids analyzed. The unforeseen fact is that the linear control law, adopted to accurately approximate the behavior of the in-plane thrust angle α, continues to provide, even for *cases A*, *B* and *C*, surprising values for the $\Delta\alpha$ range in the first set of asteroids, in which $\vartheta_e \cong \pi$.

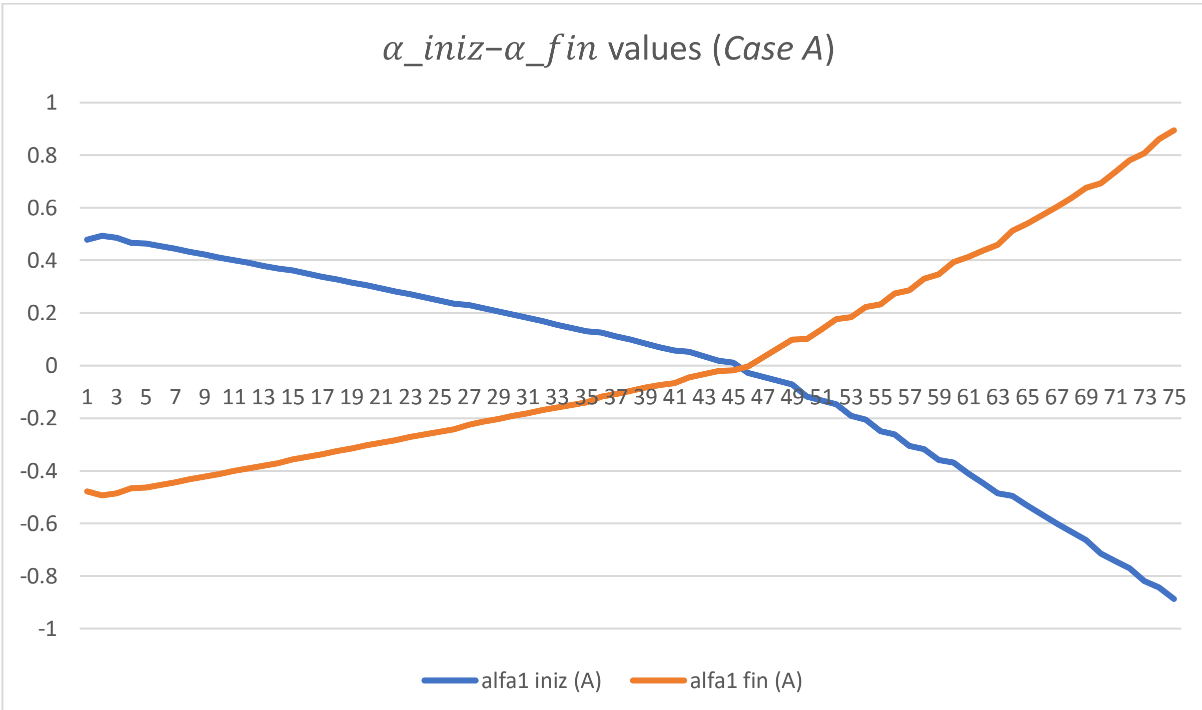

Figure 9. α_iniz–α_fin comparison for Case A - Perihelion

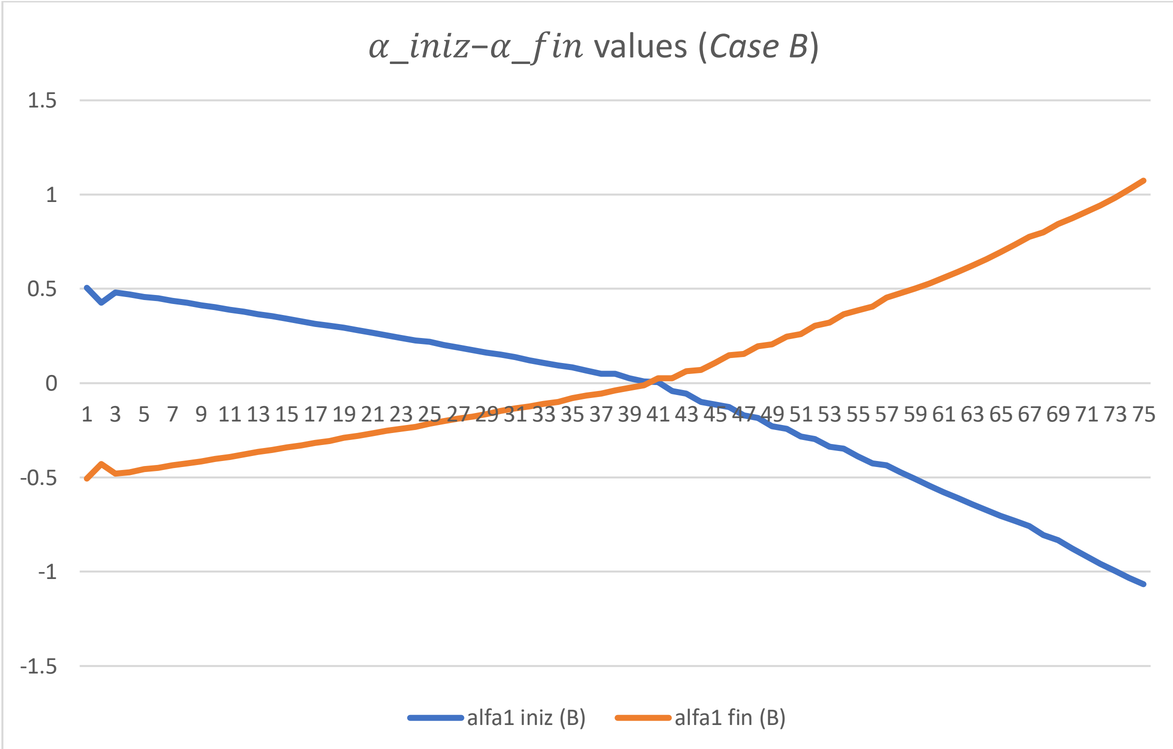

Figure 10. α_iniz–α_fin comparison for Case B - Perihelion

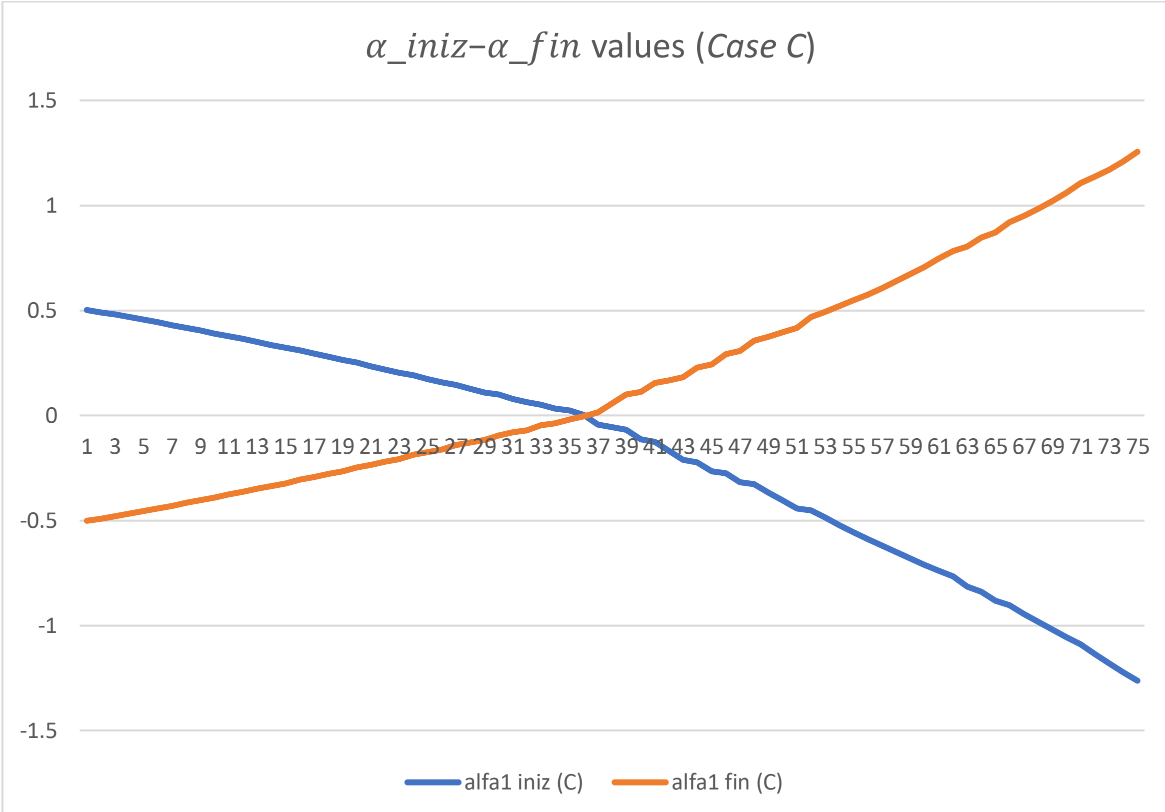

Figure 11. α_iniz–α_fin comparison for Case C - Perihelion

As indeed it can be noted, although the transition after which $\alpha_{fin} > \alpha_{iniz}$ is anticipated and shifts to the left going from *case 0* to *case C*, in all four *cases* there is still a quite consistent group of asteroids in which the maneuver appears discontinuous because is not centered at the right point. In fact, in the group of asteroids in which $\alpha_{fin} < \alpha_{iniz}$, α goes from α_{iniz} to $\Lambda\pi$, then it has a discontinuity and starts again from $-\Lambda\pi$ to α_{fin}. $\Lambda\pi$ and $-\Lambda\pi$ values are asymptotic and not random since, as reported above, $\vartheta - \vartheta_e$ must be a number between $-\pi$ and π. Furthermore, the linear control law of α is relevant to theory only if $\Delta\vartheta < \pi$. However, even the results given by the first group of asteroids can be accepted as suboptimal solutions of the utilized code. Here are the trends of the burn arc angular length for *cases 0*, *A*, *B* and *C*:

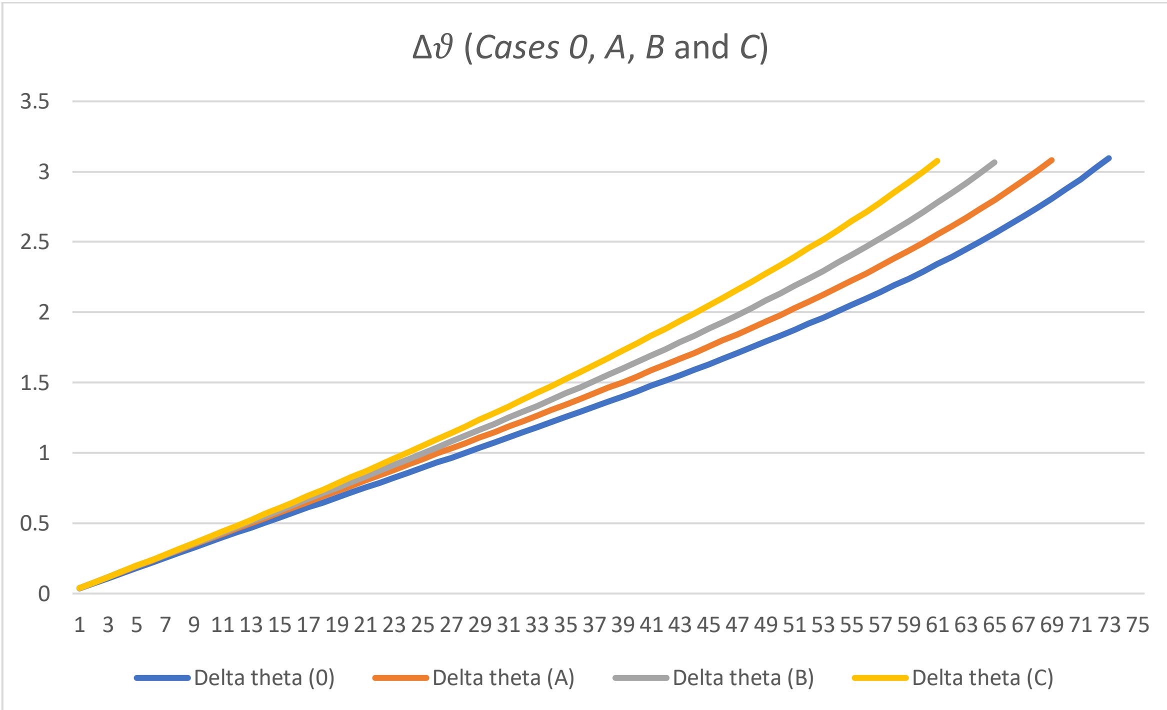

Figure 12. $\Delta\vartheta$ comparison for Cases 0, A, B and C - Perihelion

The *case* where $\Delta\vartheta$ reaches first π value is *case C* and looking the trends of the propellant consumption above it is easy to understand why: *case C* requires the largest orbital changes, consequently it is also the *case* with the longest burning arcs among the first four *cases*. Asteroid #62 in *case C* has $\Delta\vartheta \cong 3{,}07636°$, thus the last 14 asteroids must be corrected with the mathematical law shown before to get the appropriate response in terms of $\Delta\vartheta$ and their values are not shown on the graph since $\Delta\vartheta > \pi$.

2.3 Aphelion maneuver

The apoapsis (or aphelion) maneuver is generally more complicated than the periapsis (or perihelion) maneuver, mainly due to the fact that the thrust direction is not taken for granted as in the periapsis, and it is described by the parameter "*verse*" which assumes value 1 if the thrust is concurrent to the expected direction of advancement while takes value -1 if the thrust is opposite from the direction of advancement, that basically means that the spacecraft is braking. In aphelion, this trend is variable for each asteroid, and this is not a trivial information: if the vehicle brakes, α and ϑ are no longer centered in 0, but in π, and this has numerical consequences on the treated parameters which are immediately visible in the reference graphs.

2.3.1 Cases 0, A, B and C comparison

As mentioned in the previous paragraph, the aphelion maneuver may be more difficult to understand and interpret than the perihelion maneuver. The analysis of the maneuver performed in the first four *cases* can begin by observing the trends of ϑ_e.

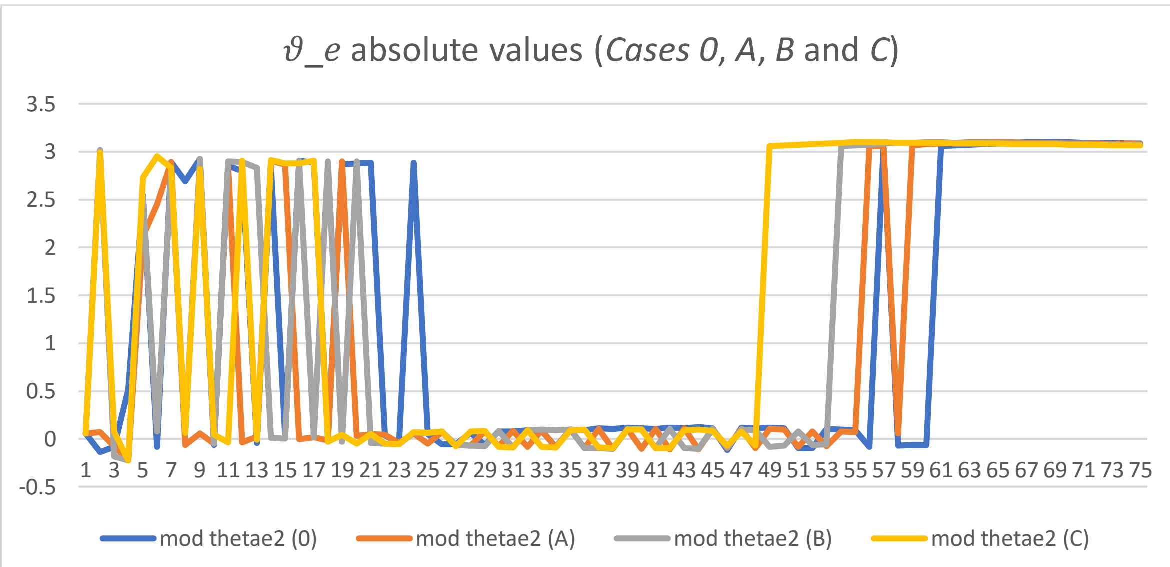

Figure 13. ϑ_e comparison for Cases 0, A, B and C - Aphelion

The reported values are ambiguous at first sight: in the first group, ϑ_e oscillates between 0 and π; in the central group it is in a range of 0, while for the final asteroids it stabilizes at π. These trends are strongly related to the verse of the thrust, as it is possible to note in the following graph.

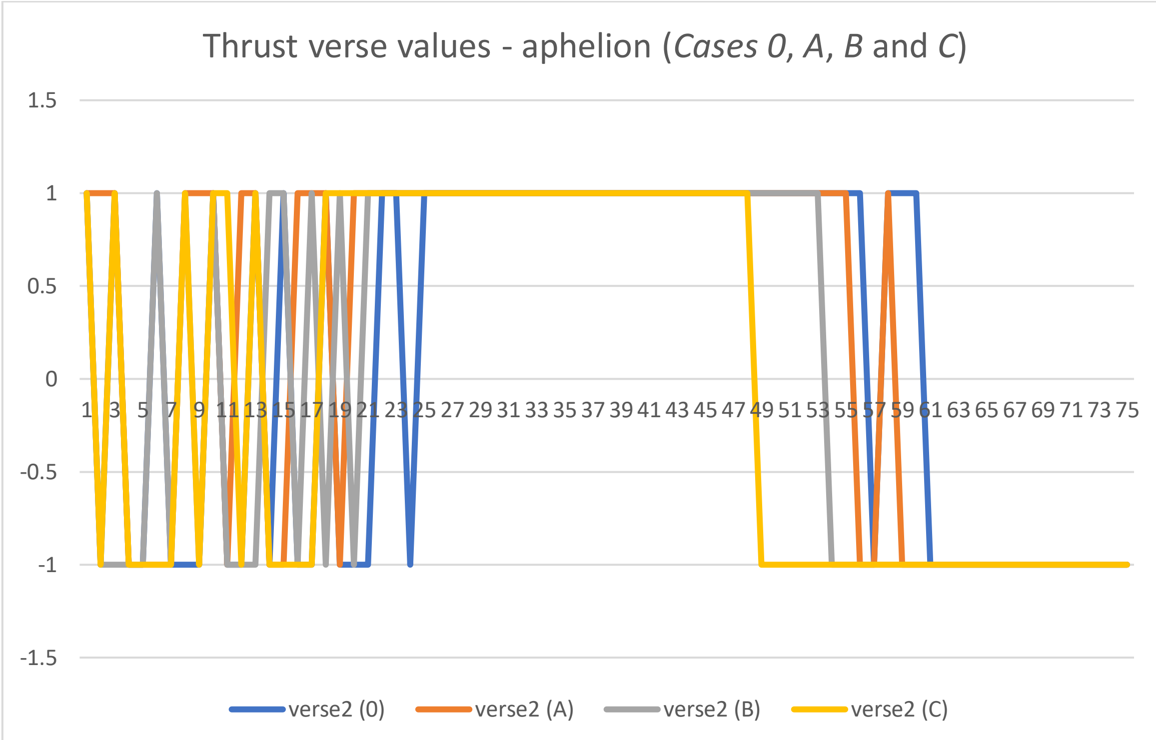

Figure 14. Thrust verse comparison for Cases 0, A, B and C - Perihelion

In the first group, the most complex to deal with, the thrust verse varies frequently, and this could be seen as a symptom of possible inaccuracy of the method. Actually, for the closest asteroids to Earth there are two possible solutions among which the code could choose: one with $verse = 1$ and $\vartheta_e \cong 0$ and the other one with $verse = -1$ and $\vartheta_e \cong \pi$; these solutions are close to each other, and the convergence algorithm tends to randomly find one or the other. Random convergence explains the reason for this apparently unclear response and therefore the presence of oscillations. It is interesting to observe that the transition from oscillating values in the first group to stable at 0 in the second group always occurs earlier (i.e., to a previous asteroid) going from *case 0* to *case C*; in fact, the first group "ends" at asteroid #26 for *case 0*, whereas this first transition takes place at asteroid #19 for *case C*. The second and last groups instead follow, at least in theory, what the linear control law of the in-plane thrust angle α imposes. When the thrust is concurrent to the expected direction of advancement [2]and so $verse = 1$, Δa is a positive value and $\alpha = \Lambda(\vartheta - \vartheta_e)$, so ϑ_e, that indicates the angular position in which the maneuver must be performed to have the thrust perfectly horizontal, must be in the closest range of 0. Subsequently, another transition occurs, and when it occurs in the four *cases* is analogous to what is written above (*case 0* → asteroid #62, *case C* → asteroid #50). Last asteroids, in each *case*, have $verse = -1$; therefore, the thrust is opposite from the direction of advancement and $\Delta a < 0$, and this causes the linear control law to be $\alpha = \pi + \Lambda(\vartheta - \vartheta_e)$. When Δa is a negative value and consequently the spacecraft has to brake, ϑ_e must be in the closest range of π, in order to have $\alpha \cong \pi$.

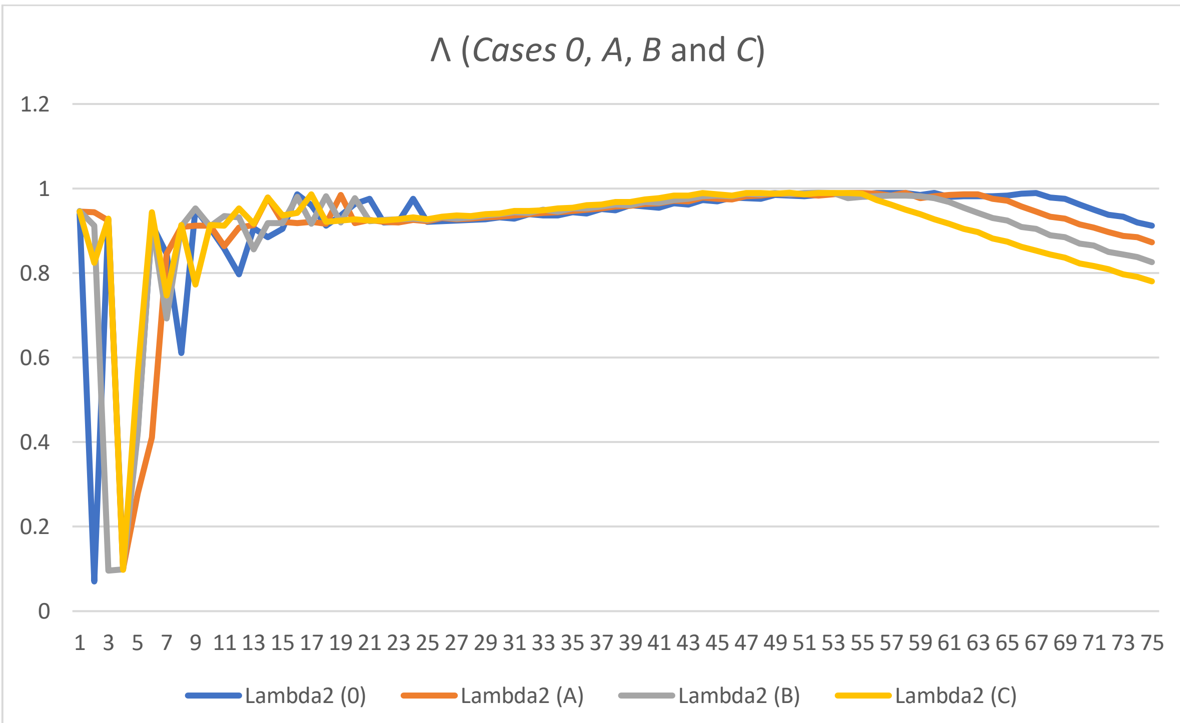

Figure 15. Λ comparison for Cases 0, A, B and C - Aphelion

Λ values are controversial. There is a very small subgroup of asteroids at the beginning which, for each *case*, has $\Lambda < 0{,}5$. Subsequently, it increases until it gets very close to 1 and then starts to decrease again (but not very much) a few asteroids away from the transition occurred for ϑ_e and *verse*.

But, if possible, the results regarding Λ are not the only ones to be complex and worthy of further study. In fact, the graphs of α_{iniz} and α_{fin} are visible below.

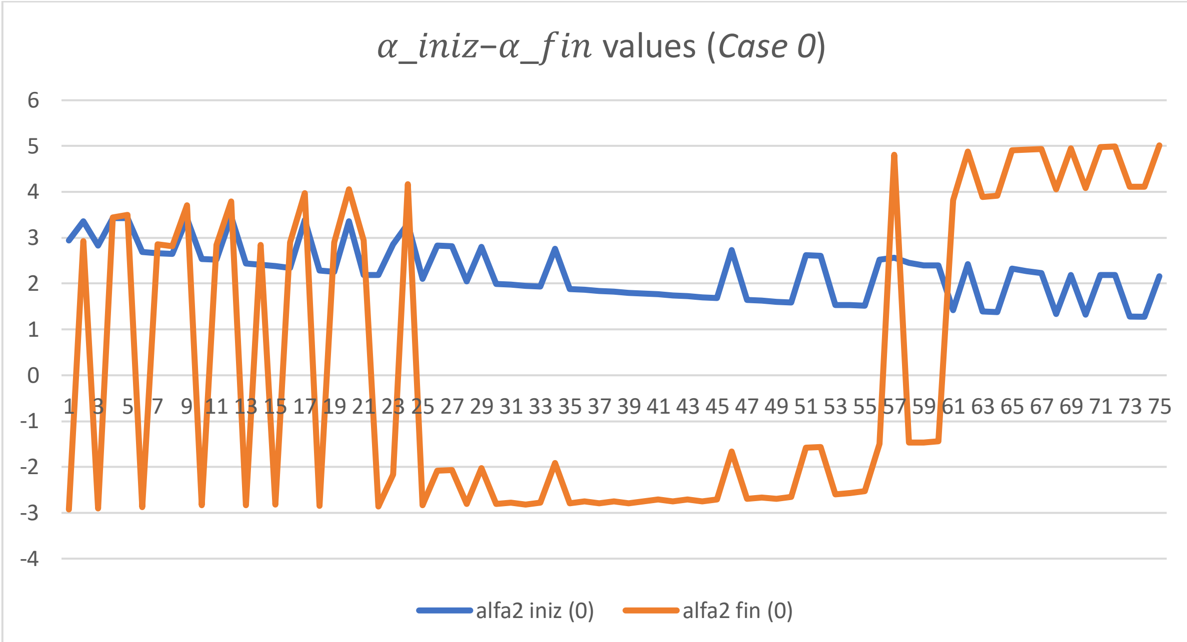

Figure 16. $\alpha\_iniz{-}\alpha\_fin$ comparison for Case 0 - Aphelion

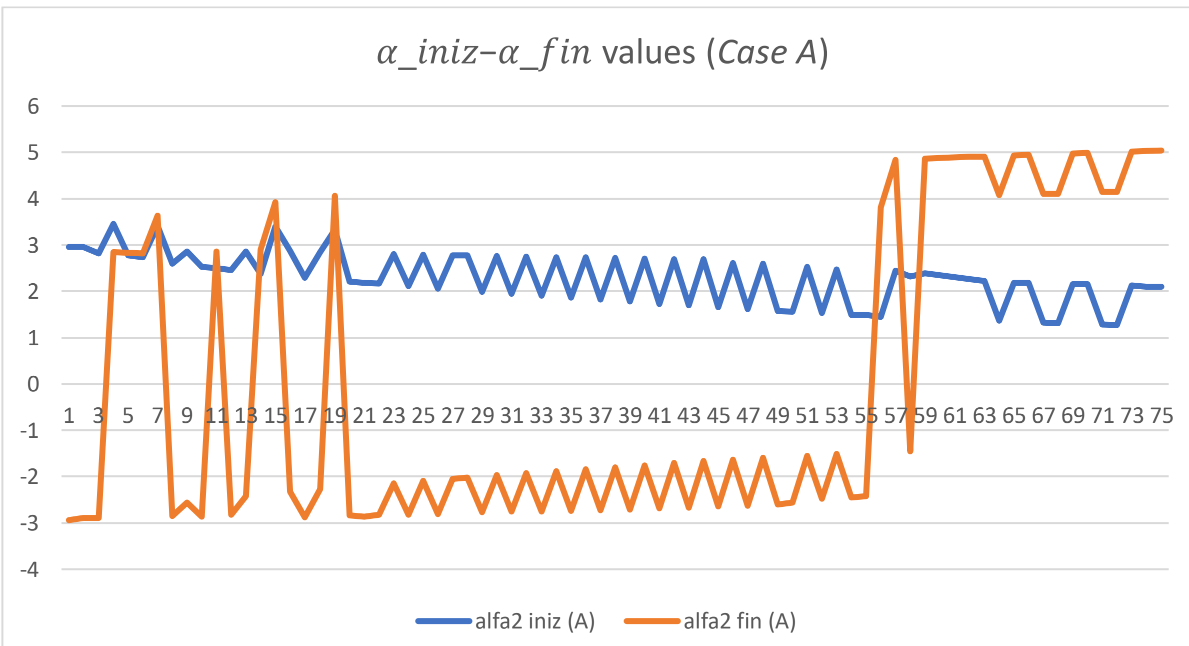

Figure 17. $\alpha\_iniz{-}\alpha\_fin$ comparison for Case A - Aphelion

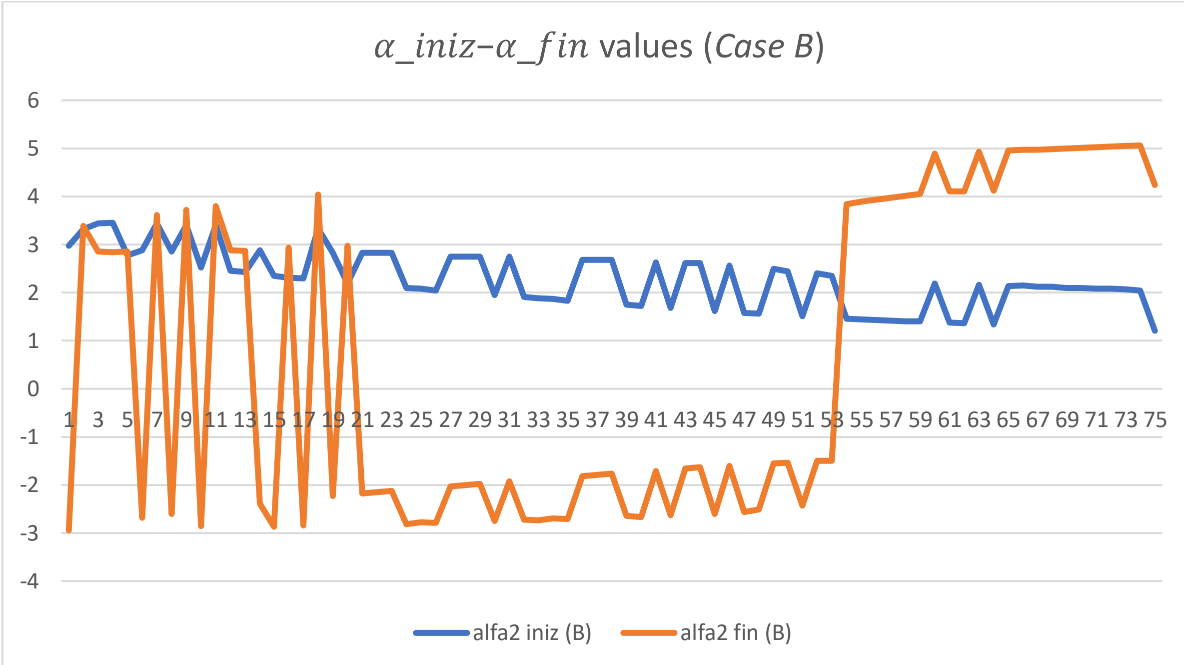

Figure 18. $\alpha\_iniz - \alpha\_fin$ comparison for Case B - Aphelion

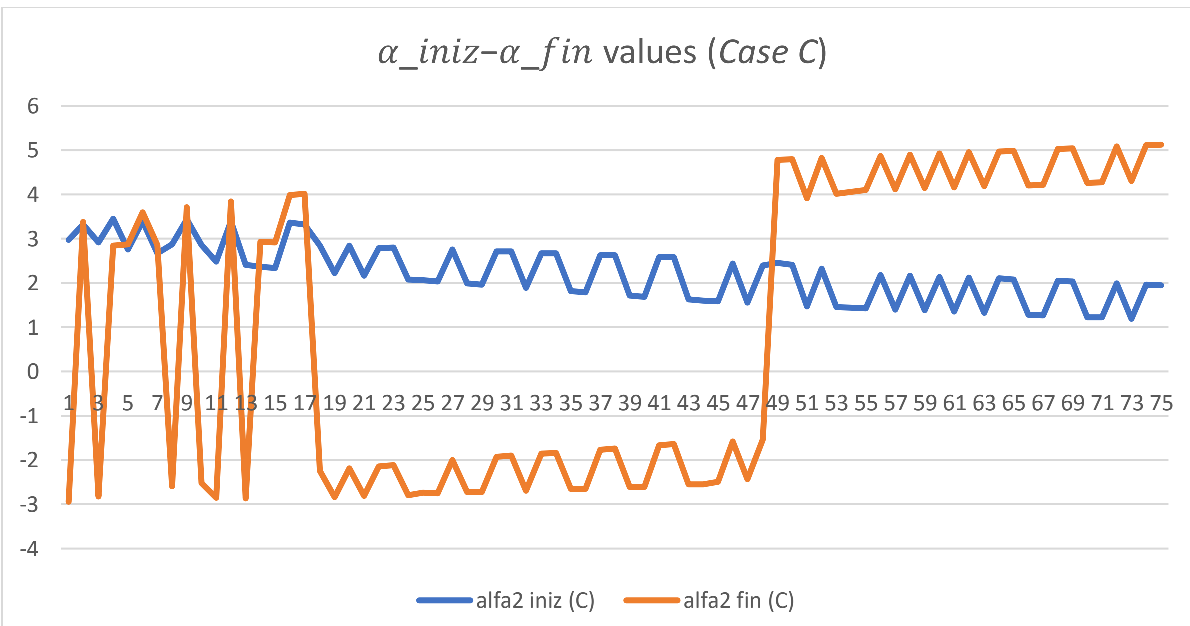

Figure 19. $\alpha\_iniz - \alpha\_fin$ comparison for Case C - Aphelion

These graphs are probably the most important to try to correctly interpret the aphelion maneuver and understand which path would be possible to follow if these models are applied in reality. Also with regard to these parameters, there is essentially a subdivision into three areas: the first one, very chaotic in which for some asteroid $\alpha_{fin} > \alpha_{iniz}$; the second one, in which one stably has $\alpha_{fin} < \alpha_{iniz}$; the last one, in which, in the same way, one has $\alpha_{fin} > \alpha_{iniz}$. Trying to analyze the situation of the first group, it is now clear that the first asteroids in these *cases* present significant oddities (due to the random convergence of the algorithm to the two possible solutions, each with their respective values of $verse$ and ϑ_e), certified by oscillating and never evident results. The second and third groups generally tend to follow the trends of ϑ_e and *verse*: particularly, the expected response is given in the area where $\alpha_{fin} > \alpha_{iniz}$, and this area coincides with the areas seen in the previous graphs in which $verse = -1$ and $\vartheta_e \cong \pi$. In the first and second areas, α tends to be discontinuous and this may be related to an odd and discontinuous centering of the maneuver.

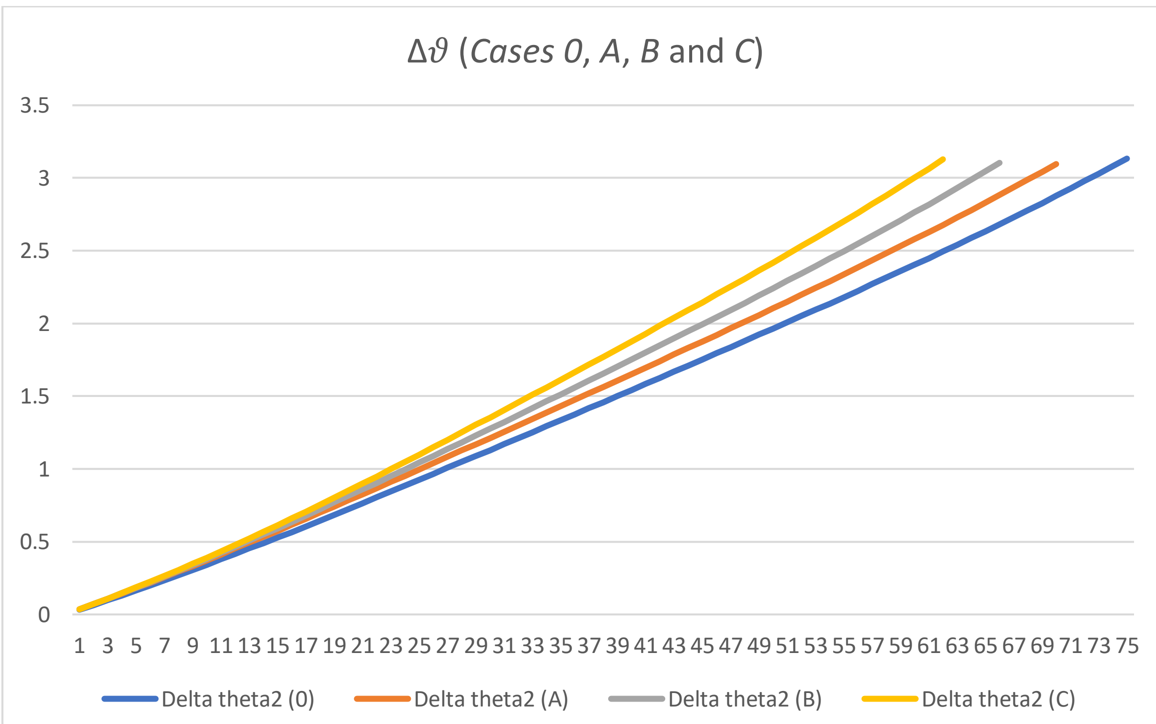

Figure 20. $\Delta\vartheta$ comparison for Cases 0, A, B and C - Aphelion

As it can be observed, making the correction already discussed in the perihelion maneuver (if $\Delta\vartheta > \pi \rightarrow \Delta\vartheta = |\Delta\vartheta_{iniz} - 2\pi|$ and the original value is not shown in the graph), the trend of $\Delta\vartheta$ does not differ from what is seen in perihelion;

nevertheless, it can be easily noted that the burning arcs are almost as long as those seen in the previous maneuver.

2.4 The relations between ϑ_e, ϑ_{iniz} and ϑ_{fin}, α_{iniz} and α_{fin}

2.4.1 Perihelion maneuver

At perihelion, one has always $\vartheta_{fin} > \vartheta_{iniz}$ and $\Delta\vartheta = \vartheta_{fin} - \vartheta_{iniz}$ (or, with the correction, $\Delta\vartheta = |\Delta\vartheta_{iniz} - 2\pi|$). At this point, it is necessary to discuss about ϑ_e, since a correct "placement" of this value makes the difference between an accurate and an imprecise output. In fact, it is possible to distinguish two possible situations by observing ϑ_e:

- If $\vartheta_{iniz} < \vartheta_e < \vartheta_{fin}$, α definitely has a continuous value, since it not only follows the approximate linear control law $\alpha = \Lambda(\vartheta - \vartheta_e)$, but knowing ϑ_{iniz}, ϑ_{fin}, α_{iniz}, α_{fin} it is possible to demonstrate trough a mathematical relationship that it varies linearly with ϑ:
$$\alpha = \alpha_{iniz} + (\alpha_{fin} - \alpha_{iniz}) \cdot \frac{\vartheta - \vartheta_{iniz}}{\vartheta_{fin} - \vartheta_{iniz}}$$
- If $\vartheta_e \notin [\vartheta_{iniz}; \vartheta_{fin}]$, then α has a discontinuous value and as written in section 2.2, it initially goes from α_{iniz} to $\Lambda\pi$, a discontinuity makes it start again from $-\Lambda\pi$ and then it grows until α_{fin}.

The observation of the graphs certainly helps the understanding of these concepts, also because in perihelion the trends for *cases 0*, *A*, *B* and *C* are similar, the only difference is the initial value for which $\vartheta_e \in [\vartheta_{iniz}; \vartheta_{fin}]$.

➢ Case 0

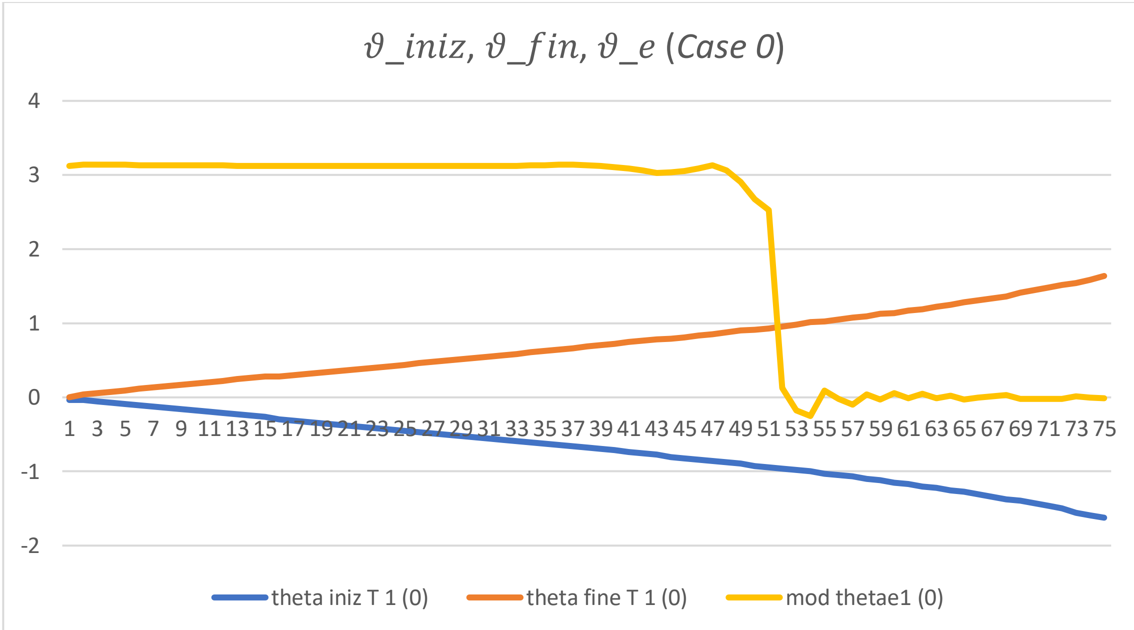

Figure 21. $\vartheta\_iniz, \vartheta\_fin, \vartheta\_e$ values for Case 0 - Perihelion

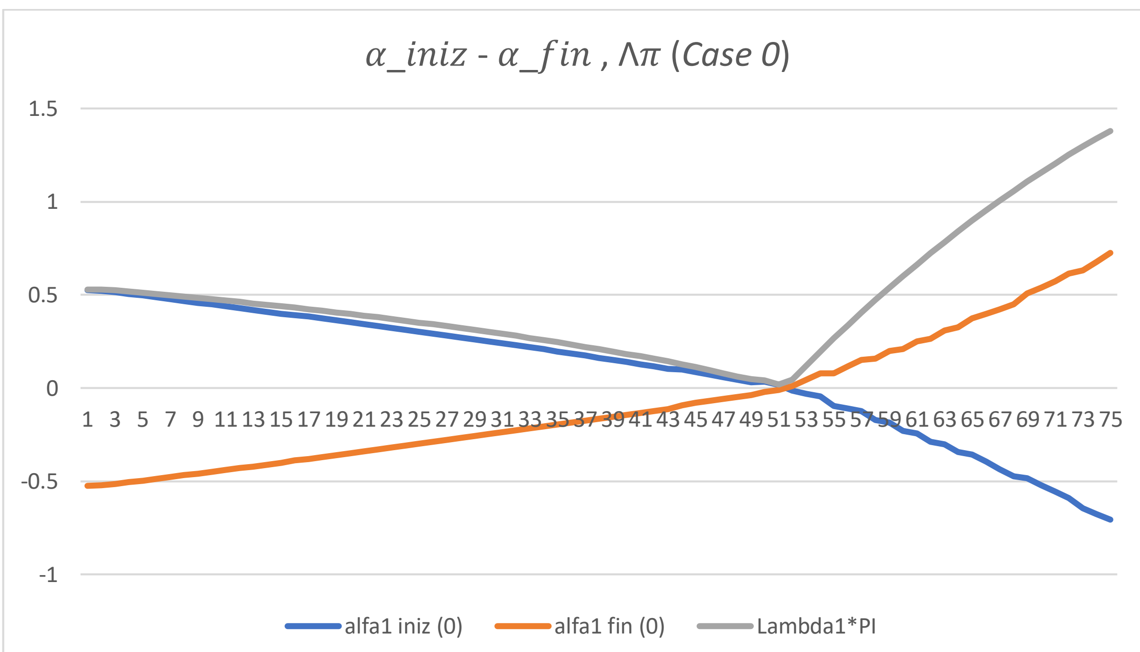

Figure 22. $\alpha\_iniz - \alpha\_fin, \Lambda\pi$ for Case 0 - Perihelion

> ➢ *Case A*

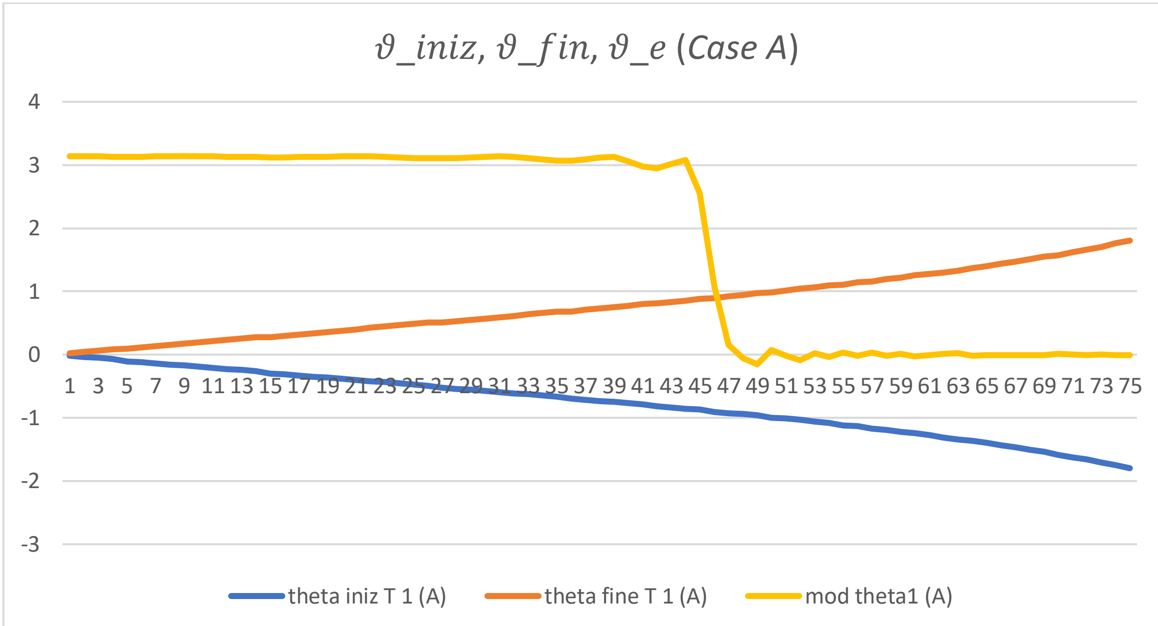

Figure 23. ϑ_iniz, ϑ_fin, ϑ_e for Case A - Perihelion

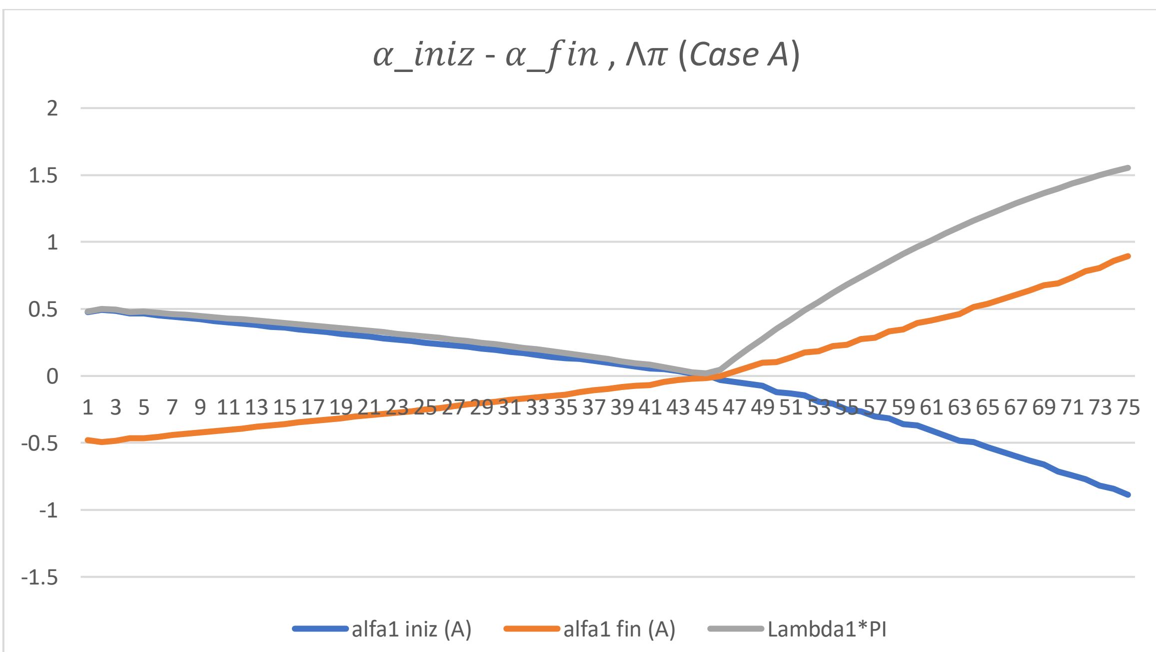

Figure 24. α_iniz - α_fin , $\Lambda\pi$ for Case A - Perihelion

➢ *Case B*

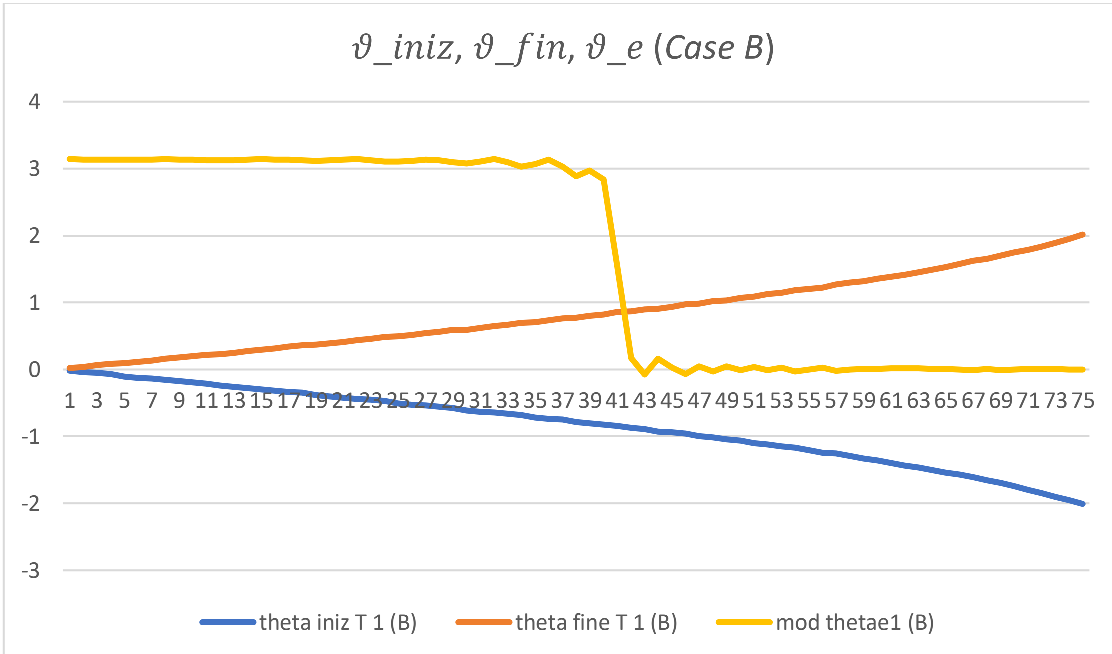

Figure 25. ϑ_iniz, ϑ_fin, ϑ_e for Case B - Perihelion

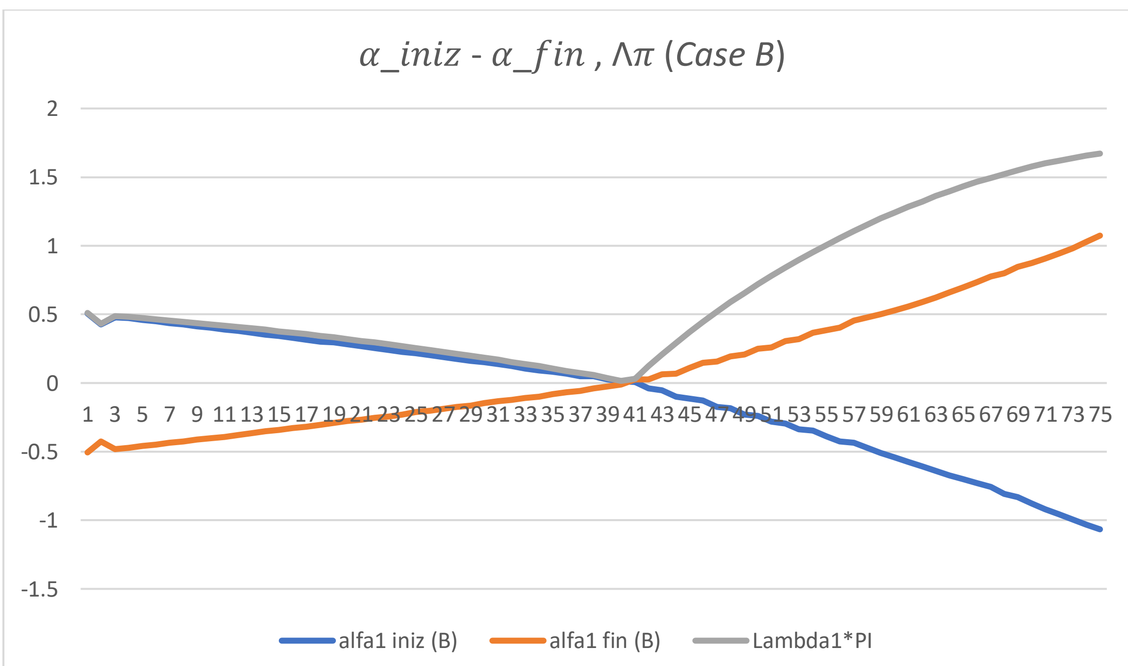

Figure 26. α_iniz - α_fin, $\Lambda\pi$ for Case B - Perihelion

- *Case C*

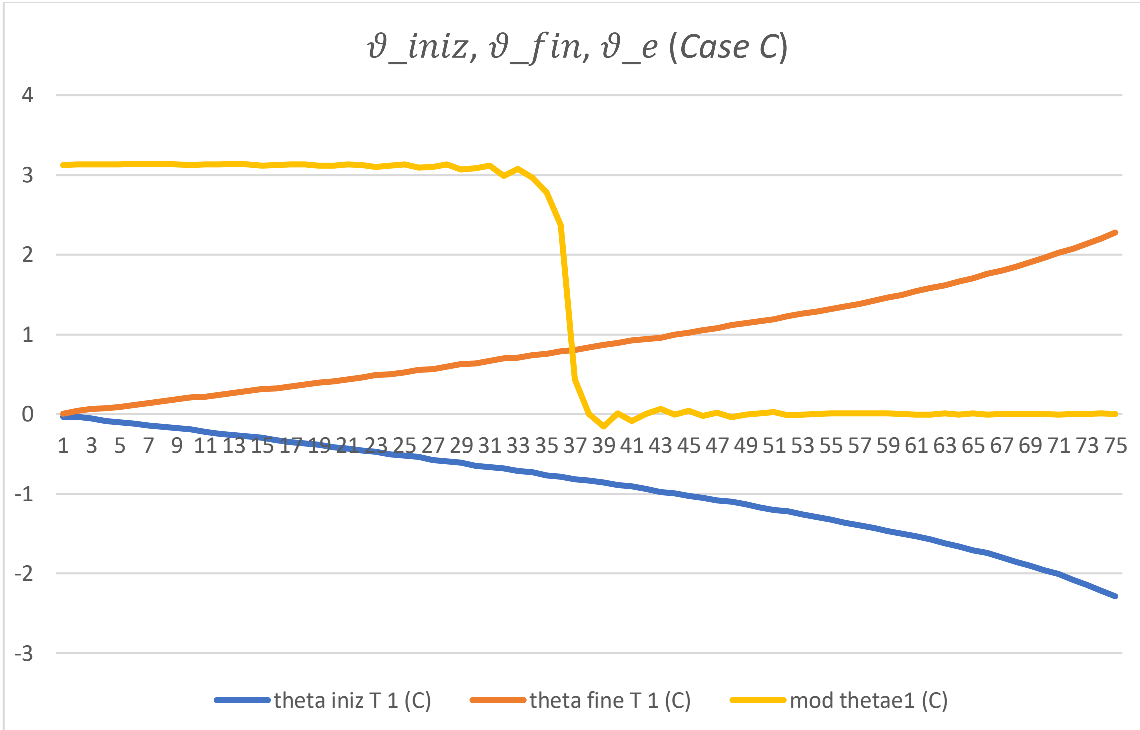

Figure 27. ϑ_iniz, ϑ_fin, ϑ_e for Case C - Perihelion

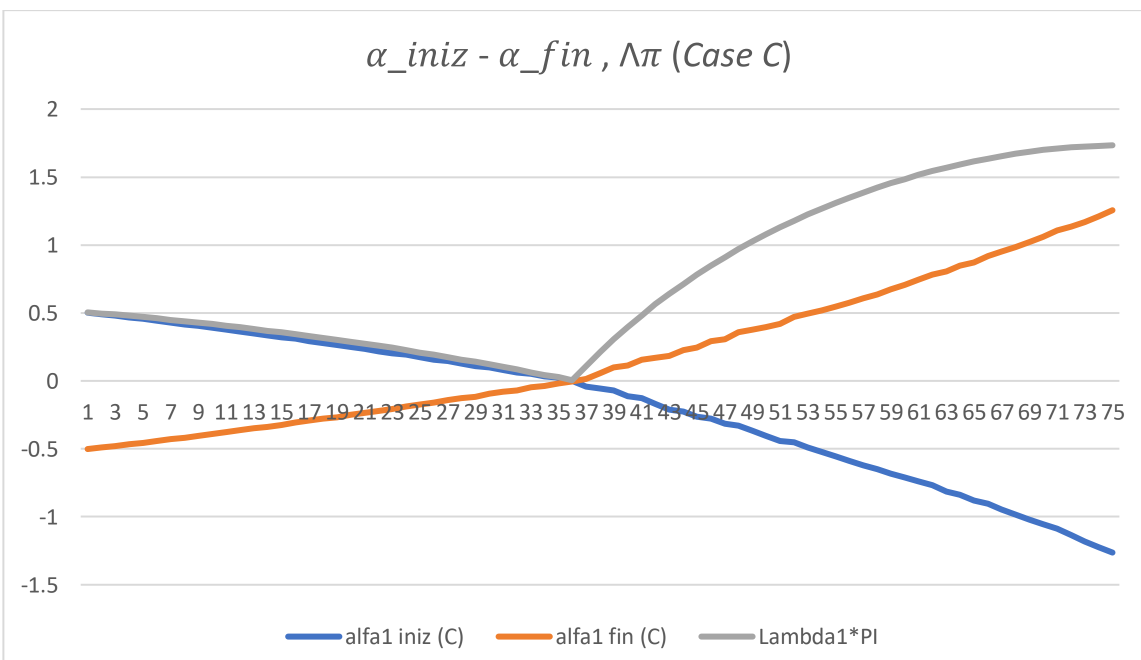

Figure 28. α_iniz - α_fin, $\Lambda\pi$ for Case C - Perihelion

It is trivial to note that, for each *case*, α graphs start to give the expected solution (hence, the area in which $\alpha_{fin} > \alpha_{iniz}$) when $\vartheta_{iniz} < \vartheta_e < \vartheta_{fin}$. Furthermore, the evolution of $\Lambda\pi$ demonstrates what has been written previously: in the first section on the left, α_{iniz} tends to the asymptotic value $\Lambda\pi$, subsequently, to the point of intersection between α_{iniz} and α_{fin}, the trend restarts from $-\Lambda\pi$ (not shown) and goes to α_{fin}; in the second section on the right, α is continuous and far from asymptotic value, which it no longer approaches.

2.4.2 Aphelion maneuver

The answer in aphelion is more complicated also as regards these relations, and the reason is the same discussed in section 2.3: the thrust verse is not taken for granted and affects the accuracy and the meaning of the results. The first step in analyzing the theoretical response of this maneuver is to observe ϑ_{iniz} and ϑ_{fin}; if, as always in perihelion, $\vartheta_{fin} > \vartheta_{iniz}$, these values are maintained; if $\vartheta_{fin} < \vartheta_{iniz}$, as often happens in aphelion, then 2π is added to ϑ_{fin} (ϑ_{fin}=$\vartheta_{fin,iniz} + 2\pi$) and one consequently has $\Delta\vartheta = \vartheta_{fin} - \vartheta_{iniz}$ reported between 0 and 2π, as expected since the maneuver seems to be centered in π and therefore ϑ_{fin} especially should have values larger than π.

However, one must remember what is initially written in chapter 2, section 2.1, paragraph 2.1.1: even if a solution may at first appear unexpected, it does not mean that is inaccurate since probably it is a suboptimal solution the algorithm chooses for a certain reason.

For each *case*, not only the graphs including $\vartheta_{e,}$ ϑ_{iniz} and ϑ_{fin} and those of α_{iniz}, α_{fin} and $\Lambda\pi$ are reported, but also those relating to the thrust verse to immediately give an idea of how much this affects the final responses.

➢ *Caso 0*

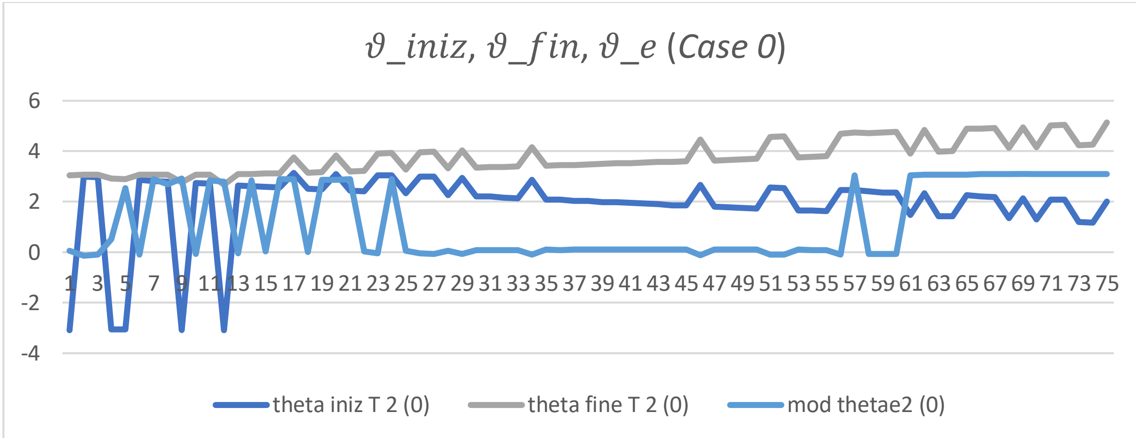

Figure 29. ϑ_iniz, ϑ_fin, ϑ_e for Case 0 - Aphelion

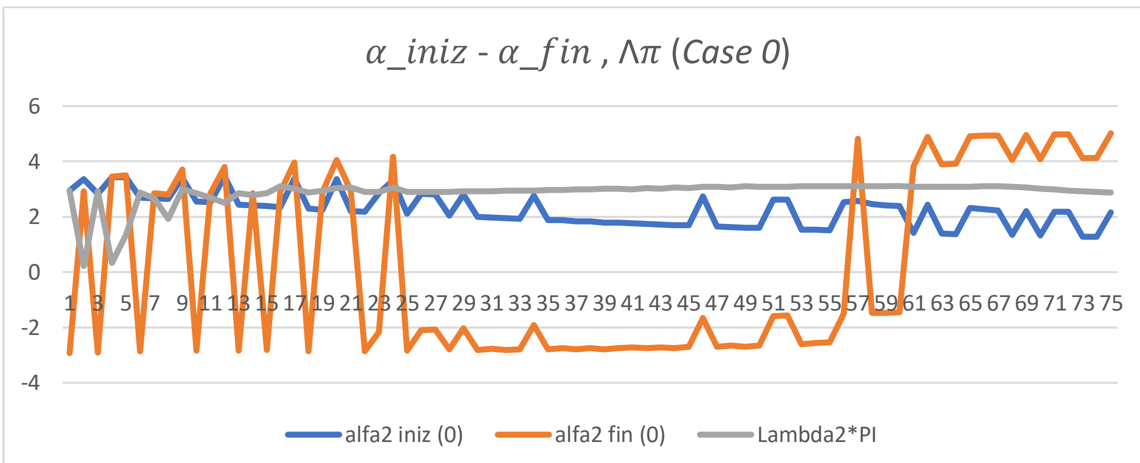

Figure 30. α_iniz - α_fin, $\Lambda\pi$ for Case 0 - Aphelion

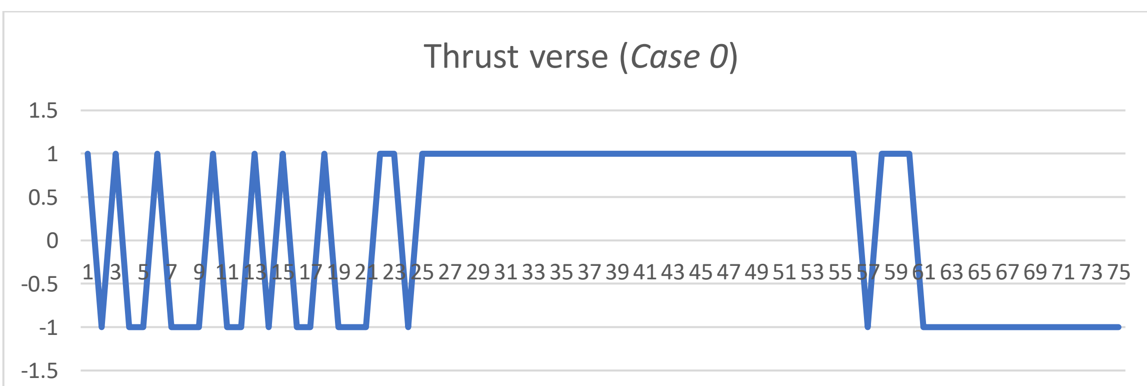

Figure 31. Thrust verse for Case 0 – Aphelion

➢ *Case A*

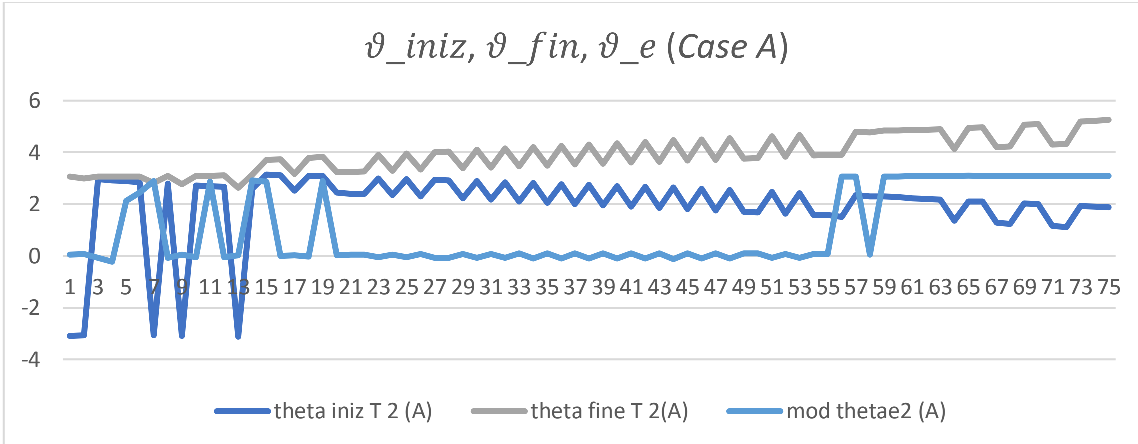

Figure 32. ϑ_iniz, ϑ_fin, ϑ_e for Case A - Aphelion

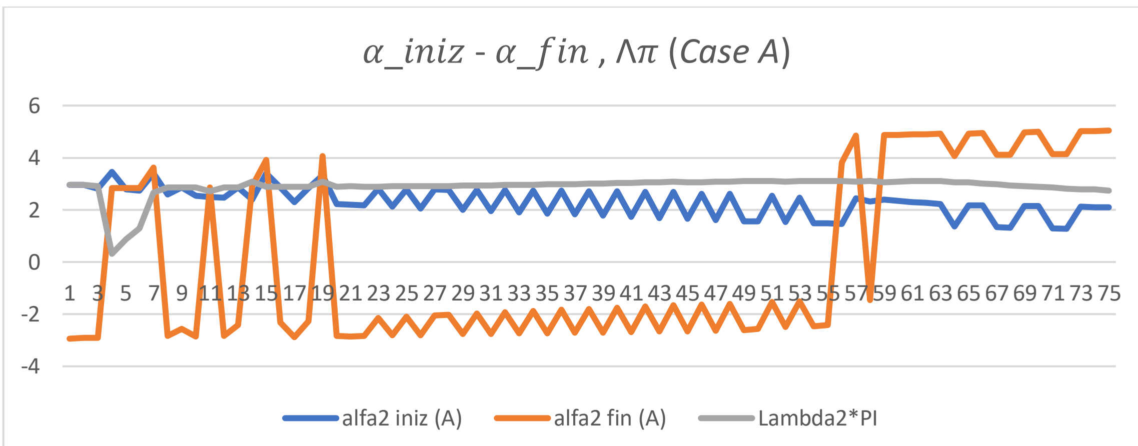

Figure 33. α_iniz - α_fin, $\Lambda\pi$ for Case A - Aphelion

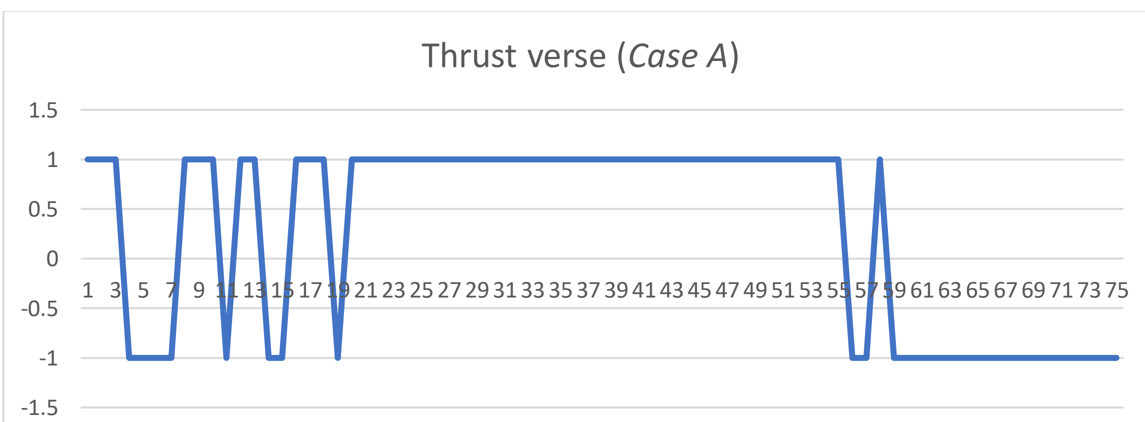

Figure 34. Thrust verse for Case A – Aphelion

➢ *Case B*

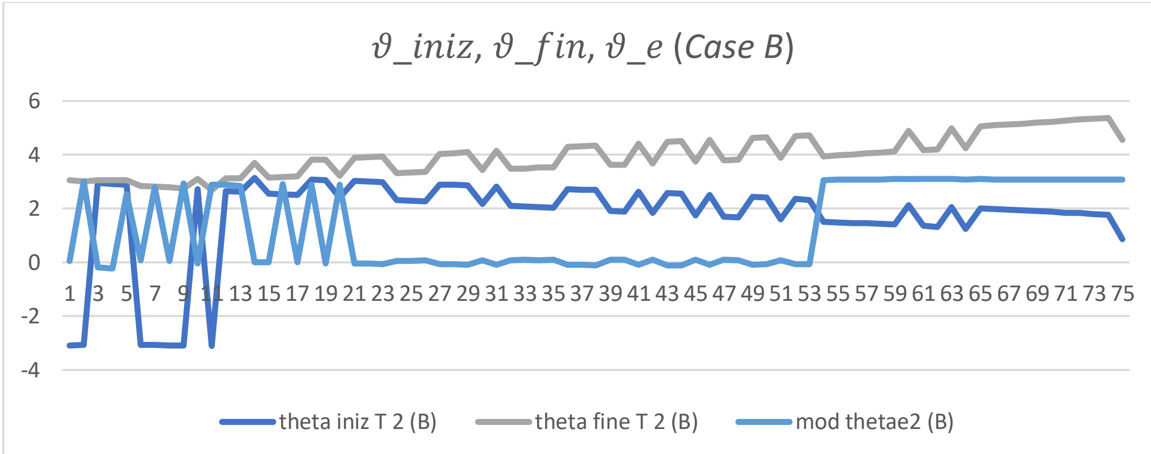

Figure 35. ϑ_iniz, ϑ_fin, ϑ_e for Case B - Aphelion

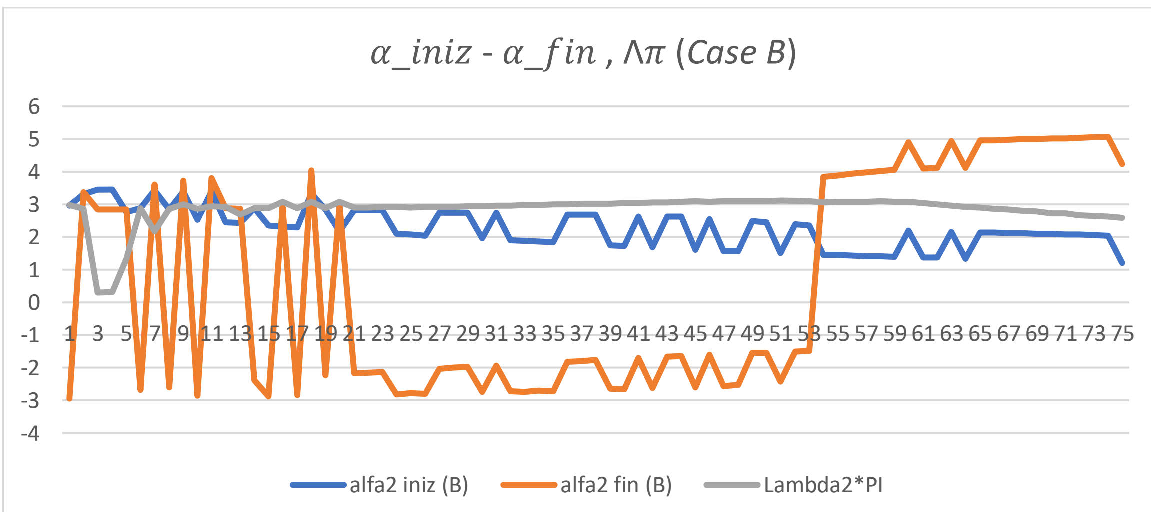

Figure 36. α_iniz - α_fin, $\Lambda\pi$ for Case B - Aphelion

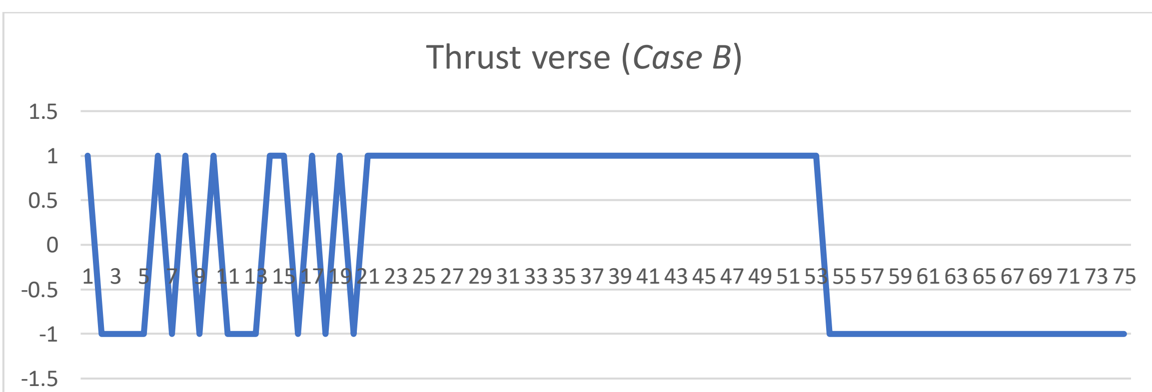

Figure 37. Thrust verse for Case B - Aphelion

- *Case C*

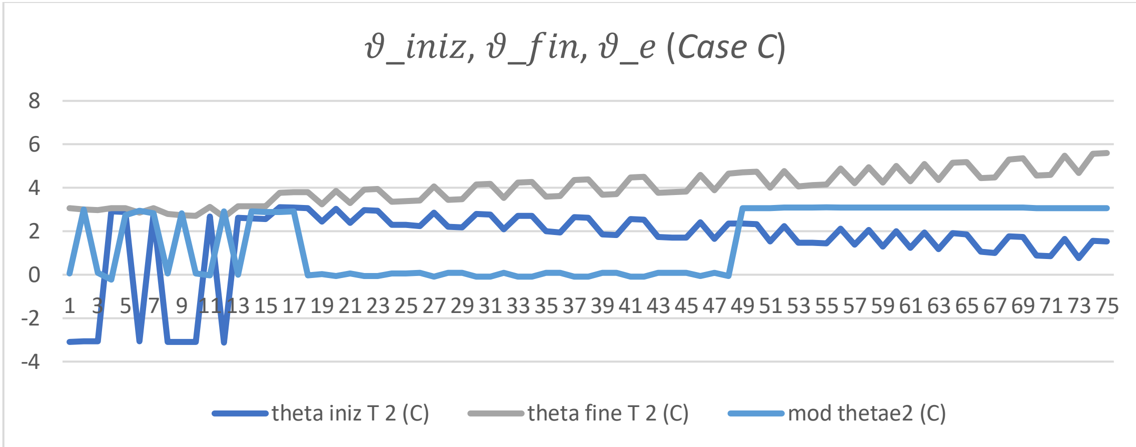

Figure 38. ϑ_iniz, ϑ_fin, ϑ_e for Case C - Aphelion

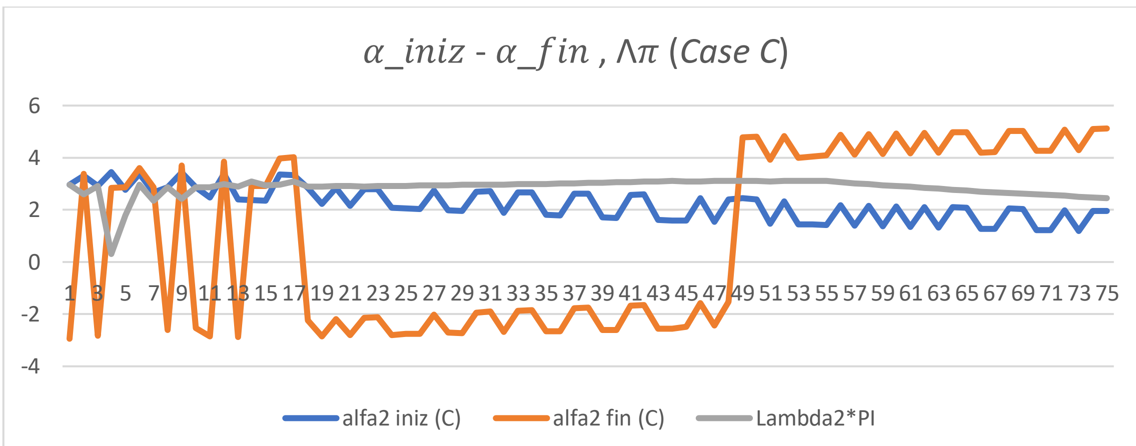

Figure 39. α_iniz - α_fin, $\Lambda\pi$ for Case C - Aphelion

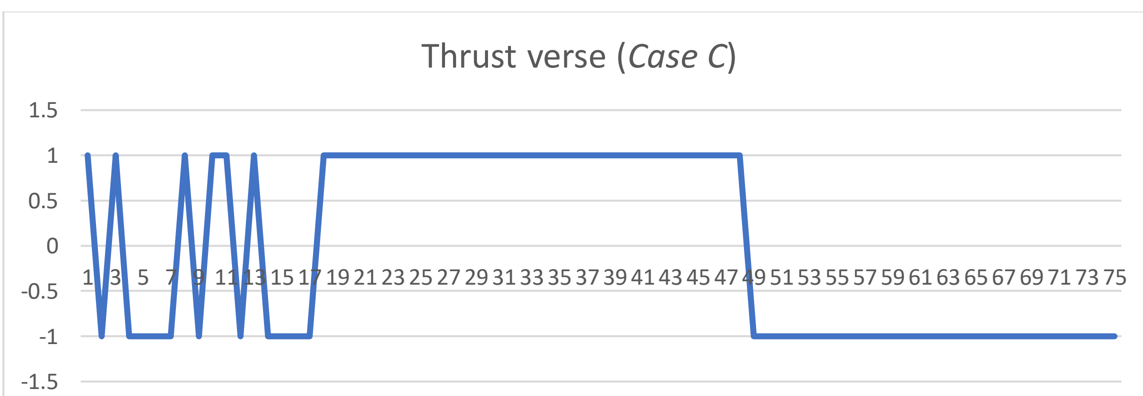

Figure 40. Thrust verse for Case C - Aphelion

The aphelion maneuver is in some ways symmetrical to the perihelion maneuver, and certainly one can have the same kind of discussion here, even if the trends show more fluctuating and less stable values. Even in these graphs there are three reference areas: the first one, very chaotic, in which the values of ϑ_e, α_{fin} and $verse$ oscillate significantly and change from asteroid to asteroid; the second one, in which $verse = 1, \vartheta_e \cong 0, \vartheta_e \notin [\vartheta_{iniz}; \vartheta_{fin}]$ and $\alpha_{fin} < \alpha_{iniz}$ and, in the end, the third one on the right, in which $verse = -1$, $\vartheta_e \cong \pi$ and $\vartheta_{iniz} < \vartheta_e < \vartheta_{fin}$, and of course $\alpha_{fin} > \alpha_{iniz}$. As in perihelion, also in aphelion the expected answer is given by the farthest fictitious asteroids from Earth, but here this result is even more interesting since the thrust is opposite from the direction of advancement, $\Delta a < 0$, the spacecraft has to brake, and the linear control law is $\alpha = \pi + \Lambda(\vartheta - \vartheta_e)$.

These results would seem to show that, with a small-to-null inclination (even because e is very low), the asteroids able to provide an adequate and expected estimation of the theoretical predictions are those distant beyond a certain amount. By separating the perihelion from the ascending node, that is, $\Omega \neq 0$, this distance is reduced, and more asteroids have an accurate output, at the cost of a small increase in consumption. Especially when the line of apsides and the line of nodes are in quadrature ($\Omega = \pi/2$), the perihelion response is accurate for about 50% of the 75 asteroids and the aphelion response for about 33%.

In the next chapter, the *cases* in which i is fixed have been analyzed. Particularly in the last two *cases* studied with $i = 4.5°$ and $i = 6°$, the inclination assumes larger values than those obtained with the linear dependence from eccentricity (but not so high to still adhere to Edelbaum's approximation), and this, together with an obvious but not huge increase in consumption and some oddities in the very first asteroids, improves the overall accuracy of the preliminary estimation.

3. RESULTS WITH FIXED INCLINATION: IMPROVEMENTS AND COSTS

The four cases treated in the previous chapter have in common, as seen, the linear dependence of the inclination on the eccentricity, a very positive factor in terms of consumption especially for the closest fictitious asteroids of the group: the orbits of these asteroids are almost-circular, thus the relation $i = (1/8)e$ suggests an infinitesimal plane change and ΔV and the overall cost are contained.

The responses provided by these *cases* in terms of ϑ_e, Λ, $\Delta\vartheta$ and α_{iniz}-α_{fin} are however unexpected, particularly, precisely for the closest asteroids, although generally acceptable as suboptimal solutions. The aim of this chapter is to analyze the possible improvements and the eventual additional costs of fixing the inclination to a certain value from the very first asteroid and maintaining it for the whole set. The inclination values analyzed for each *case* are the following: $i = 1.5°$, $i = 3°$, $i = 4.5°$ and $i = 6°$. Performing a plane change with an inclination larger than 6° would have probably meant departing too much from one of the fundamental hypotheses of Edelbaum's approximation [6] and, for this reason, invalidating the results obtained and making the estimation method useless.

The answers obtained are first compared between the various *cases* by corresponding inclination values (for example, *A3*, *B3*, *C3*), to study the influence of the RAAN variation as the inclination value increases; only later there are comparisons for each *case* seen but at different inclinations (ex. *A*, *A1.5*, *A3*, *A4.5*, *A6*).

3.1 <u>Perihelion maneuver</u>

3.1.1 $\boldsymbol{i = 1.5°}$

The first fixed inclination value to be treated is $i = 1.5°$. Initially, the graphs of the consumed propellant mass are shown to observe any differences in trends with the cases treated in chapter 2.

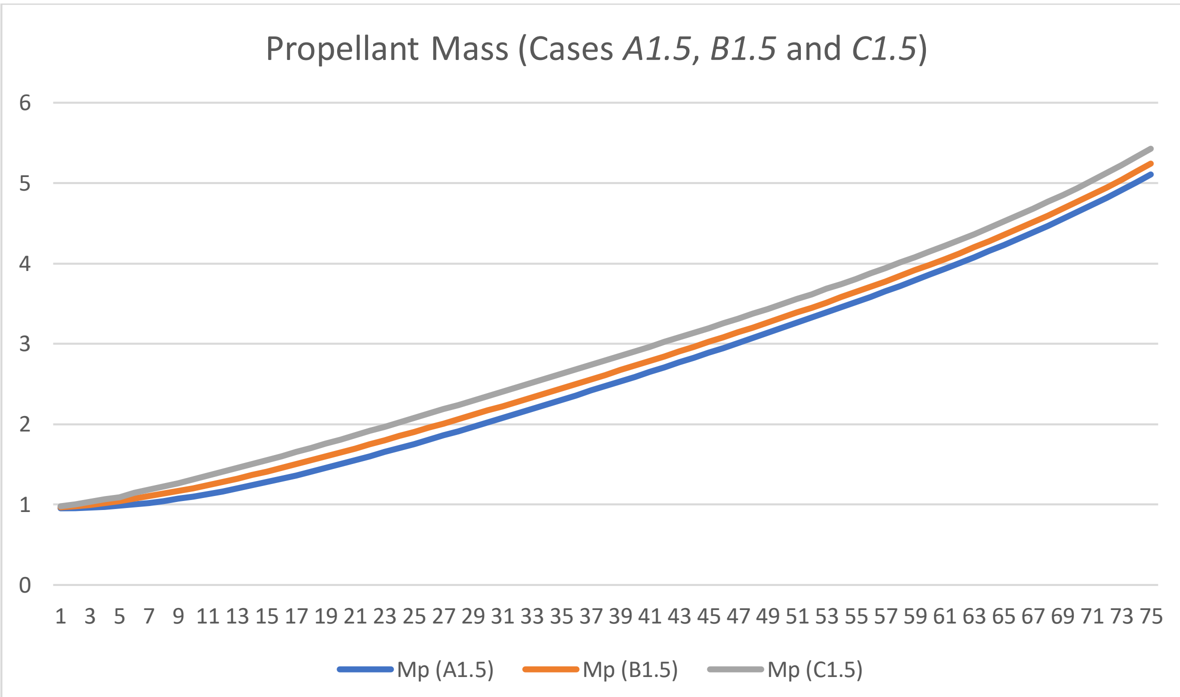

Figure 41. Propellant Mass comparison with i=1.5°

As one can see, the trends in the propellant mass present smoother and less elevated curves than in the *cases* with variable inclination. Going into details, these curves, as shown in few paragraphs, intersect the curves of the cases treated in chapter 2. In fact, taking *cases A* and *A1.5* as examples, the propellant mass consumed for asteroid #2 is $0{,}06363\ kg$ in *case A* and $0{,}954\ kg$ in *case A1.5*, so there is a $6{,}67\%$ increase in consumption and this actually makes it clear that for the closest asteroids the cost of this plane change is slight, but present; instead, the propellant mass consumed for asteroid #76 is $5{,}40704\ kg$ in *case A* and $5{,}10758\ kg$ in *case A1.5*, with a decrease of $5{,}53\%$ with fixed inclinations. This means that the farthest fictious asteroids from Earth perform, with inclination increasing and linearly dependent from eccentricity, a larger plane change than the 1.5° imposed here. Hence it is also easy to guess that the central group of asteroids has almost-similar consumption in these two *cases*. The trends are identical for *cases* B and $B1.5$, C and $C1.5$, and so are the percentage of increase for asteroid #2 (6,64% going from B to $B1.5$, 6,57% going from C to $C1.5$), while the gap widens as regards asteroid #76 ($-11{,}05\%$ going from B to $B1.5$, ($-16{,}59\%$ going from C to $C1.5$). Therefore, fixing the inclination to a low value significantly decreases the propellant consumption as regards the farthest asteroids, especially in *cases* where $\Omega \neq 0$, at the expense of a slight increase in asteroids close to Earth.

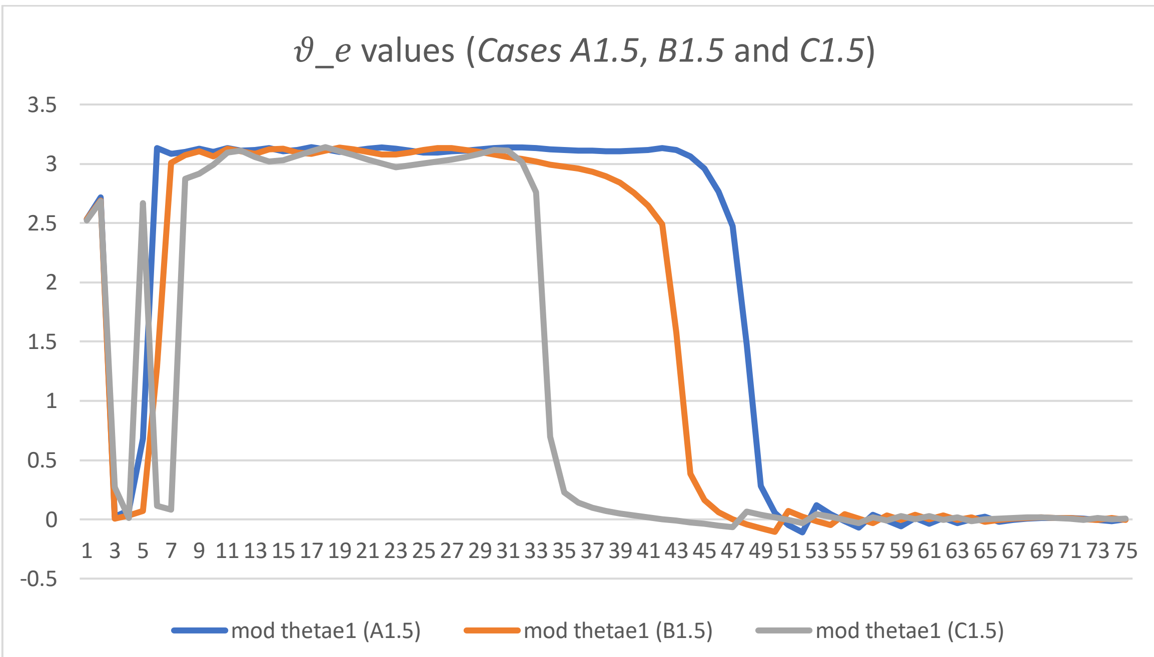

Figure 42. θ_e values comparison with i=1.5° - Perihelion

As one could easily imagine, even the graph of ϑ_e trends for cases $A1.5$, $B1.5$ and $C1.5$ recalls what has been seen in *cases* with variable inclination. Given an initial oscillation caused, as already reported, by the proximity of the two possible solutions, the trends indeed appear very similar to those of the *cases* seen previously: initially, ϑ_e values settle at π, then at a certain asteroid a transition to the expected solution ($\vartheta_e \cong 0$) takes place. Two considerations are particularly interesting: the first one is that the transition occurs “delayed” by 1-2 asteroids with respect to *cases*

A, B and C, and the almost identical answer demonstrates how this low inclination value has little impact on the final response; in the end, in *case C* the transition takes place much earlier than in the other two cases with $i = 1.5°$. Another signal that the quadrature between the perihelion and the ascending node speeds up the transition of the algorithm to the expected solution.

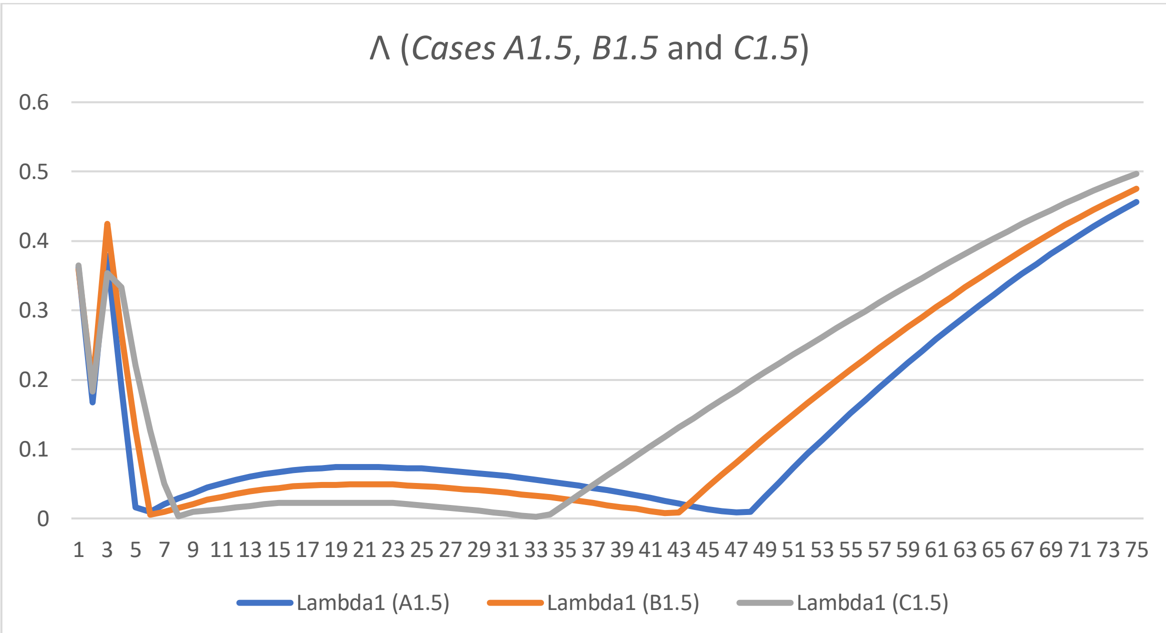

Figure 43. Λ values comparison with i=1.5° - Perihelion

Even the graph with Λ values is quite similar to the graph seen for *cases A*, *B* and *C*. One can easily notice that here too, in correspondence with the section in which $\vartheta_e \cong \pi$, Λ is very low, less than 0,1. Then, approximately at the same asteroids of the transition happened with ϑ_e, Λ starts to increase until values near 0,5 in the same area in which $\vartheta_e \cong 0$. The only difference between the current *cases* and *cases* with variable inclination is the is the very first stretch, where there is a little oscillation probably derived from the ϑ_e response, chaotic and fluctuating. In this area Λ is in a range between about 0,18 and 0,42.

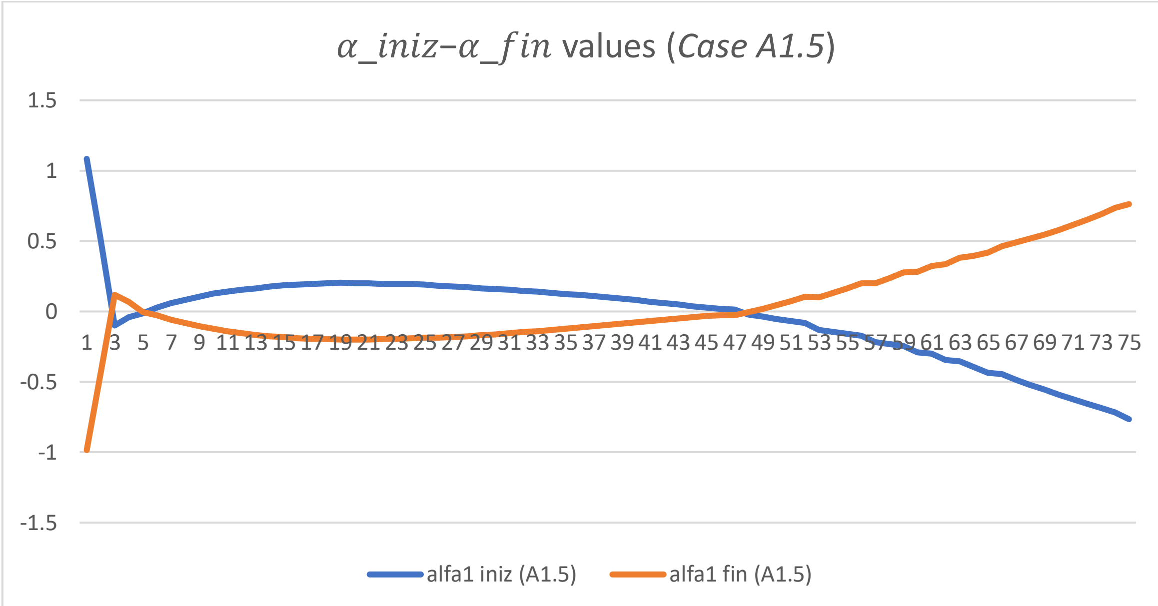

Figure 44. $\alpha\_iniz{-}\alpha\_fin$ values for Case A1.5 – Perihelion

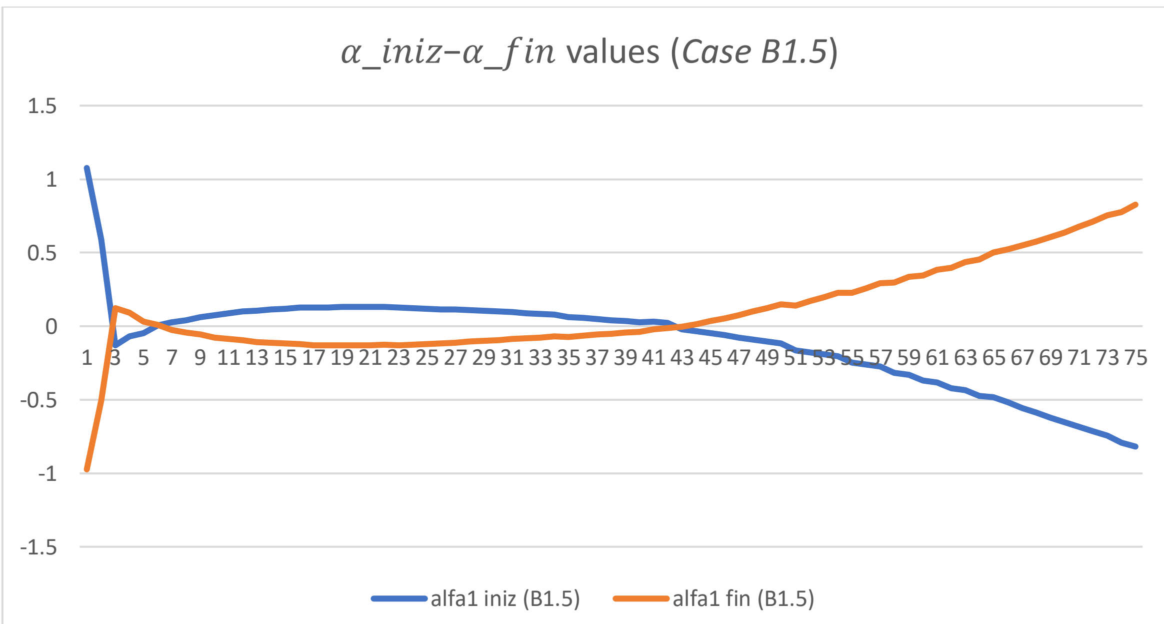

Figure 45. $\alpha\_iniz{-}\alpha\_fin$ values for Case B1.5 – Perihelion

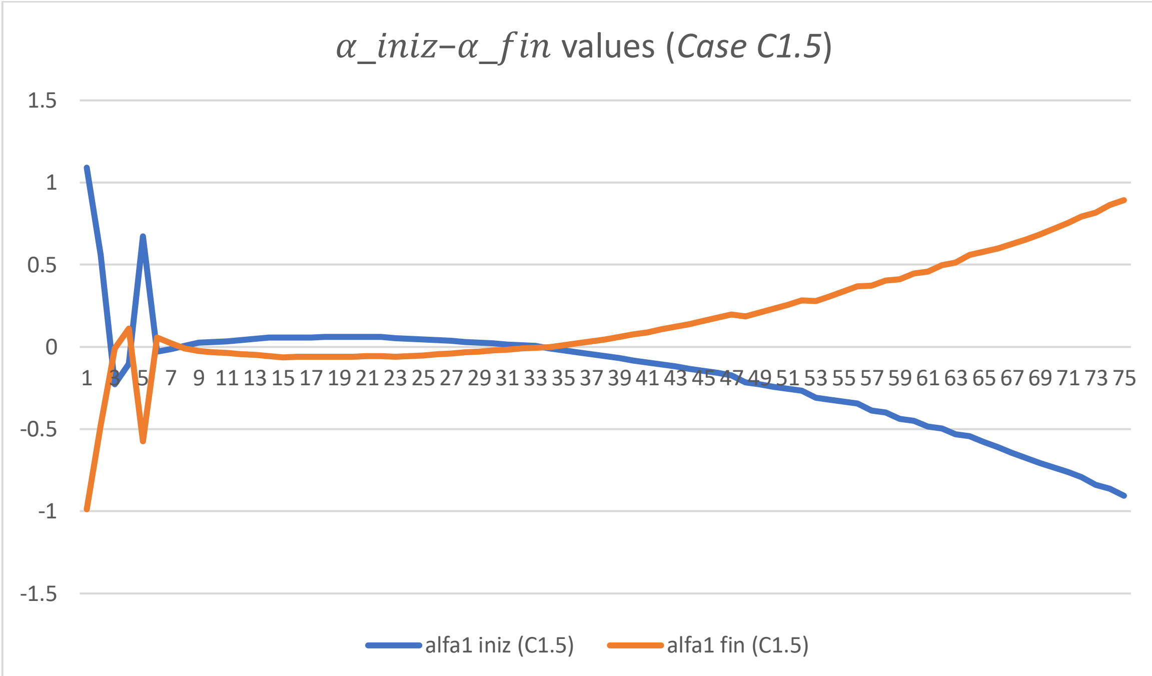

Figure 46. α_iniz–α_fin values for Case C1.5 – Perihelion

The graphs of $\alpha_{iniz} - \alpha_{fin}$ trace those of Λ and ϑ_e, presenting the same subdivision into three zones: the first one, characterized by the random convergence value of the algorithm and therefore with some oddities; the second one, with $\alpha_{fin} < \alpha_{iniz}$, and the last one, with $\alpha_{fin} > \alpha_{iniz}$. Even with this inclination, α in the first two zone is discontinuous, and the code has produced suboptimal responses. As expected, the transition to the foreseen answer occurs in *case C* before the other *cases*.

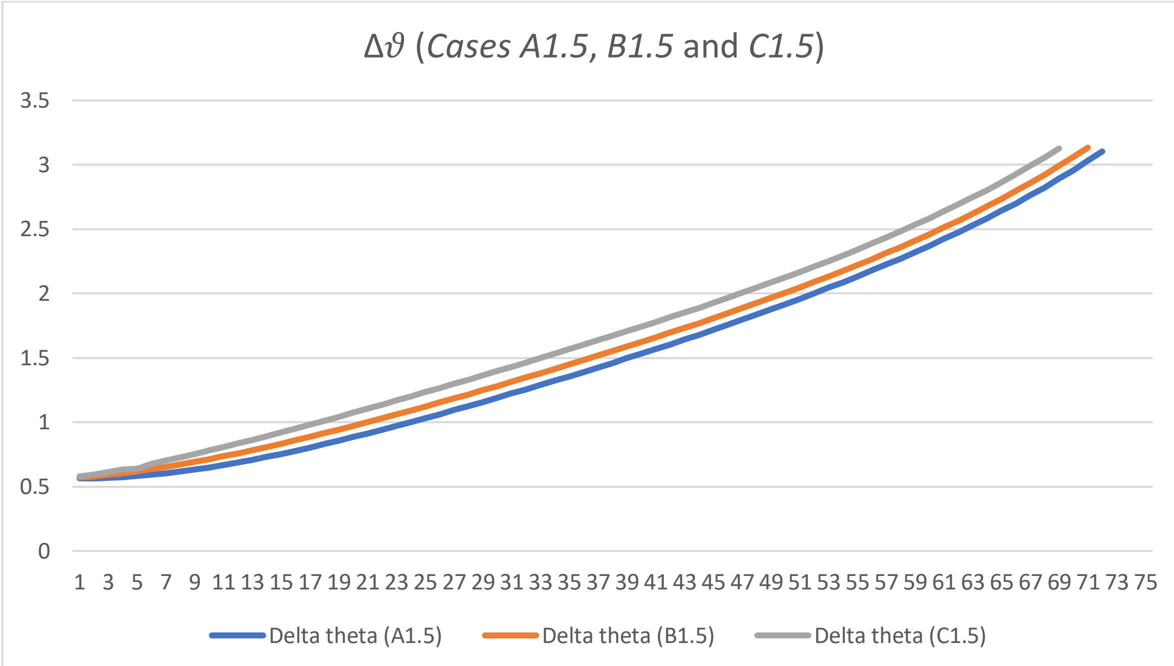

Figure 47. Δϑ values comparison with i=1.5° - Perihelion

In this graph, it is easy to note that the value of the last asteroid before $\Delta\vartheta > \pi$ is very close for all the cases (#69 for *case C1.5*, #71 for *case B1.5* and #72 for *case A1.5*), while in cases A, B and C these values are more widely spaced. It is very interesting to observe that for *case C* ($\Omega = \pi/2$) four more asteroids fall within the hypothesis of validity of the method ($\Delta\vartheta < \pi$), in fact for *case C* the last asteroid is #65. This means perhaps that for *case C* $i = 1.5°$ helps to slightly shorten the burning arcs.

3.1.1.1 The relations between ϑ_e, ϑ_{iniz} and ϑ_{fin}, α_{iniz} and α_{fin}

Descriptive graphs of ϑ_e, ϑ_{iniz} and ϑ_{fin}, α_{iniz} and α_{fin} parameters and their relations are presented below for cases A1.5, B1.5 and C1.5.

Obviously, one must remember that being a perihelion maneuver, the thrust verse is taken for granted and is $verse = 1$.

➢ *Case A1.5*

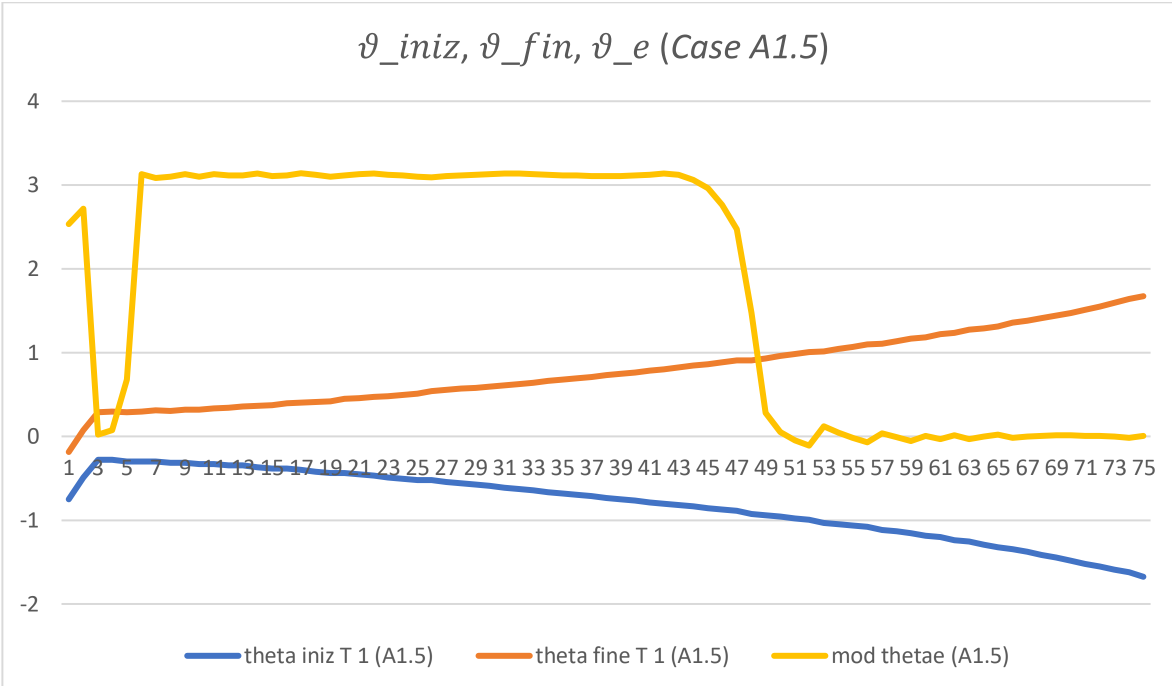

Figure 48. ϑ_iniz, ϑ_fin, ϑ_e values for Cases A1.5 – Perihelion

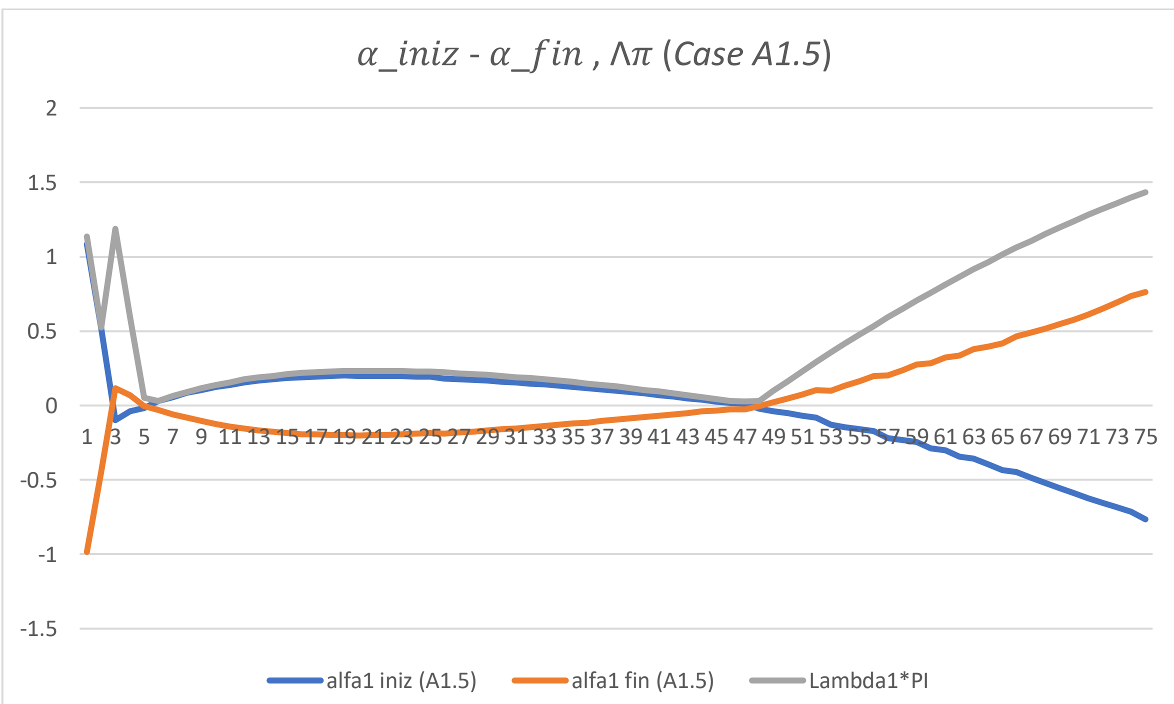

Figure 49. α_iniz - α_fin, $\Lambda\pi$ values for Case A1.5 – Perihelion

- *Case B1.5*

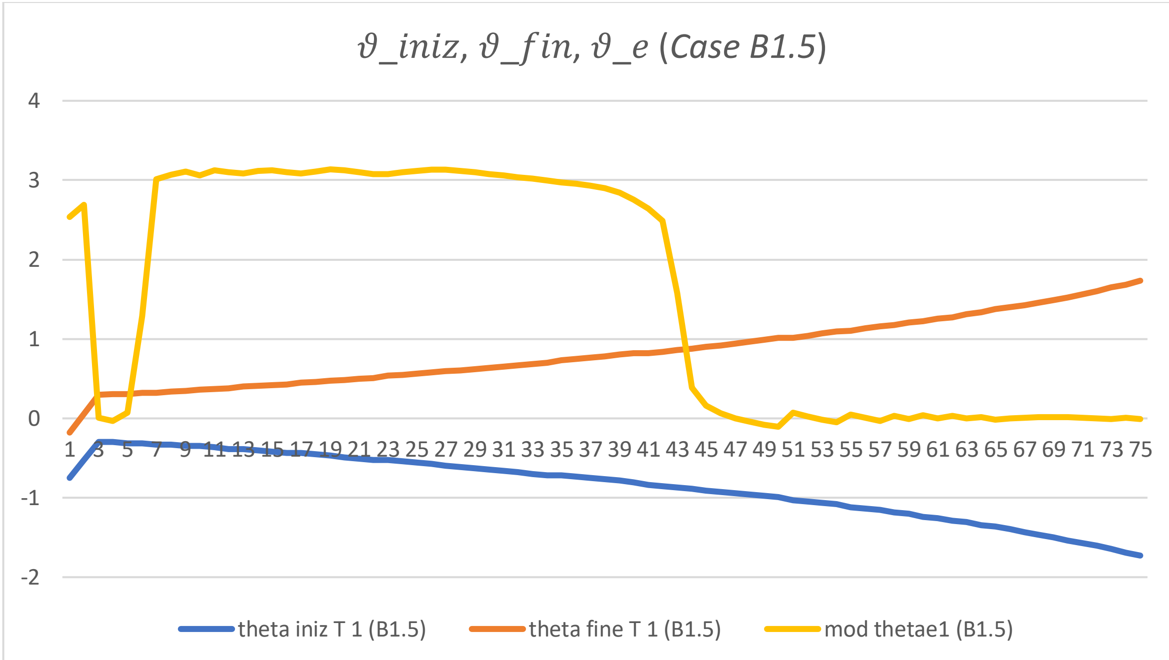

Figure 50. $\vartheta\_iniz, \vartheta\_fin, \vartheta\_e$ values for Cases B1.5 – Perihelion

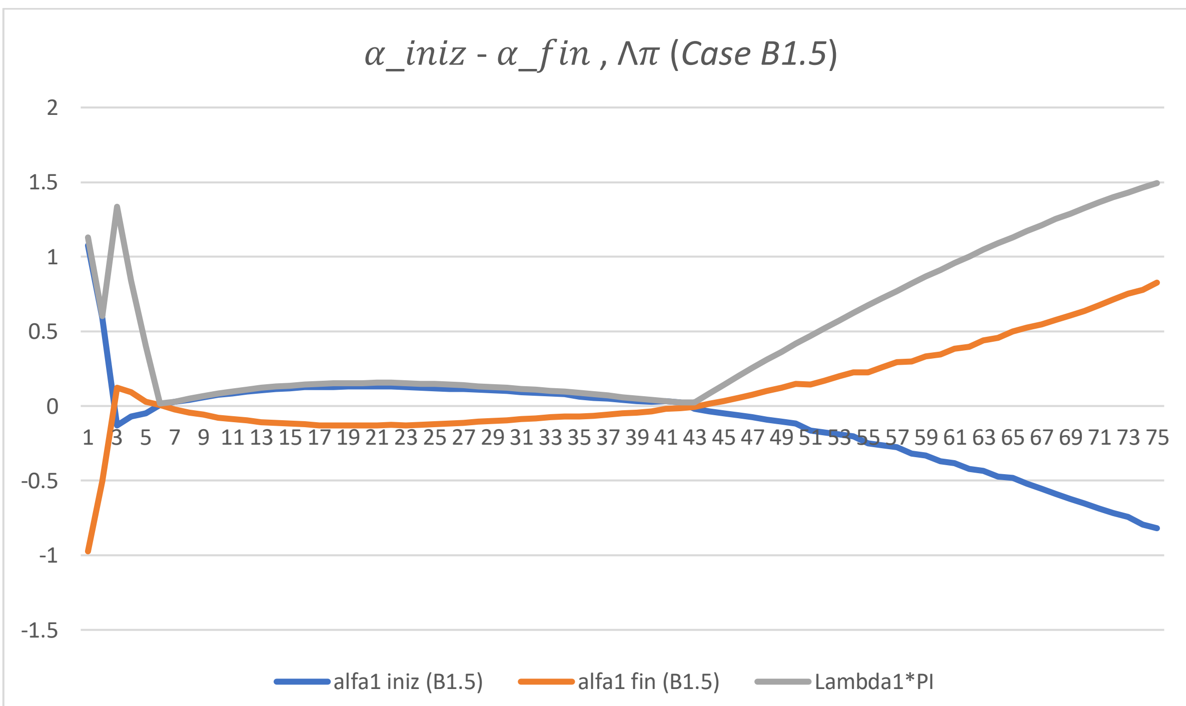

Figure 51. α_iniz - α_fin, $\Lambda\pi$ values for Case B1.5 – Perihelion

- *Case C1.5*

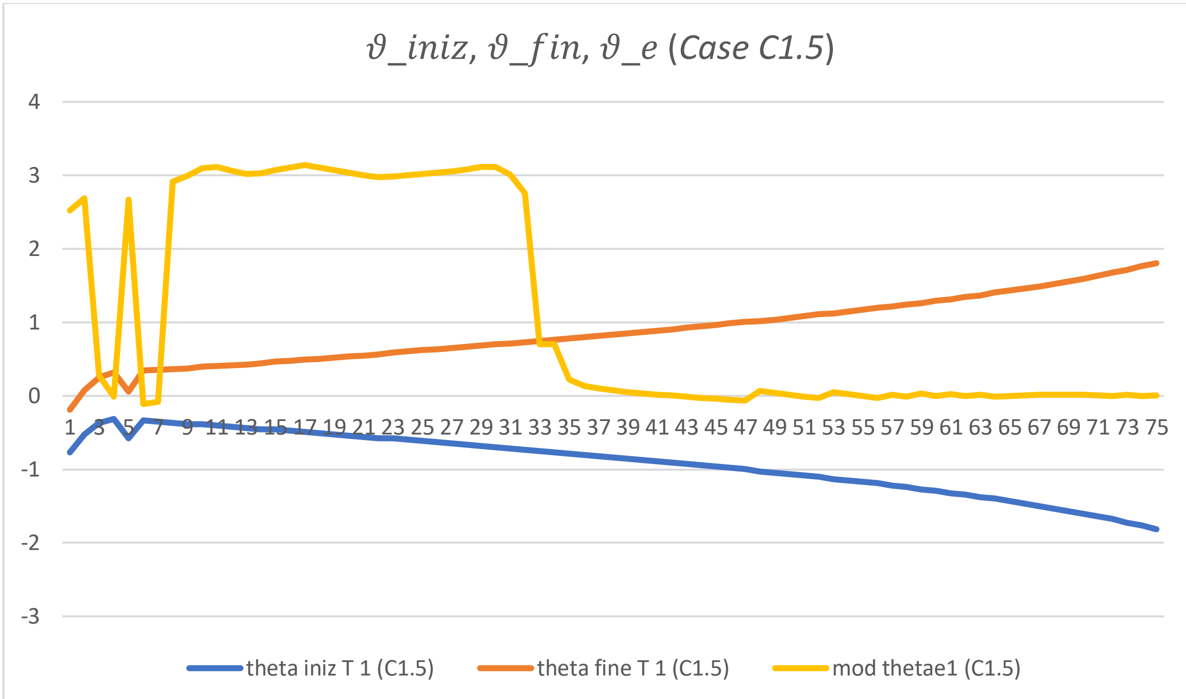

Figure 52. $\vartheta\_iniz, \vartheta\_fin, \vartheta\_e$ values for Cases C1.5 – Perihelion

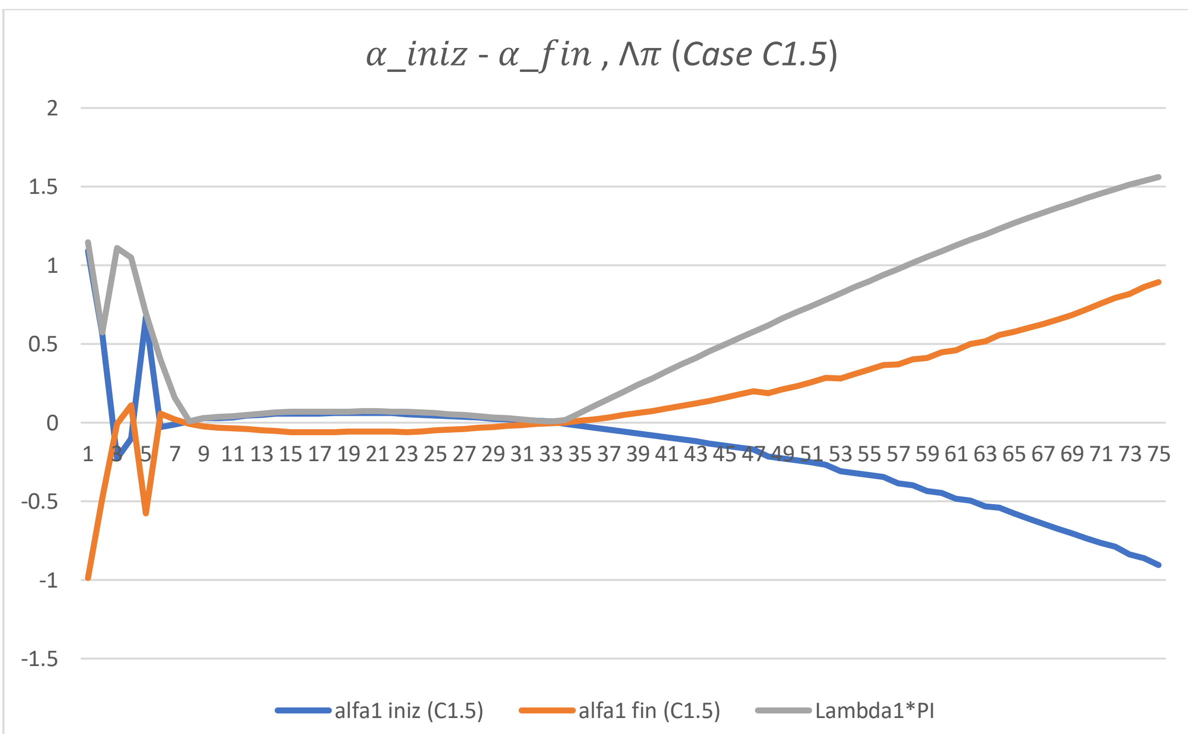

Figure 53. α_iniz - α_fin, $\Lambda\pi$ values for Case C1.5 – Perihelion

As expected, it can be observed that the situation for these *cases* with $i = 1.5°$ is similar to what has been described for *cases* with variable inclination, and the only difference is represented once again by the fluctuating values in the first area of the graph in which something unclear happens. Even with this inclination, in the first zone and in the zone in which $\alpha_{fin} < \alpha_{iniz}$, the trend of α is discontinuous and the same: it starts from α_{iniz} and goes until $\Lambda\pi$, then restarts from $-\Lambda\pi$ and proceeds until α_{fin}.

3.1.2 $i = 3°$

The next cases treated are those with $i = 3°$. Even here, the first interesting thing to notice is in the graph of the propellant mass consumed.

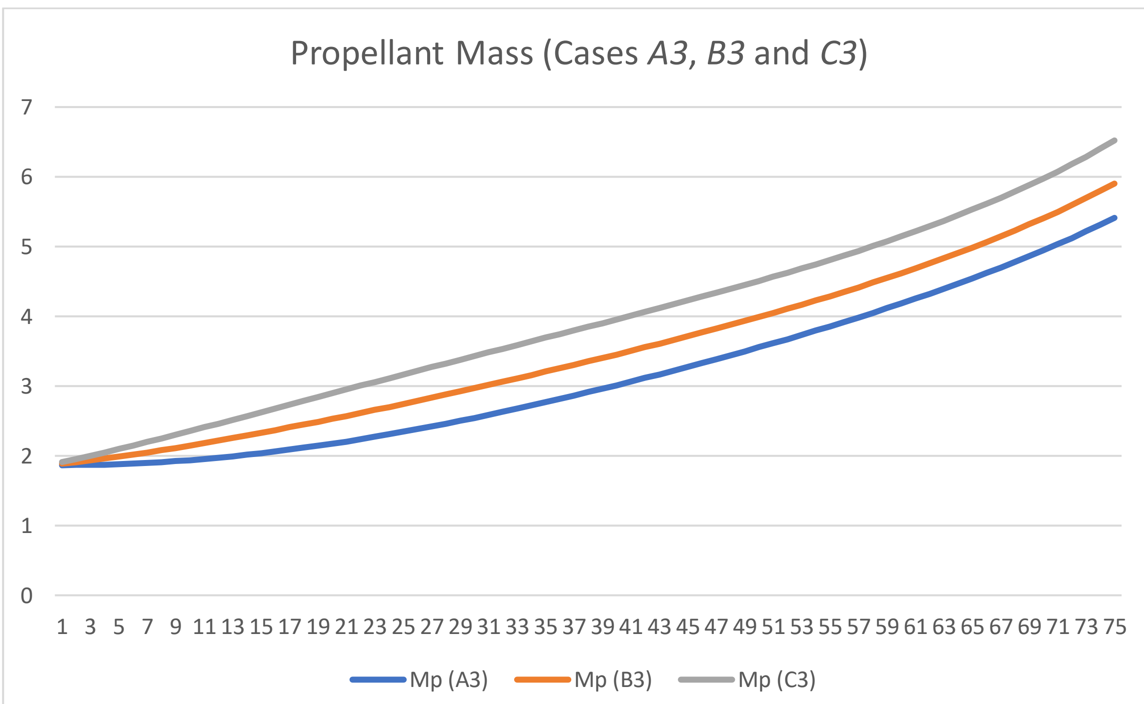

Figure 54. Propellant Mass comparison with i=3°

Trivially, consumption goes up in all *cases*, but unexpectedly, not all along the set of asteroids. In fact, the increase is tangible particularly for the closest asteroids: all *cases* with $i = 3°$ burn nearly twice the propellant with respect to the *cases* with $i = 1.5°$ and almost 30 times the propellant consumed in the *cases* with variable inclination (1,86375 kg, 1,88785 kg and 1,91022 kg respectively in *cases A3*, *B3* and *C3* for asteroid #2). But moving toward the farthest asteroids from Earth, this substantial difference becomes very thin with cases A1.5, B1.5 and C1.5 (5,41121 kg, 5,90279 kg and 6,5211 kg respectively in *cases A3*, *B3* and *C3* for asteroid #76) and almost zeroes completely with respect to *cases A*, *B* and *C*, with a deviation of approximately 1% of the values. If the final consumption values of *cases* with $i = 3°$ and *cases* with variable inclination are almost identical, then one can say that the inclination values reached with the relation $i = (1/8)e$ for the farthest asteroids are very close to or equal to 3°.

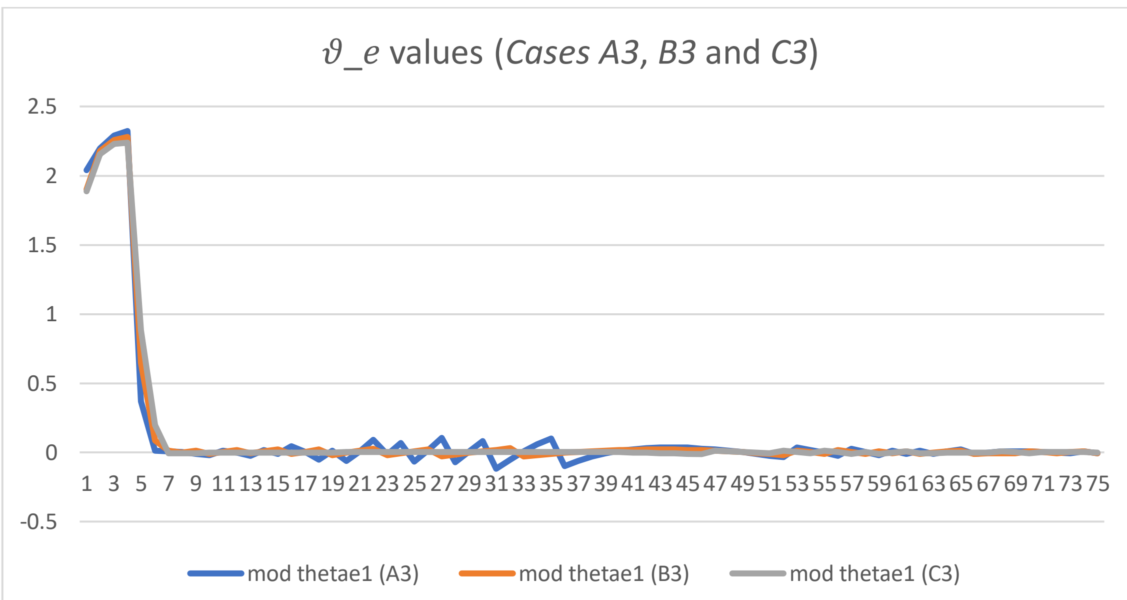

Figure 55. ϑ_e values comparison with i=3° - Perihelion

This is a perihelion maneuver, so $verse = 1$ and ϑ_e should be in a range of 0. As it easily observable, except for an initial subgroup of about 5 asteroids, the whole set of the fictitious asteroids presents the solutions predicted by the theory. Therefore, having further increased the inclination value by 1.5° helps the algorithm to choose among the possible answers the one foreseen by the theoretical studies.

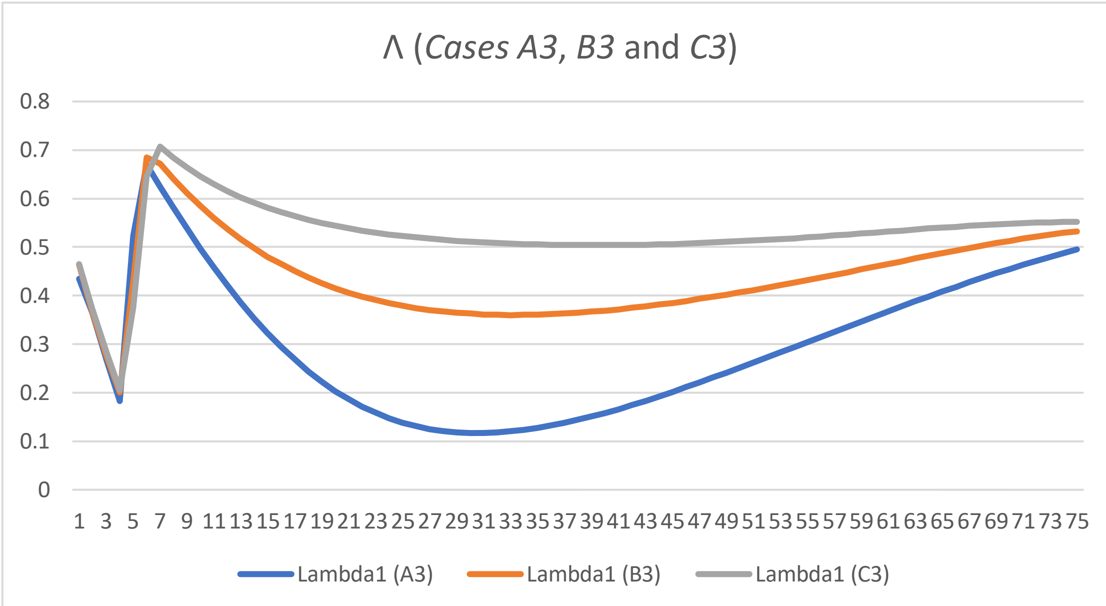

Figure 56. Λ values comparison with i=3° - Perihelion

Λ demonstrates also with this inclination value that has a quite strange behavior with respect to ϑ_e, but pretty much acceptable: when ϑ_e presents some oddities, in the very first zone, Λ assumes quite low values, less than 0,5; then a rapid transition brings the values close to 0,7, value from which begins to descend with different slopes for the various *cases*, to finally settle down in a range between 0,49 (*case A3* value) and 0,55 (*case C3* value). Λ could perhaps be the only parameter, together of course with propellant mass consumed, to be negatively affected by the raise of inclination. More exhaustive considerations are reported in the next paragraphs, where *cases* with $i = 4.5°$ and $i = 6°$ are dealt with.

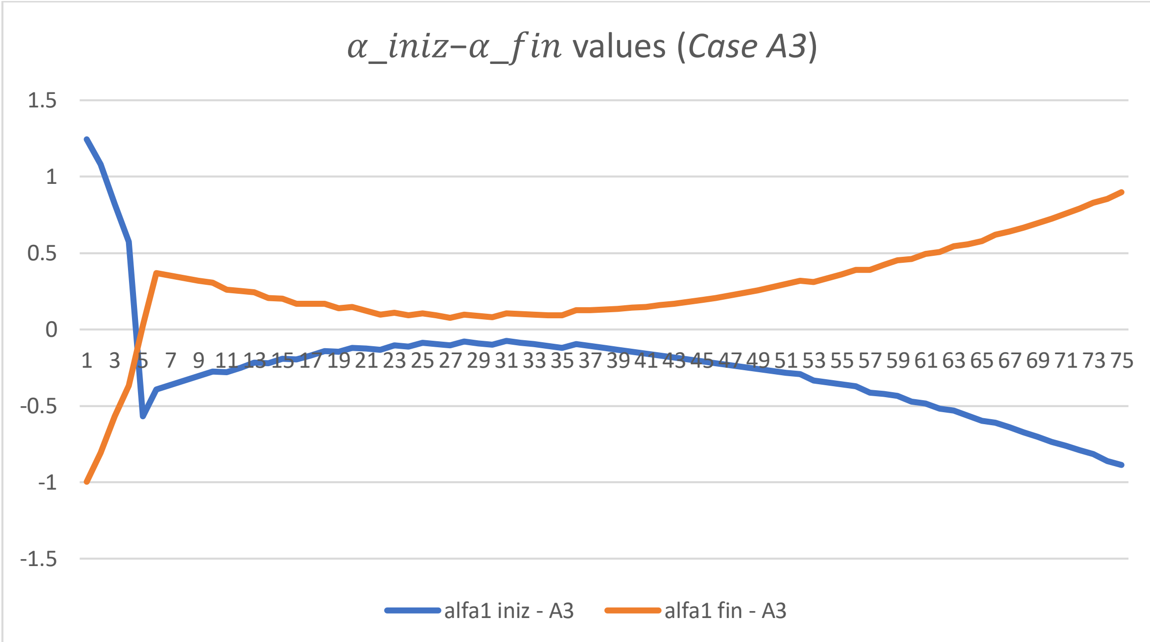

Figure 57. $\alpha\_iniz{-}\alpha\_fin$ values for Case A3 – Perihelion

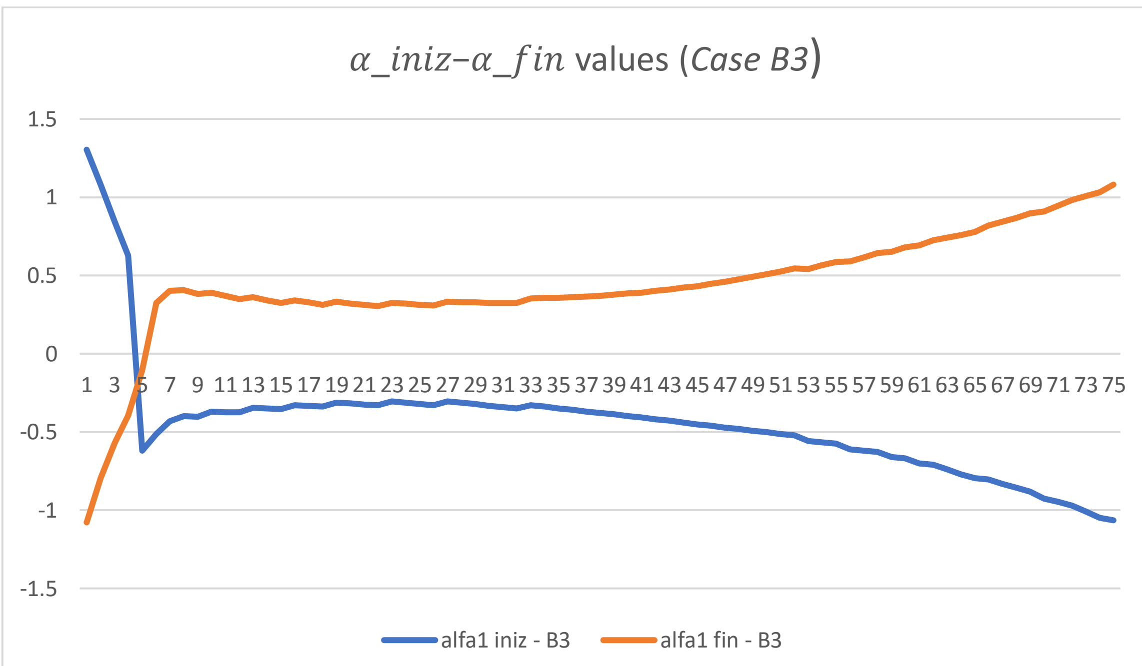

Figure 58. $\alpha\_iniz{-}\alpha\_fin$ values for Case B3 – Perihelion

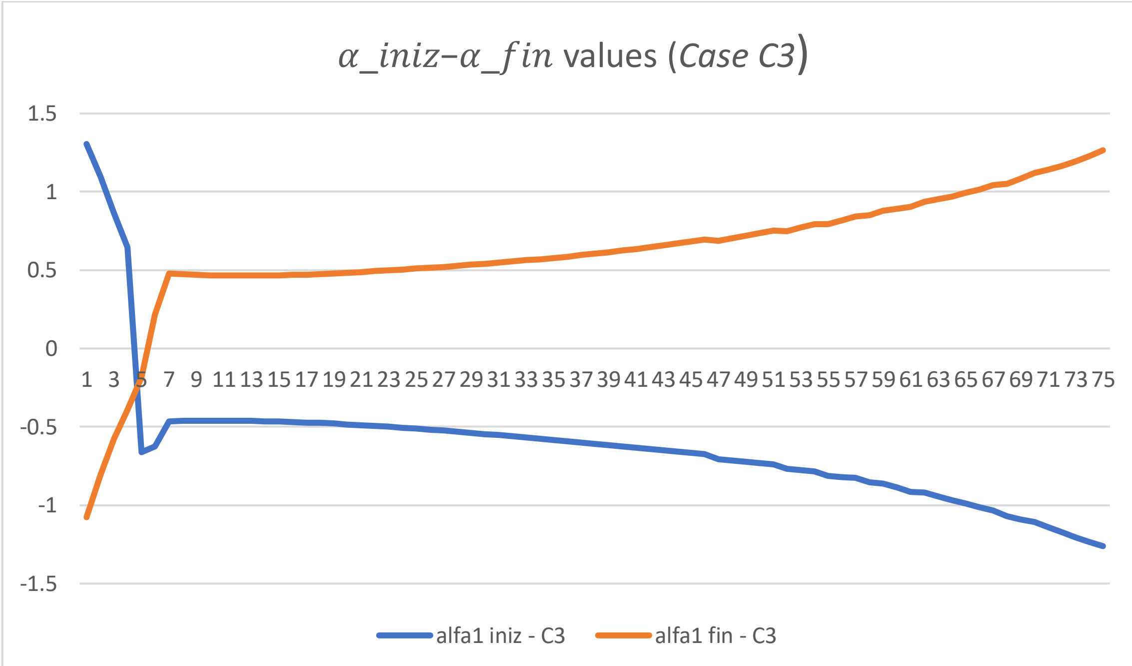

Figure 59. α_iniz–α_fin values for Case C3 – Perihelion

The $\alpha_{iniz} - \alpha_{fin}$ graph is the consequence of what has been seen regarding ϑ_e and Λ. In fact, expect for the first zone, even these parameters return the expected solution, in which $\alpha_{fin} > \alpha_{iniz}$. It is interesting to observe that the distance between α_{iniz} and α_{fin} widens going towards the farthest asteroids, and this suggest that the burn arc angular lengths still grow.

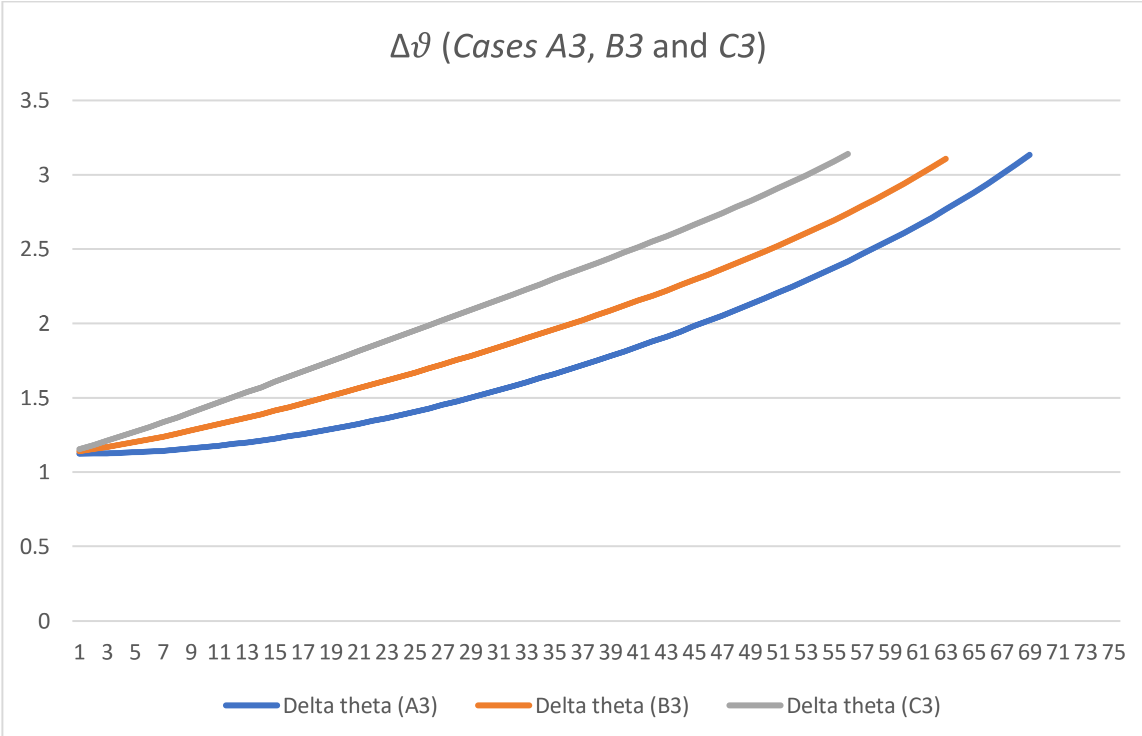

Figure 60. Δϑ values comparison with i=3° - Perihelion

The raise of inclination is highly tangible as regards the cases in which $\Omega \neq 0$. For *case A3*, the last asteroid where $\Delta\vartheta < \pi$ is indeed asteroid #69, not so much different from asteroid #72 for *case A1.5*; for *cases B3* and *C3*, instead, the last asteroids to fall within the hypothesis of validity of the method are respectively asteroids #63 and #56, unlike the *cases B1.5* and *C1.5* (#71 and #69). Hence, it is reasonable to expect that in the next *cases*, where the inclination is further raised, these trends (especially *case C*) tend to move rapidly to the right of the graphs.

3.1.2.1 The relations between ϑ_e, ϑ_{iniz} and ϑ_{fin}, α_{iniz} and α_{fin}

The relations between the fundamental parameters of the estimation method reveal what has already been understood in the previous paragraph, namely that this inclination value makes the algorithm choose the solution foreseen by the theory.

➢ *Caso A3*

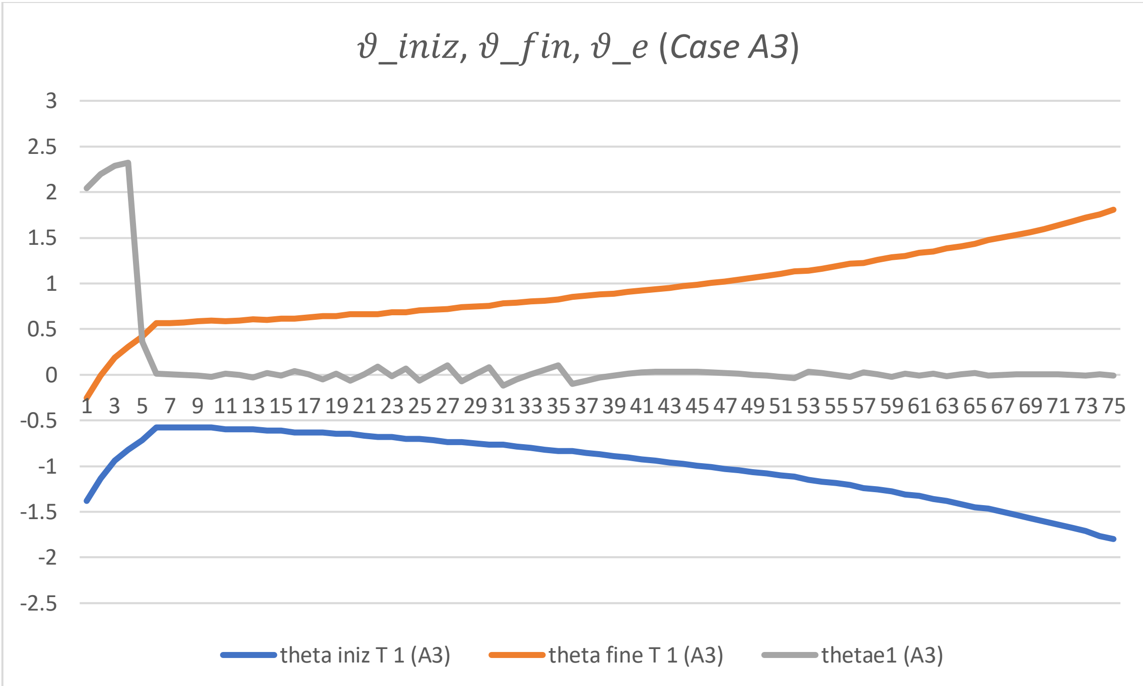

Figure 61. ϑ_iniz, ϑ_fin, ϑ_e values for Case A3 – Perihelion

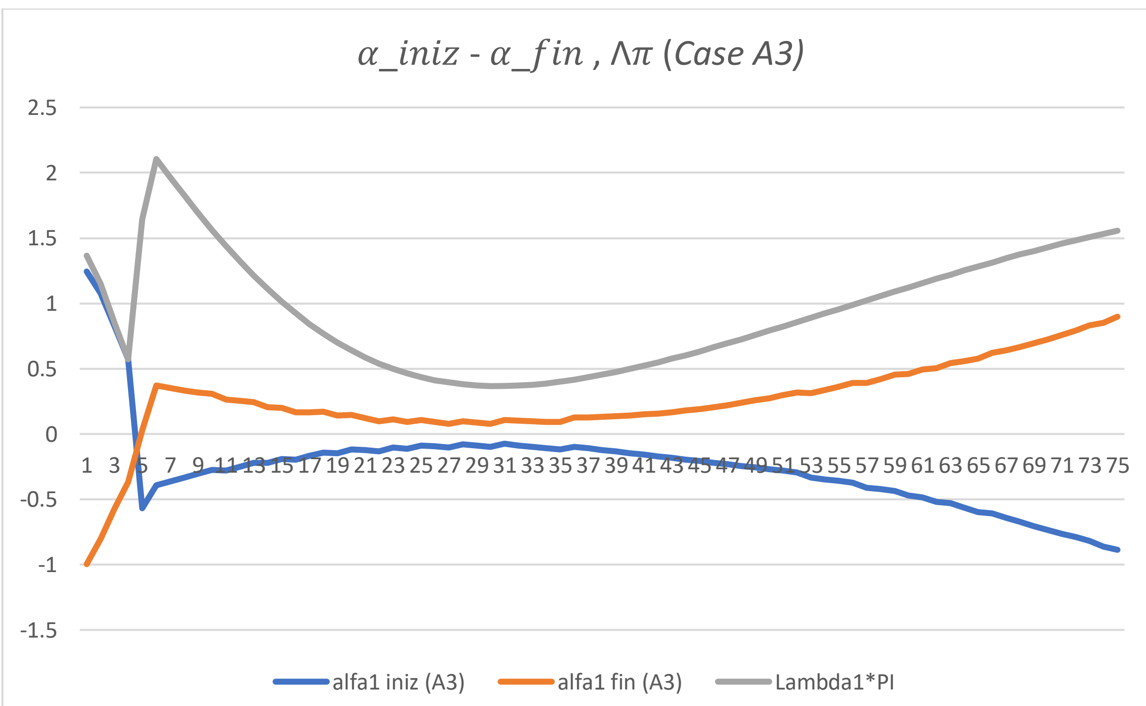

Figure 62. α_iniz - α_fin, $\Lambda\pi$ for Case A3 – Perihelion

➢ *Case B3*

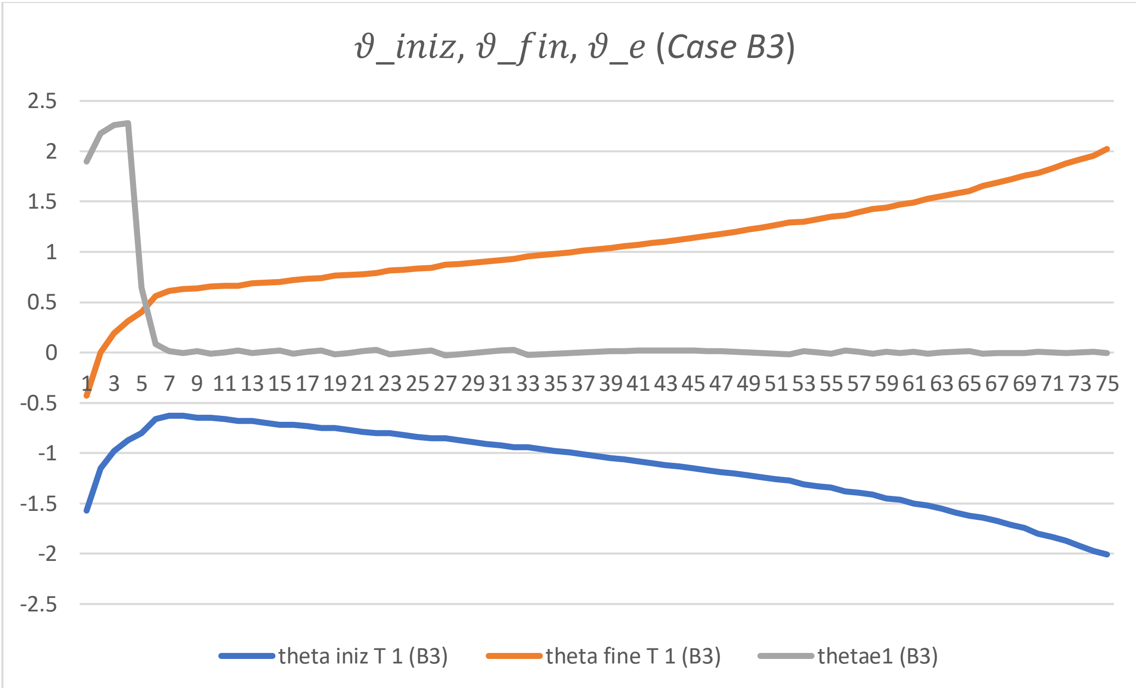

Figure 63. ϑ_iniz, ϑ_fin, ϑ_e for Case B3 – Perihelion

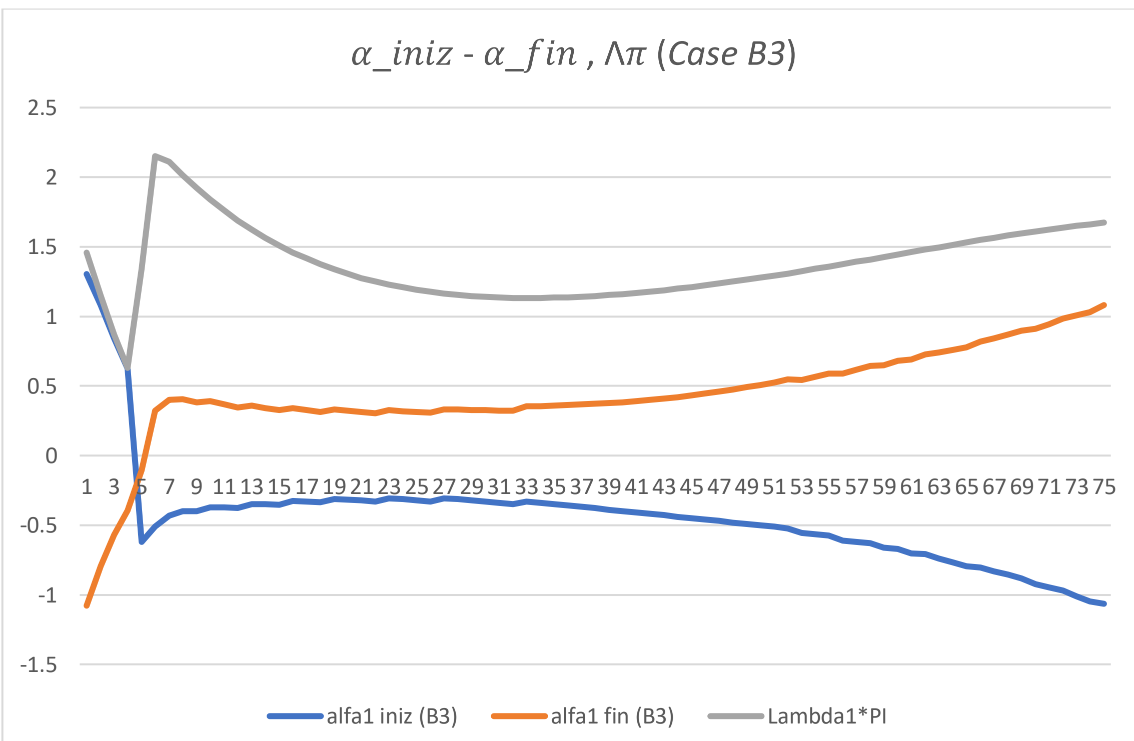

Figure 64. α_iniz - α_fin, $\Lambda\pi$ values for Case B3 – Perihelion

➢ Case C3

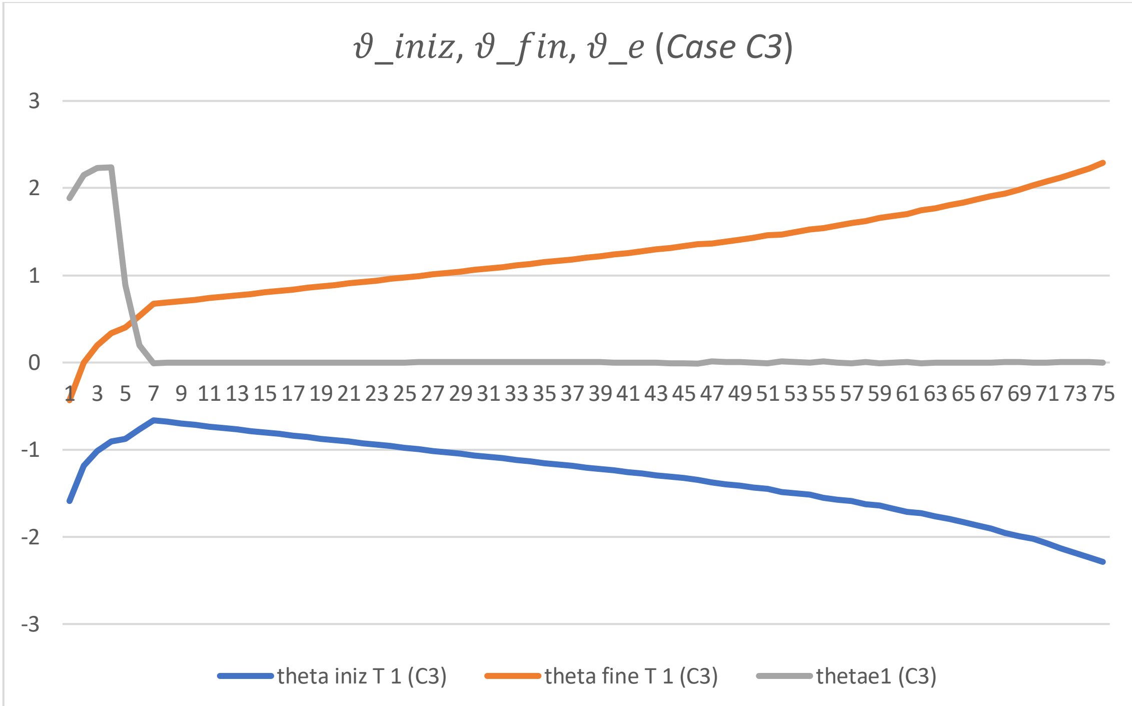

Figure 65. $\vartheta\_iniz, \vartheta\_fin, \vartheta\_e$ values for Case C3 – Perihelion

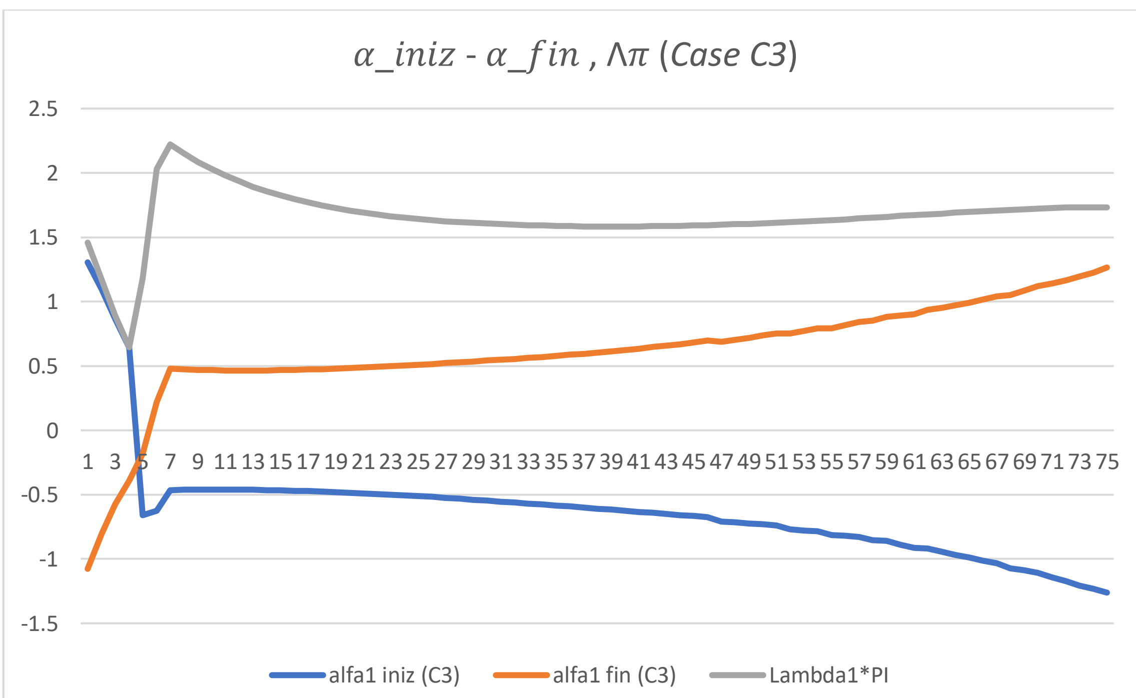

Figure 66. α_iniz - α_fin, $\Lambda\pi$ values for Case C3 – Perihelion

For all three *cases*, there are the initial area on the right of about 5 asteroids, in which $\vartheta_e \notin [\vartheta_{iniz}; \vartheta_{fin}]$ and α is discontinuous ($\alpha_{fin} < \alpha_{iniz}$), and the rest of the set where the expected solution is clearly visible and α is continuous and quite far from the asymptotic value $\Lambda\pi$ (particularly with $\Omega \neq 0$). So, with $i = 3°$ one has both an increase in consumption (at least for the first group of asteroids) and an early transition to the expected answers in terms of ϑ_e, Λ and $\alpha_{iniz} - \alpha_{fin}$.

3.1.3 $\boldsymbol{i = 4.5°}$

It is possible to observe what happens if the inclination is further increased and its value reaches $i = 4.5°$. First comment is obviously on the propellant mass.

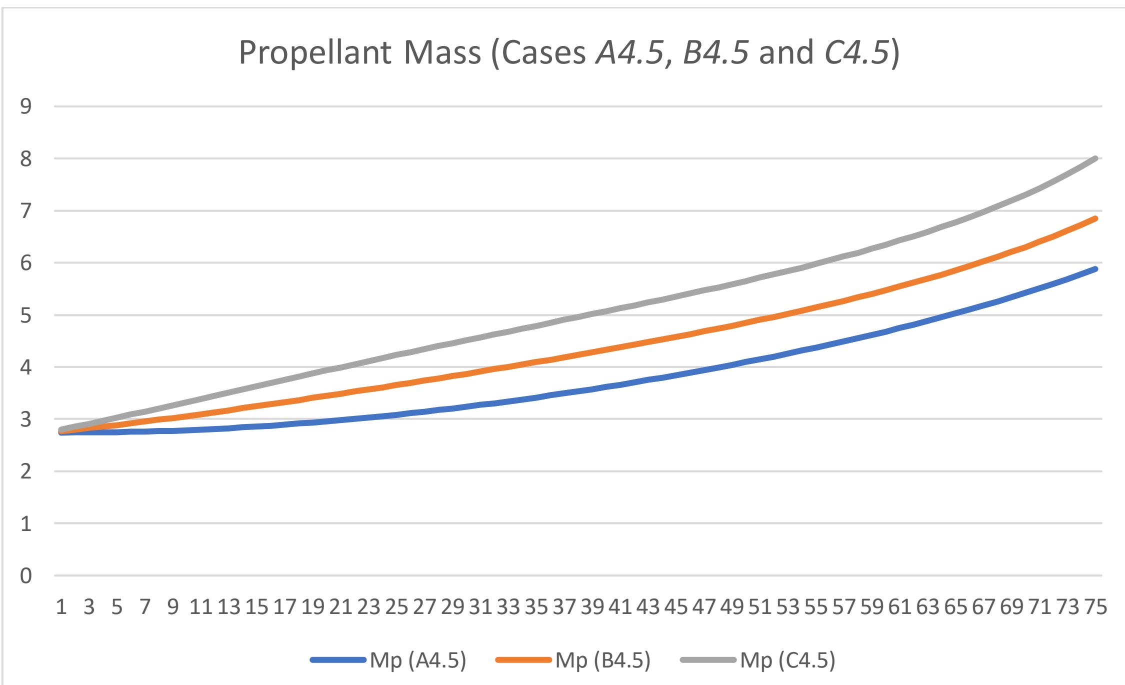

Figure 67. Propellant Mass comparison with i=4.5°

As it is normal, the propellant mass consumed still increases in all three *cases* following the rise of the inclination, and this time it is completely above the trends of the respective fuel masses seen in the previous *cases*. The increase is palpable already from asteroid #2: consumption in cases with $i = 4.5°$ exceeds the corresponding in cases with $i = 3°$ by 47% as regards *cases A4.5* and *A3*, 46,6% as regards *cases B4.5* and *B3*, 46,5% as regards *cases C4.5* and *C3*. Once again, the larger required changes in orbital elements imposes in *cases* with $\Omega \neq 0$ affect the results as one moves farther away from Earth, hence for the final asteroids. Regarding asteroid #76, there is a growth in consumption percentage of 8,66% going from *A3* to *A4.5*, of 16% going from *B3* to *B4.5* and of 22,7% going from *C3* to *C4.5* (consuming in the latter 8,00152 kg when $\Omega = \pi/2$).

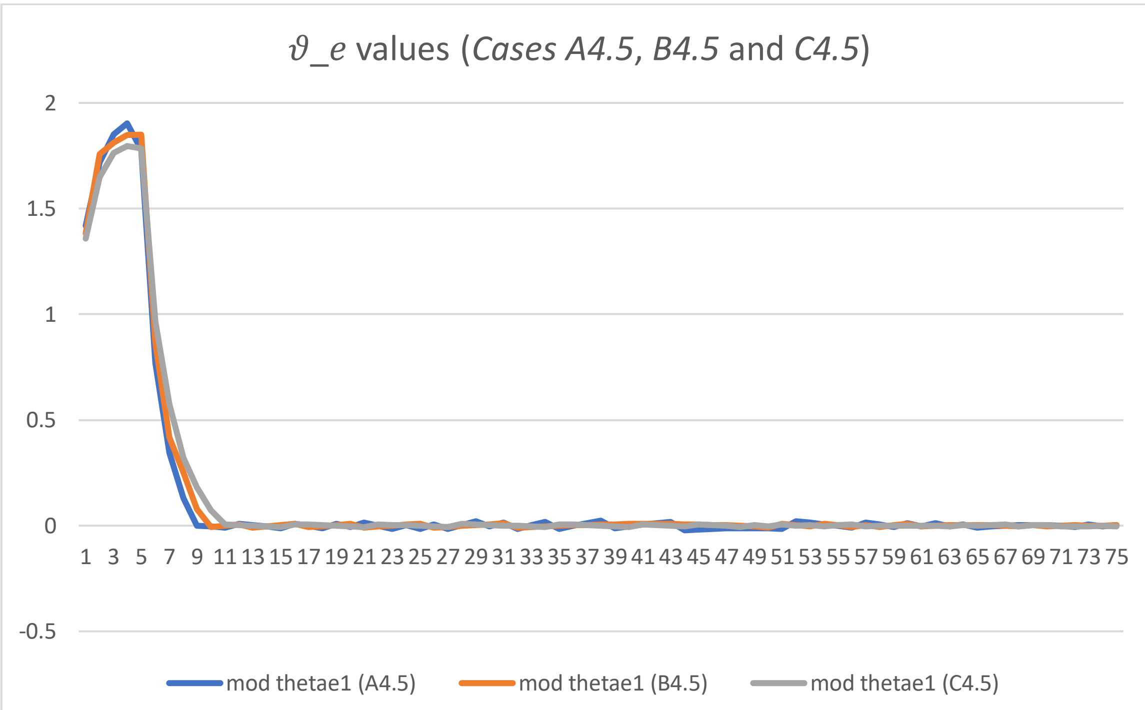

Figure 68. ϑ_e values comparison with i=4.5° - Perihelion

The trends of ϑ_e are almost identical to what has been seen for *cases* with $i = 3°$, and here more than in the previous *cases* these trends are so similar that they can be confused with each other. There is an initial subgroup of asteroids in which ϑ_e are far from 0; the first value is close to $1{,}35 - 1{,}40\ rad$, it arrives to $1{,}78 - 1{,}90\ rad$ and then decreases and is in the range of 0. Two small differences between these *cases* and *cases* with $i = 3°$ are now reported: firstly, the transition here takes place at asteroid #9 for case A4.5 and at asteroid #10 for cases B4.5 and C4.5 (remember that a value is considered in a range of 0 or in the closest range of 0 if it is less than 0,2), hence "delayed" by a few asteroids with respect to the transition for *cases A3*, *B3* and *C3*, occurred for each *case* after 5 asteroids (and so at asteroid #6); secondly, while the *cases B3*, *C3*, *B4.5* and *C4.5* have the same trends in the zone where the expected solution is present, *case A3* has some small fluctuation (which in any case do not destabilize the results) that almost completely disappear in case *A4.5*.

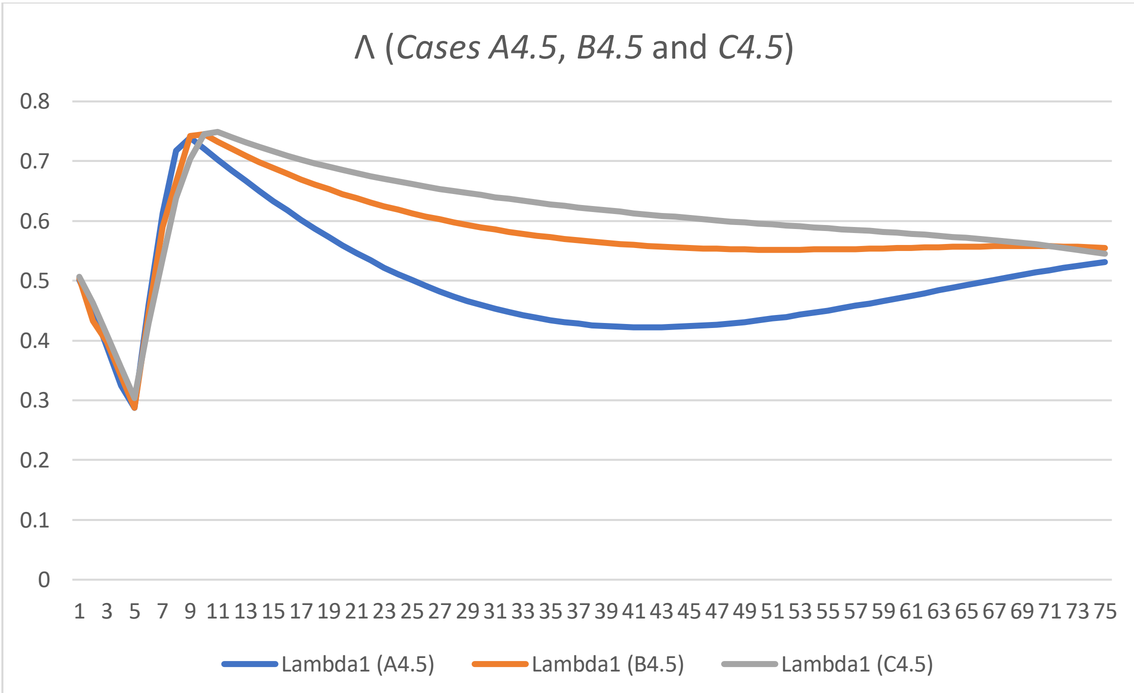

Figure 69. Λ values comparison for i=4.5° - Perihelion

Even for this parameter, the trends recall the behavior of Λ in cases *A3*, *B3* and *C3*, but there are differences that cannot be ignored and begin to clarify the influence of inclination on Λ. In fact, initially the value reaches about 0,3 (and not about 0,2 as in cases with $i = 3°$), it arrives to a value between 0,7 and 0,8 and then assumes a decreasing trend until it reaches a value between 0,5 and 0,6. As it is easy to note, the trend from about asteroid #10 until asteroid #76 are no longer so far apart, and this means that for each case Λ values has risen on average (it should be noted how the very pronounced curve that distinguishes *case A3* is now much higher in *case A4.5*). The only current case in which Λ value for asteroid #76 is lower than in the case with $i = 3°$ is *case C4.5*; this may suggest that the quadrature between the line of apsides and the line of nodes is capable of mitigating, at least for the farthest asteroids from Earth, the effect of inclination on this parameter.

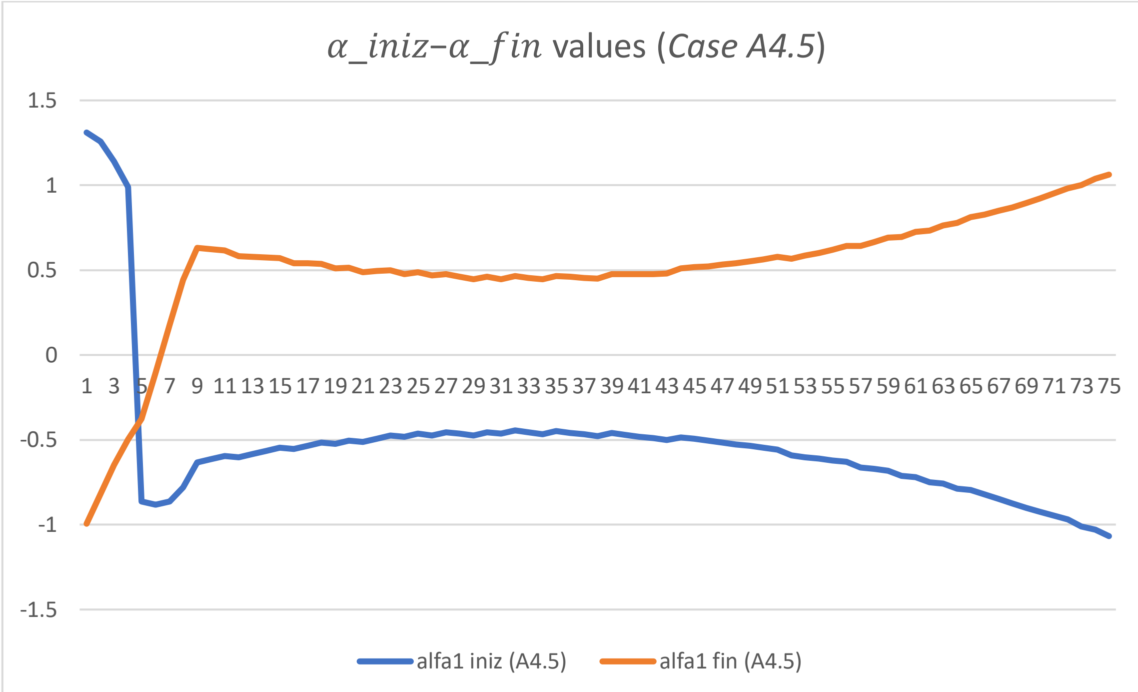

Figure 70. $\alpha\_iniz-\alpha\_fin$ values for Case A4.5 - Perihelion

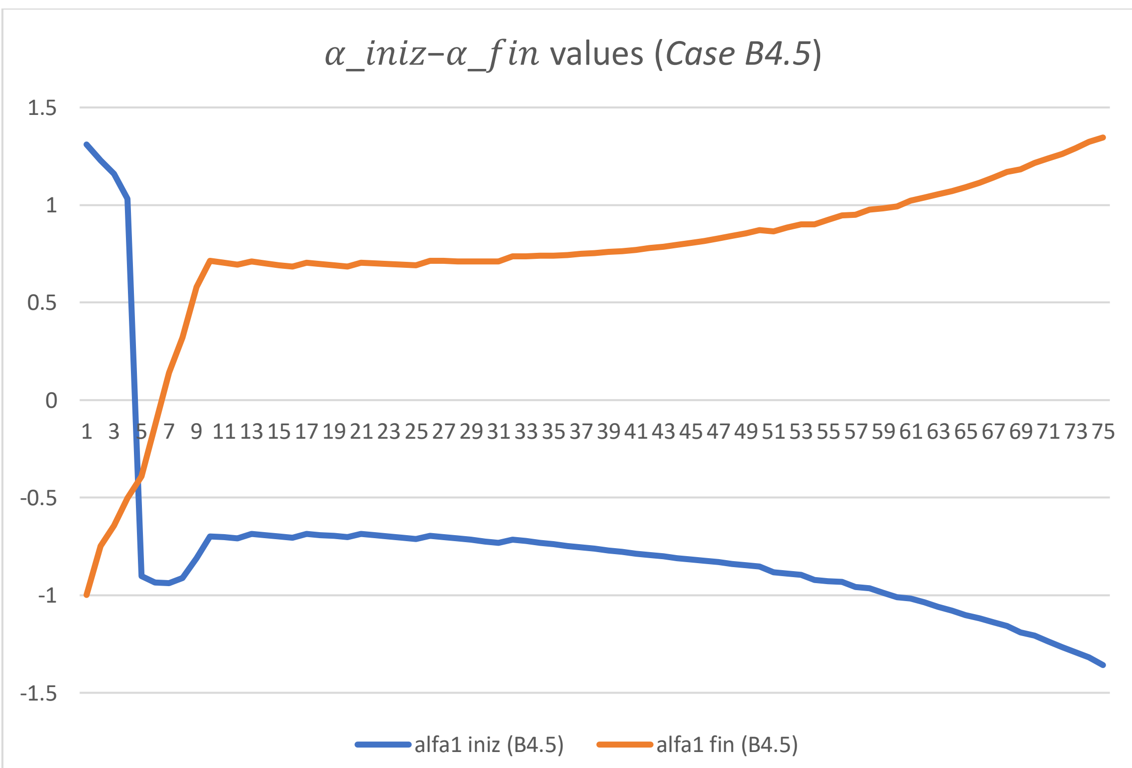

Figure 71. $\alpha\_iniz-\alpha\_fin$ values for Case B4.5 - Perihelion

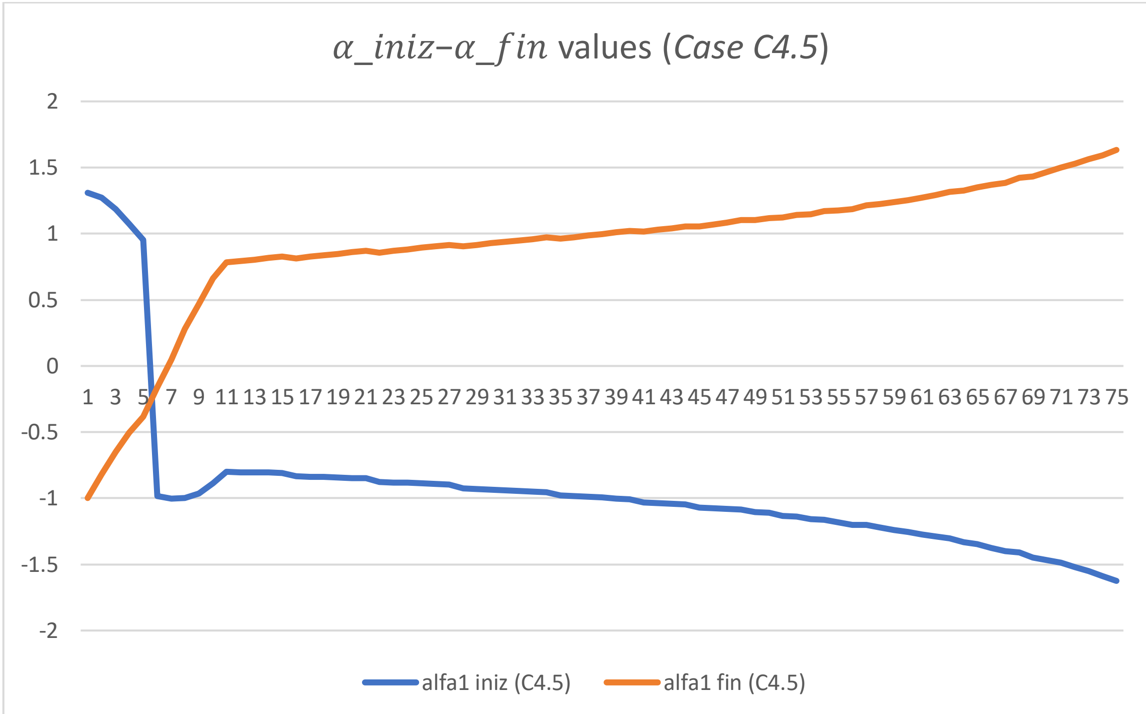

Figure 72. α_iniz–α_fin values for Case C4.5 - Perihelion

After an initial subgroup of about 5 asteroids in which some oddities happen, the trends of these parameters are what is expected for about the whole set of asteroids. In fact, $\alpha_{fin} > \alpha_{iniz}$ from asteroid #6 for *cases A4.5* and *B4.5* and form asteroid #7 for case *C4.5*. Even with these cases, the considered burning arcs are very long and the length of many of them does not fall within the hypothesis of validity of the method.

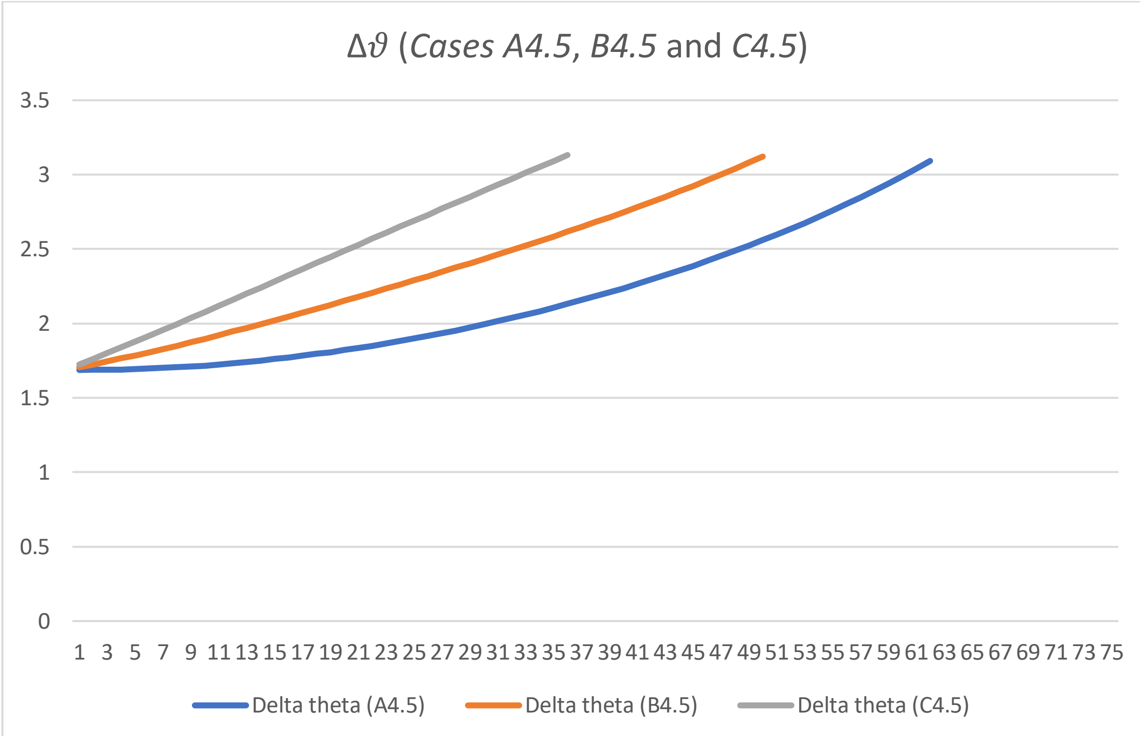

Figure 73. Δϑ values comparison for i=4.5° - Perihelion

As it is trivial to notice, the burn arc angular lengths are further increased with $i = 4.5°$, and this basically means that more asteroids need the correction introduced in chapter 2, section 2.1, paragraph 2.1.1. In fact, as already written, $\Delta\vartheta$ values larger than π are always defined by subtracting 2π and their reported value is between 0 and 2π, but they are not shown in the graph since they are outside one of the fundamental hypotheses of the estimation method. Then, as expected, the trends appear to be shortened and shifted to the right of the graph. About this parameter, closely related to the propellant mass consumed, it seems that Ω significantly affects both $\Delta\vartheta$ and consumption since the trend of *case C4.5* for the asteroids in which $\Delta\vartheta < \pi$ is basically a straight line that grows much faster than the observed curves for *cases A4.5* and *B4.5*, as it is predicted by the theory which assumes that both ΔV and the cost of transfer is significantly related to the required orbital changes from the starting orbit to the arrival orbit [2].

3.1.3.1 The relations between ϑ_e, ϑ_{iniz} and ϑ_{fin}, α_{iniz} and α_{fin}

Even in these cases the predominant answer is the expected one, present in almost the whole set of fictitious asteroids.

- *Case A4.5*

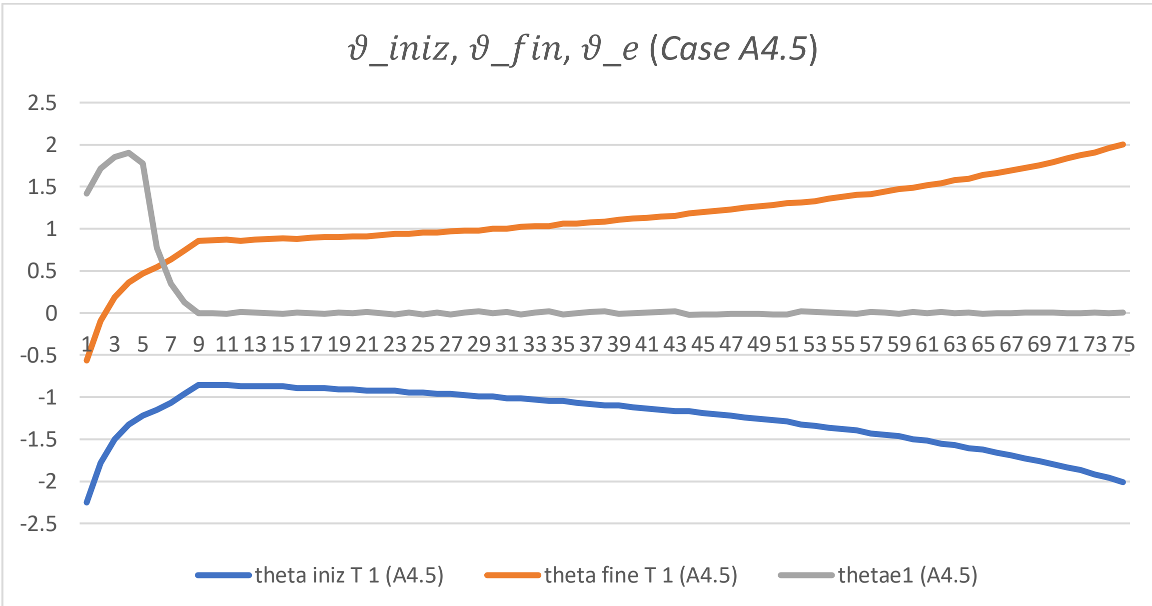

Figure 74. ϑ_iniz, ϑ_fin, ϑ_e values for Case A4.5 - Perihelion

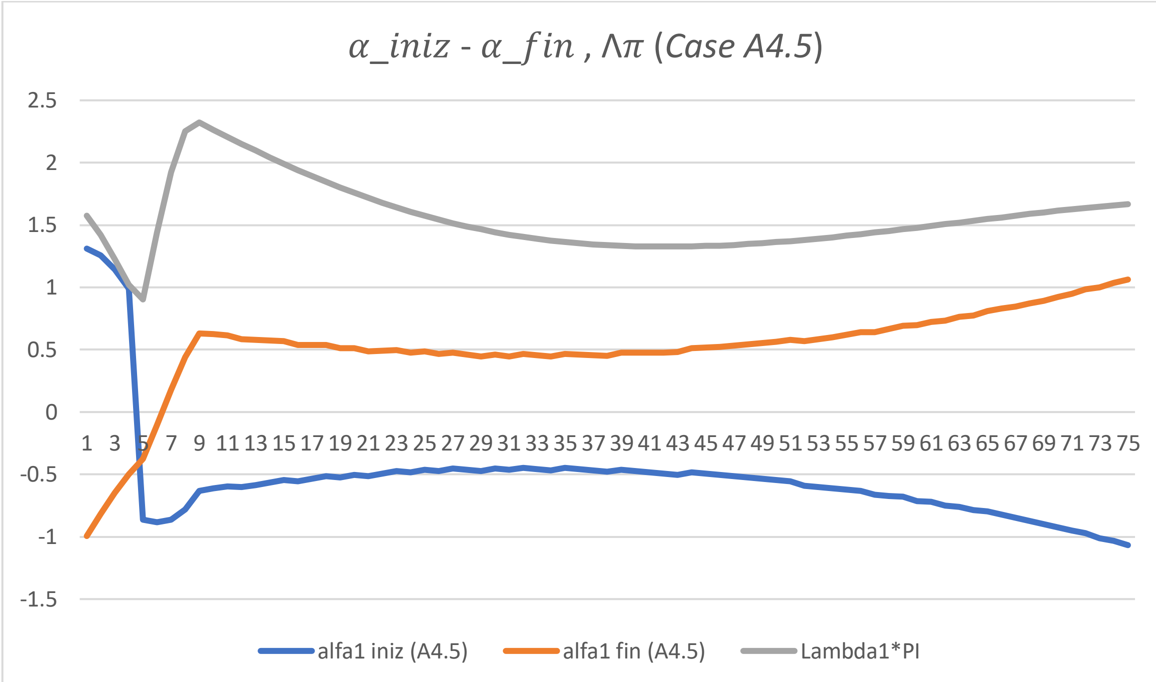

Figure 75. α_iniz - α_fin, $\Lambda\pi$ values for Case A4.5 - Perihelion

- *Case B4.5*

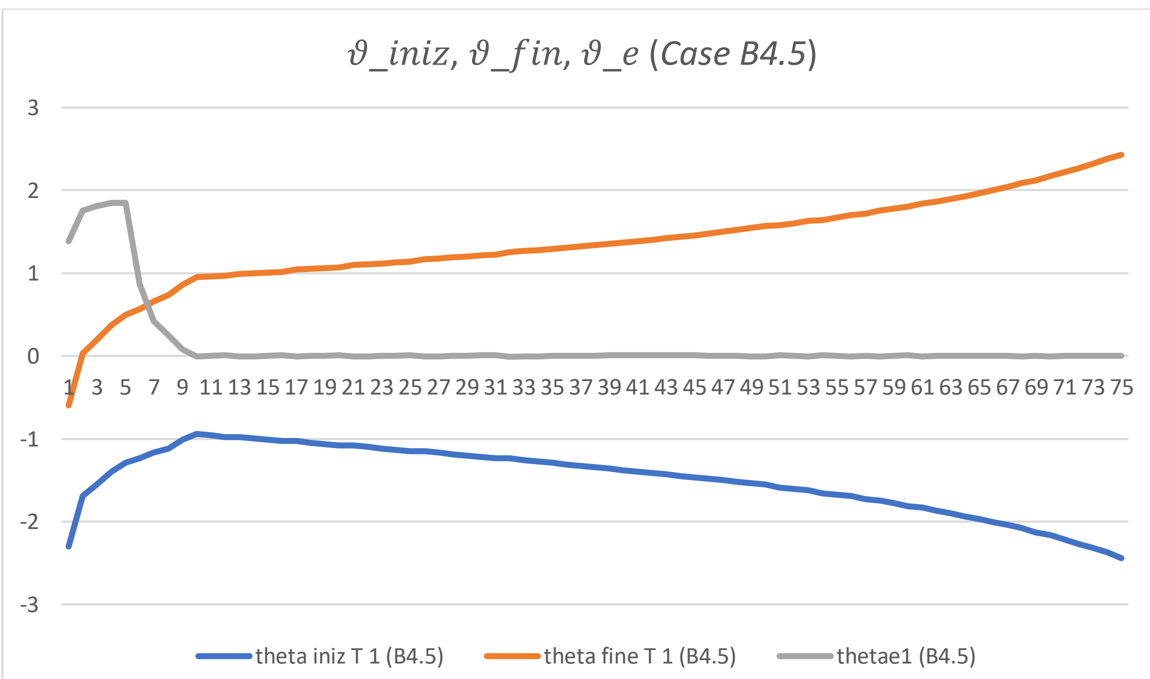

Figure 76. ϑ_iniz, ϑ_fin, ϑ_e values for Case B4.5 - Perihelion

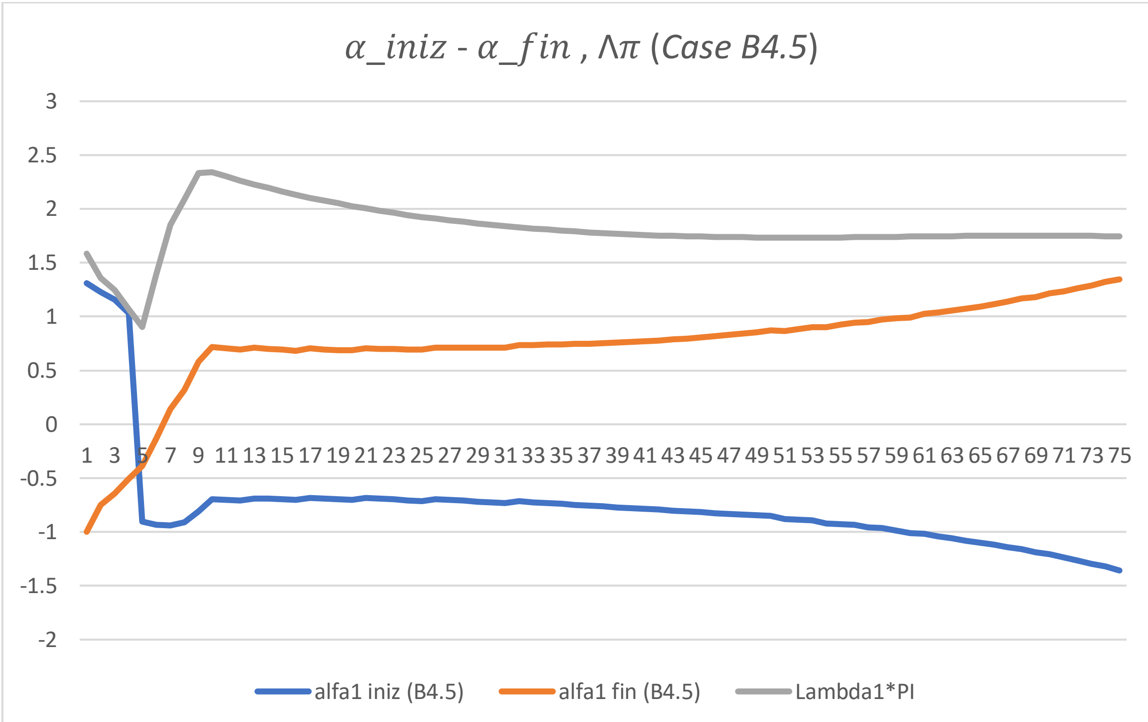

Figure 77. α_iniz - α_$f$in, $\Lambda\pi$ values for Case B4.5 - Perihelion

➢ *Case C4.5*

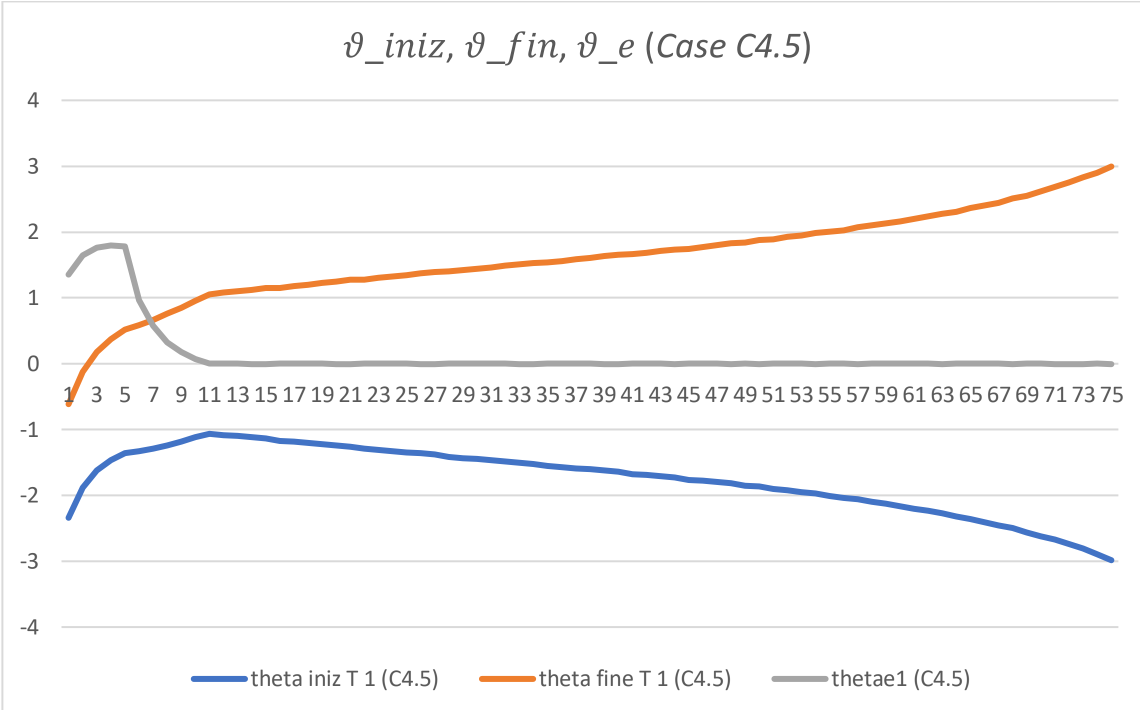

Figure 78. $\vartheta\_iniz, \vartheta\_fin, \vartheta\_e$ values for Case C4.5 – Perihelion

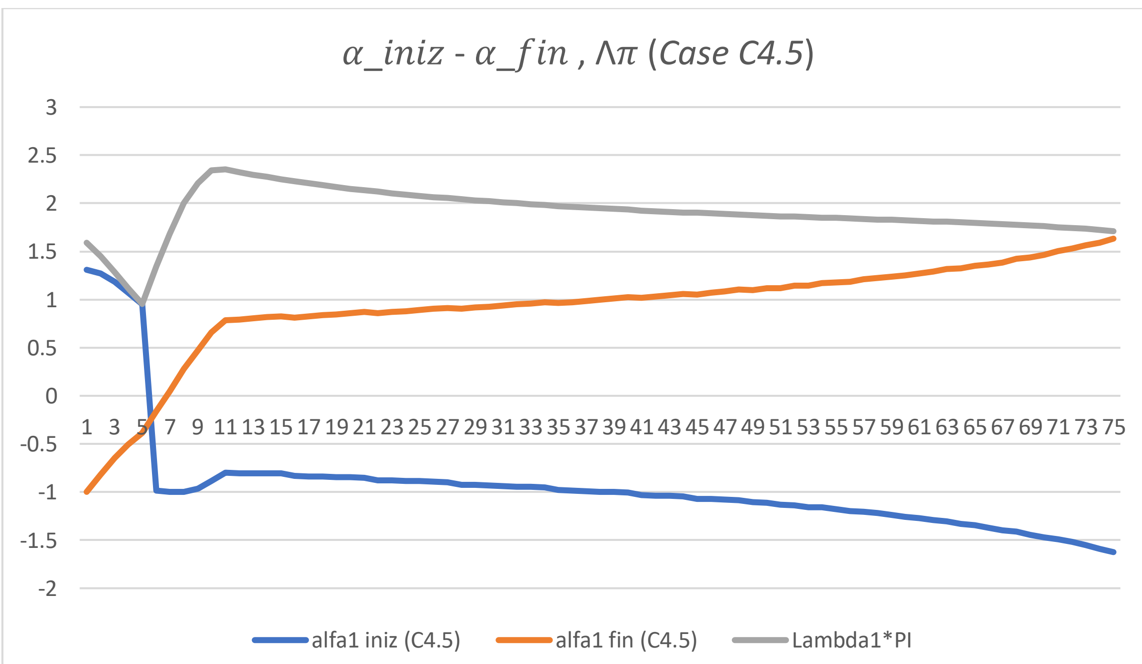

Figure 79. α_iniz - α_fin, $\Lambda\pi$ values for Case C4.5 – Perihelion

As it can be seen, the responses are very similar to those of the cases with $i = 3°$, but there are still some small diversities. It has already been mentioned above the damping of the oscillations in the central section as regards ϑ_e values in *case A4.5*; the solution predicted by the theory is present in all *cases* in a range of about $87 -$ 89% of the asteroids, similarly to what happens in *cases A3*, *B3* and *C3*, but here the higher inclination value lengthens the burning arcs and this can be observed from the larger distance between ϑ_{iniz} and ϑ_{fin}. This larger burn arc angular length can also be seen in the graphs of α_{iniz}, α_{fin} and $\Lambda\pi$. For the latest asteroids of the set α_{fin} value, especially in cases B4.5 e C4.5 (respectively $\Omega = \pi/4$ and $\Omega = \pi/2$), almost reaches the asymptotic value $\Lambda\pi$, which is the upper limit that the relation $\alpha = \Lambda(\vartheta - \vartheta_e)$ must not exceed.

3.1.4 $i = 6°$

The last and largest inclination value imposed in the various *cases* is $i = 6°$. A check is performed to see if with such a value it can still be considered within Edelbaum's approximation: $\cos(6°) = 0{,}9945 \cong 1$, $\sin(6°) = 0{,}1045 \approx 0$ [7], adherence to the approximation is still confirmed. Despite this, the current inclination leads, in addition to an obvious and substantial increase in consumption, to a strange situation as regards asteroid #2, the one hypothetically closest to Earth: about this asteroid, in all three *cases* the propellant consumption is $20\ kg$, the entire amount of fuel available for the mission; moreover, $\vartheta_{iniz} = \vartheta_{fin} = 0$, $\alpha_{iniz} = \alpha_{fin} = \pi$ and both ϑ_e and Λ are null. These odd values can be explained by the fact that the algorithm has probably calculated too long burning arcs to be performed in a mission with $n = 3$ arcs in 3 years. In fact, a check can be carried out by imposing this inclination value to a mission with $n = 4$ arcs in 4 years: the output results are normal since the time of flight increases and the higher number of arcs performed means that they can be shortened. For all these reasons, in the following discussion the values of asteroid #2 are excluded from the graphs and it is therefore considered, only for *cases* with $i = 6°$, a group of 74 asteroid (asteroid #3 is now the closest to Earth, which is always considered asteroid #1).

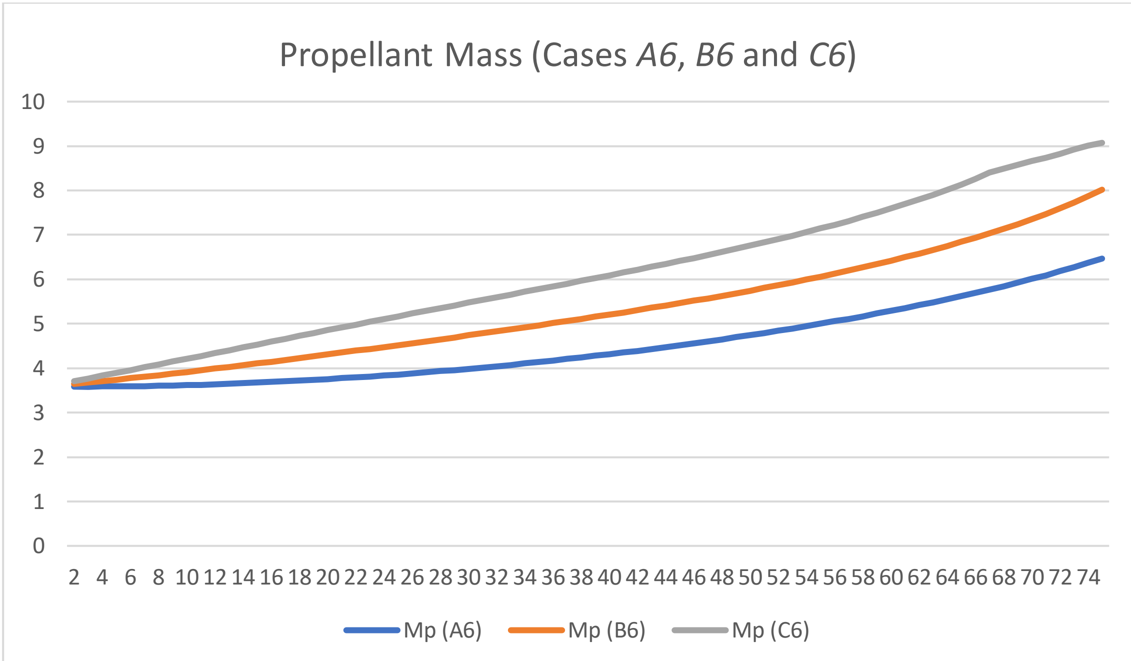

Figure 80. Propellant Mass comparison with i=6°

As it is easy to note, values are higher for all asteroids of the set with respect to the *cases* with $i = 4.5°$. As with all other inclination values, the very first asteroids consume a similar amount of propellant, while the difference between the various *cases* in the required changes of the orbital parameters is felt more as one moves farther from Earth. In fact, the trends of *case B4.5* and above all *case C4.5* are those which differ the most from the trends of the previous *cases*. About asteroid #76, consumption is, respectively, $6{,}46658\,kg$ for *A4.5*, $8{,}01814\,kg$ for *B4.5* and $9{,}07338\,kg$ for *C4.5*.

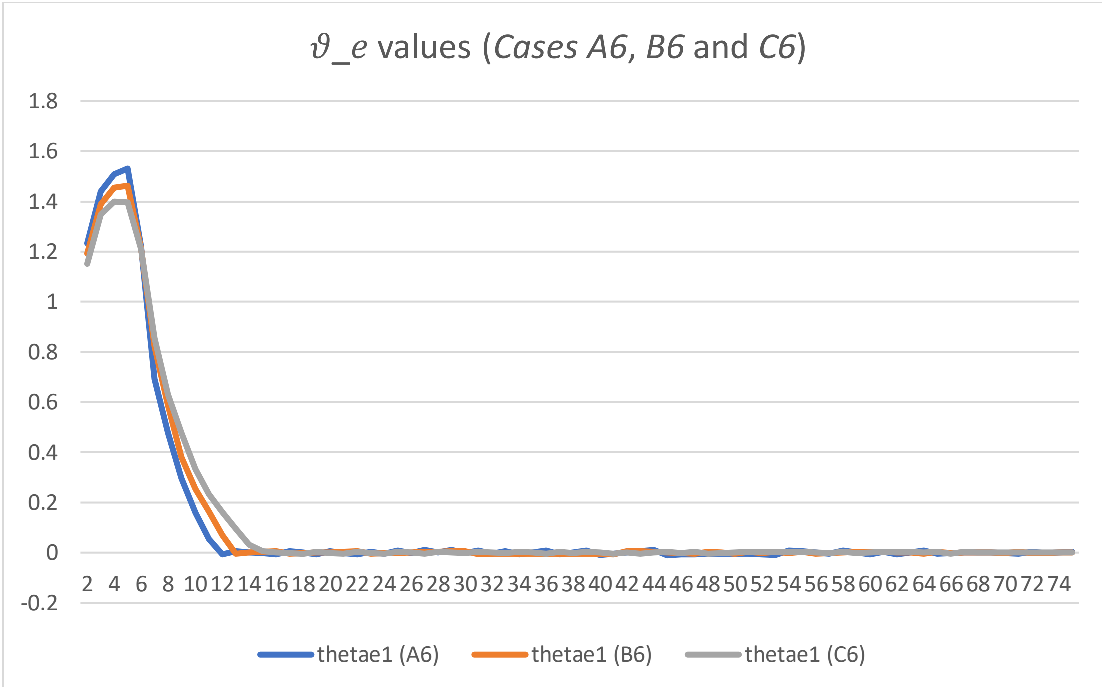

Figure 81. ϑ_e values with i=6° - Perihelion

It is now clear that, beyond $i = 3°$, the algorithm maintains the expected solution from a certain asteroid (even here, relatively close to Earth) to asteroid #76. However, it is particularly interesting to note that while the maximum value of ϑ_e in the suboptimal solution in the first zone decreases globally (for *cases A3*, *A4.5* and *A6*, it is respectively $2{,}32238\ rad$, $1{,}90332\ rad$ and $1{,}53125\ rad$), the range of asteroids in which the code chooses this answer widens slightly (asteroid #11 for *case A6*, #12 for *case B6* and #13 for *case C6*); hence, as the inclination raises, the transition from the suboptimal solution to the optimal solution moves towards a farther asteroid (i.e., in the graphs it shifts to the right).

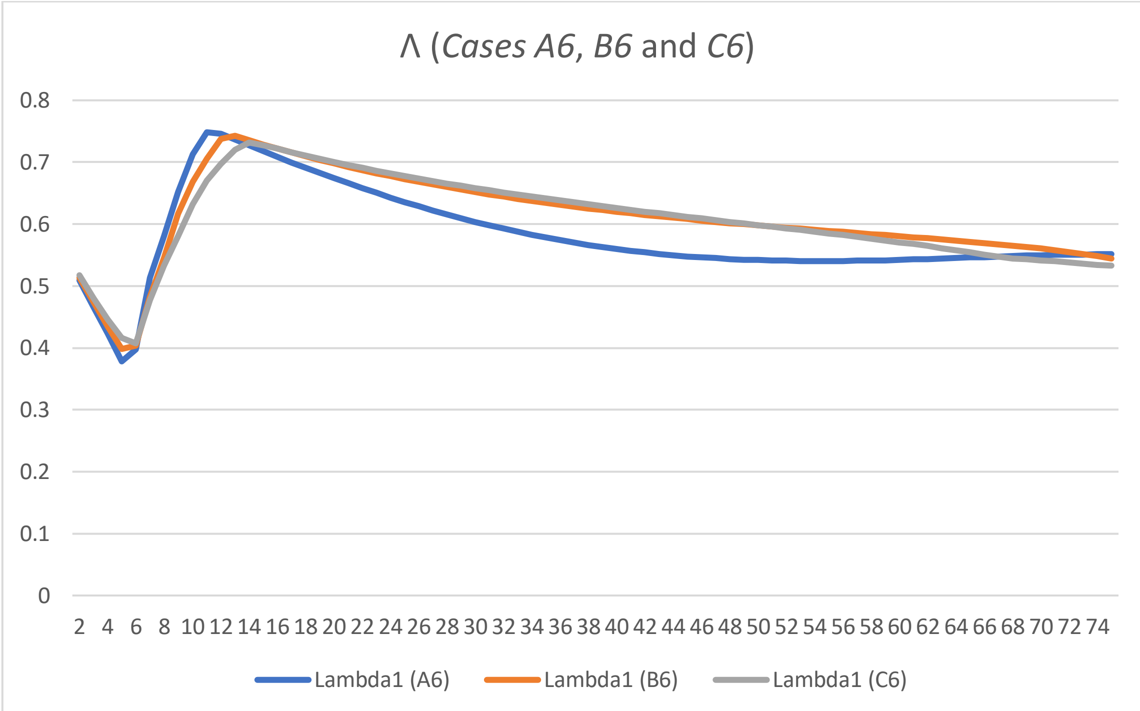

Figure 82. Λ values with i=6° - Perihelion

Λ trends shown in the graph are similar to those of the cases with $i = 4.5°$, but even here the further rise of the inclination has slightly influenced them: after the initial subgroup of asteroids, in which there is first a descent to about 0,4 and then a rise up to 0,73-0,75, the trend are much less curved, especially in *case A6*, and much closer to each other. Indeed, *cases B6* and *C6* seem to assume an almost rectilinear trend in the central and final sections of the graph and, especially in the central section, they can be confused with each other. As already mentioned in *cases* with $i = 4.5°$, in the farthest asteroids Ω tends to slightly lower Λ: about asteroid #76, for *case A6* $(\Omega = 0) \rightarrow\ \Lambda = 0{,}55112$, for *case B6* $(\Omega = \pi/4) \rightarrow\ \Lambda = 0{,}54458$ and for *case C6* $(\Omega = \pi/2) \rightarrow\ \Lambda = 0{,}53254$.

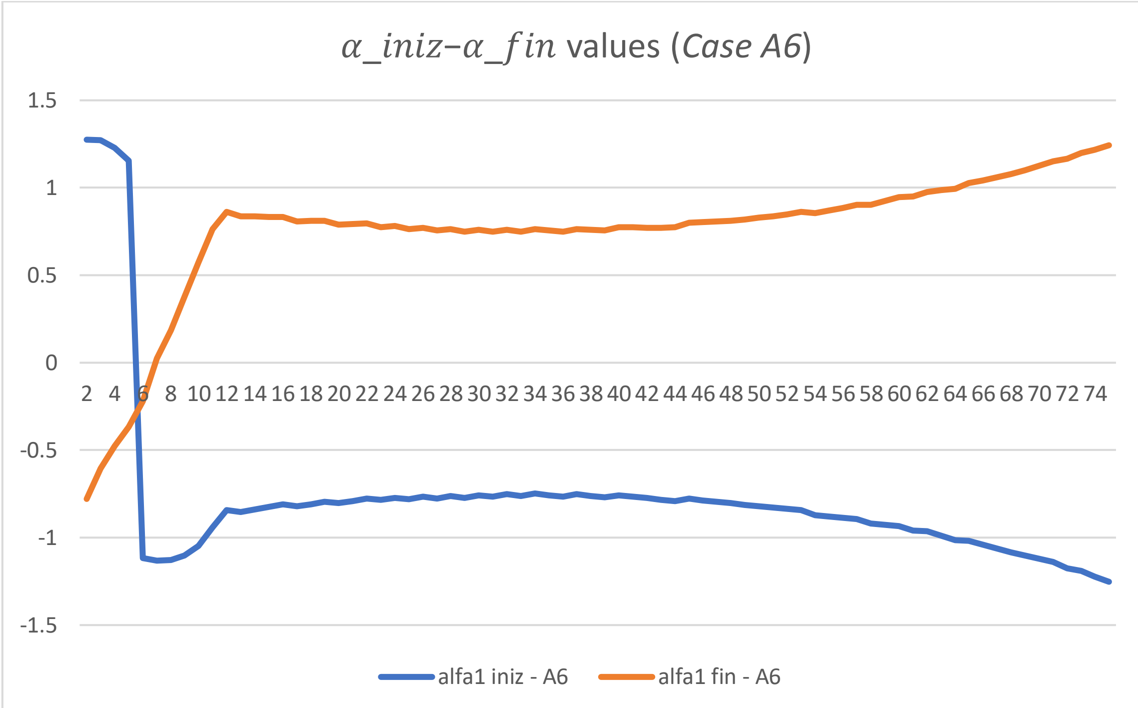

Figure 83. α_iniz–α_fin values for Case A6 - Perihelion

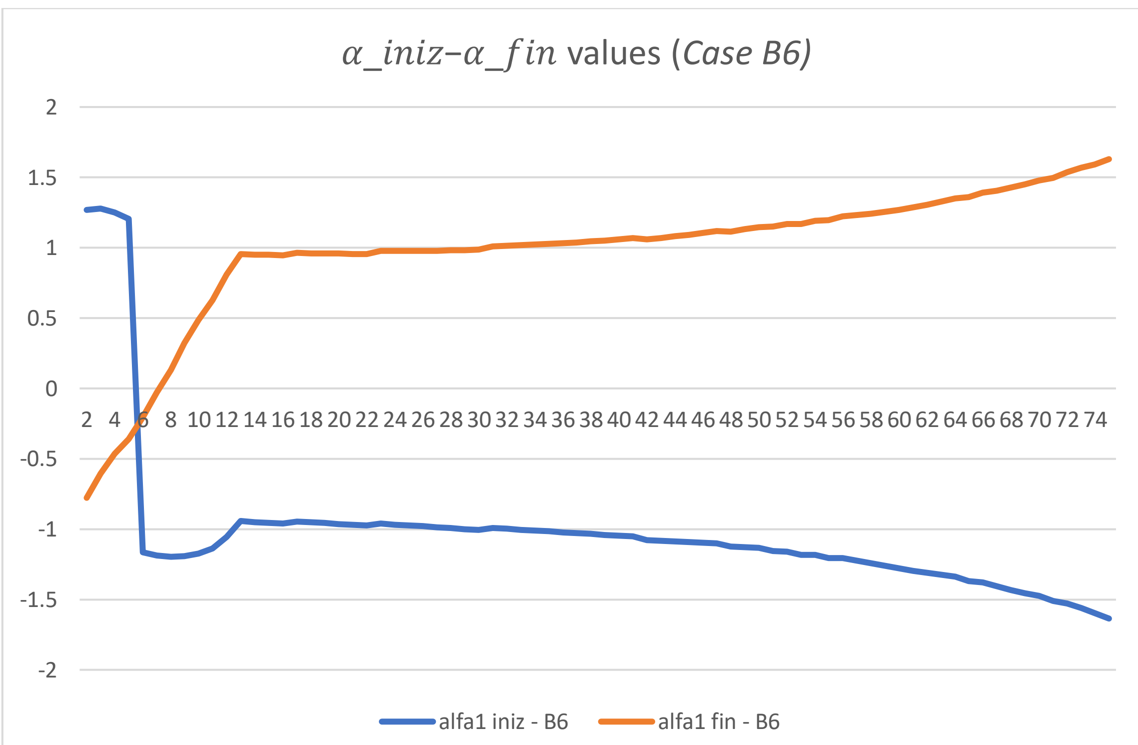

Figure 84. α_iniz–α_fin values for Case B6 – Perihelion

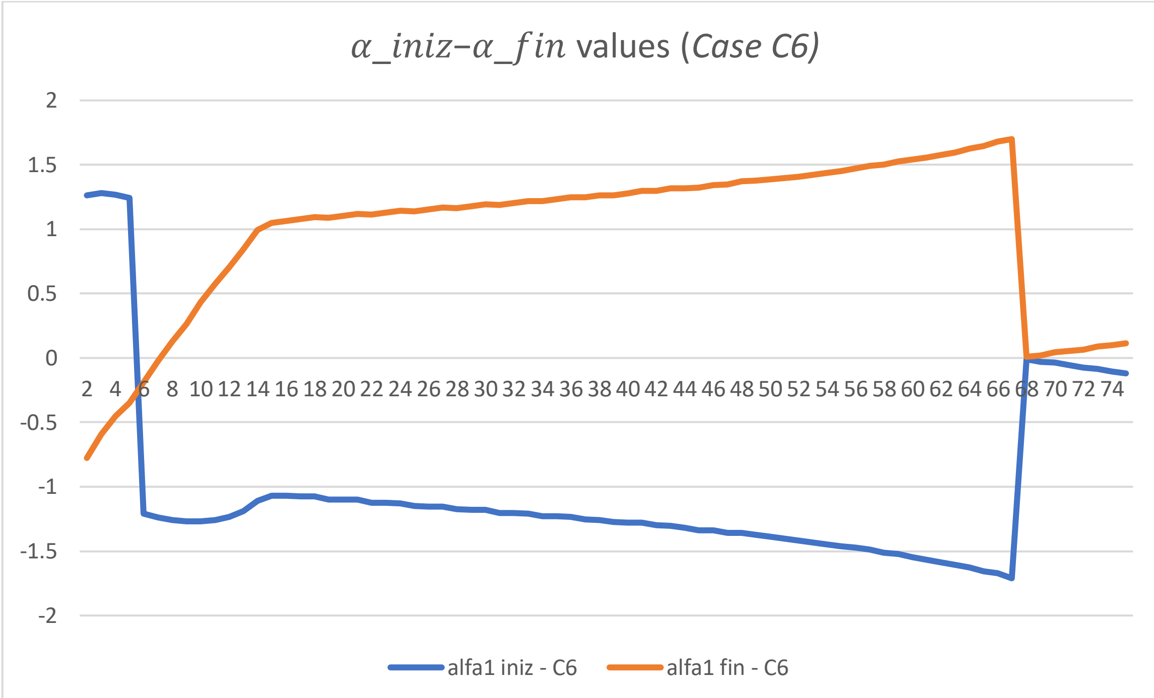

Figure 85. $\alpha\_iniz{-}\alpha\_fin$ values for Case C6 - Perihelion

Even for α_{iniz} and α_{fin} the graphs show no particular oddities. The first area where $\alpha_{fin} < \alpha_{iniz}$ is now taken for granted since it is repeated with any inclination value, and with $i \geq 3°$ about 93% of the set returns the expected solution represented by $\alpha_{fin} > \alpha_{iniz}$. An almost obvious detail can be seen: with this further elevated plane change, the burning arcs become even longer (and this heavily affects the next analyzed parameter). Indeed, from about asteroid #69 for *case C6*, it seems that α_{iniz} and α_{fin} values suddenly decrease very significantly; actually, the burning arcs for these latter asteroids are so long they are theoretically larger than 2π, hence no oddities are detected in this zone.

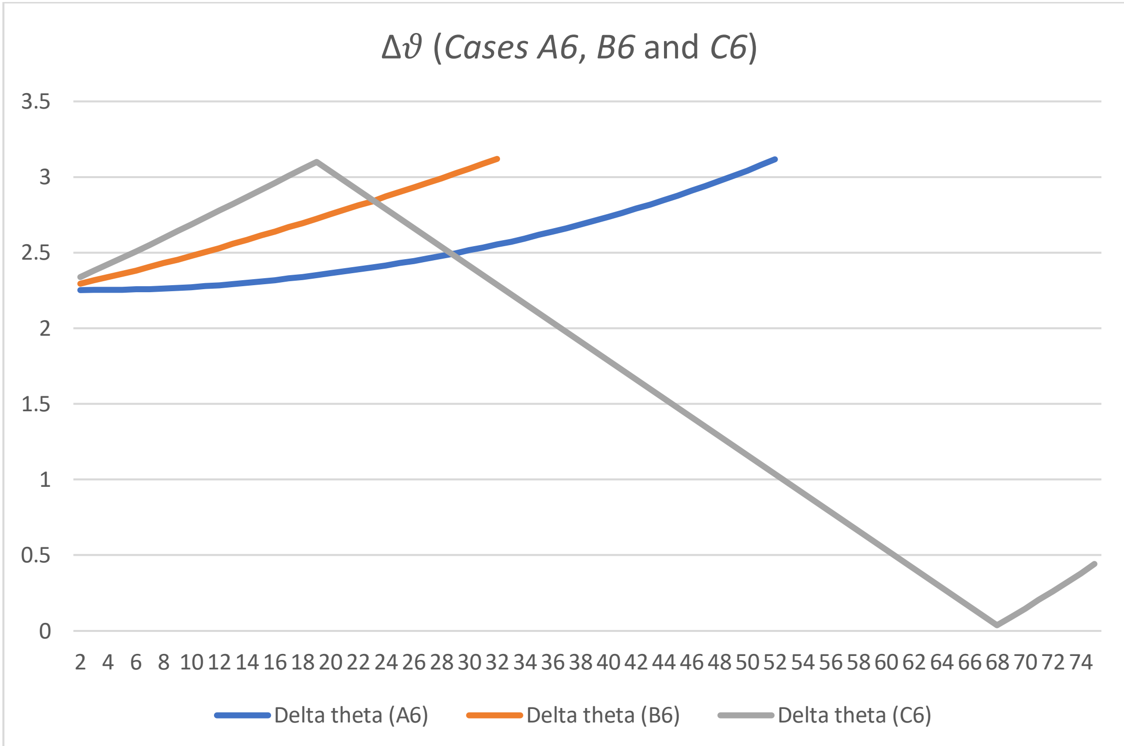

Figure 86. $\Delta\vartheta$ values comparison with i=6° - Perihelion

As explained above, the burn arc angular lengths react to the new rise of i growing even more. *Case A6* is the only one with a number of asteroids for which $\Delta\vartheta < \pi$ larger than half of the group, counting 51 asteroids: in fact, there are 31 asteroids for *case B6* and 26 for *case C6* which actually fall within the hypothesis of validity of the method. Even here it is possible to observe that, for *C6*, from asteroid #69 to #76 $\Delta\vartheta > 2\pi$, therefore the values are calculated as they start from $0\ rad$ and are regularly included in trends.

3.1.4.1 The relations between ϑ_e, ϑ_{iniz} and ϑ_{fin}, α_{iniz} and α_{fin}

In this section, the relations between the fundamental parameters of the theory are analyzed. The situation is similar to that of the cases with $i = 4.5°$, but as the previous section has shown, case C6 has a peculiarity which however does not affect the validity of the solution.

➢ *Case A6*

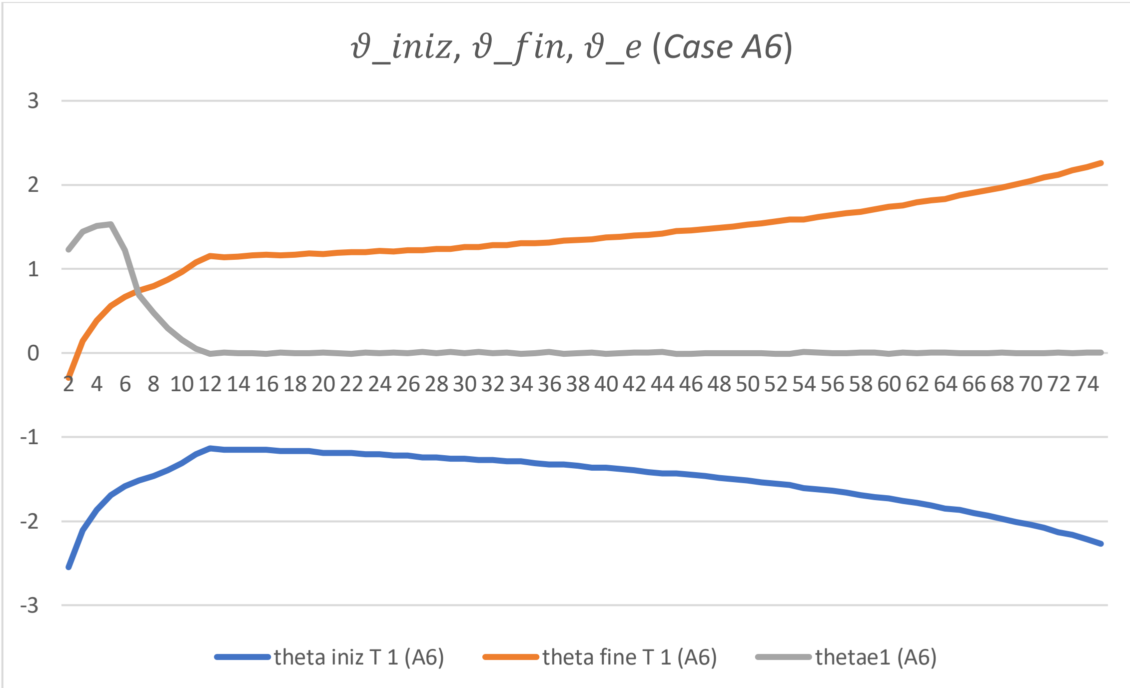

Figure 87. ϑ_iniz, ϑ_fin, ϑ_e values for Case A6 - Perihelion

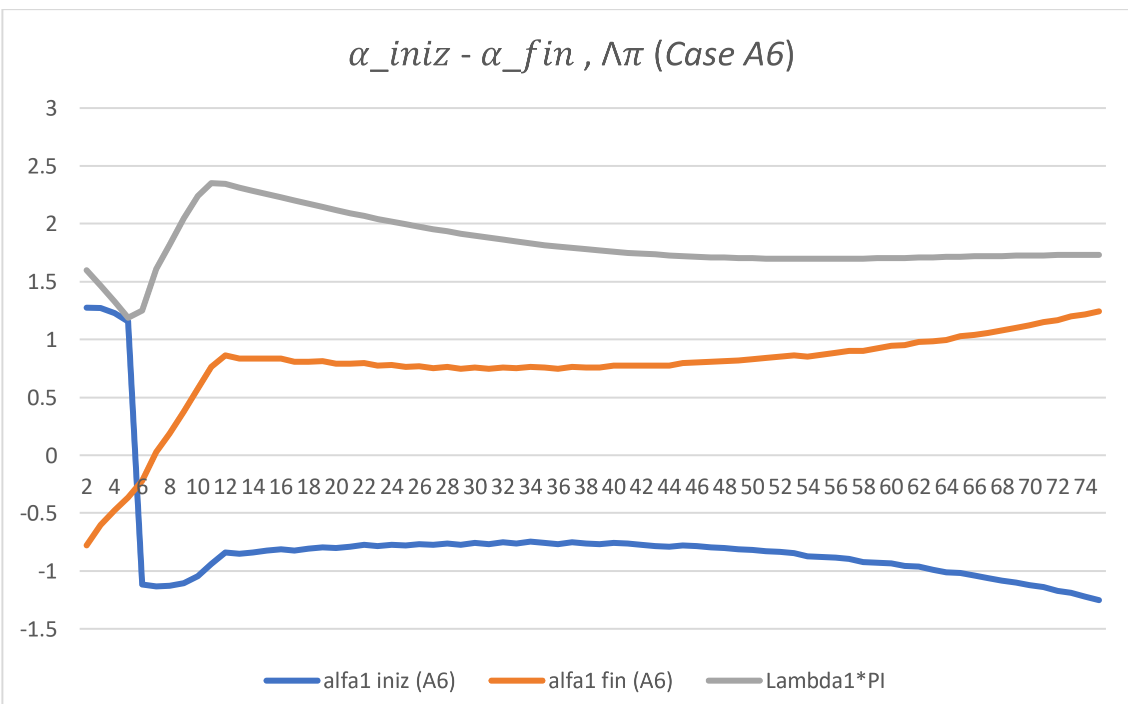

Figure 88. α_iniz - α_fin, $\Lambda\pi$ values for Case A6 - Perihelion

➢ *Case B6*

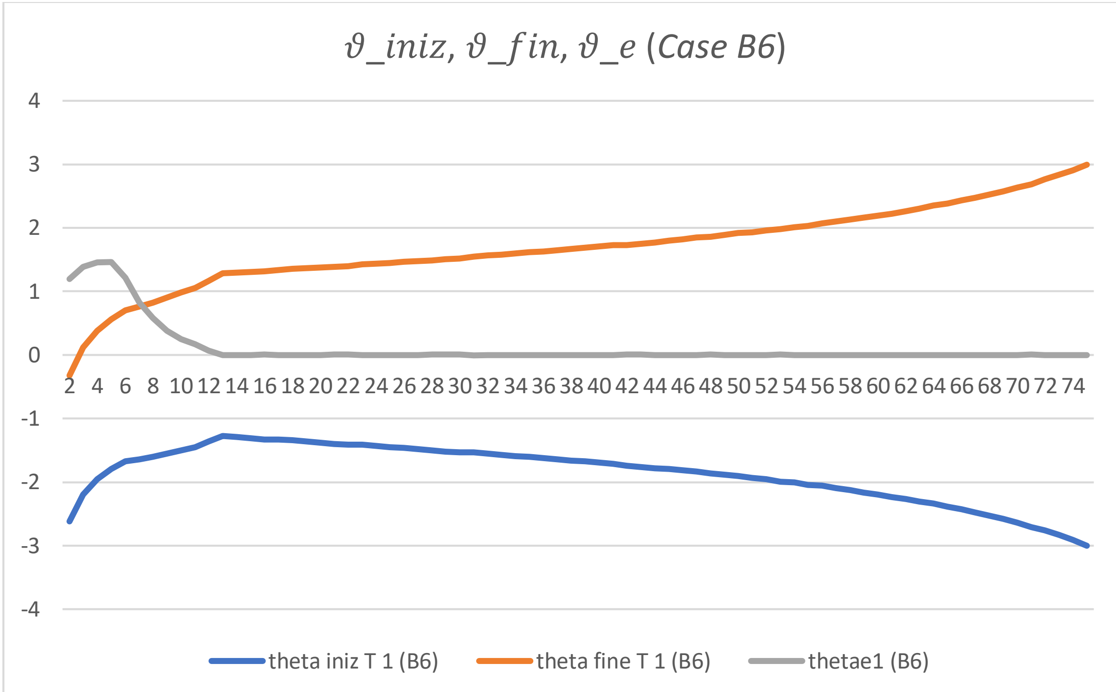

Figure 89. ϑ_iniz, ϑ_fin, ϑ_e values for Case B6 - Perihelion

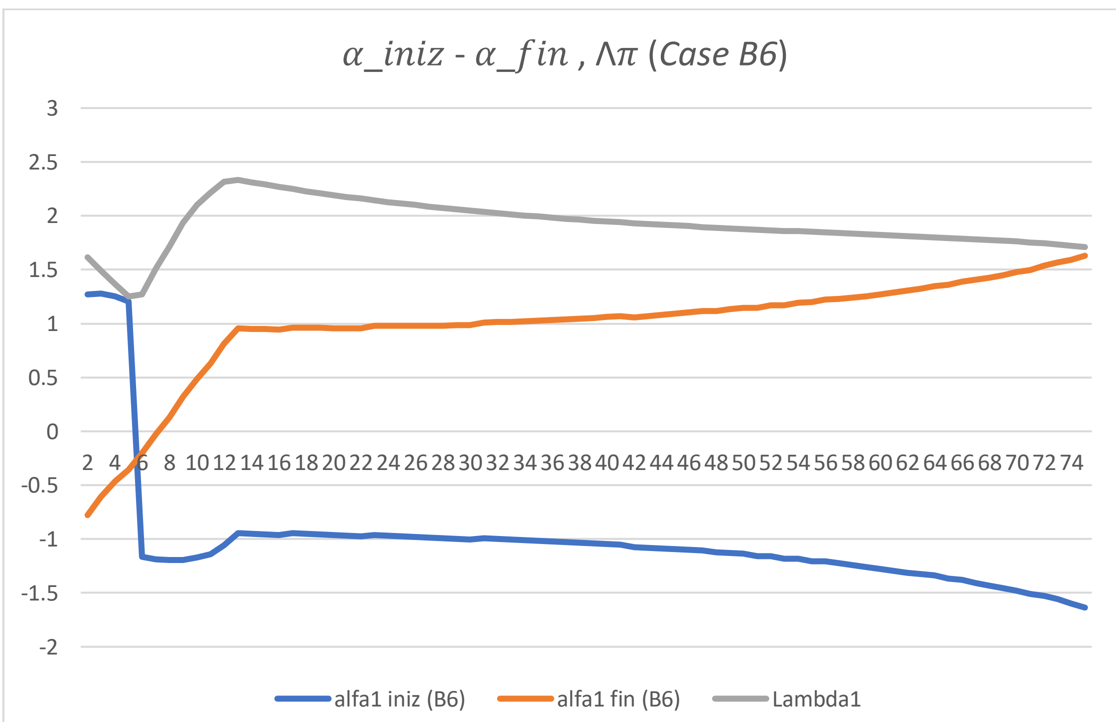

Figure 90. α_iniz - α_fin, $\Lambda\pi$ values for Case B6 – Perihelion

➢ *Case C6*

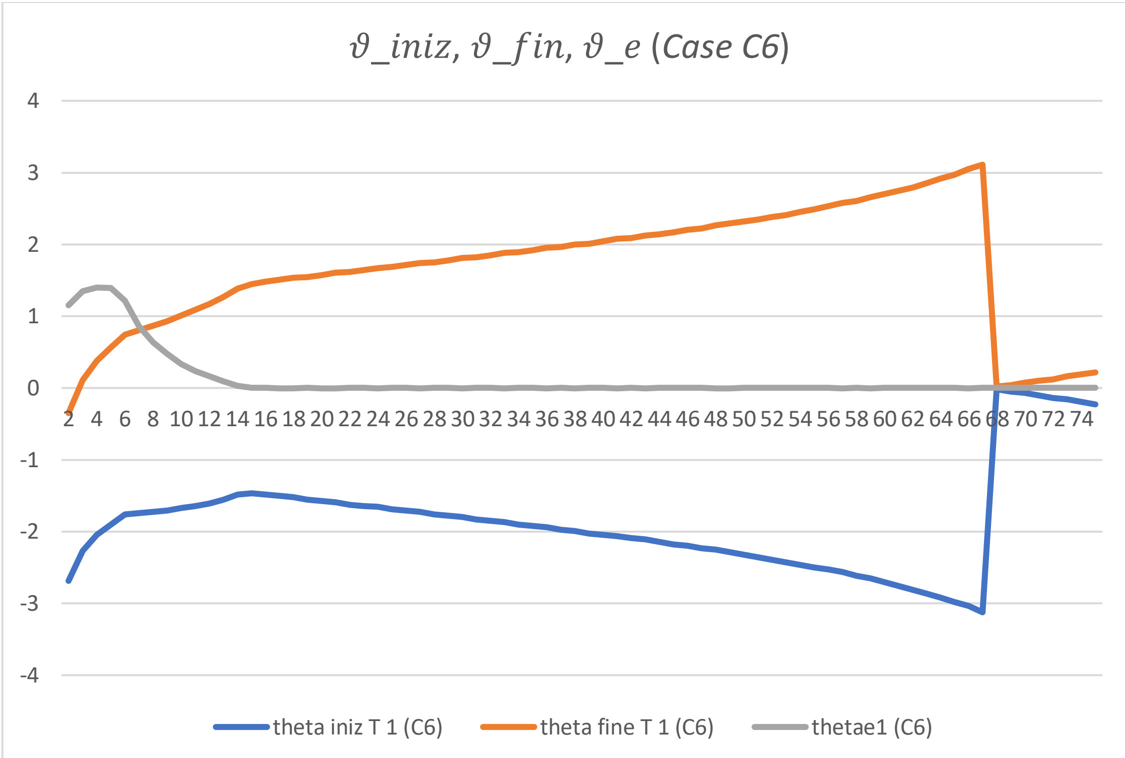

Figure 91. ϑ_iniz, ϑ_fin, ϑ_e values for Case C6 – Perihelion

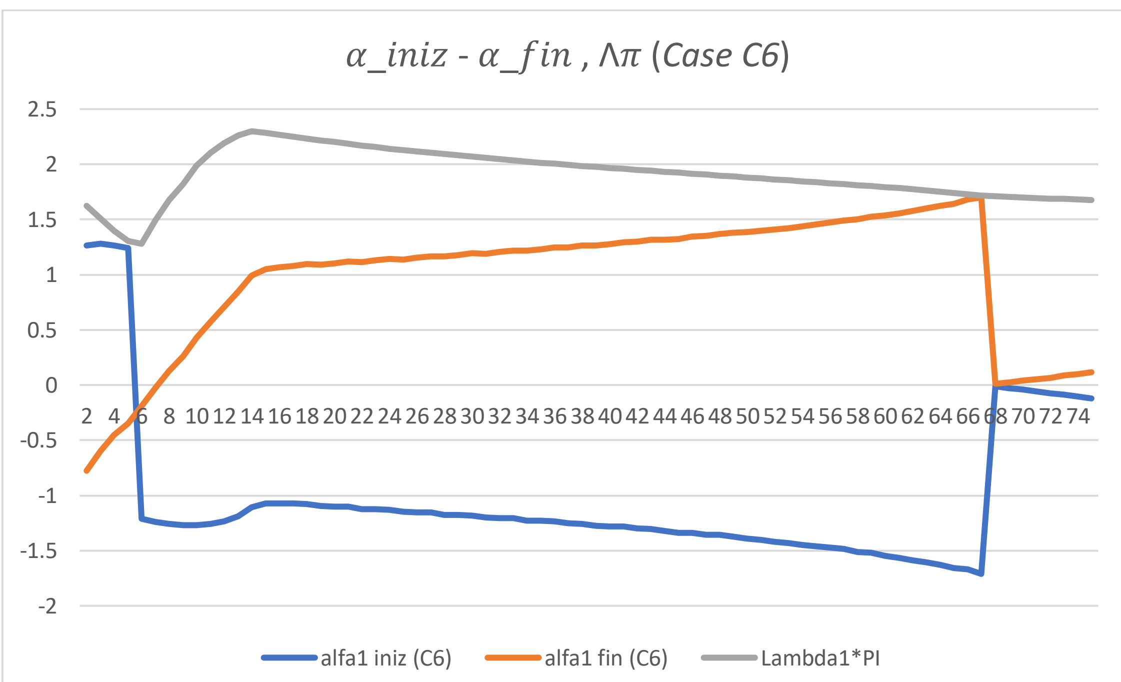

Figure 92. α_iniz - α_fin, $\Lambda\pi$ values for Case C6 - Perihelion

There are no substantial anomalies in these graphs either. After the now usual oddities in the very first subgroup of asteroids, the predominant solution is that foreseen by the theory, that is, $\vartheta_e \in [\vartheta_{iniz};\ \vartheta_{fin}]$ with $\vartheta_e \cong 0$ and $\alpha_{fin} > \alpha_{iniz}$. The particularly interesting results to observe and analyze concern *case C6*, as it can also be seen at a quick glance. Firstly, when $\Delta\vartheta > 2\pi$ and ϑ_{iniz} and ϑ_{fin} "restart the circle" with very small values at asteroid #69, ϑ_e's answer is perfectly aligned with the theory since it is $\vartheta_e \equiv 0$. Afterwards, it is necessary to analyze, again regarding *C6*, α_{fin} values immediately before $\Delta\vartheta > 2\pi$; in fact, as it is can be understood from the graph above, some values (asteroids #67 and #68) go very close to the asymptotic value $\Lambda\pi$, especially asteroid #68 with a difference of only $0{,}018947\ rad$, but the never intersect it or surpass it.

3.2 Perihelion maneuver: overall comparison

After having analyzed the *cases* separately by the inclination value, now an overall comparison is made essentially based on the value of RAAN. Thus, the cases that are now compared are those with:

- $\Omega = 0$ (*Cases A*, *A1.5*, *A3*, *A4.5* and *A6*);
- $\Omega = \pi/4$ (*Cases B*, *B1.5*, *B3*, *B4.5* and *B6*);
- $\Omega = \pi/2$ (*Cases C*, *C1.5*, *C3* and *C6*).

3.2.1 $\boldsymbol{\Omega = 0\ rad}$

The overall comparison is performed by analyzing the fundamental parameters of the theory: the propellant mass consumed, ϑ_e and Λ. $\Delta\vartheta$ has an identical trend to the propellant mass even if they are interrupted due to the hypothesis $\Delta\vartheta < \pi$, while $\alpha_{iniz} - \alpha_{fin}$ are single parameters already exhaustively observed and studied in the previous section; hence, now these parameters are not treated. First cases to be dealt with are those with $\Omega = 0$.

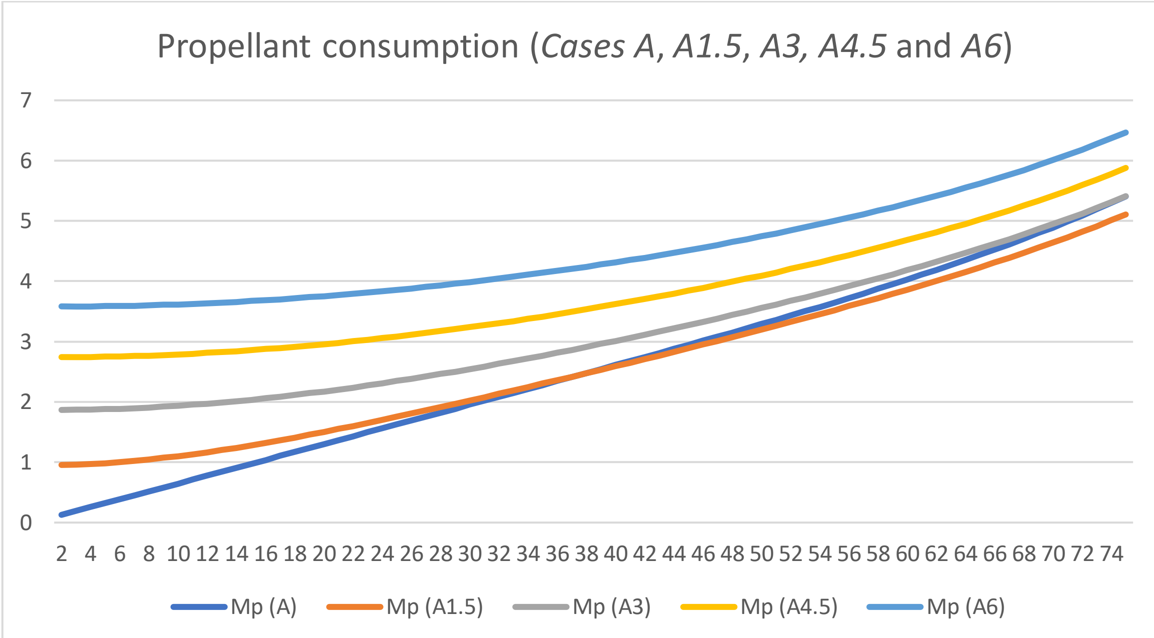

Figure 93. Propellant consumption values comparison with Ω=0 rad - Perihelion

Cases with $\Omega = 0$ are undoubtedly those which consume the least, and this is expected since they require the least number of orbital changes (a, e and i) [2]. It is possible to see, as described above, the trend for *case* $A1.5$ which intersect A since the first asteroids consume more, but the last significantly less, and trend for *case* $A3$ which at the beginning has a higher consumption than A and $A1.5$, but at the end it presents very similar consumption values with the *case* with variable inclination. Finally, *cases* $A4.5$ and $A6$ are detached from the first three analyzed since their inclination value significantly raise the consumption. As one can notice, they have basically identical, slightly spaced patterns.

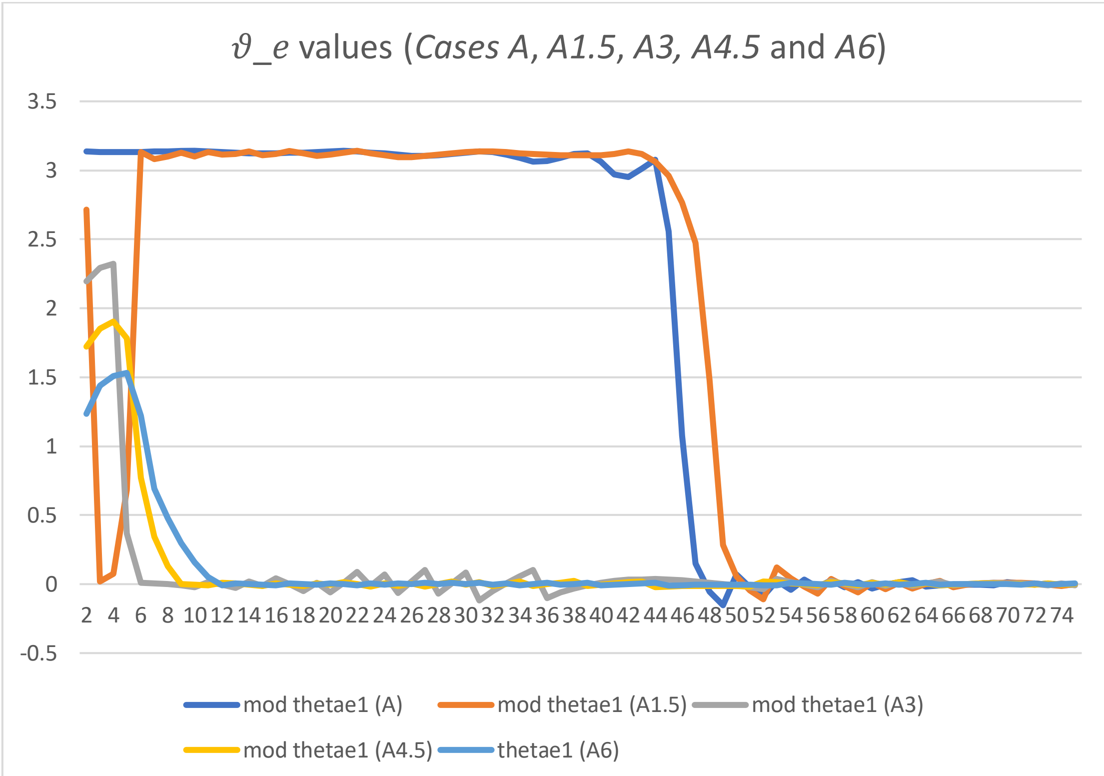

Figure 94. ϑ_e values comparison with Ω=0 rad - Perihelion

Even here, it is possible to see the effect of the gradual rise of inclination given Ω. This effect on ϑ_e is certainly positive, since, as one can see, with $i = (1/8)e$ and $i = 1.5°$ 60% of the asteroids presents the suboptimal solution with $\vartheta_e \cong \pi$ and only much later the transition to the expected solution takes place. Raising the inclination, the following events occur: not only the range of asteroids in which the suboptimal solution is present narrows (8% of asteroids for *A3*, about 11% for *A4.5* and 13% for *A6*), but the peak value of ϑ_e in this range get lower. Thus, with $i \geq 3°$ almost in the whole set of asteroids there is the foreseen solution by the theory.

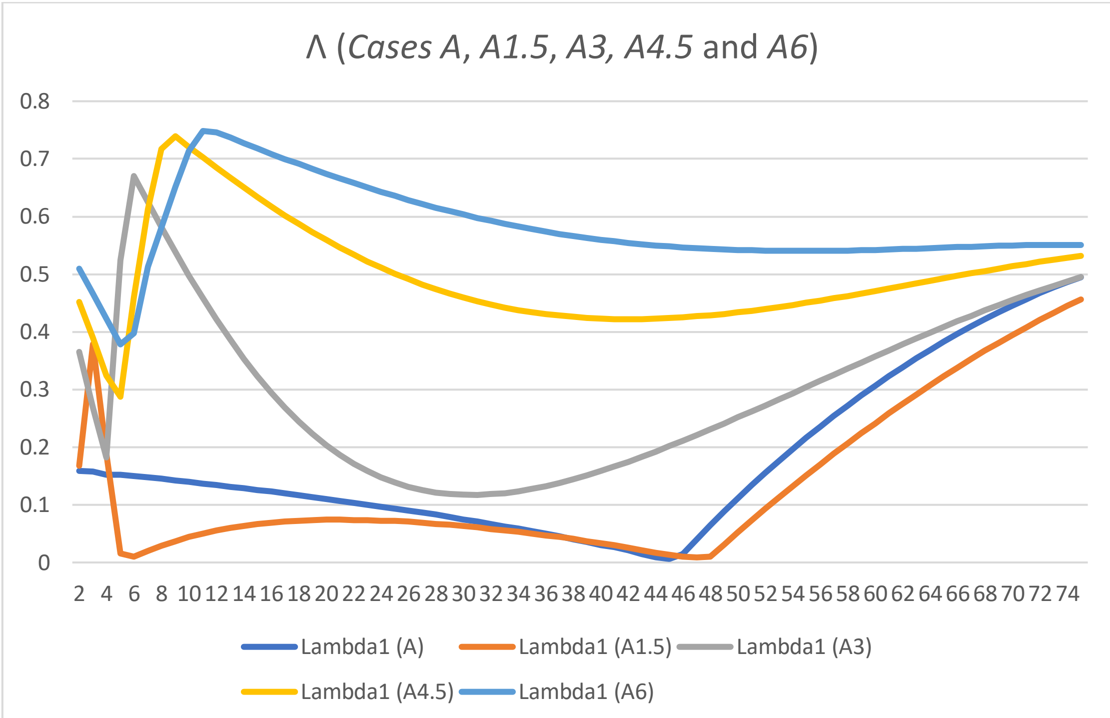

Figure 95. Λ values comparison with Ω=0 rad - Perihelion

About Λ, there is a basically opposite behavior, at least in the first and the central part of the group, with respect to ϑ_e. In fact, *cases A* and *A1.5* presents in these stretches of the graph optimal values that fall within the prediction of the theory; *case A3* has a high peak of almost 0,7 in the first section and then in the central one gets lower and goes close to *A* and *A1.5*; instead, in *cases A4.5* and *A6*, the trends after their peak (between 0,7 and 0,8) do not drop that much (*A6* do not get lower than 0,5). In the final zone, it seems that values tend to converge, but not enough. This effect is much more visible in *cases* with $\Omega = \pi/4$ and $\Omega = \pi/2$.

3.2.2 $\boldsymbol{\Omega = \pi/4\ rad}$

Cases with $\Omega = \pi/4$ are now treated.

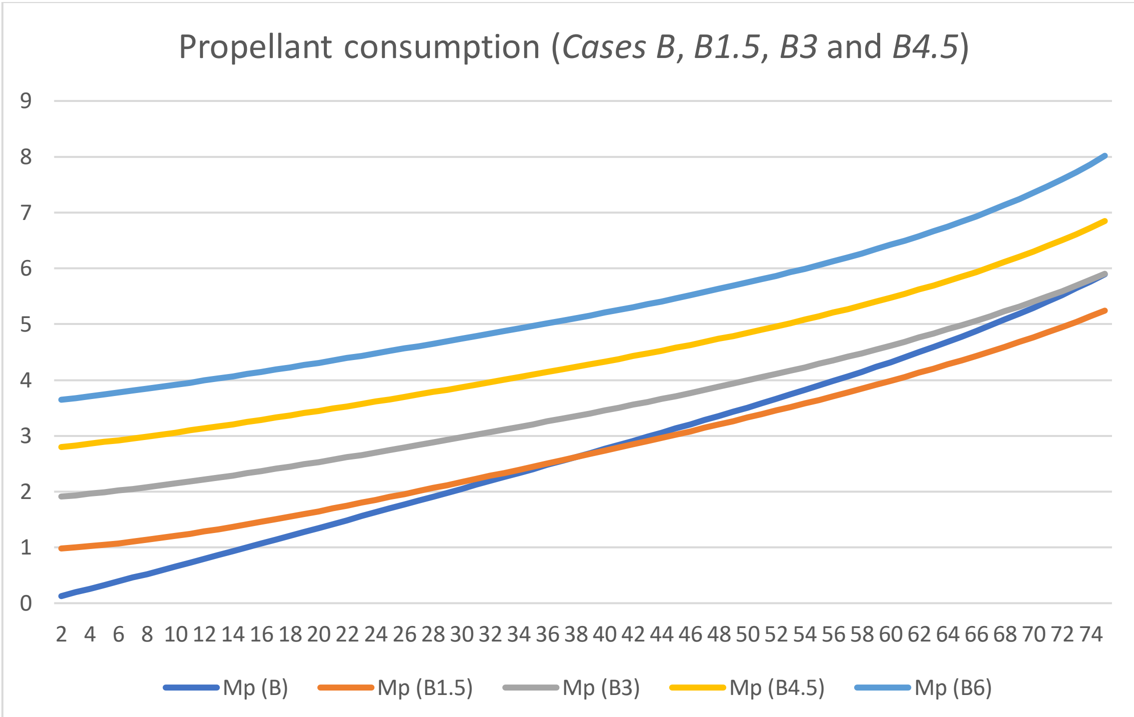

Figure 96. Propellant consumption values comparison with Ω=π⁄4 rad - Perihelion

As it can be easily observed, the patterns are identical to those with $\Omega = 0$, but higher, meaning that the change of an additional orbital parameter significantly affects the total cost of the mission [2]. Moreover, the increase in inclination contributes as well to raise fuel consumption, thus the trends for the various *cases* are more distant from each other.

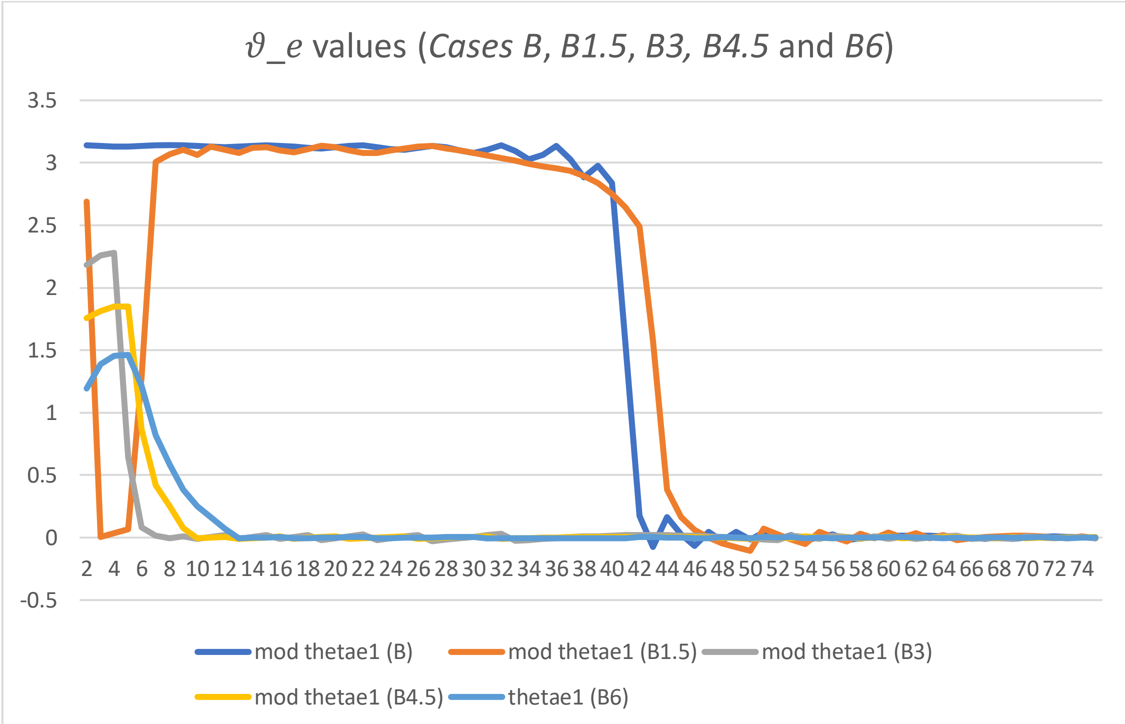

Figure 97. ϑ_e values comparison with Ω=π/4 rad – Perihelion

$\Omega = \pi/4$ improves results especially for *cases* with variable or low inclination (*B* and *B1.5*. As it can be observed, for *B* and *B1.5* the transition occurs a few asteroids before with respect to cases *A* and *A1.5*; furthermore, the same thing does not happens in the very first section of asteroids, in which the transition from the suboptimal solution to the optimal solution is more gradual and occurs about at the same asteroids with respect to cases *A3*, *A4.5* and *A6*.

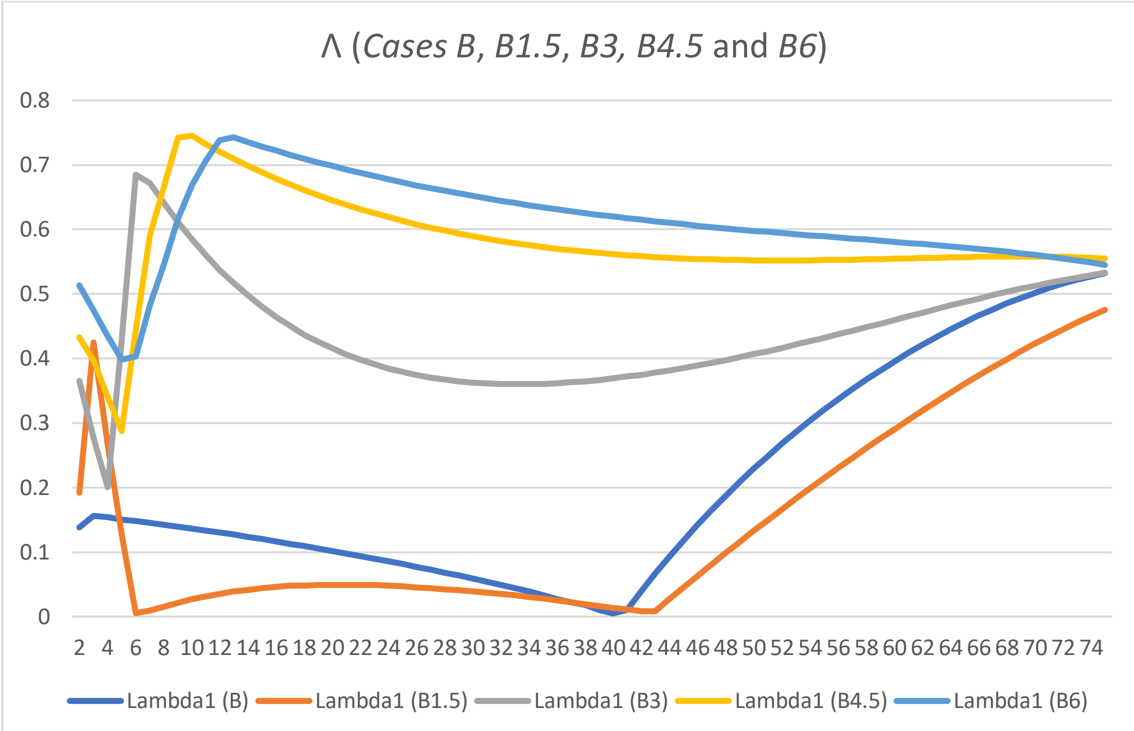

Figure 98. Λ values comparison with Ω=π⁄4 rad – Perihelion

Two things are very interesting in this graph: first, the trend of *B3*, with the influence of $\Omega = \pi/4$, outdistances the patterns of *B* and *B1.5* and assumes higher values in the central section of the graph; secondly, the only *case* that do not converge to a certain point is B1.5, that reaches a value less than 0,5.

3.2.3 $\Omega = \pi/2\ rad$

Cases that present the quadrature between the perihelion and the ascending node are now dealt with.

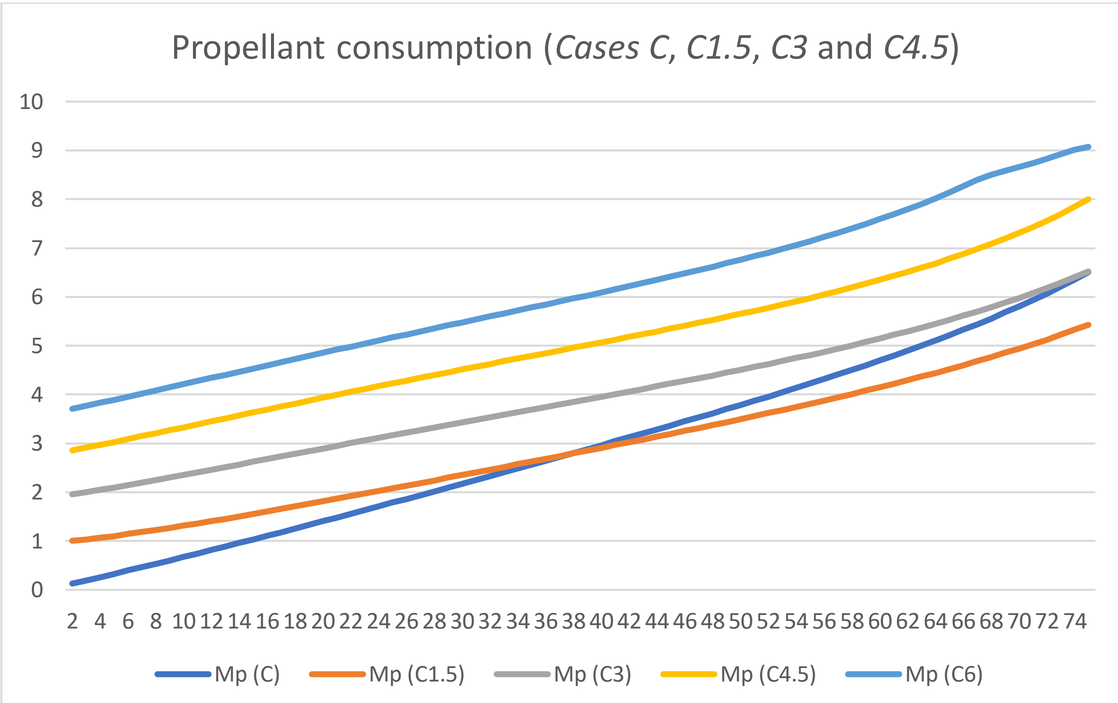

Figure 99. Propellant consumption values comparison with Ω=π⁄2 rad – Perihelion

The trends are now usual, but take on even higher values. Asteroid #76 for case C6, so with the highest inclination value studied, consumes $9{,}07338\ kg$, that is, almost half the propellant used for the mission. It is indeed the highest consumption value of all sixteen *cases* treated according with the fact that, together with the highest values of inclination and RAAN, asteroid #76 is the farthest one from the Earth and the one with the most eccentric orbit [2]. Hence the required orbital changes are massive and heavily affect the consumption.

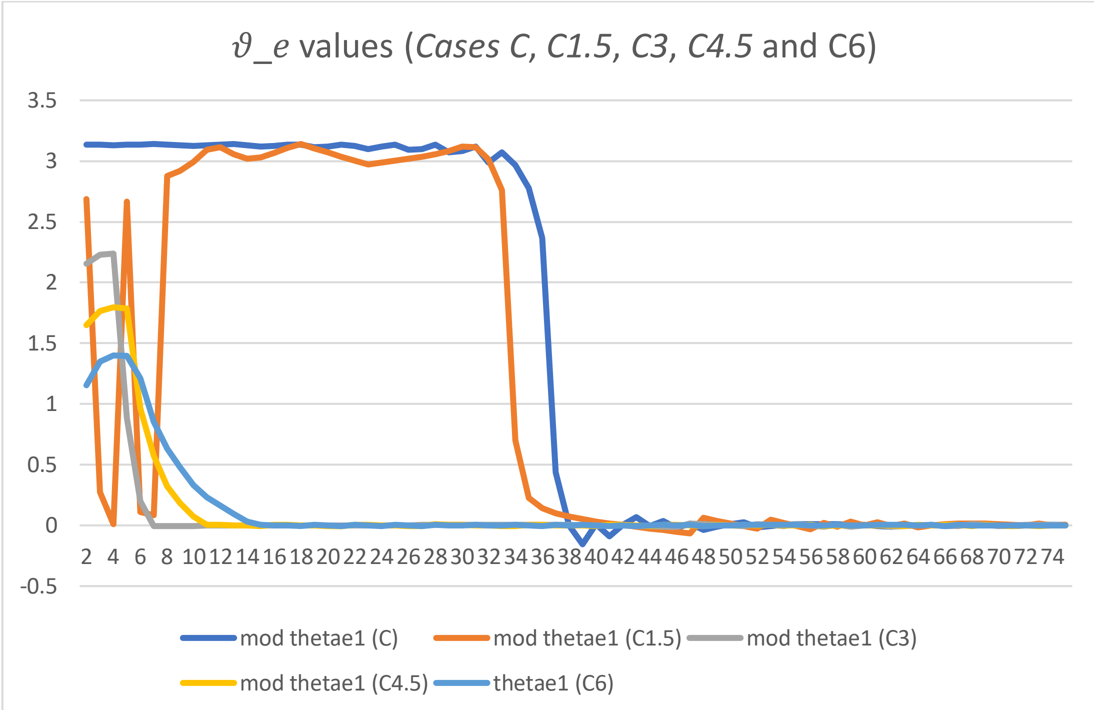

Figure 100. ϑ_e values comparison with Ω=π/2 rad – Perihelion

Even here, there are no surprises about the trends. The quadrature between the line of apsides and the line of nodes further anticipates the transition from $\vartheta_e \cong \pi$ to $\vartheta_e \cong 0$, proving that for orbits with small inclination and eccentricity $\Omega \neq 0$ helps to reach to reach the solution predicted by the theory some asteroids before with respect to the cases with $\Omega = 0$. In the first section, in which occurs the suboptimal solution for *cases* with $i \geq 3°$, almost nothing changes for *C3* with respect to *A3* and B3, while the transition for *C4.5* and *C6* appears even more spread on various asteroids.

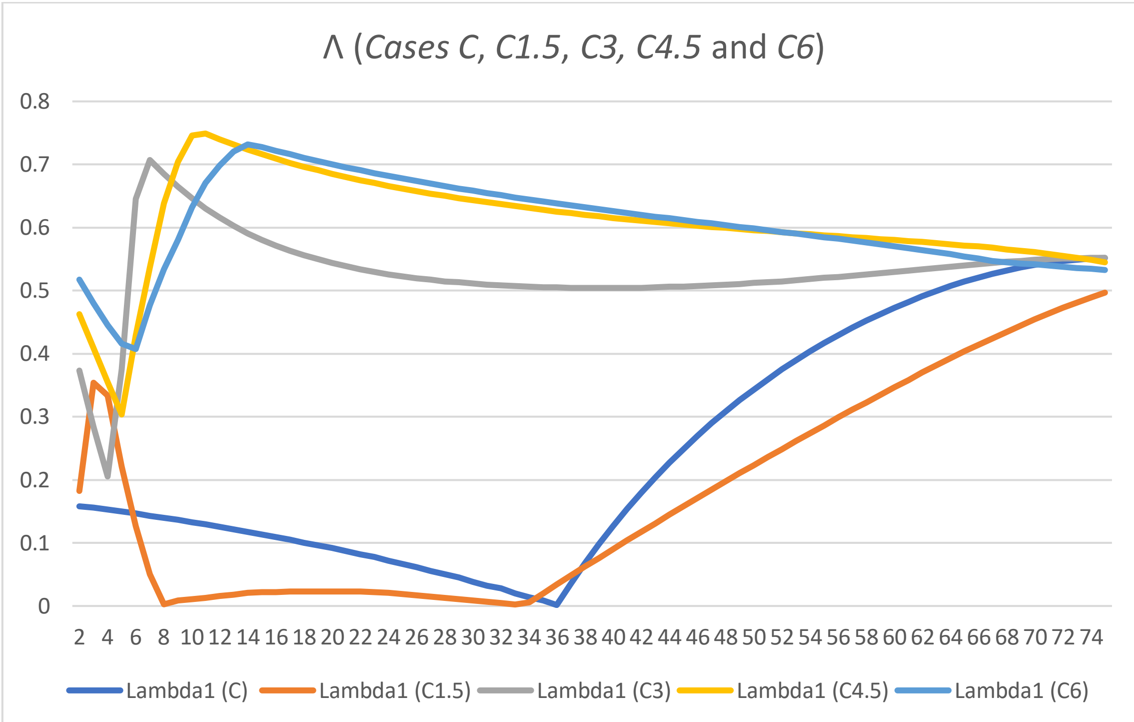

Figure 101. Λ values comparison with Ω=π⁄2 rad – Perihelion

The first thing that catches the eye in this graph is the large distance that separates *cases C* and *C1.5* from *cases* with $i \geq 3°$, *C3*, *C4.5* and *C6*. With $\Omega = \pi/2$, even case C3 after its peak does not drop below 0,5, but in the central section it touches this value. In the final stretch of the graph, *cases C*, *C3*, *C4.5* and *C6* almost converge to a value around 0,53-0,54.

3.3 Aphelion maneuver

Even with the fixed inclination, aphelion maneuver is complex and deserves an in-depth analysis. As already seen in chapter 2, section 2.4, paragraph 2.4.2, thrust verse can be concurrent with ($verse = 1$, $\vartheta_e \cong 0$, $\alpha \cong 0$) or opposite to ($verse = -1$, $\vartheta_e \cong \pi$, $\alpha \cong \pi$) the direction of advancement [2], and for *cases* with variable inclination the optimal solution has been recognized as the zones of the various graphs in which $verse = -1$, hence at the aphelion of the orbits of these asteroids the spacecraft has to brake. It is interesting from now on to analyze whether this fact changes or remains the same. For all cases dealt with for the aphelion maneuver with fixed inclination, the first parameter to be studied is precisely the thrust verse to observe the behavior of the other parameters (especially ϑ_e) in relation to it. The optimal solution is instead identified for this maneuver in the description of the relations between ϑ_e, ϑ_{iniz} and ϑ_{fin}, α_{iniz} and α_{fin}, since only in these graphs it is possible to see the belonging of the parameters to certain ranges.

3.3.1 $\boldsymbol{i = 1.5°}$

First studied cases in aphelion are those with $i = 1.5°$.

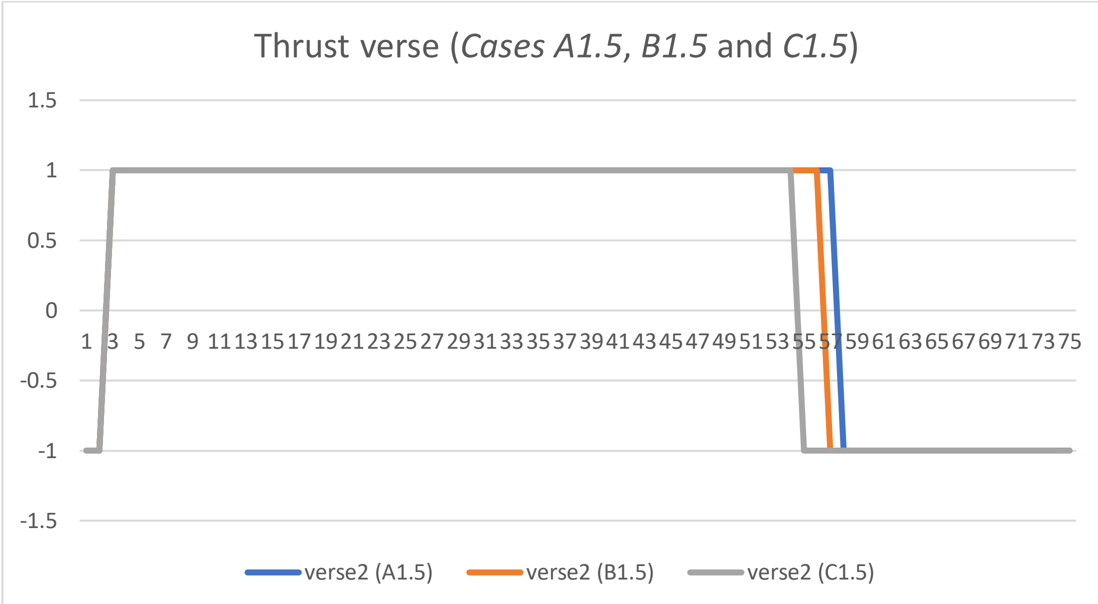

Figure 102. Thrust verse values comparison with i=1.5° - Aphelion

The trends of the thrust verses for cases with $i = 1.5°$ are well defined and also very similar. In fact, except for the first two asteroids, a subdivision into two zones is clearly visible: a larger area encompassing the initial and central segments of the set in which one has $verse = 1$ and the final stretch where the spacecraft must instead brake and so $verse = -1$. The transition from the central section to the final section takes place a few asteroids before going from *case A1.5* to *case C1.5*.

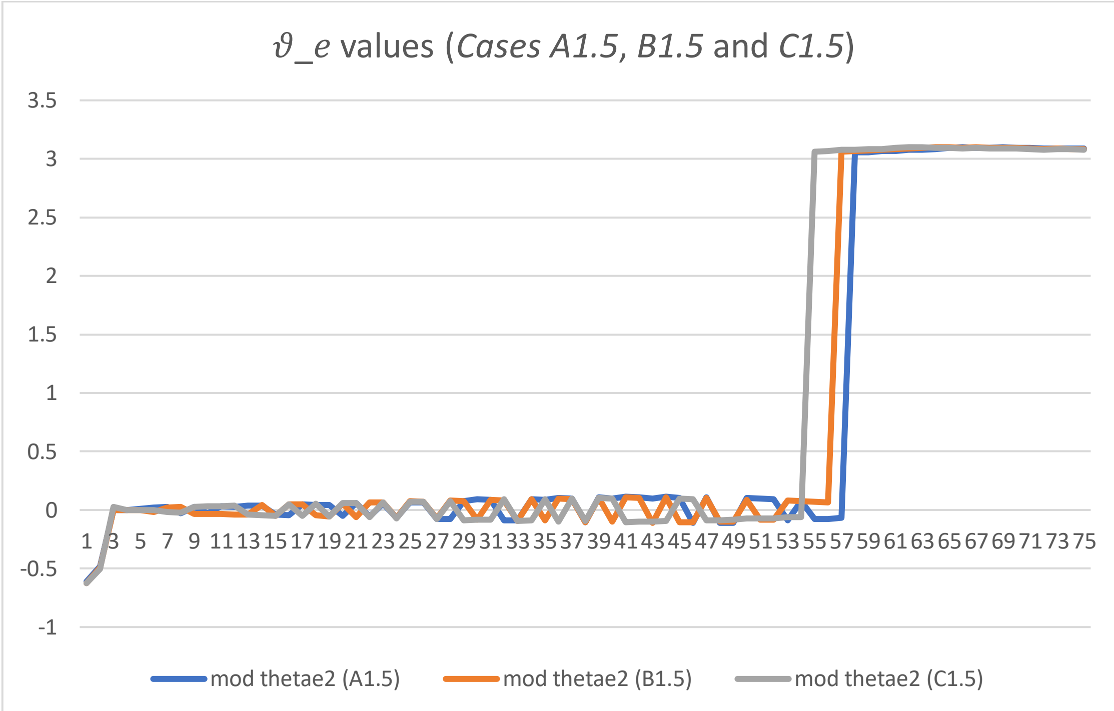

Figure 103. ϑ_e values comparison with i=1.5° - Aphelion

As it is easy to notice, excluding some oddities for the very first fictitious asteroids, ϑ_e perfectly follows the trend of the thrust verse in each *case* and assumes the values that are predicted by the theory for certain segments of the graph, i.e., $\vartheta_e \cong 0$ where $verse = 1$ and $\vartheta_e \cong \pi$ where $verse = -1$. The transition between these values occurs at exactly the same asteroids it occurs for the thrust verse.

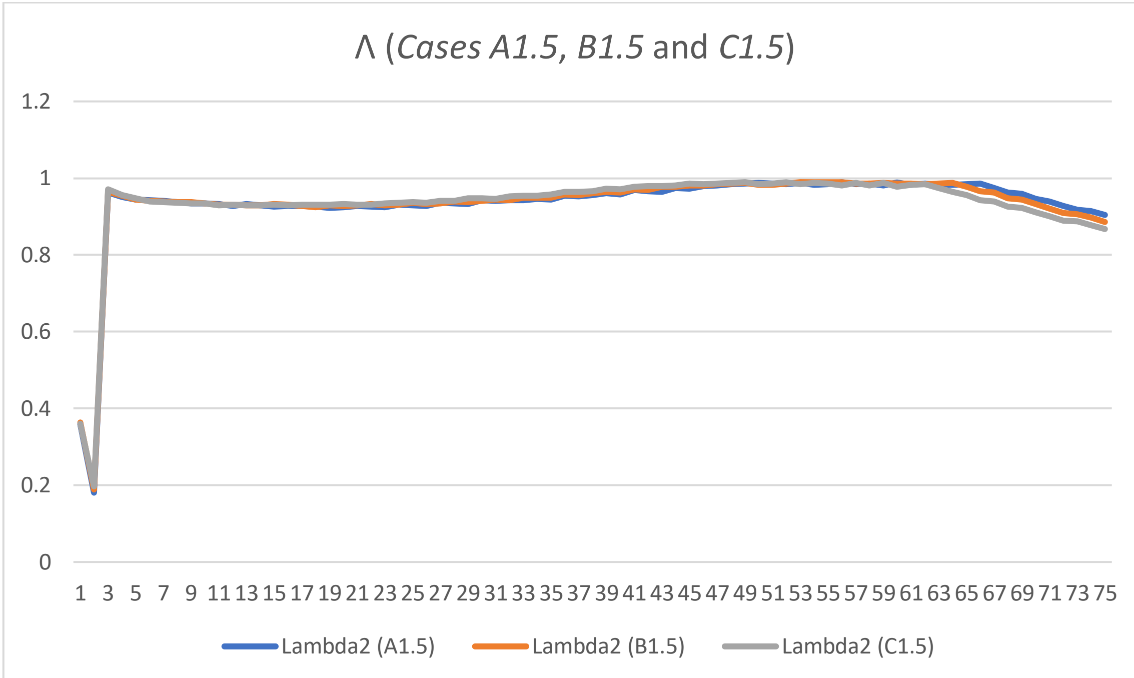

Figure 104. Λ values comparison with i=1.5° - Aphelion

Λ values are very high with $i = 1.5°$. In fact, except for the first section, for about 60 asteroids for case C1.5, 65 for B1.5 and 67 for A1.5 it is in a range between 0,92-0,97. It is interesting to see the evolution of this parameter in the following cases to understand how the inclination affects it.

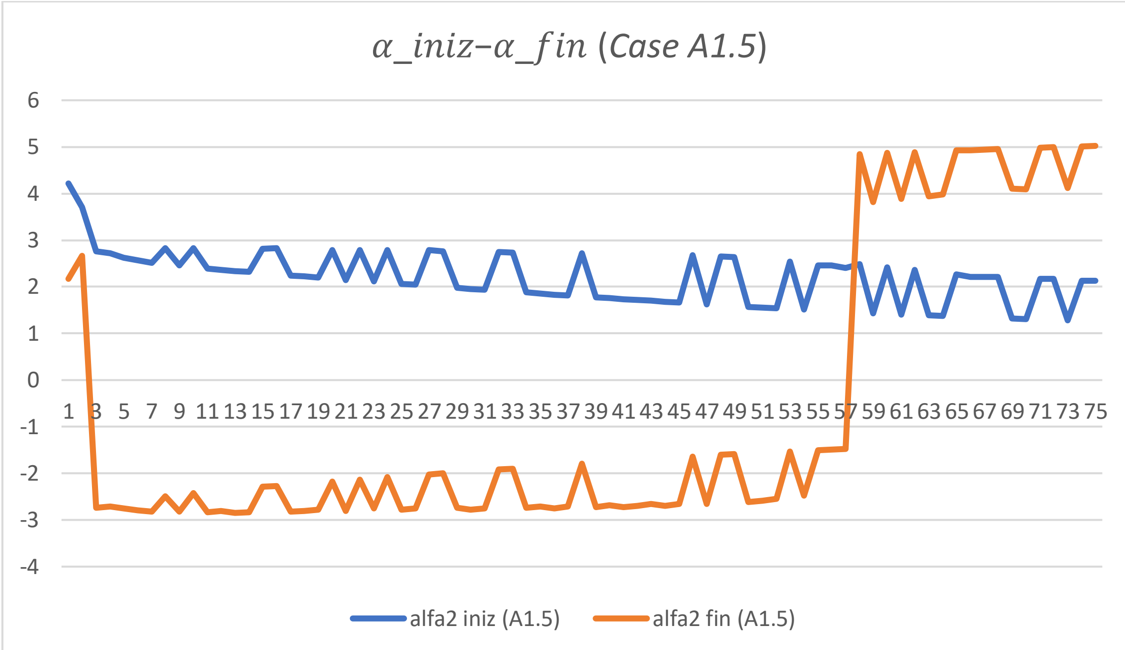

Figure 105. α_iniz-α_fin values for Case A1.5 - Aphelion

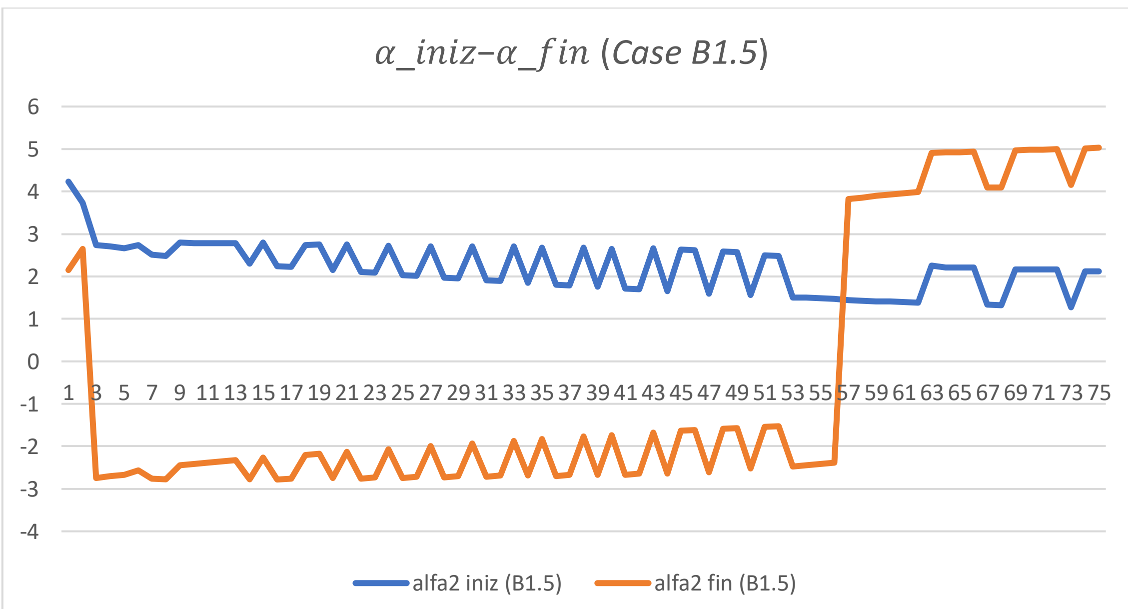

Figure 106. $\alpha\_iniz\text{-}\alpha\_fin$ values for Case B1.5 – Aphelion

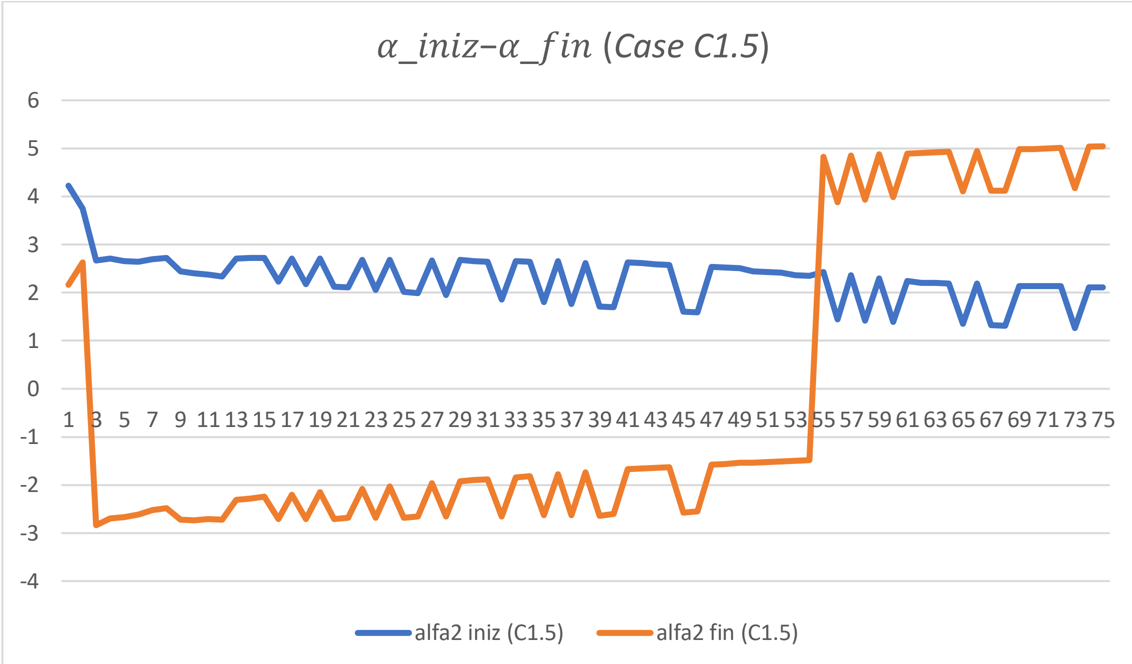

Figure 107. α_iniz–α_fin values for Case C1.5 - Aphelion

By observing these graphs, it is already possible to guess in which area of them there is the optimal solution. In fact, the expected solution foresees $\alpha_{fin} > \alpha_{iniz}$ and it is the current situation for the last few asteroids in each graph. However, what happens in the initial and central sections can be safely considered a suboptimal solution since ϑ_e is in a range of the value predicted by the theory in relation to $verse$, but $\alpha_{fin} < \alpha_{iniz}$.

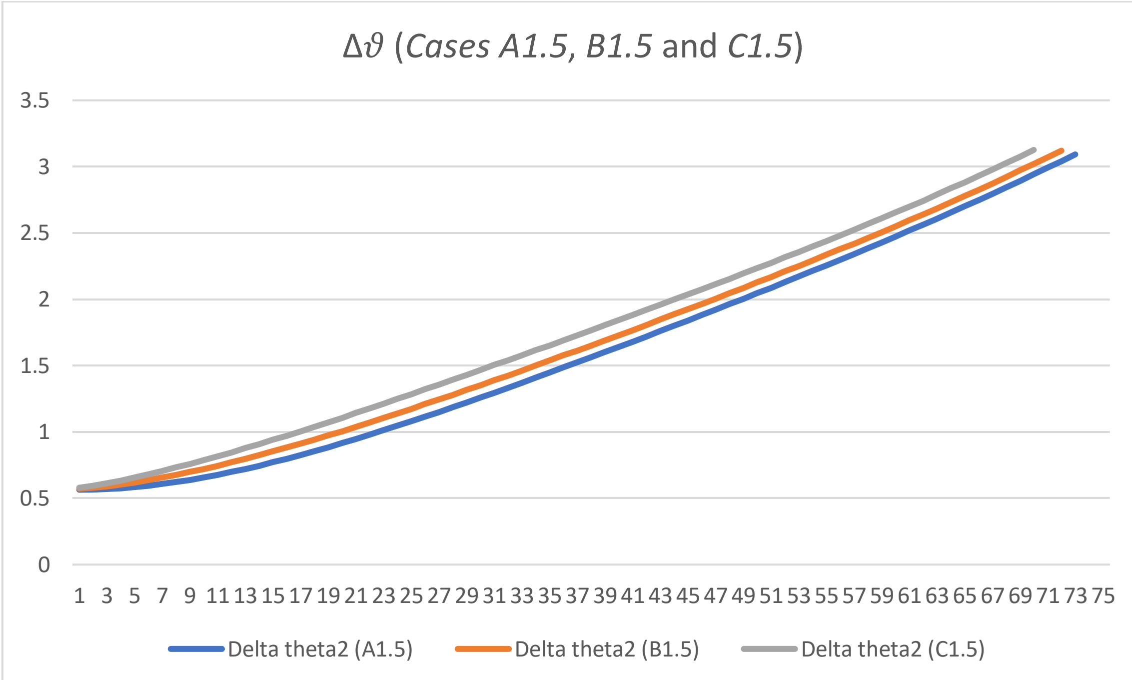

Figure 108. $\Delta\vartheta$ values comparison with i=1.5° - Aphelion

About the burn arc angular lengths in aphelion, the concept is the same as in the aphelion maneuver for *cases* with variable inclination (chapter 2, section 2.4, paragraph 2.4.2): if $\vartheta_{fin} < \vartheta_{iniz}$, then 2π is added to ϑ_{fin} (i.e., ϑ_{fin}=$\vartheta_{fin,iniz} + 2\pi$) and one consequently has $\Delta\vartheta = \vartheta_{fin} - \vartheta_{iniz}$ reported between 0 and 2π, but if $\Delta\vartheta > \pi$ the result is not shown as it does not fall within one of the hypotheses of validity of the method. The trends show an almost perfect symmetry with respect to the $\Delta\vartheta$ values shown in the perihelion maneuver with the same *cases*. In fact, the interruption occurs at asteroid #74 for case A1.5 (in perihelion, at #73), at #73 for B1.5 (in perihelion, at #72) and at #71 for C1.5 (in perihelion, at #70).

3.3.1.1 The relations between ϑ_e, ϑ_{iniz} and ϑ_{fin}, α_{iniz} and α_{fin}

In aphelion, one has to take into account the thrust verse to understand where the optimal solution is.

- *Case A1.5*

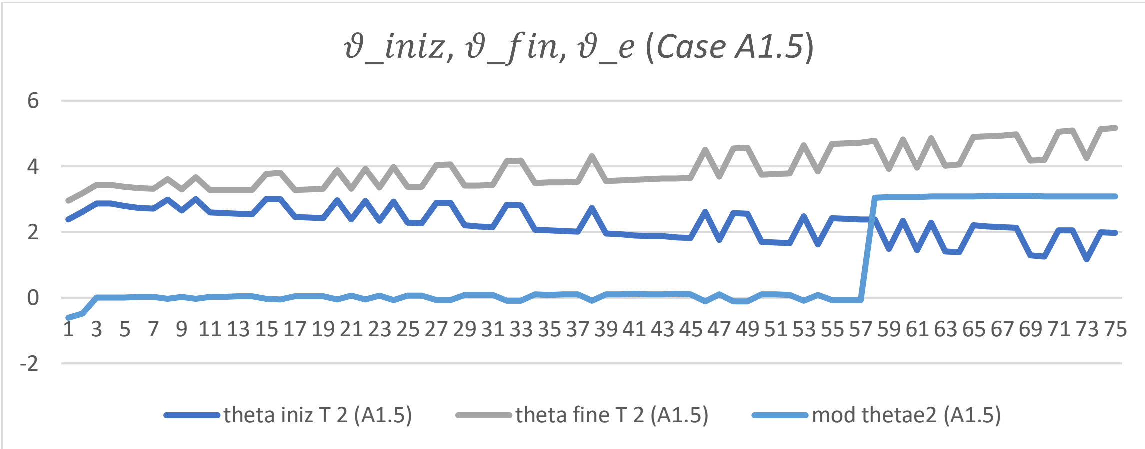

Figure 109. ϑ_iniz, ϑ_fin, ϑ_e values for Case A1.5 - Aphelion

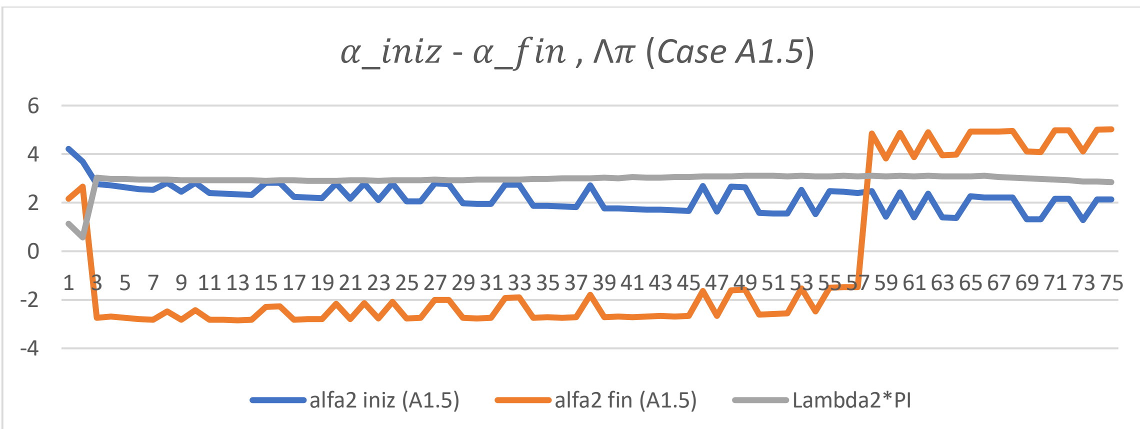

Figure 110. α_iniz - α_fin, $\Lambda\pi$ values for Case A1.5 - Aphelion

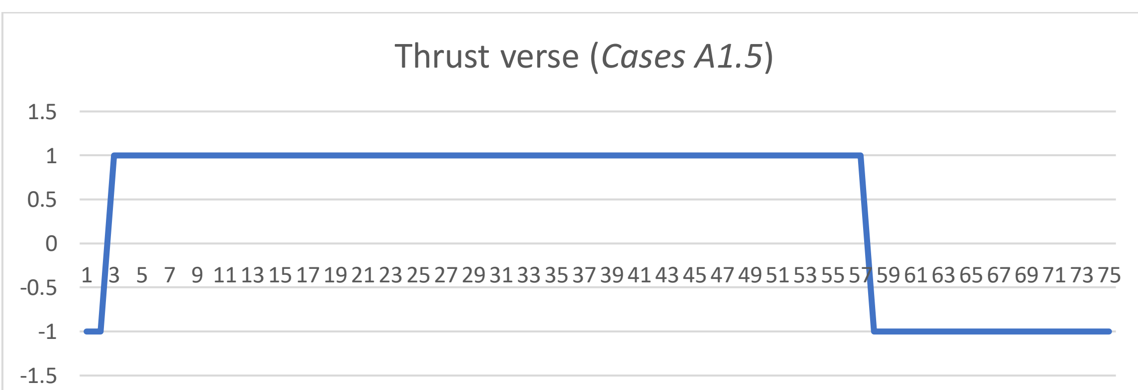

Figure 111. Thrust verse for Case A1.5 – Aphelion

➢ *Case B1.5*

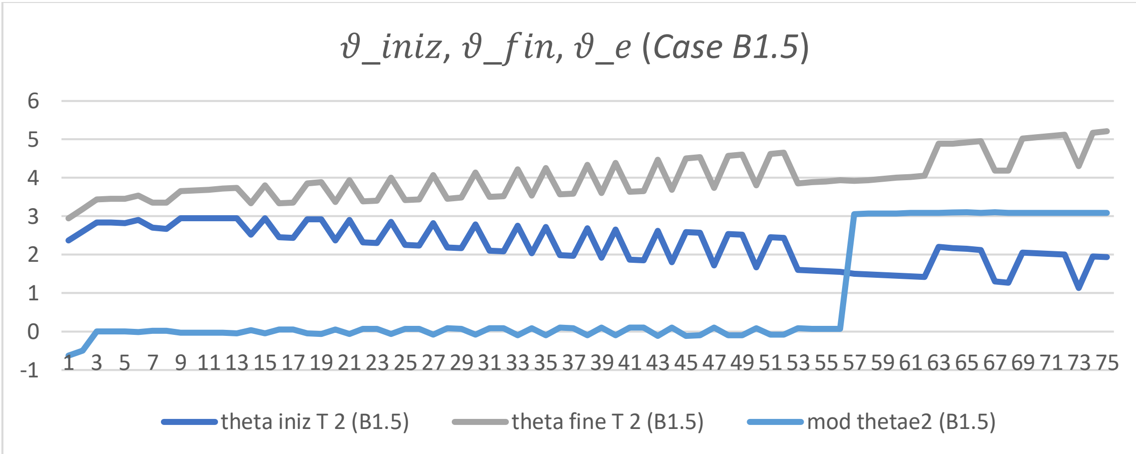

Figure 112. ϑ_iniz, ϑ_fin, ϑ_e values for Case B1.5 - Aphelion

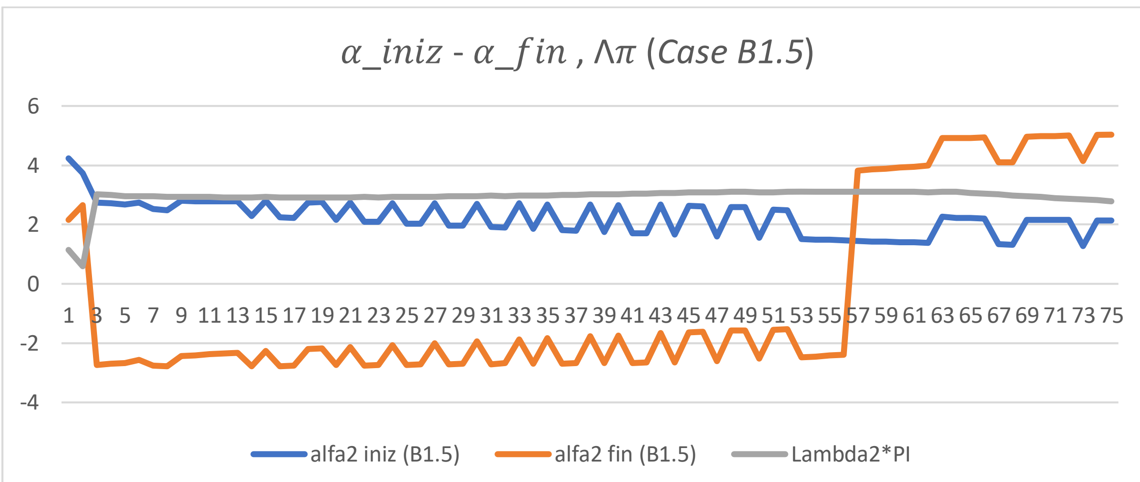

Figure 113. α_iniz - α_fin, $\Lambda\pi$ values for Case B1.5 - Aphelion

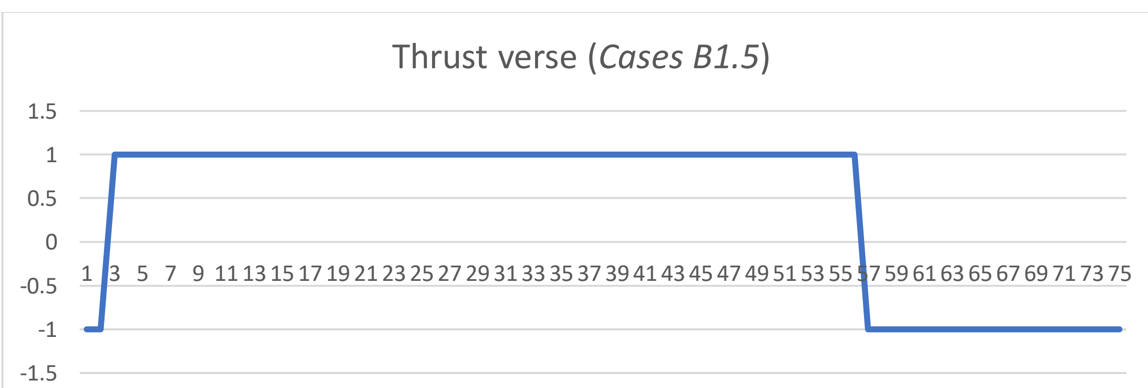

Figure 114. Thrust verse for Case B1.5 - Aphelion

- *Case C1.5*

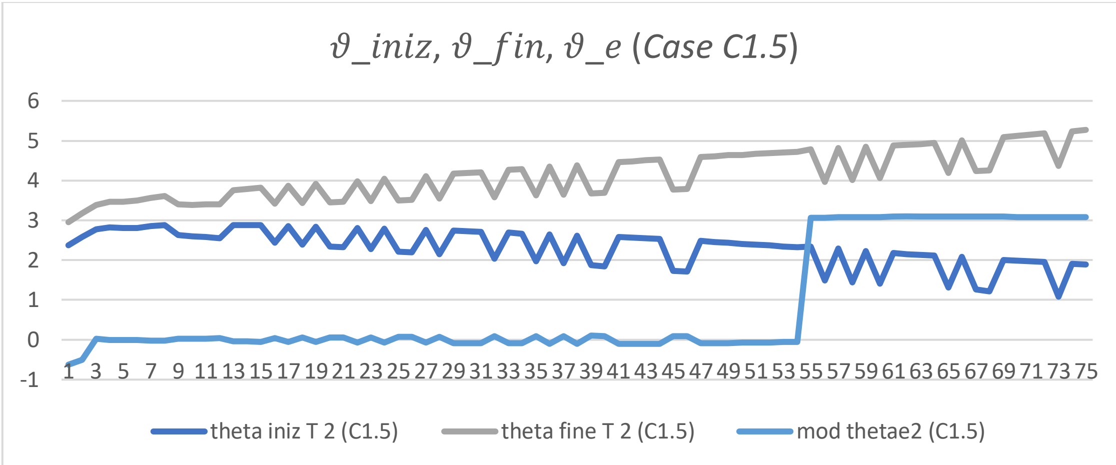

Figure 115. $\vartheta\_iniz, \vartheta\_fin, \vartheta\_e$ values for Case C1.5 - Aphelion

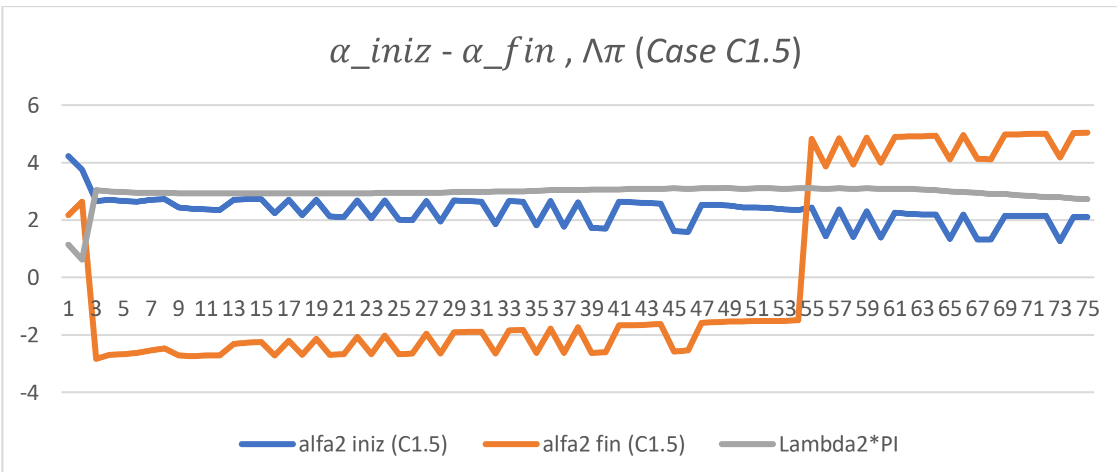

Figure 116. α_iniz - α_fin, $\Lambda\pi$ values for Case C1.5 – Aphelion

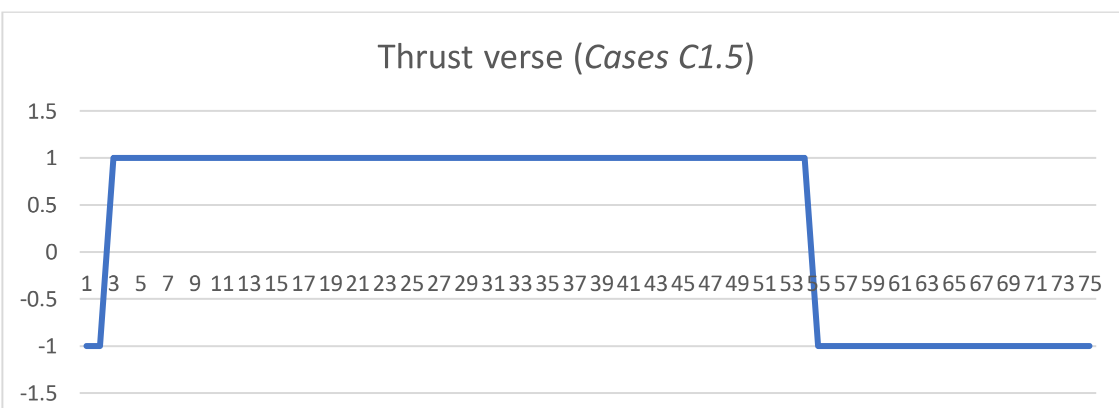

Figure 117. Thrust verse for Case C1.5 - Aphelion

From these graphs is clearly possible to see what one could only guess from $\alpha_{iniz} - \alpha_{fin}$ graphs. There is indeed an area where $\vartheta_e \in [\vartheta_{iniz}; \vartheta_{fin}]$ and $\alpha_{fin} > \alpha_{iniz}$, which is in the right stretch and corresponds to the latter asteroids of the group. It can also be understood from the trends that both ϑ and α are centered in π (in addition of course to ϑ_e), hence the maneuver theoretically foreseen is *braking* and the optimal solutions are in the zones of the graphs which corresponds to $verse = -1$. It also seems correct that $\Lambda\pi$ is between α_{fin} and α_{iniz} trends where the expected solution is present, since when $verse = -1$ one has $\Delta a < 0$ and of course $\alpha = \pi + \Lambda(\vartheta - \vartheta_e)$ [2], and whereas $\Lambda\pi$ is the maximum value that $\Lambda(\vartheta - \vartheta_e)$ can reach (and never touches it). Therefore, calculating α_{fin} it is plausible to think that by adding π to $\Lambda(\vartheta - \vartheta_e)$ then $\alpha_{fin} > \Lambda\pi$, at least in the area with the expected solution. In the central area it seems instead, at least in terms of α, that the algorithm chooses the maneuver centered in 0, but and $\alpha_{fin} < \alpha_{iniz}$. It probably is a suboptimal answer of the problem and further studies may show why the code chooses an unexpected solution for these asteroids.

3.3.2 $\boldsymbol{i = 3°}$

Now *cases* with $i = 3°$ are treated.

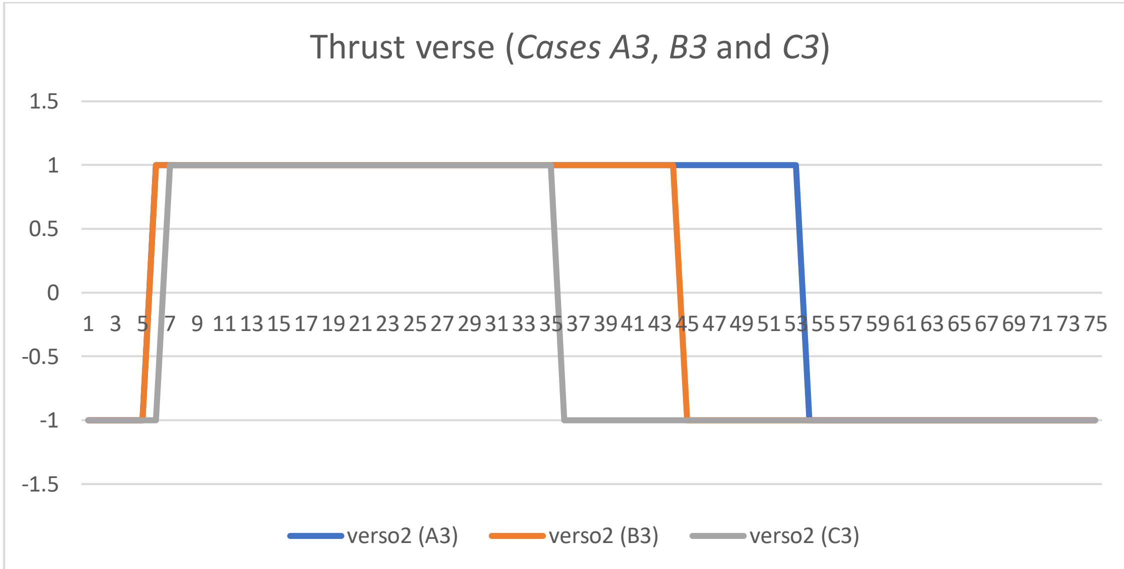

Figure 118. Thrust verse values comparison with i=3° - Aphelion

The increase in inclination already shows some significant changes in the thrust verses, at least as regards the transition and the asteroid to which it occurs. In fact, while the transition for *cases A1.5*, *B1.5* and *C1.5* is compressed into a small range of asteroids (respectively #59, #58 and #56), now it is anticipated in each case and the asteroids to which it occurs are farther away from each other (#55, #45 and #37). In addition to the inclination, the positive influence of the non-zero RAAN on the response must be mentioned since cases B3 and especially C3 ($\Omega = \pi/2$) have many more fictitious asteroids with the expected solution.

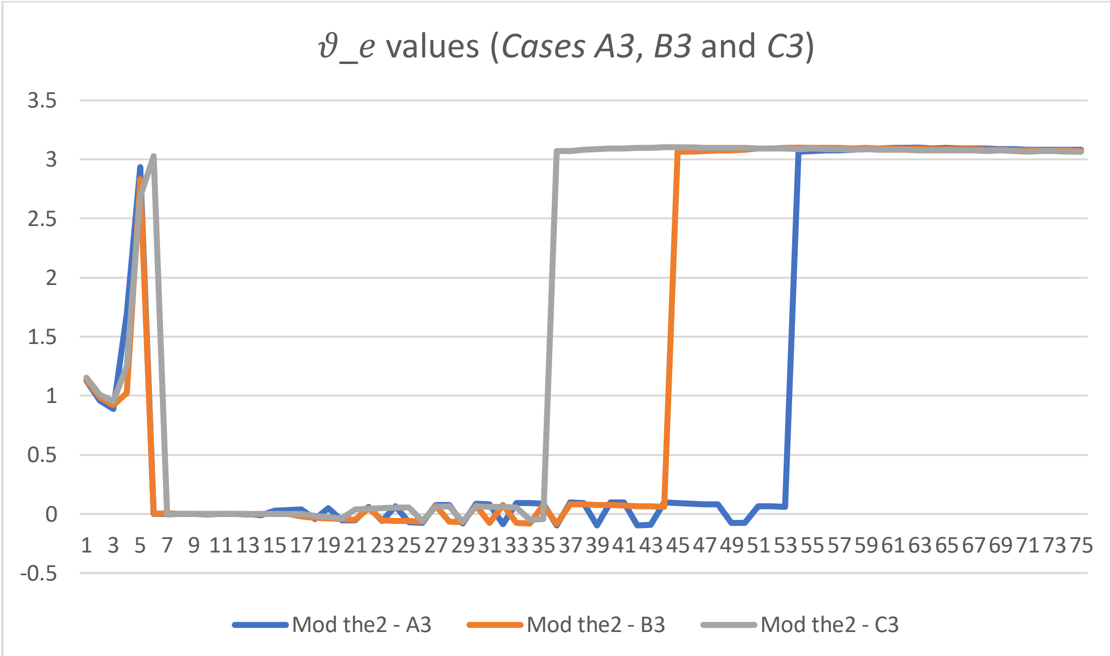

Figure 119. ϑ_e values comparison with i=3° - Aphelion

Not taking into consideration an initial fluctuation of the results (probably due to the proximity of the two possible answers at the first asteroids of the set), ϑ_e essentially follows the path of the trust verses, being close to 0 where $verse = 1$ while it is in a range of π where $verse = -1$, and having a transition that starts at the same asteroid to which, for each *case*, the transition of $verse$ occurs.

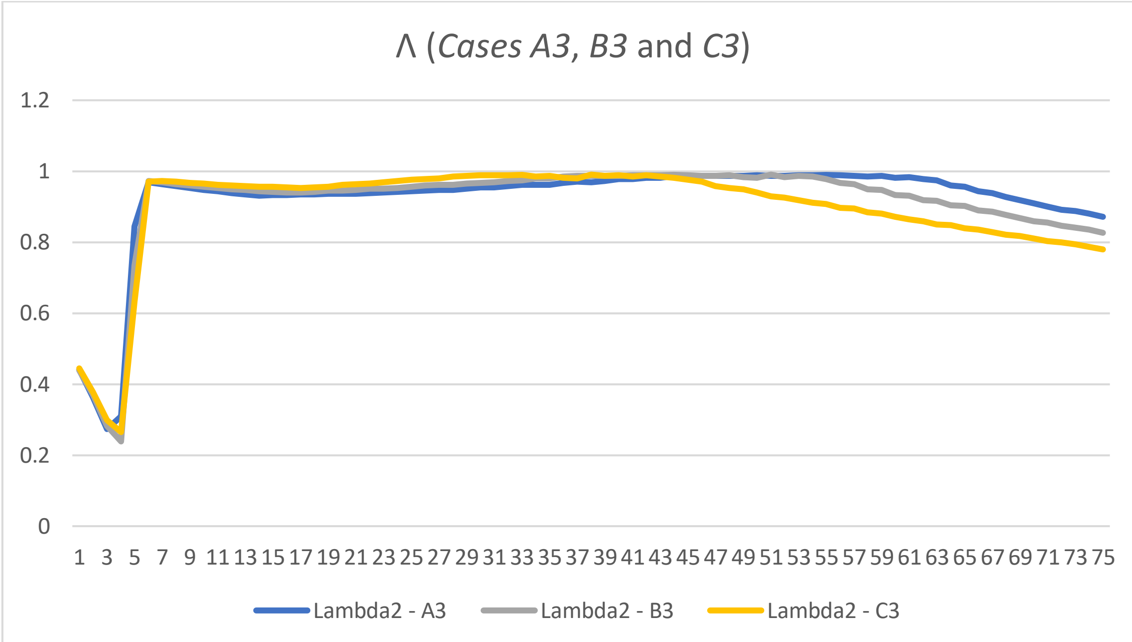

Figure 120. Λ values comparison with i=3° - Aphelion

Λ trends do not change very much with respect to the trends with $i = 1.5°$. Values are still very high in almost the whole set, but approximately starting from a close asteroid to which, for each case, the transition of $verse$ and ϑ_e takes place, Λ begin to slightly decrease.

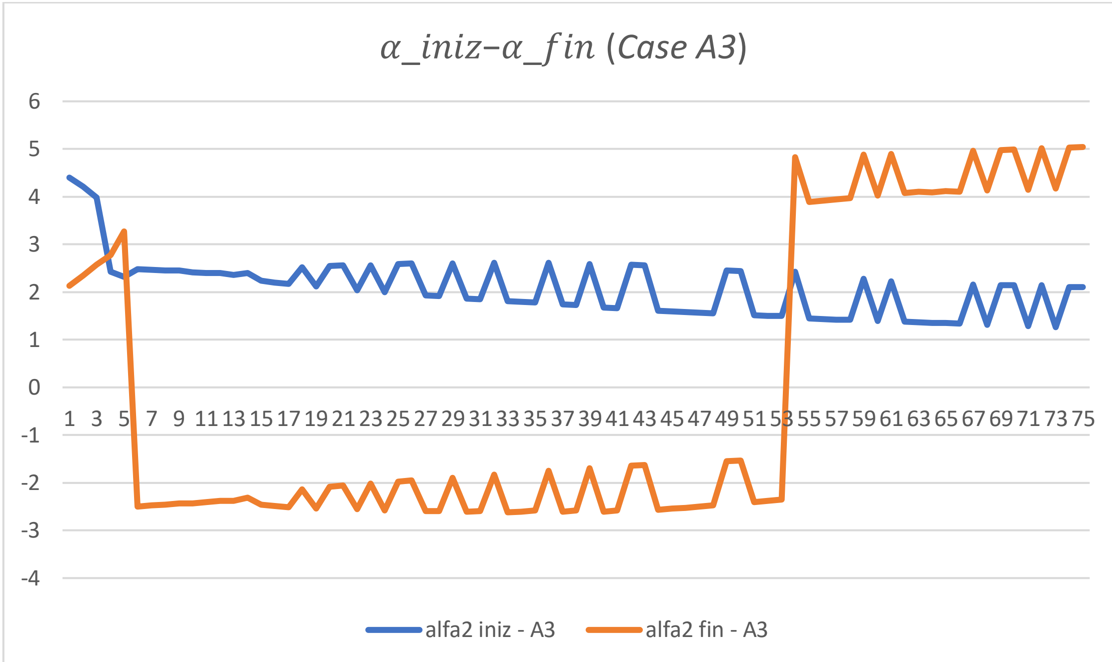

Figure 121. $\alpha\_iniz{-}\alpha\_fin$ values for Case A3 – Aphelion

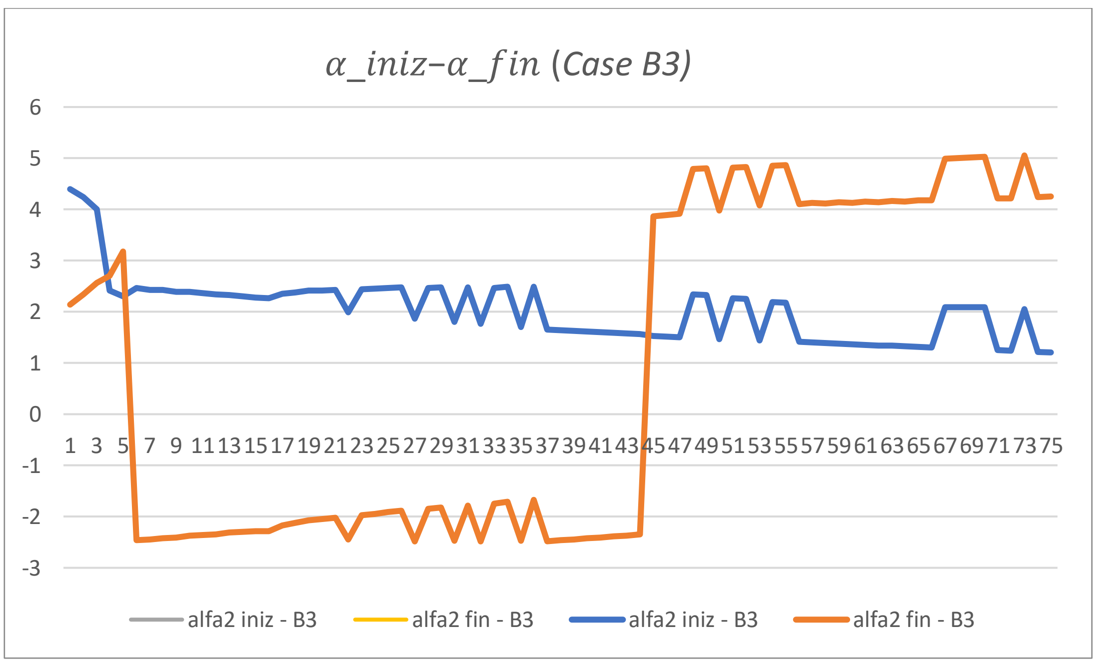

Figure 122. $\alpha\_iniz{-}\alpha\_fin$ values for Case B3 – Aphelion

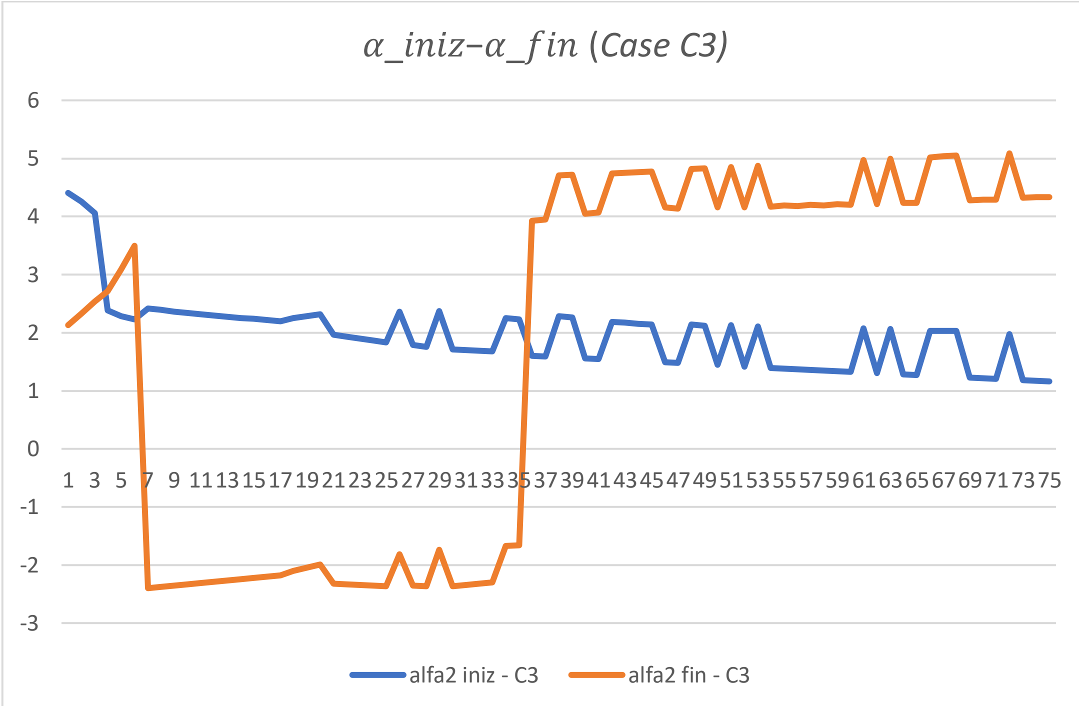

Figure 123. $\alpha\_iniz{-}\alpha\_fin$ values for Case C3 - Aphelion

The areas to the right of the graphs in which the foreseen solution is present is larger by increasing the inclination to 3°. Even here, except for the first zone in which there are oscillating values, two distinct areas can be distinguished: the central area with $\alpha_{fin} < \alpha_{iniz}$ and the final area with the farthest fictitious asteroids from Earth with $\alpha_{fin} > \alpha_{iniz}$. The influence of $\Omega \neq 0$ is also clearly visible in these trends.

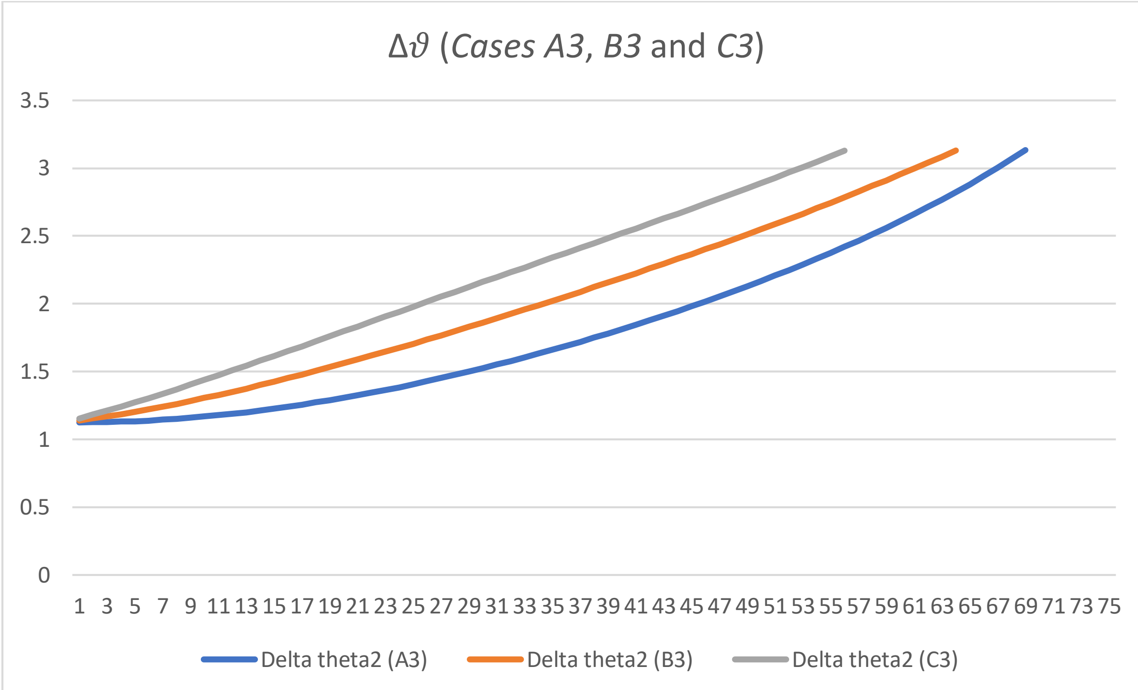

Figure 124. Δϑ values comparison with i=3° - Aphelion

The symmetry with the same maneuver in perihelion is clearly visible and almost perfect: the transition between asteroids with $\Delta\vartheta < \pi$ and $\Delta\vartheta > \pi$ basically occurs at the same asteroid for each *case*. A small curiosity is now reported: *case A3* is the only one where $\vartheta_{fin} > \vartheta_{iniz}$ always, instead of *B3* and *C3* in which the usual correction must be imposed for almost di entire set of asteroids.

3.3.2.1 The relations between ϑ_e, ϑ_{iniz} and ϑ_{fin}, α_{iniz} and α_{fin}

The fundamental parameters for the estimation have reported visible variations compared to the cases with $i = 1.5°$. Now one can see what happens to their particular relations.

- *Case A3*

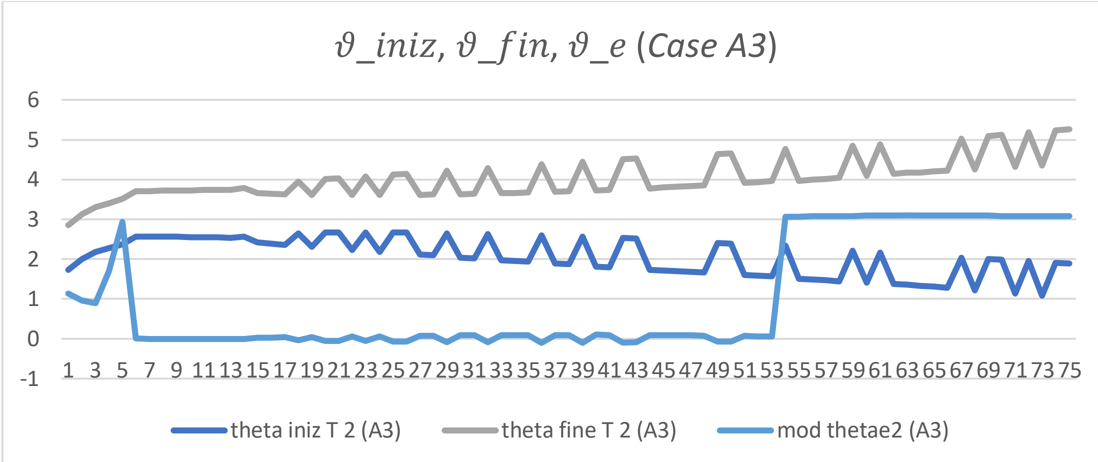

Figure 125. ϑ_iniz, ϑ_fin, ϑ_e values for Case A3 - Aphelion

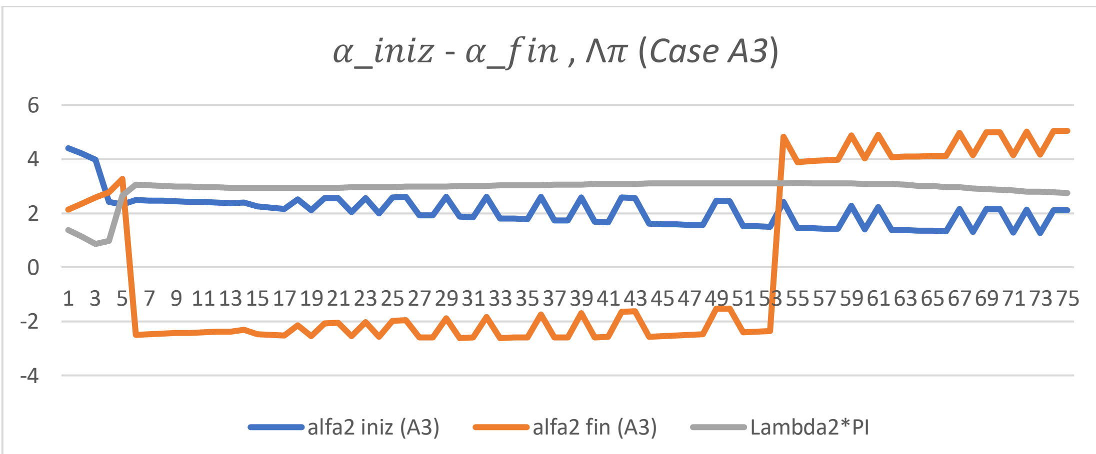

Figure 126. α_iniz - α_fin, $\Lambda\pi$ values for Case A3 – Aphelion

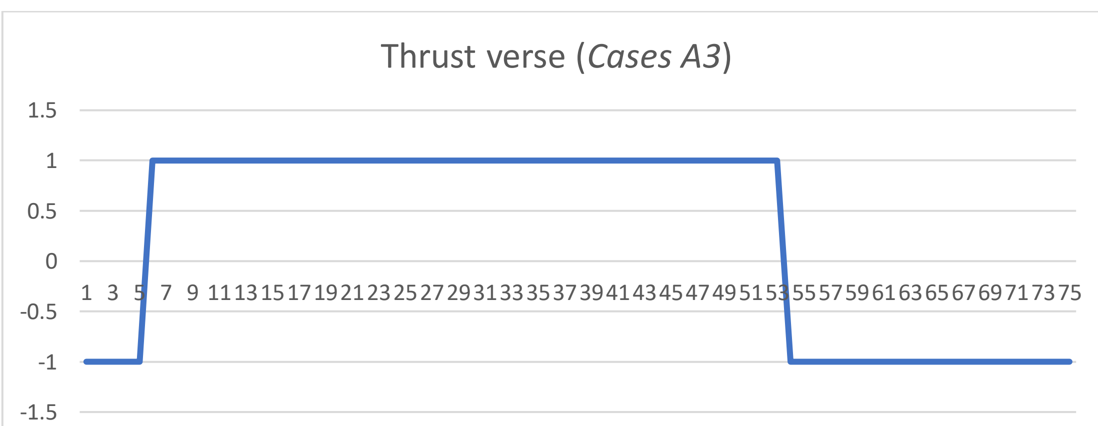

Figure 127. Thrust verse for Case A3 – Aphelion

➢ *Case B3*

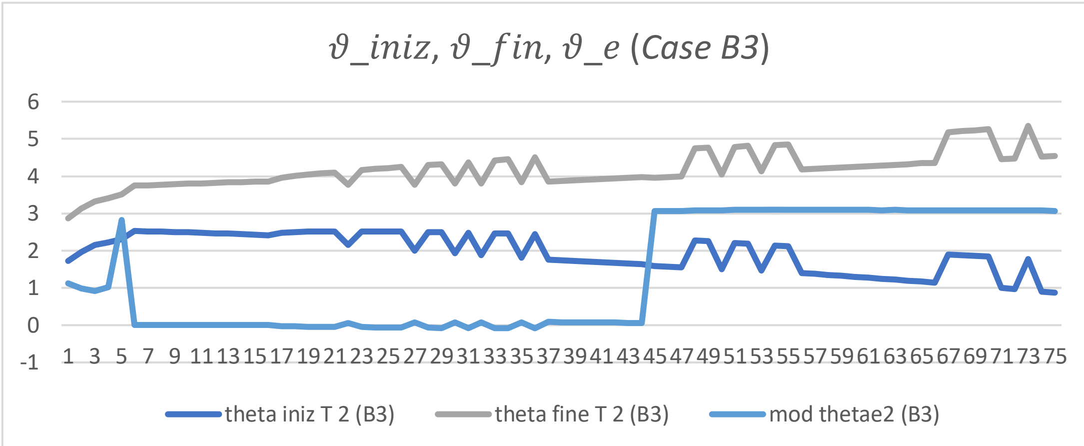

Figure 128. ϑ_iniz, ϑ_fin, ϑ_e values for Case B3 - Aphelion

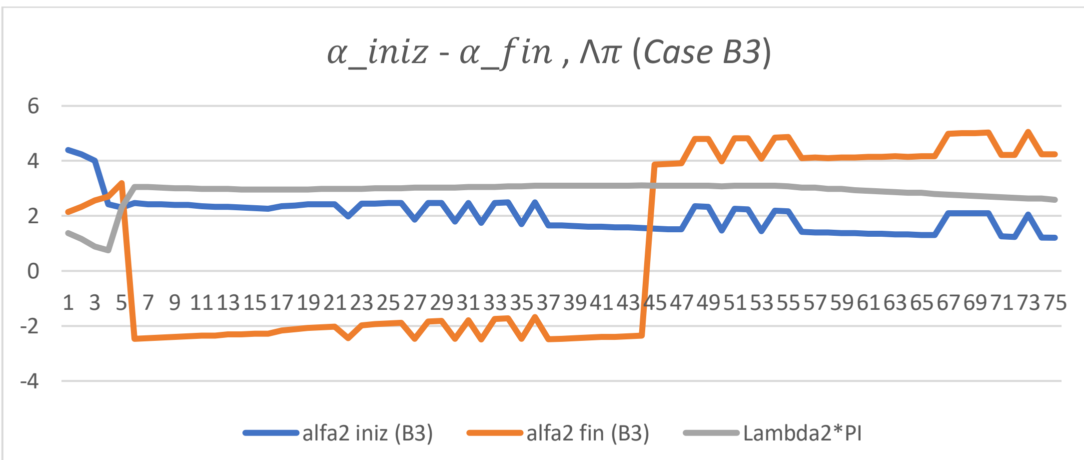

Figure 129. α_iniz - α_fin, $\Lambda\pi$ values for Case B3 - Aphelion

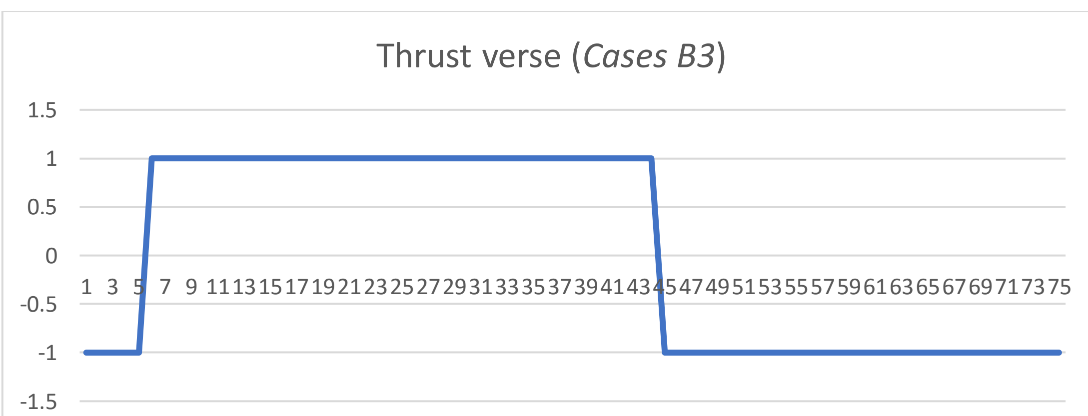

Figure 130. Thrust verse for Case B3 – Aphelion

➢ *Case C3*

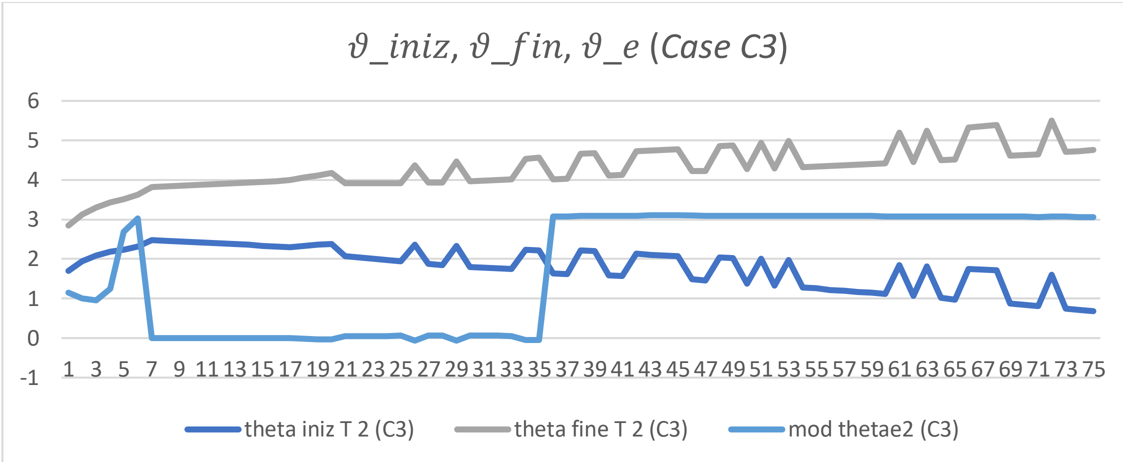

Figure 131. $\vartheta\_iniz, \vartheta\_fin, \vartheta\_e$ values for Case C3 - Aphelion

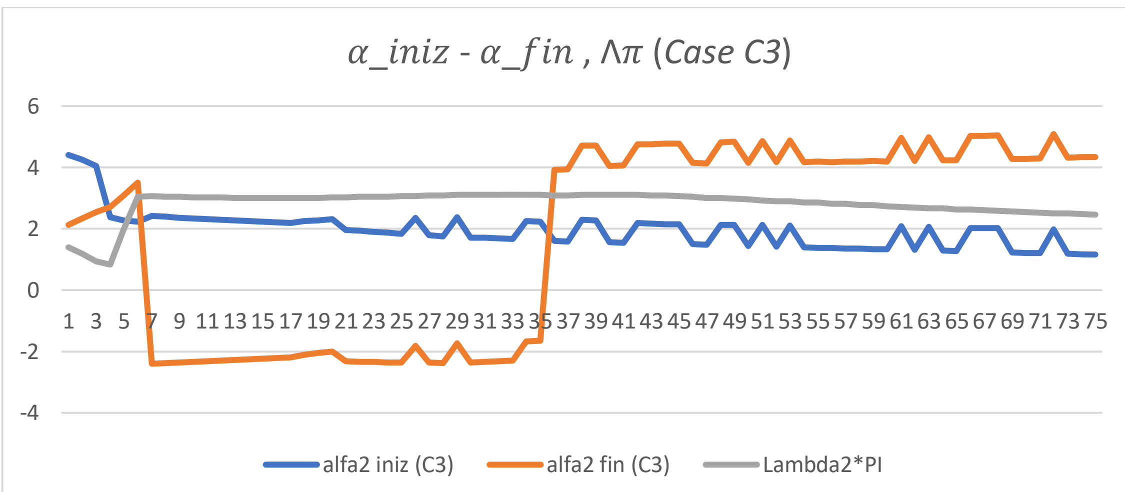

Figure 132. α_iniz - $\alpha\_fin, \Lambda\pi$ values for Case C3 – Aphelion

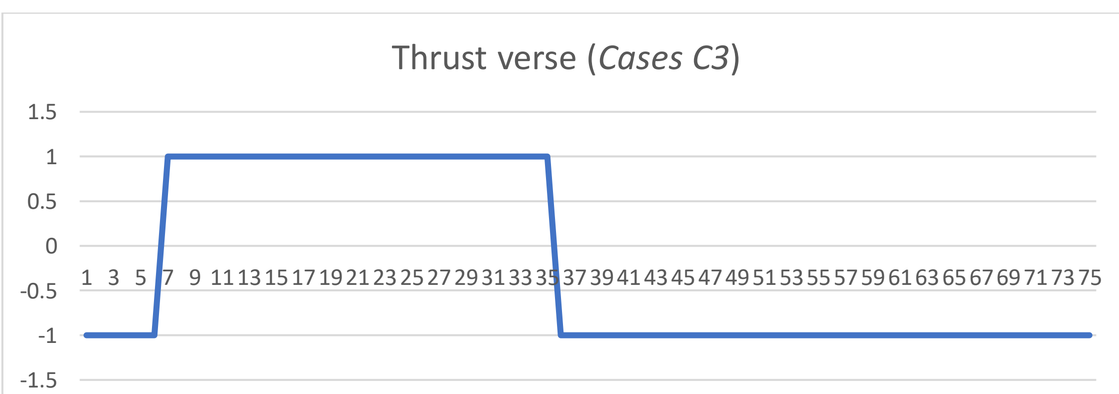

Figure 133. Thrust verse for Case C3 – Aphelion

The situation is basically the same as in the cases dealt with in the previous section, except for the various transitions that take place, as already seen, some asteroids before. The optimal solution is always the one in which the vehicle brakes and is described by $verse = -1$, $\vartheta_e \in [\vartheta_{iniz}; \vartheta_{fin}]$ and $\alpha = \pi + \Lambda(\vartheta - \vartheta_e)$. A detail is very interesting: while with $i = 1.5°$ the trends of α_{iniz} almost touches the asymptotic value $\Lambda\pi$ especially in the central stretch, with $i = 3°$ the values are more spaced. Even Ω, in cases with the same inclination, contributes positively to this by moving α_{iniz} away from the asymptote.

3.3.3 $i = 4.5°$

The aphelion maneuver is analyzed for *cases* with $i = 4.5°$. It is noted from the very first graphs that, especially with regard to a specific case, the increase in inclination made the output results very accurate.

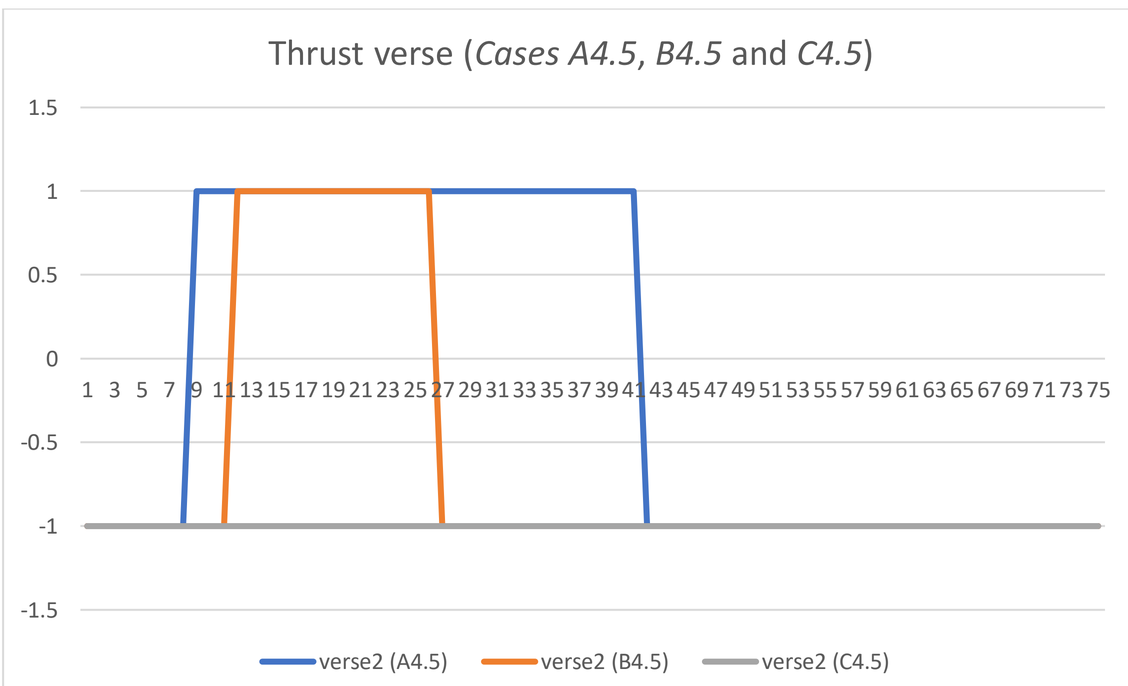

Figure 134. Thrust verse values with i=4.5° - Aphelion

As it is possible to see, while *cases A4.5* and *B4.5* still improve their outcomes not only by anticipating the right transition to a previous asteroid, but also for the actual appearance of the first area of the graph with $verse = -1$, *case C4.5* is the first *case* in the aphelion maneuver discussion to reach, at least in terms of trust verse, the optimal solution for the whole group of 75 asteroids. It is certainly a result for which not only the inclination value, but also the quadrature between the perihelion and the ascending node, heavily contribute.

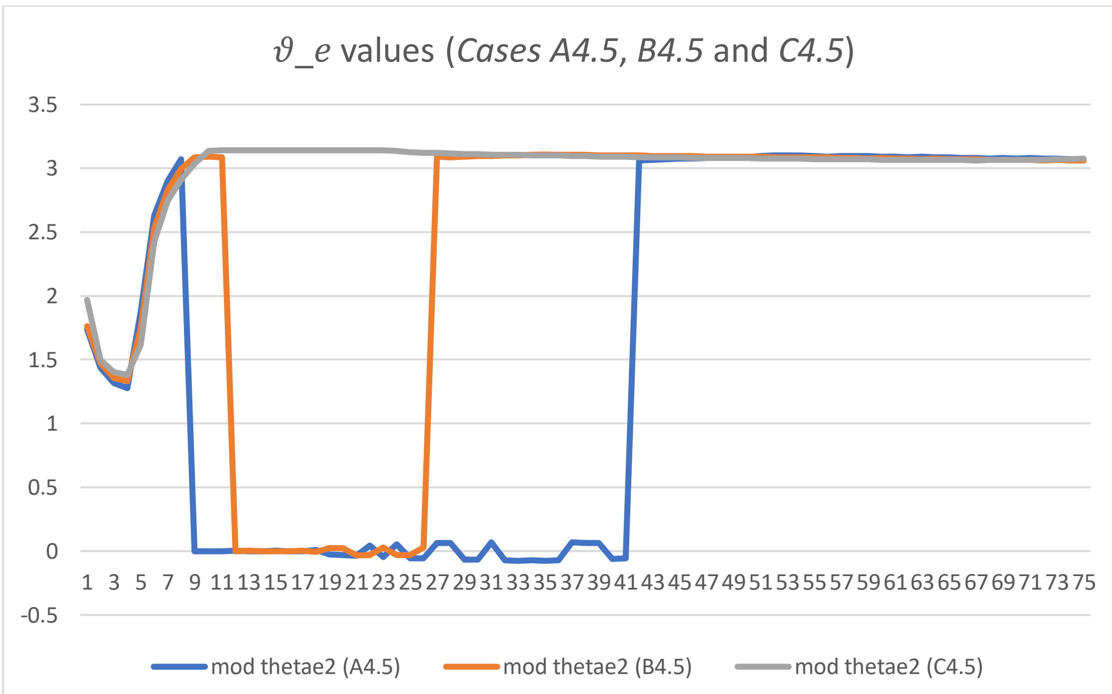

Figure 135. ϑ_e values comparison for i=4.5° - Aphelion

Even the graph with ϑ_e trends is influenced by the thrust verses. In fact, for *cases A4.5* and *B4.5* there is basically a subdivision into three zones: the first one, in which each case starts with a value close to 2 rad, it decreases to a value less the 1,5 rad and then increases to reach π; the second one, that starts immediately after a transition from $\vartheta_e \cong \pi$ to $\vartheta_e \cong 0$; the final one, where a second transition occurs, but this time is from 0 to π. Analyzing just these two cases one can clearly see the contribution of the RAAN, which going from 0 (for *A4.5*) to $\pi/4$ (for *B4.5*) anticipates the second transition of about 15 asteroids with respect to *A4.5*. For *case C4.5* there is an almost total predominance of the answer foreseen by the theory for this maneuver, that is, $\vartheta_e \cong \pi$. In the first section of about 9-11 asteroids, the pattern for *C4.5* is similar to those already analyzed for *A4.5* and *B4.5*.

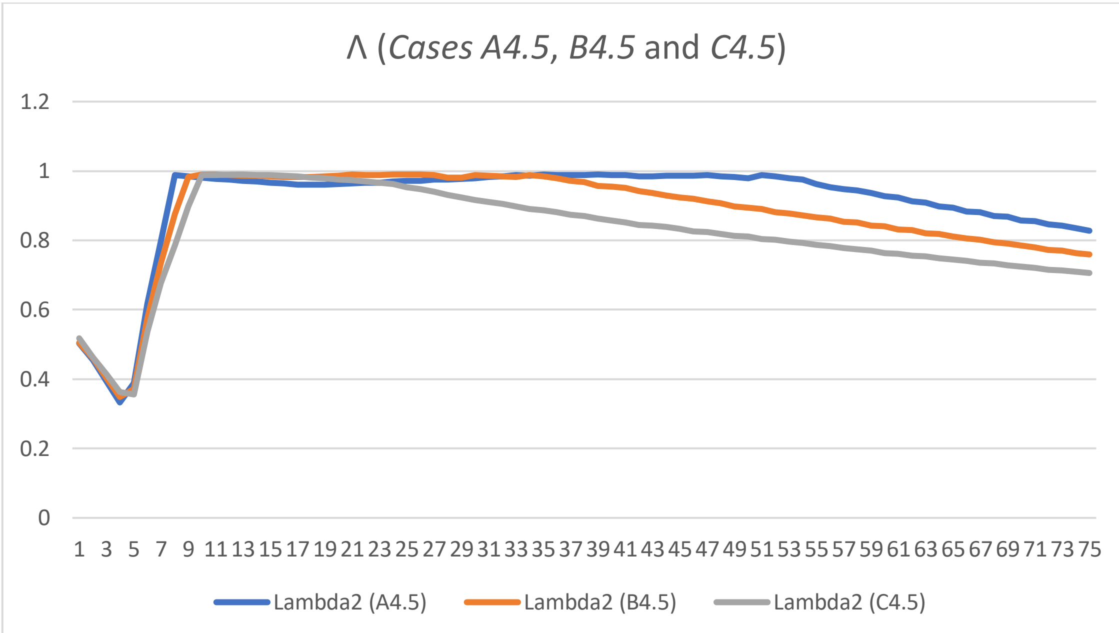

Figure 136. Λ values comparison with i=4.5° - Aphelion

Λ trends for about the first 23 asteroids are identical to those seen with $i = 1.5°$ and $i = 3°$. But even here, together with this inclination value, Ω too gives a huge contribution to improve responses. In fact, the first case to lower its Λ values is C4.5 at asteroid #24, followed by B4.5 at asteroid #37 and A4.5 at asteroid #54. Values remains still high, considering that asteroid #76 in case C4.5 (the best in terms of accurate results with $i = 4.5°$) has $\Lambda = 0{,}70687$.

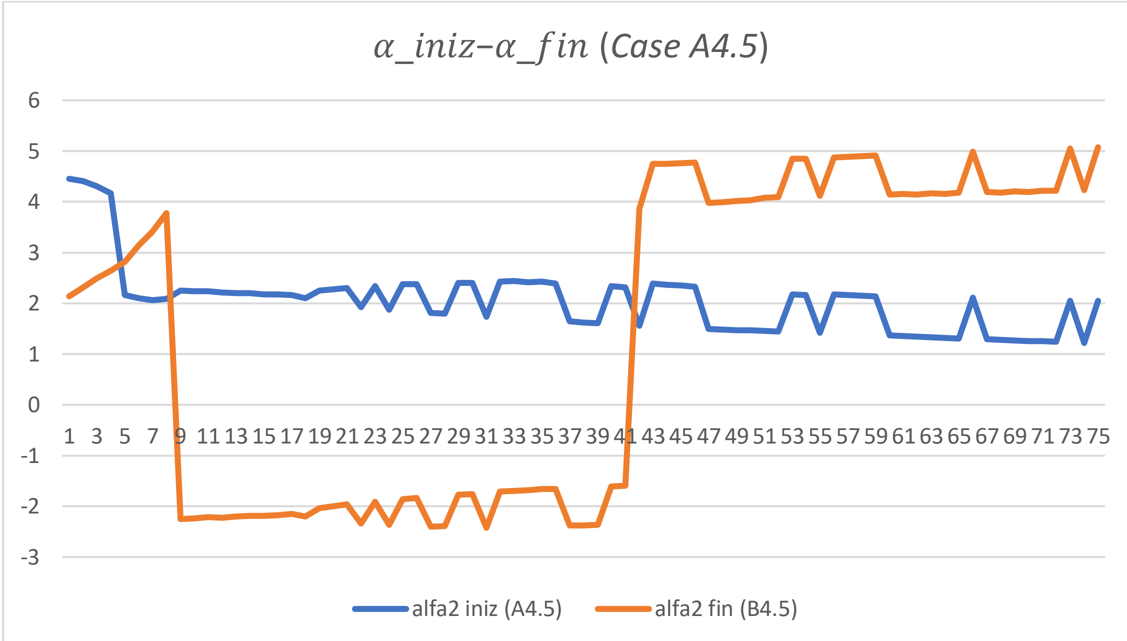

Figure 137. $\alpha\_iniz{-}\alpha\_fin$ *values for Case A4.5 - Aphelion*

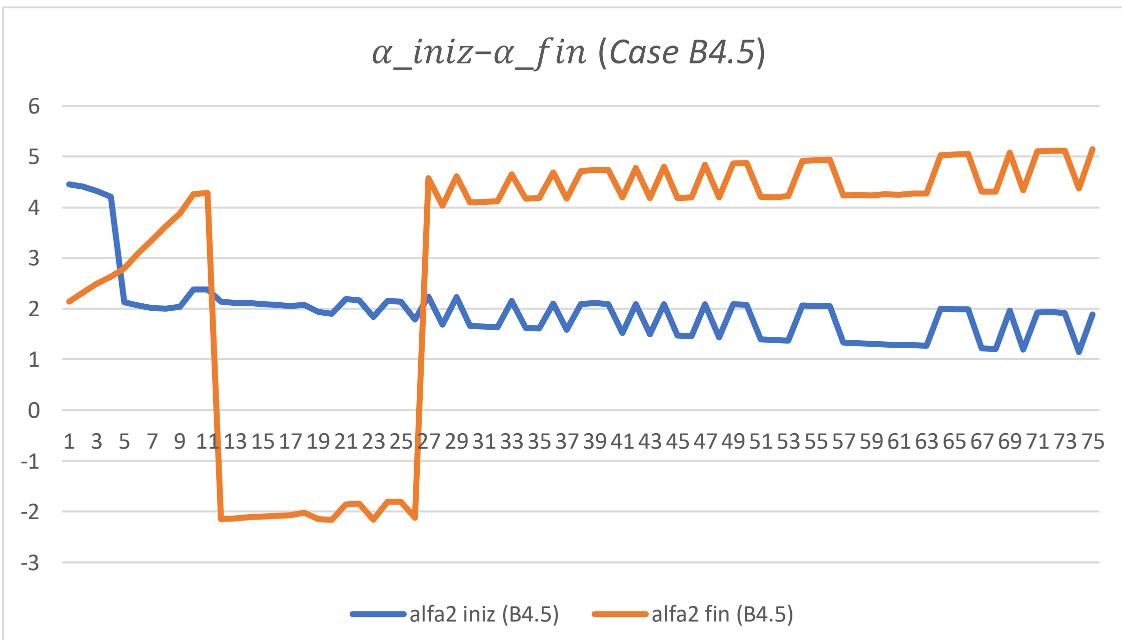

Figure 138. $\alpha\_iniz{-}\alpha\_fin$ *values for Case B4.5 - Aphelion*

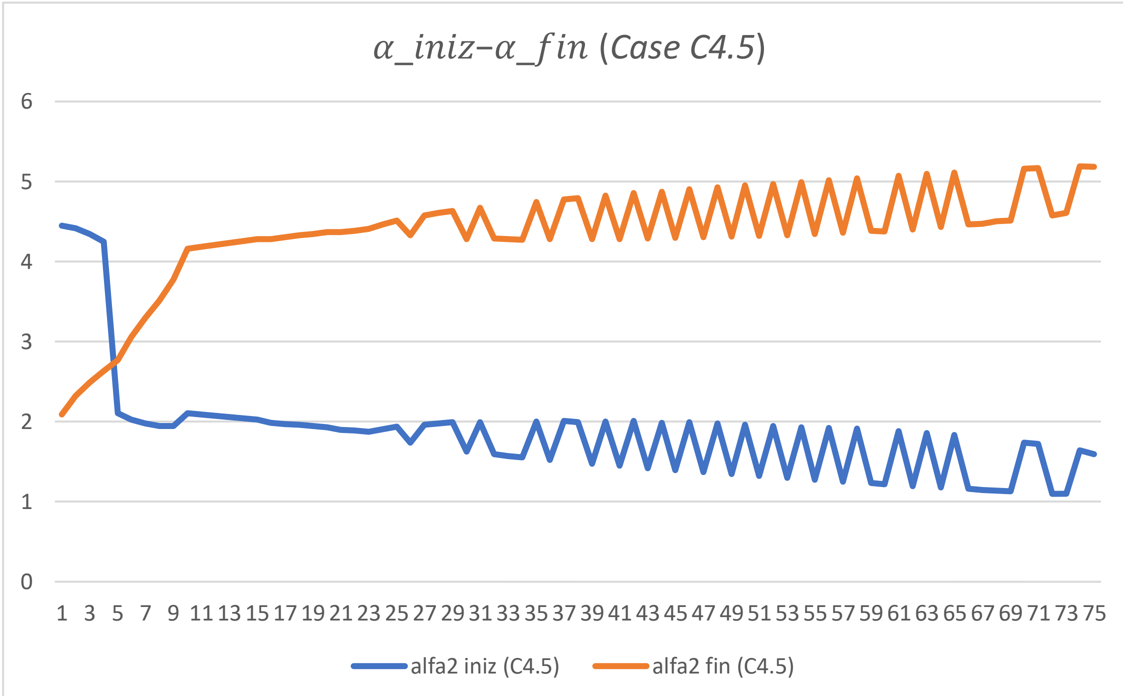

Figure 139. α_iniz−α_fin values for Case C4.5 – Aphelion

Cases A4.5 and B4.5 have similar trends of $\alpha_{iniz} - \alpha_{fin}$. Both have, initially, the first section where the situation is chaotic since probably the two possible solutions are close to each other and the algorithm randomly chooses one instead of the other; then, two well separated and distinct areas are present; the central section, where $\alpha_{fin} < \alpha_{iniz}$, and the final section with the optimal solution $\alpha_{fin} > \alpha_{iniz}$. The only difference is that for A4.5 the optimal solution includes about 34 asteroids, while for B4.5 the asteroids for which $\alpha_{fin} > \alpha_{iniz}$ are about 48. The situation is different for case C4.5 since, except for the now usual initial stretch with some oddities, the entire set of fictitious asteroids present the optimal and expected solution. $i = 4.5°$ and $\Omega = \pi/2$, although are quite significative and hence expensive orbital changes [2], give a huge contribution to the accuracy of the method.

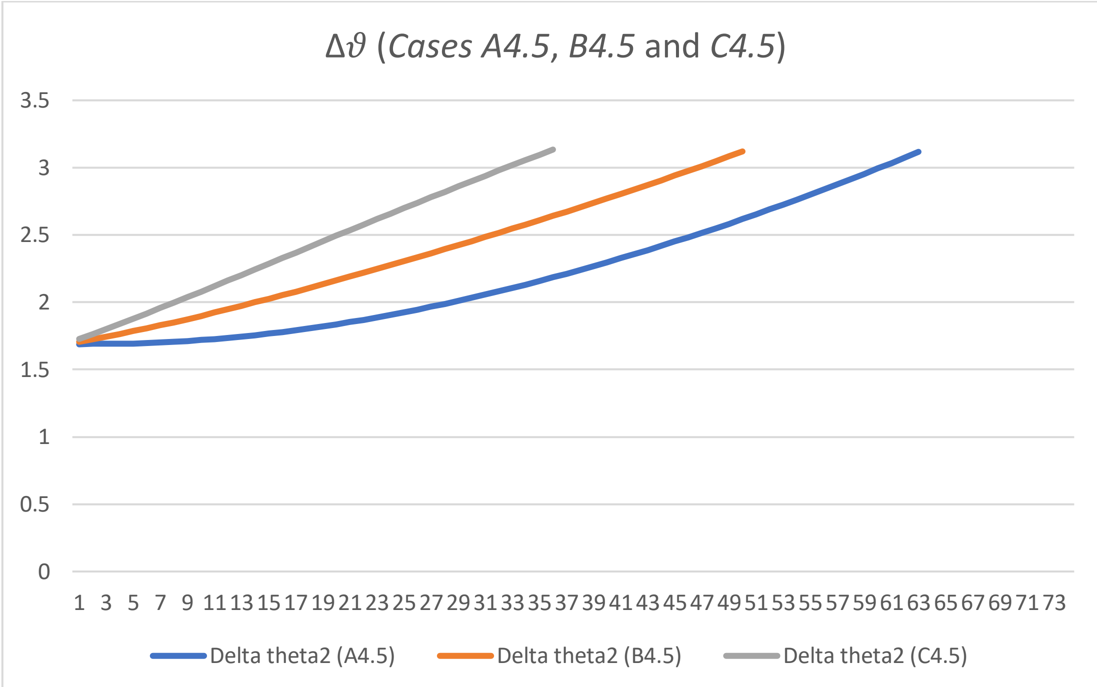

Figure 140. Δϑ values comparison with i=4.5° - Aphelion

Even with this inclination value, there is an almost perfect symmetry between this maneuver and the perihelion maneuver. *Cases A4.5*, *B4.5* and *C.5* have indeed, respectively, 63, 50 and 36 asteroids in which $\Delta\vartheta < \pi$. These numbers of asteroids are basically confirmed in perihelion: 62, 50 and 36. The symmetry between the maneuvers, also considering that the effects of one maneuver on the other (in this case, those of the perihelion maneuver on this one) are neglected [2], is an excellent indicator of overall accuracy for the estimation method.

3.3.3.1 The relations between ϑ_e, ϑ_{iniz} and ϑ_{fin}, α_{iniz} and α_{fin}

The graphs which describe the relations between the fundamental parameters are studied. With $i = 4.5°$, the difference between the various cases is basically evident.

➢ *Case A4.5*

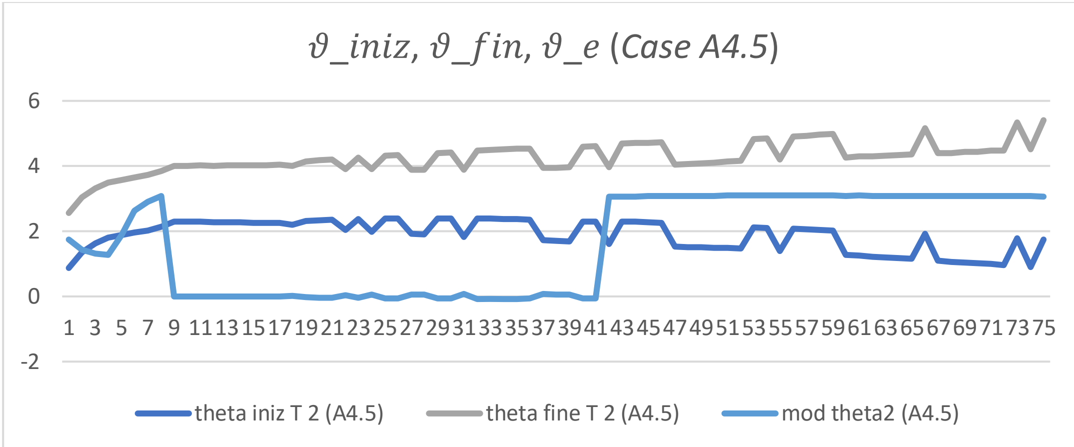

Figure 141. ϑ_iniz, ϑ_fin, ϑ_e values for Case A4.5 - Aphelion

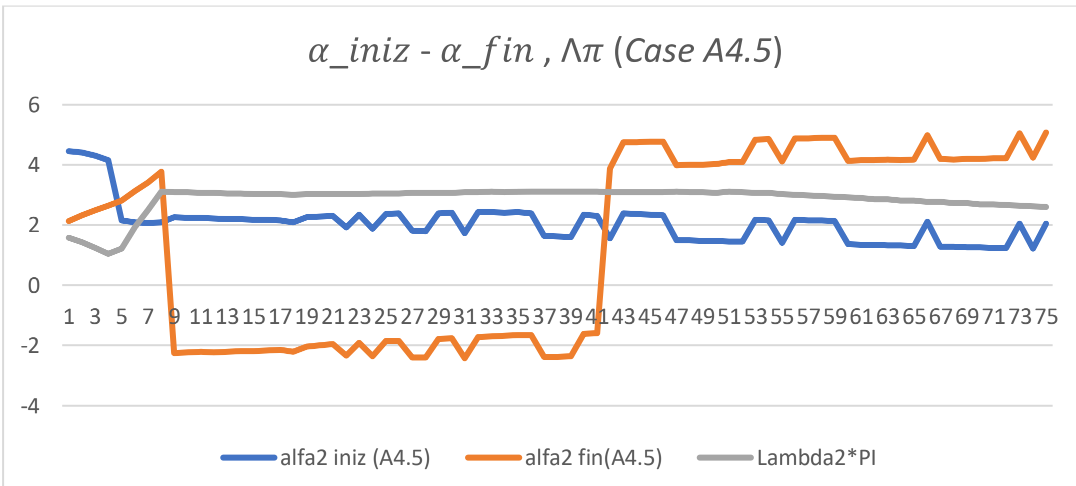

Figure 142. α_iniz - α_fin, $\Lambda\pi$ values for Case A4.5 - Aphelion

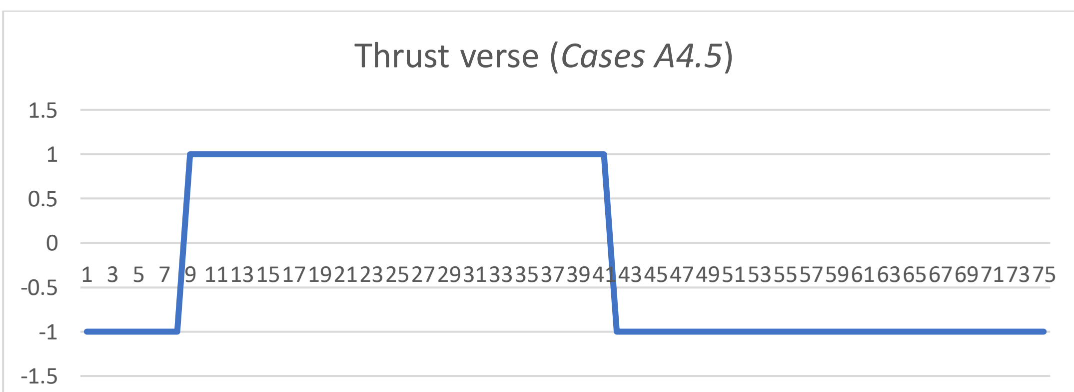

Figure 143. Thrust verse for Case A4.5 - Aphelion

- *Case B4.5*

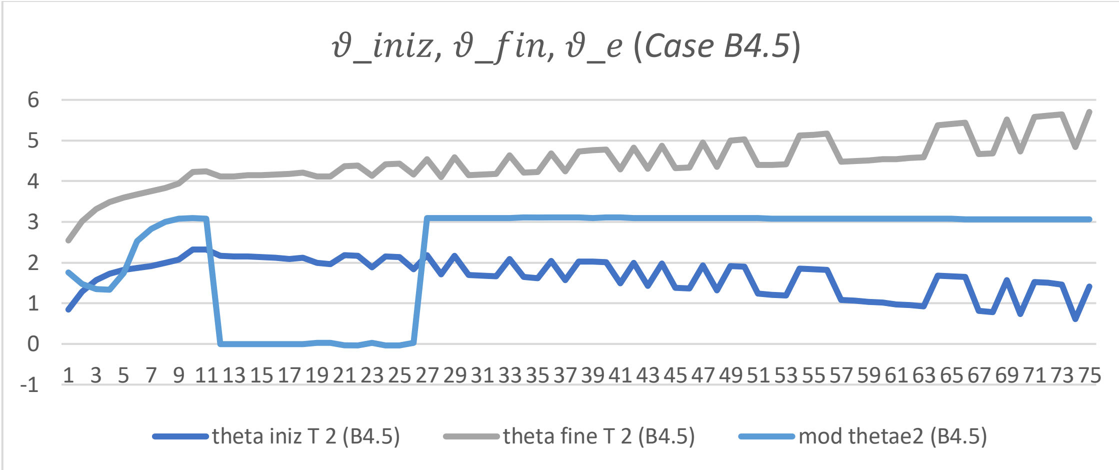

Figure 144. ϑ_iniz, ϑ_fin, ϑ_e values for Case B4.5 - Aphelion

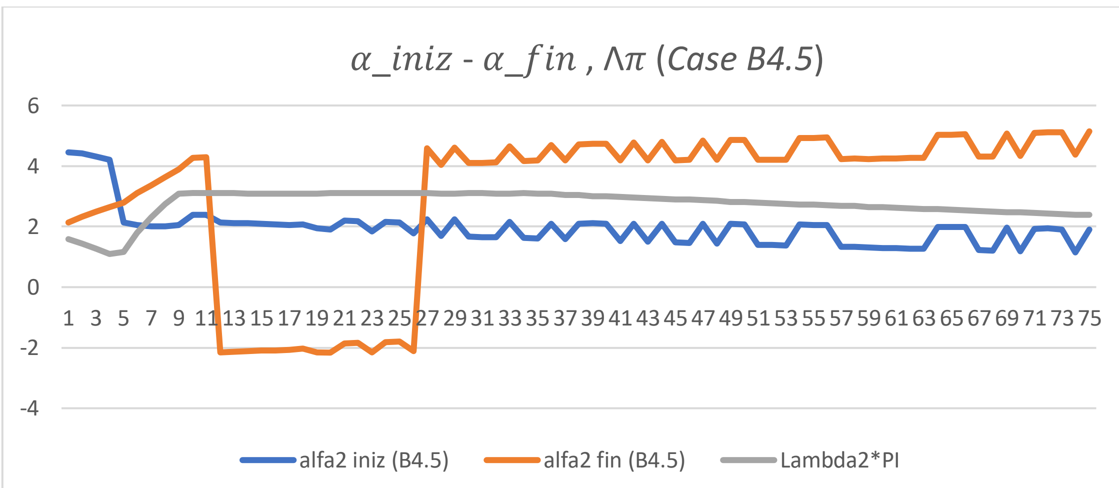

Figure 145. α_iniz - α_fin, $\Lambda\pi$ values for Case B4.5 - Aphelion

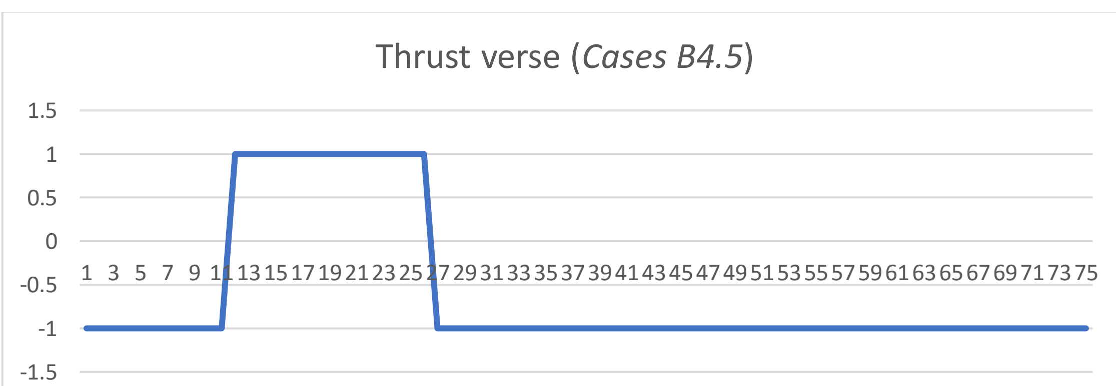

Figure 146. Thrust verse for Case B4.5 - Aphelion

➢ *Case C4.5*

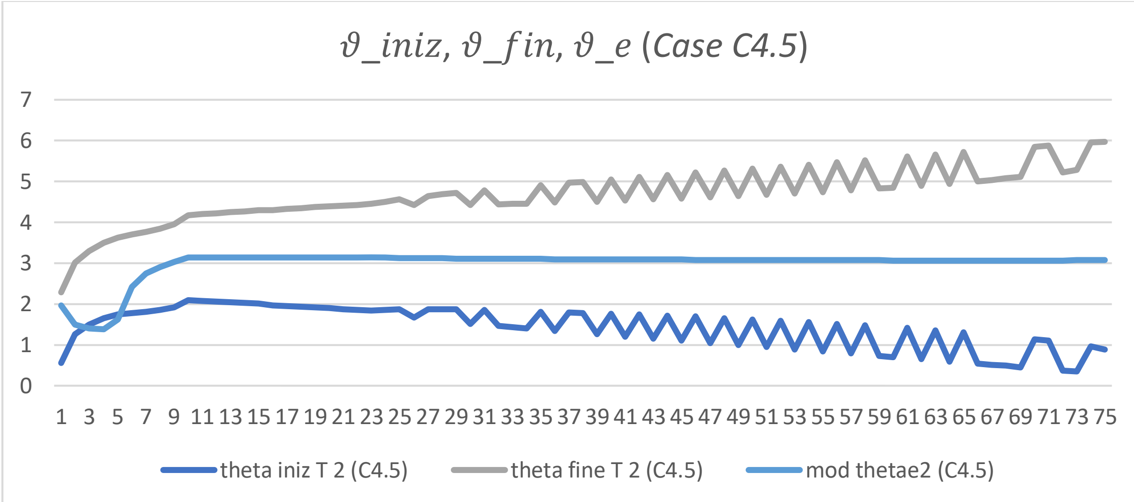

Figure 147. ϑ_iniz, ϑ_fin, ϑ_e values for Case C4.5 - Aphelion

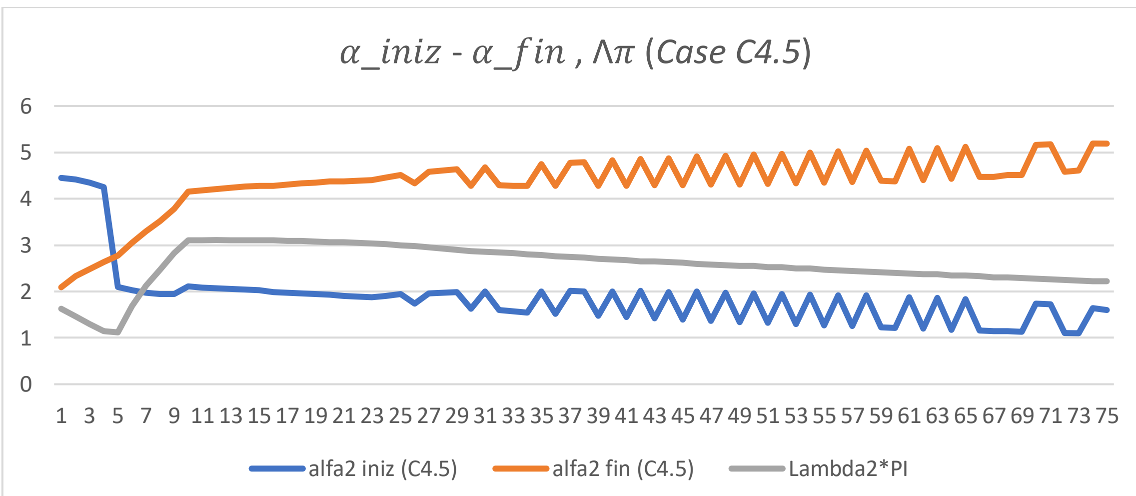

Figure 148. α_iniz - α_fin, $\Lambda\pi$ values for Case C4.5 - Aphelion

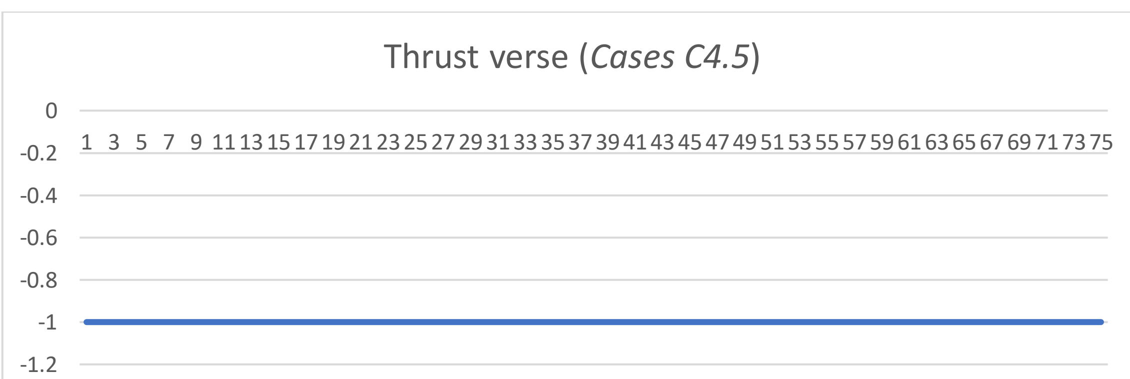

Figure 149. Thrust verse for Case C4.5 - Aphelion

As it is clearly possible to see, the only section that differentiates these graphs, for each parameter (ϑ_e, α_{fin}, $verse$), is the central one where there is the suboptimal solution. In fact, for *A4.5* it is larger and includes 32 asteroids, for *B4.5* it shrinks and contains 14 asteroid and, finally, for *C4.5* it disappears completely including almost the whole set of fictitious asteroids in the optimal solution predicted by the theory, since the first area always presents some oddities.

3.3.4 $\boldsymbol{i = 6°}$

Last cases treated are those with $i = 6°$. Despite this inclination value significantly increases consumption (as it is shown and explained in paragraph 3.1.4), the final responses in terms of the fundamental parameters of the estimation method (ϑ_e and $\alpha_{iniz} - \alpha_{fin}$ above all, but also Λ is safely acceptable) are very accurate. One must remember that asteroid #2 is neglected for the reasons seen in paragraph 3.1.4.

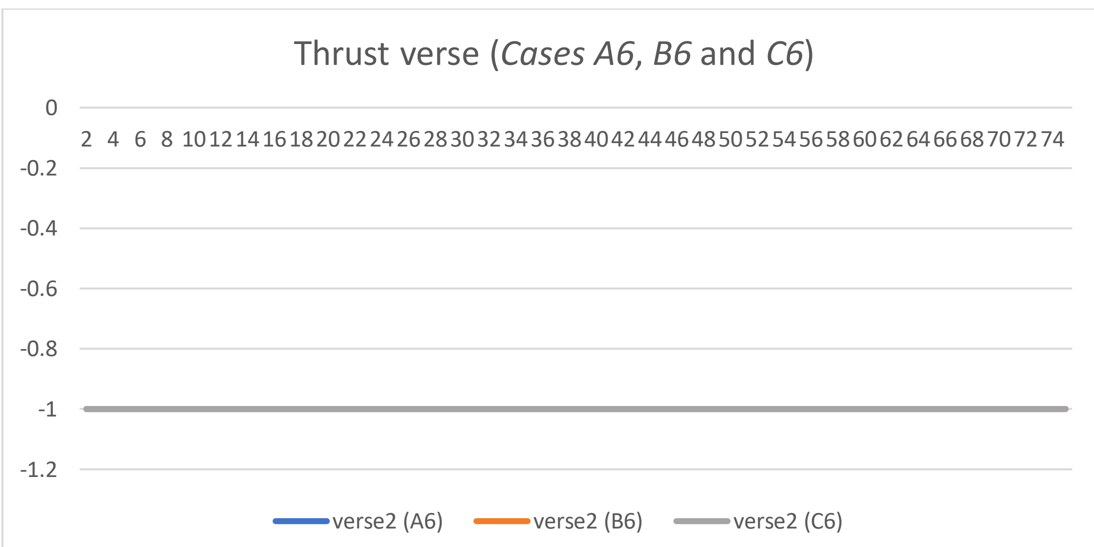

Figure 150. Thrust verse values with i=6° - Aphelion

With $i = 6°$ a significant result is achieved: all asteroids present, in each *case* treated, the optimal solution, in which the spacecraft that maneuver in aphelion must necessarily brake.

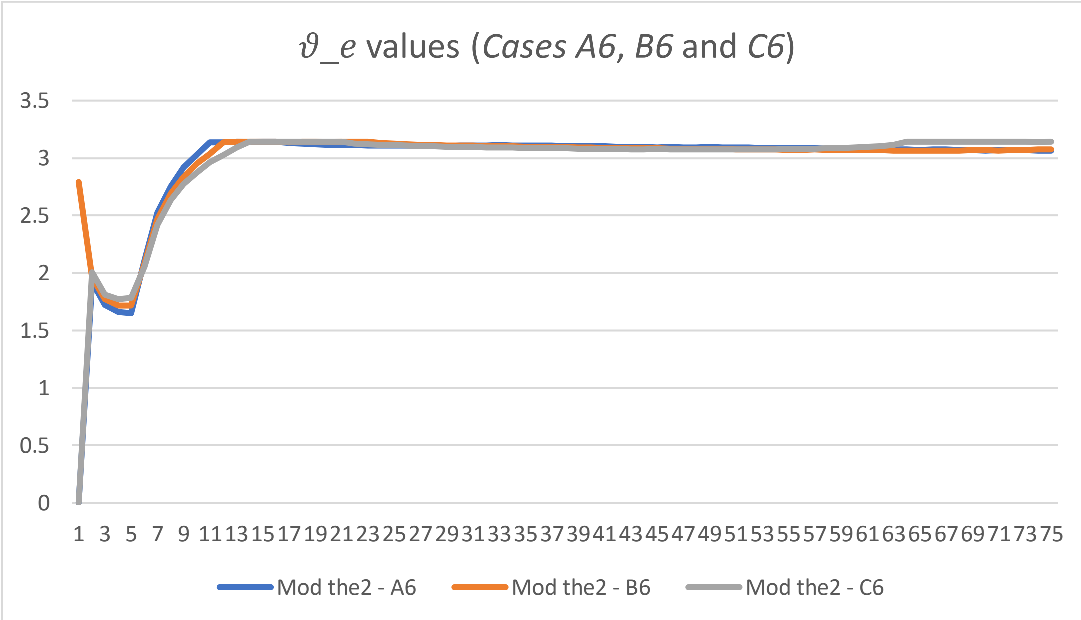

Figure 151. ϑ_e values comparison with i=6° - Aphelion

Except for the first zone of very few asteroids, in each *case* $\vartheta_e \cong \pi$ just as theory predicts.

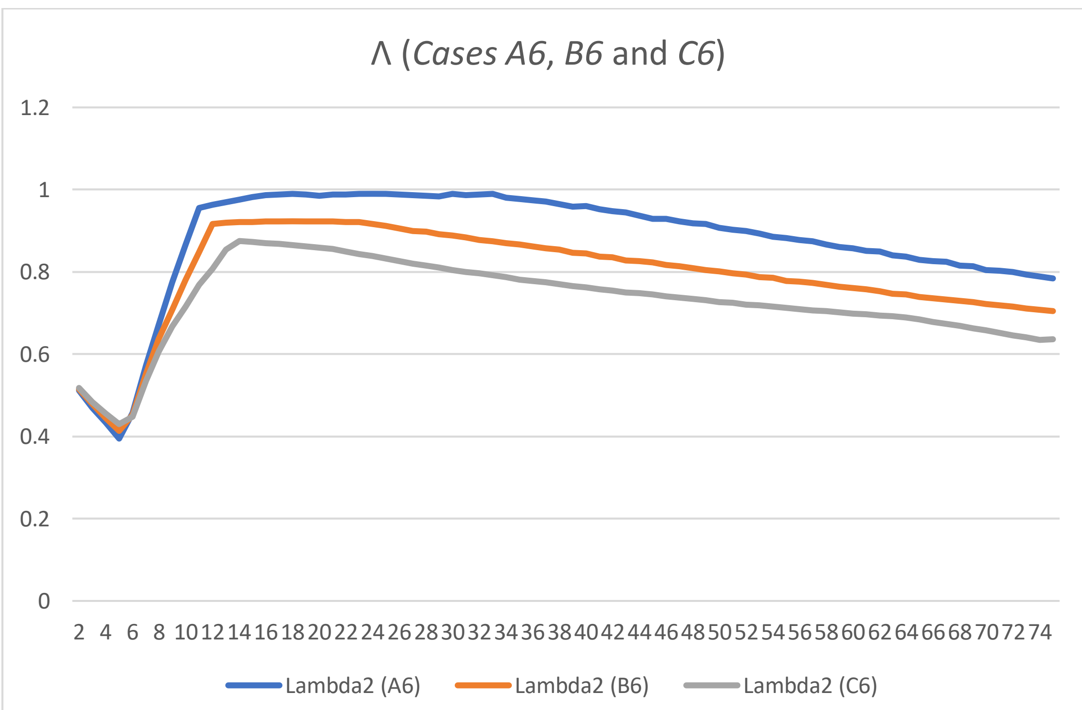

Figure 152. Λ values comparison with i=6° - Aphelion

Despite Λ values are still high for each *case*, the improvements are noticeable as now only *case A6* almost touches the unit in the first part of the graph. *Cases B6* and *C6* have lower values along the entire group of asteroids. These results are however acceptable since they do not seem to affect the overall accuracy of the method and both ϑ_e and $\alpha_{iniz} - \alpha_{fin}$ basically the whole set presents the optimal solution.

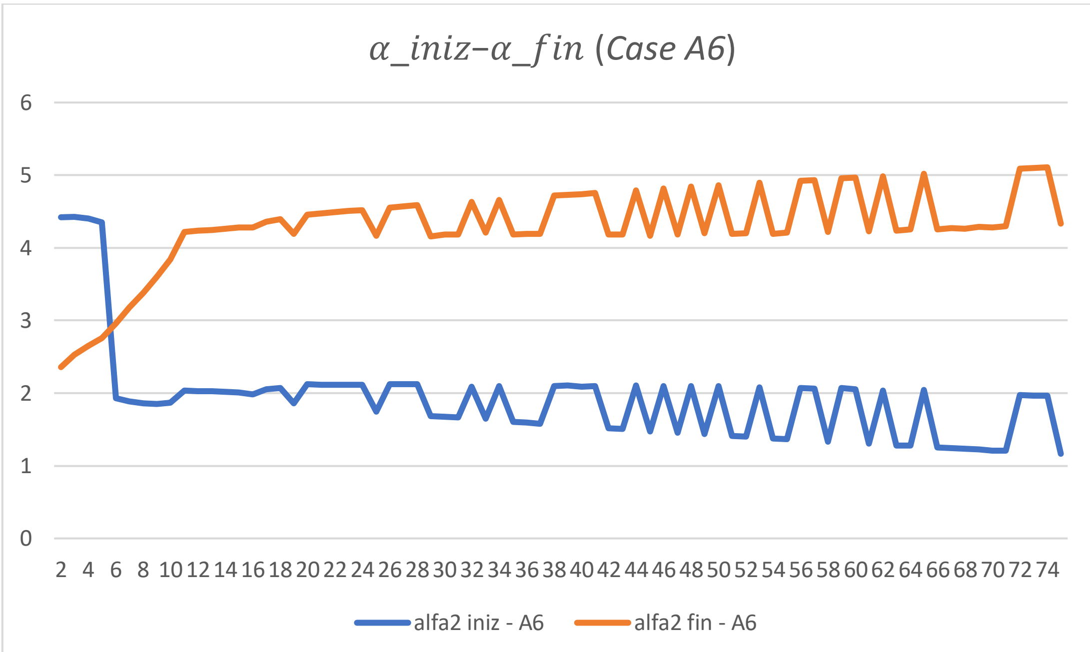

Figure 153. $\alpha\_iniz-\alpha\_fin$ values for Case A6 - Aphelion

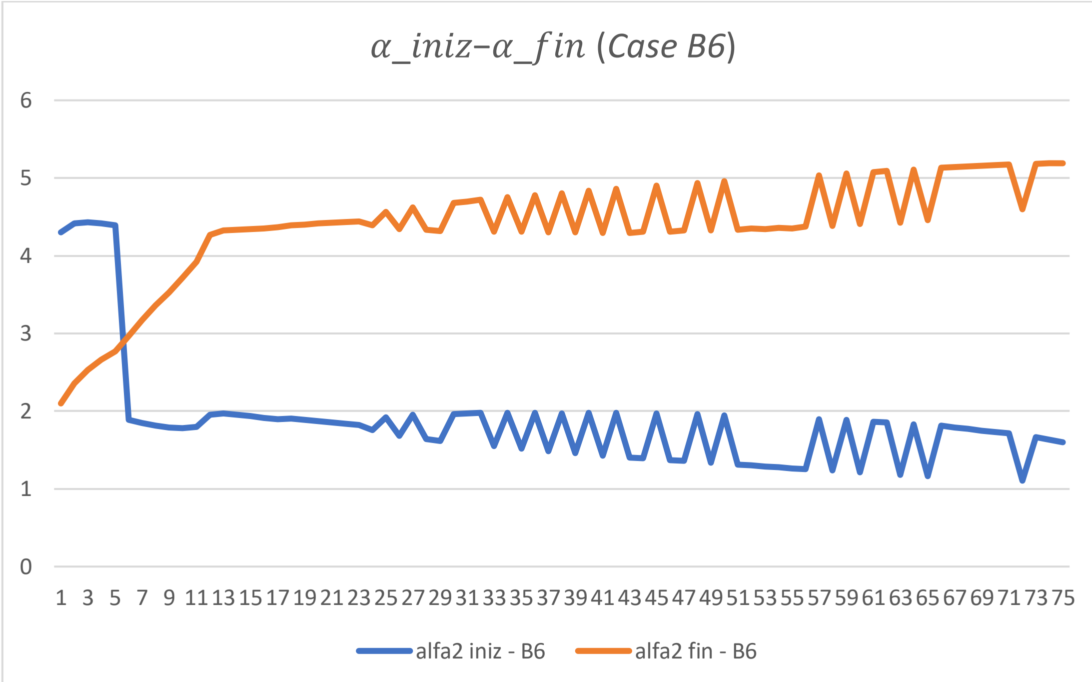

Figure 154. $\alpha\_iniz – \alpha\_fin$ values for Case B6 – Aphelion

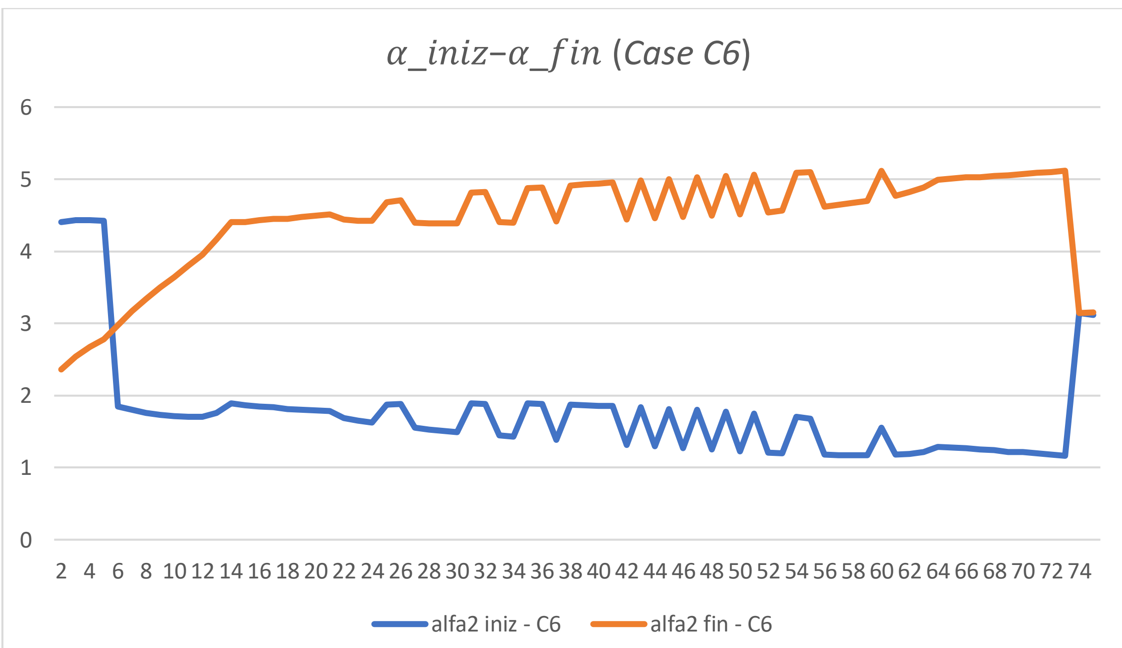

Figure 155. $\alpha\_iniz – \alpha\_fin$ values for Case C6 - Aphelion

The graphs above are clear: with this inclination value the algorithm chooses for each *case* the optimal solution for almost the entire set of 75 fictitious asteroids. It is easy to notice for *case C6* the same behavior seen for the same *case* in the perihelion maneuver (symmetry in the burning arcs, as it also can be seen with $\Delta\vartheta$), but there the maneuver is centered in 0, the aphelion maneuver is centered in π: from asteroid #74 until the end the burning arcs are so long that they become larger than 2π and it is possible to count them from the beginning (in this maneuver, π).

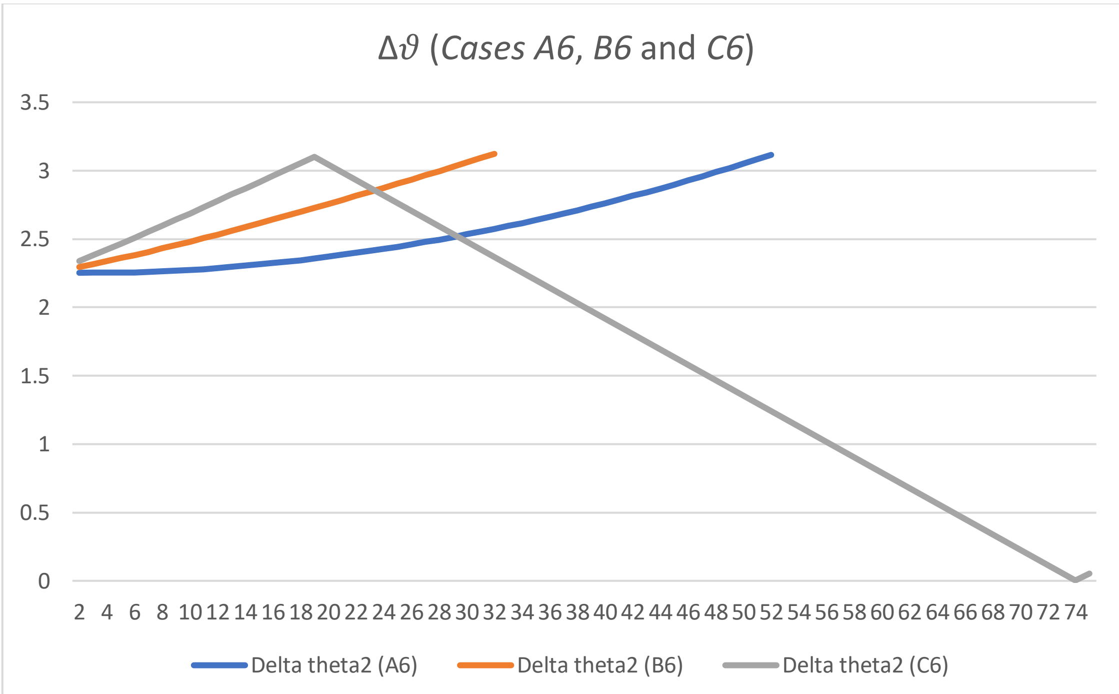

Figure 156. Δθ values with i=6° - Aphelion

Even here the symmetry between perihelion and aphelion maneuver is basically perfect since the transition from $\Delta\vartheta < \pi$ to $\Delta\vartheta > \pi$ occurs at the same asteroids for each *case* in both maneuvers (#52, #32 and #19 respectively). A small difference can be found for the final asteroids of the group. It has been seen that for the farthest asteroids from Earth with $i = 6°$ one can have $\Delta\vartheta > 2\pi$ and hence count the relative asteroids as they start from the beginning (that is, once again, 0 at perihelion and π at the aphelion); perihelion maneuver is a bit longer than aphelion maneuver since in perihelion the asteroids where $\Delta\vartheta > 2\pi$ go from asteroid #69 to #76, while in aphelion only asteroids #75 and #76 presents $\Delta\vartheta > 2\pi$.

3.3.4.1 The relation between ϑ_e, ϑ_{iniz} and ϑ_{fin}, α_{iniz} and α_{fin}

The relations that link the fundamental parameters of the theory are now studied through the respective graphs. The answers with $i = 6°$ are particularly accurate.

- *Case A6*

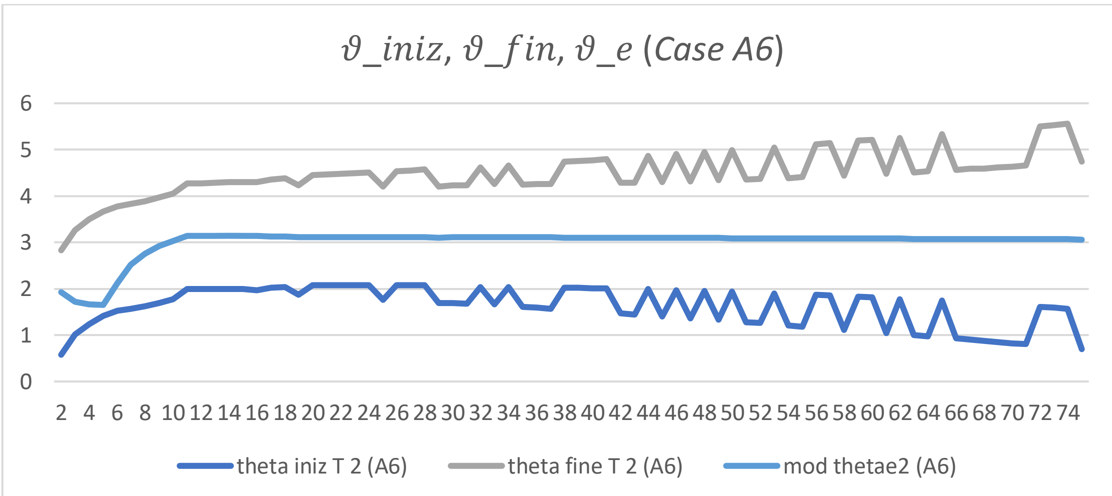

Figure 157. ϑ_iniz, ϑ_fin, ϑ_e values for Case A6 - Aphelion

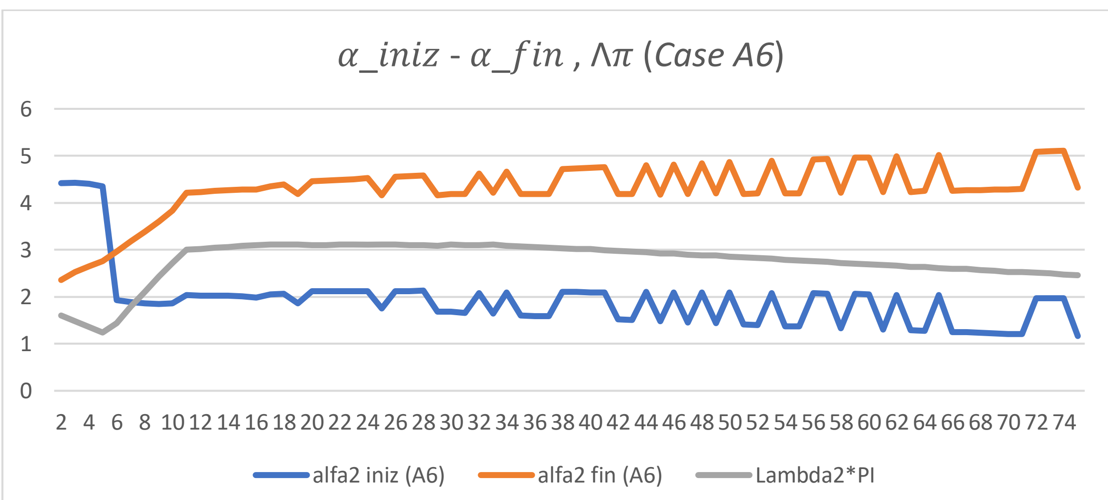

Figure 158. α_iniz - α_fin, $\Lambda\pi$ for Case A6 - Aphelion

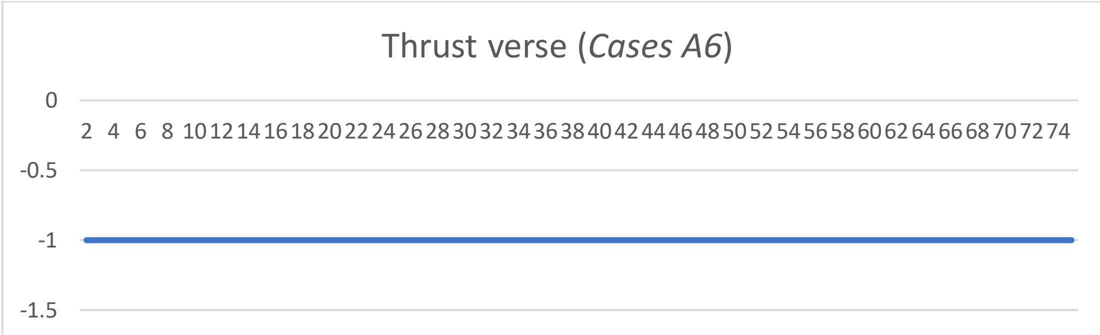

Figure 159. Thrust verse for Case A6 - Aphelion

- *Case B6*

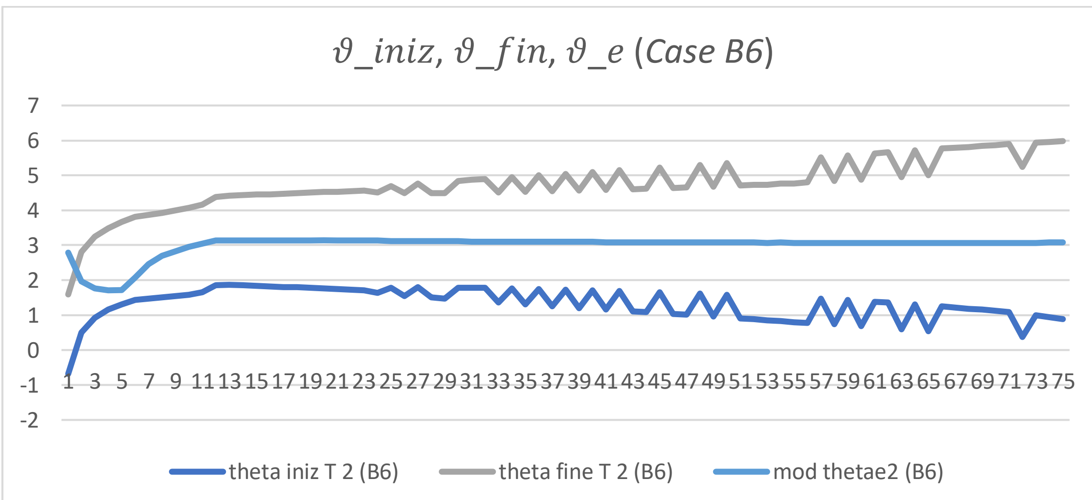

Figure 160. ϑ_iniz, ϑ_fin, ϑ_e values for Case B6 - Aphelion

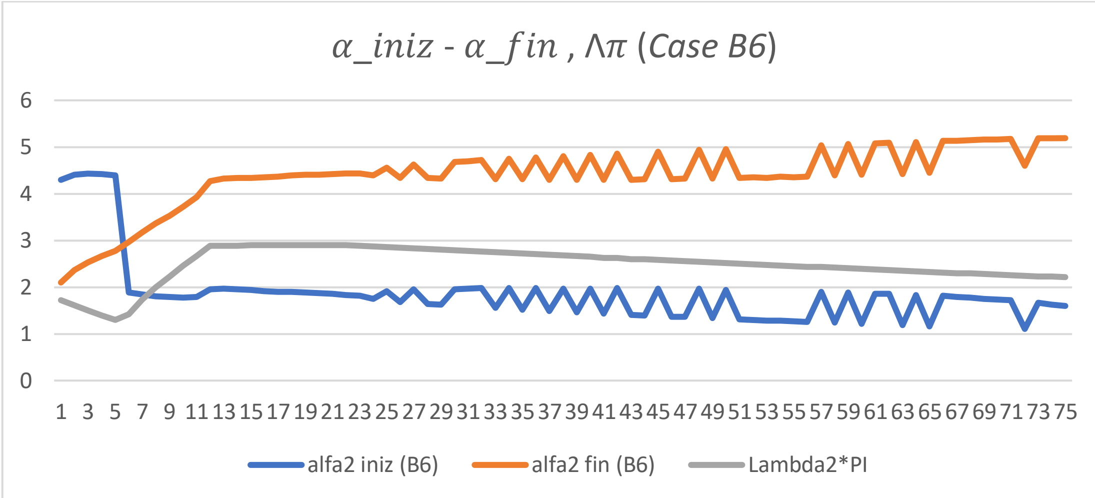

Figure 161. α_iniz - α_fin, $\Lambda\pi$ values for Case B6 - Aphelion

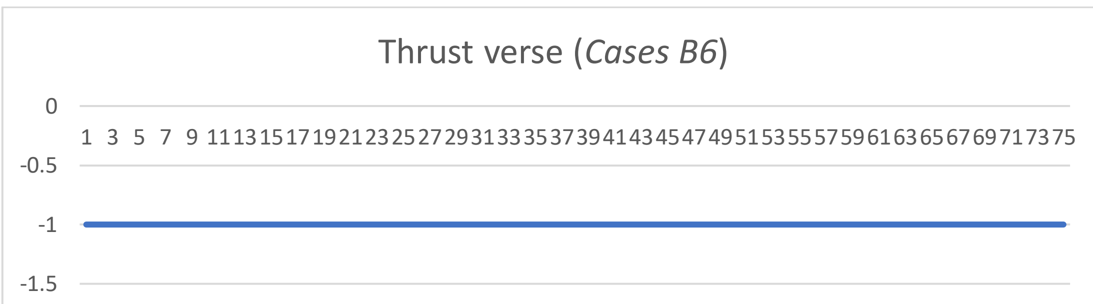

Figure 162. Thrust verse for Case B6 – Aphelion

- *Case C6*

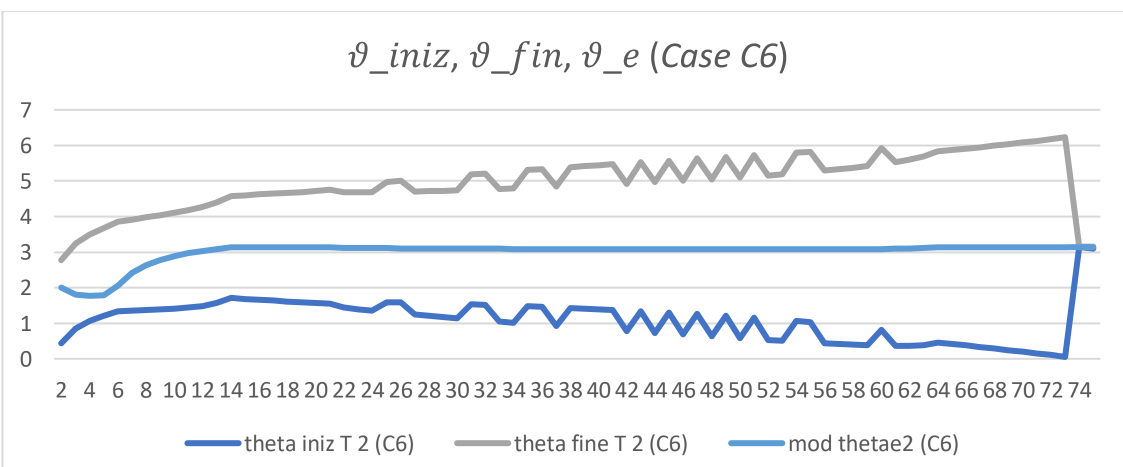

Figure 163. ϑ_iniz, ϑ_fin, ϑ_e values for Case C6 - Aphelion

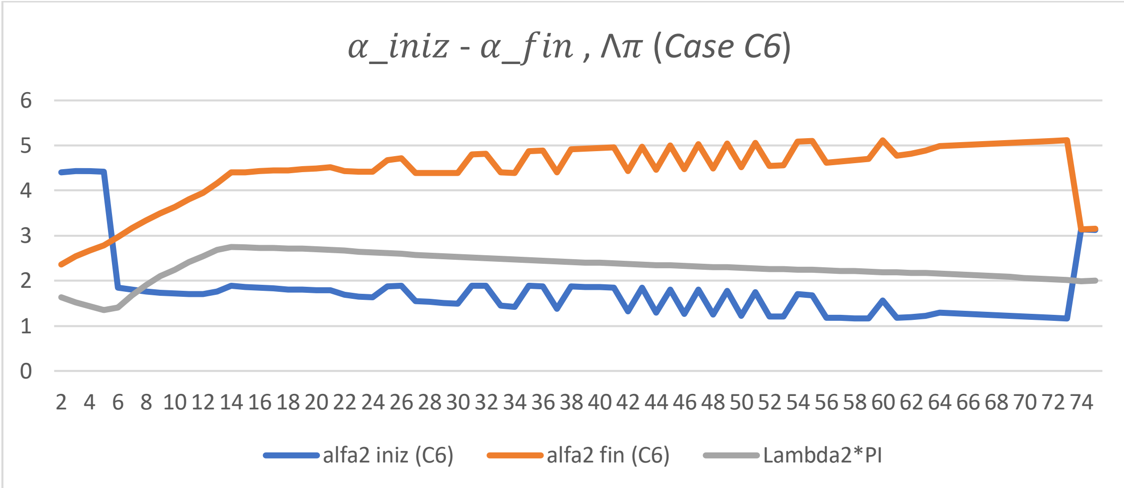

Figure 164. α_iniz - α_fin, $\Lambda\pi$ values for Case C6 - Aphelion

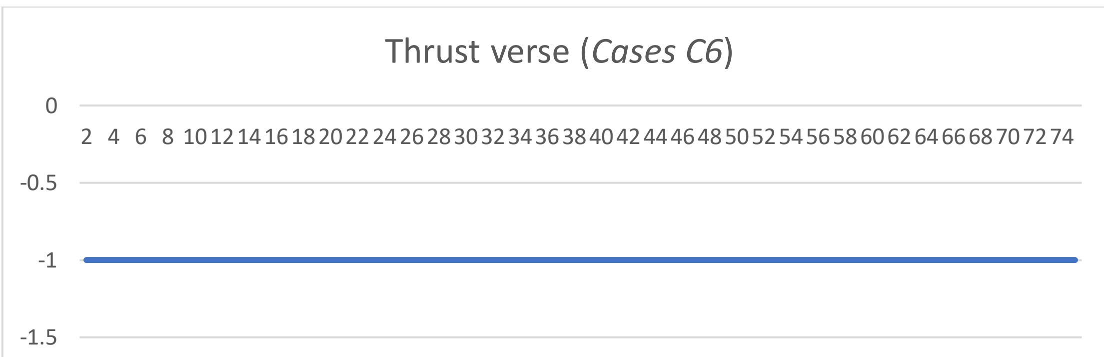

Figure 165. Thrust verse for Case C6 – Aphelion

All cases have the thrust opposite to the direction of advancement; hence the optimal answer requires $\vartheta_e \in [\vartheta_{iniz}; \vartheta_{fin}]$, $\vartheta_e \cong \pi$, $\alpha \cong \pi$, $\alpha_{fin} > \alpha_{iniz}$. As it can clearly be seen, for all *cases* the first section presents as usual some oddities for the reasons explained throughout the paper, while the rest of the set perfectly behave in terms of the fundamental parameters.

<u>3.4</u> <u>Aphelion maneuver: overall comparison</u>

Now it is time, after having studied the *cases* separately by the inclination value, to do an overall comparison for the aphelion maneuver essentially based on the value of RAAN. So, the cases compared even here are those with:

- $\Omega = 0$ (*Cases A*, *A1.5*, *A3*, *A4.5* and *A6*);
- $\Omega = \pi/4$ (*Cases B*, *B1.5*, *B3*, *B4.5* and *B6*);
- $\Omega = \pi/2$ (*Cases C*, *C1.5*, *C3* and *C6*).

The propellant consumption comparison has been made for the perihelion maneuver, thus now the only parameters to be compared are ϑ_e and Λ.

3.4.1 $\boldsymbol{\Omega = 0\ rad}$

First cases to be compared are of course those where the perihelion and the ascending node coincide, i.e., $\Omega = 0$.

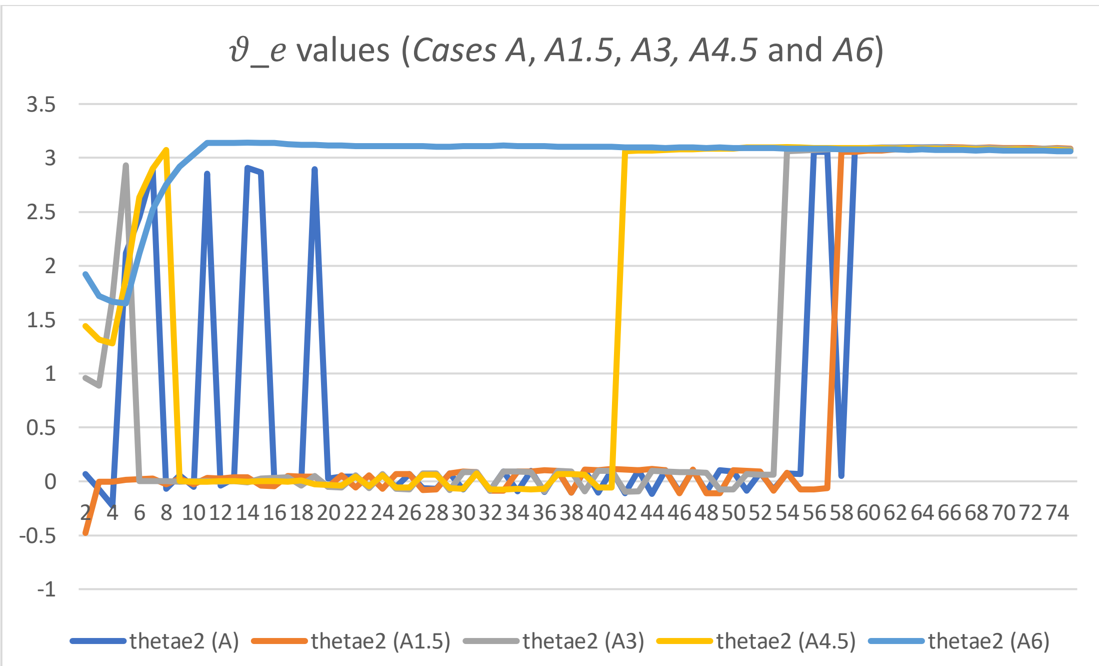

Figure 166. ϑ_e values comparison with Ω=0 rad - Aphelion

The graph is very chaotic in its first part since there are a lot of fluctuation between 0 and π for *case A*. For *cases A*, *A1.5* and *A3* the transitions to the right of the graph occur a few asteroids away, while raising the inclination to 4.5° significantly improves this result anticipating the transition of about 10 asteroids. With $i = 6°$ almost the whole set presents the optimal solution. $\Omega = 0$ is positive for the consumption, but it somehow penalizes the results, as one can also understand by reading the next two paragraphs.

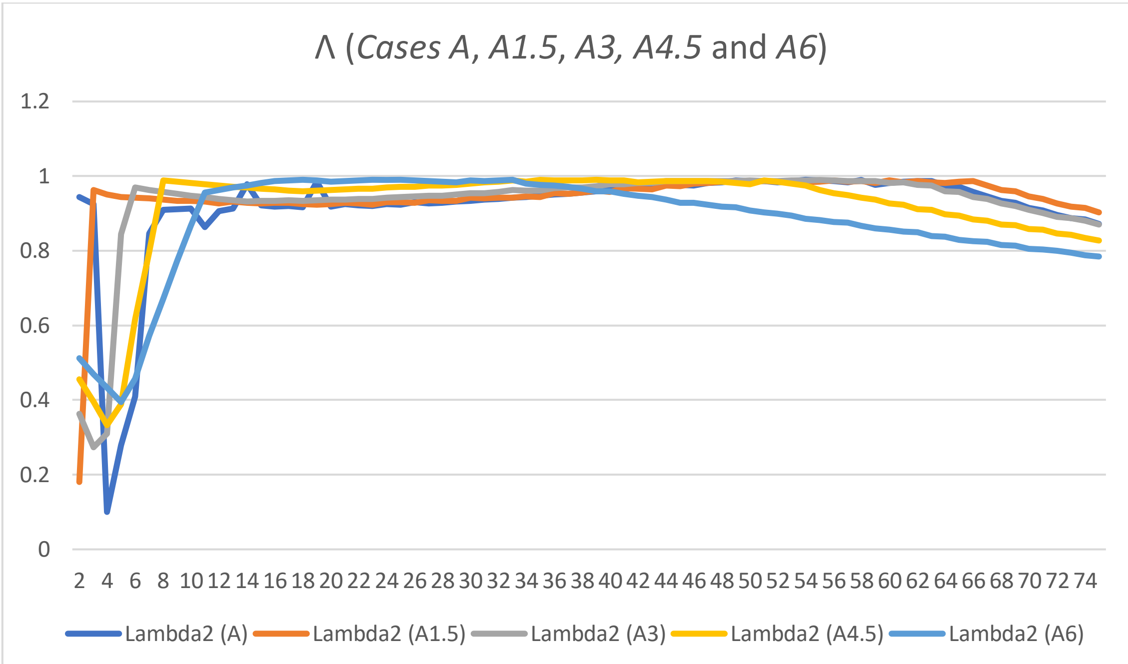

Figure 167. Λ values comparison with Ω=0 rad – Aphelion

Even as regards Λ, *cases* with null RAAN have the worst results, as it is clearly visible. Each *case* has a trend very close to 1 for at least 16-17 asteroids (*case A6*, the best between those with $\Omega = 0$) and despite all the trends having a descending stroke at the end (which begins earlier when the inclination increases), the values always remain very high.

3.4.2 $\boldsymbol{\Omega = \pi/4\ rad}$

Cases with the lines of nodes shifted by 45° with respect to the line of apsides are now dealt with.

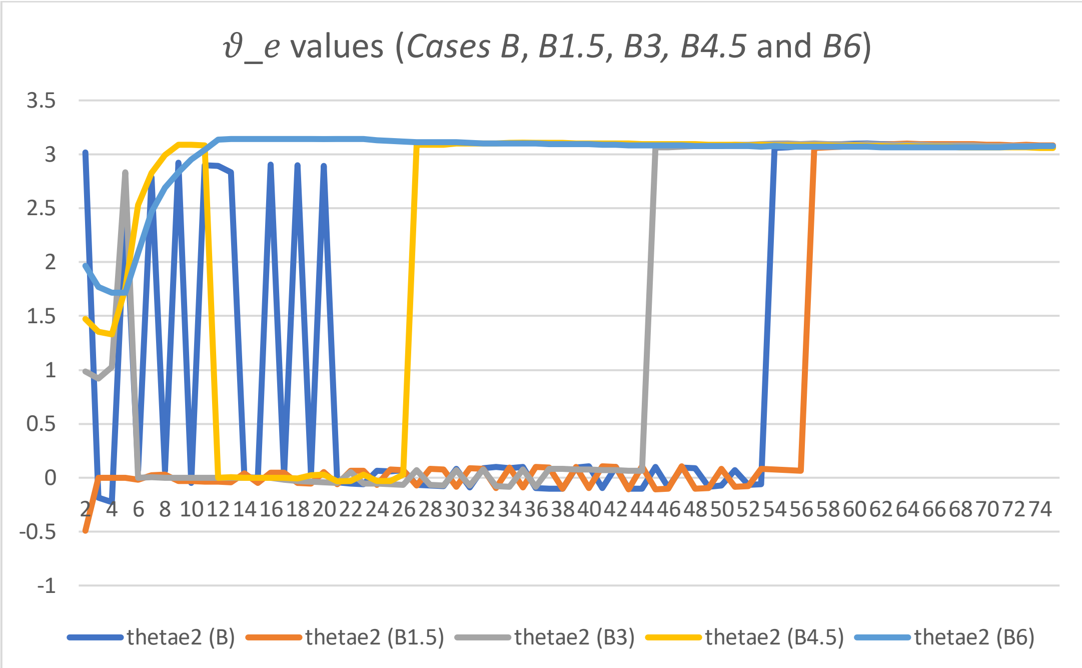

Figure 168. ϑ_e values comparison with $\Omega=\pi/4$ rad – Aphelion

About the first section, the situation for case B is similar that for case A with many fluctuations between 0 and π. Case B1.5 has a globally worse result than case B since the transition from 0 and π takes place a few asteroids after, and this means that fixing very low values of inclination makes little sense because the results do not improve compared to a *case* with a low and variable inclination. With $i = 3°$ and $i = 1.5°$ the response significantly improves since the section with the asteroids having optimal solution becomes way larger under the effect of the growth of the inclination and of non-zero RAAN. With $i = 6°$ one has of course the expected solution for almost the entire set of asteroids.

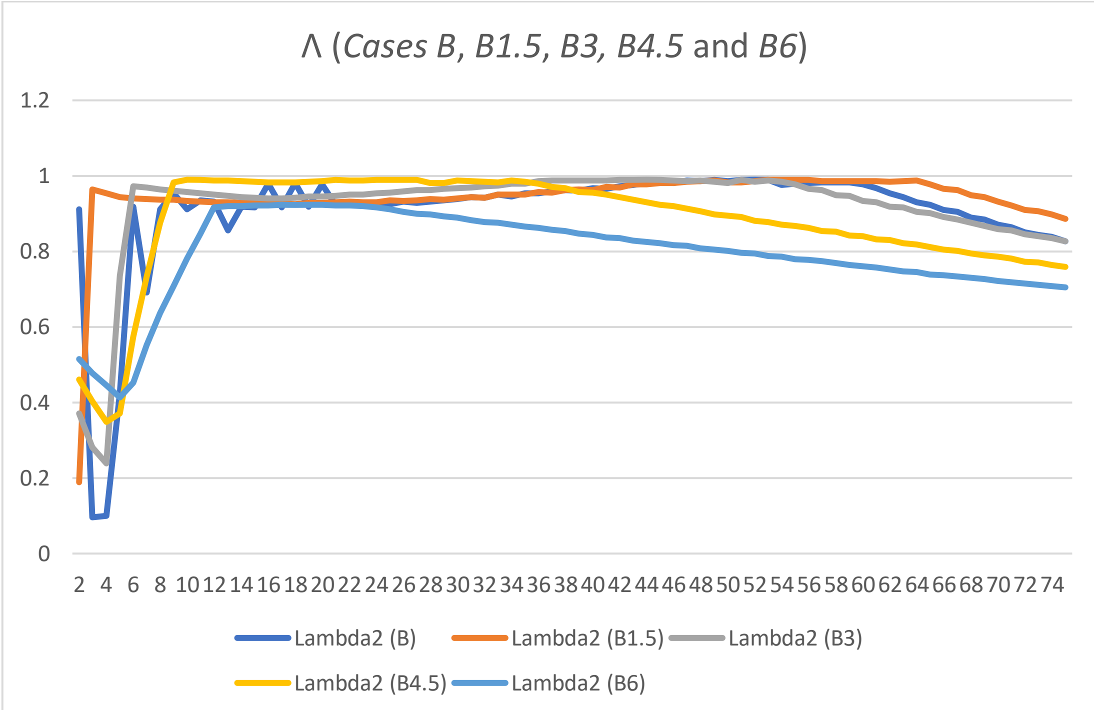

Figure 169. Λ values comparison with Ω=π⁄4 rad – Aphelion

As it was written for the whole discussion of the aphelion maneuvers, Λ values are very high, but with $\Omega = \pi/4$ the situation improves a bit compared to the cases with $\Omega = 0$. The cases with the worst values are *B* and *B1.5*, while raising the inclination helps slightly to lower the trends.

3.4.3 $\boldsymbol{\Omega = \pi/2\ rad}$

Finally, a comparison of the cases in which the perihelion and the ascending node are in quadrature is made. These are the cases with the highest values in consumption, but with also the best results obtained in terms of adherence to the theory.

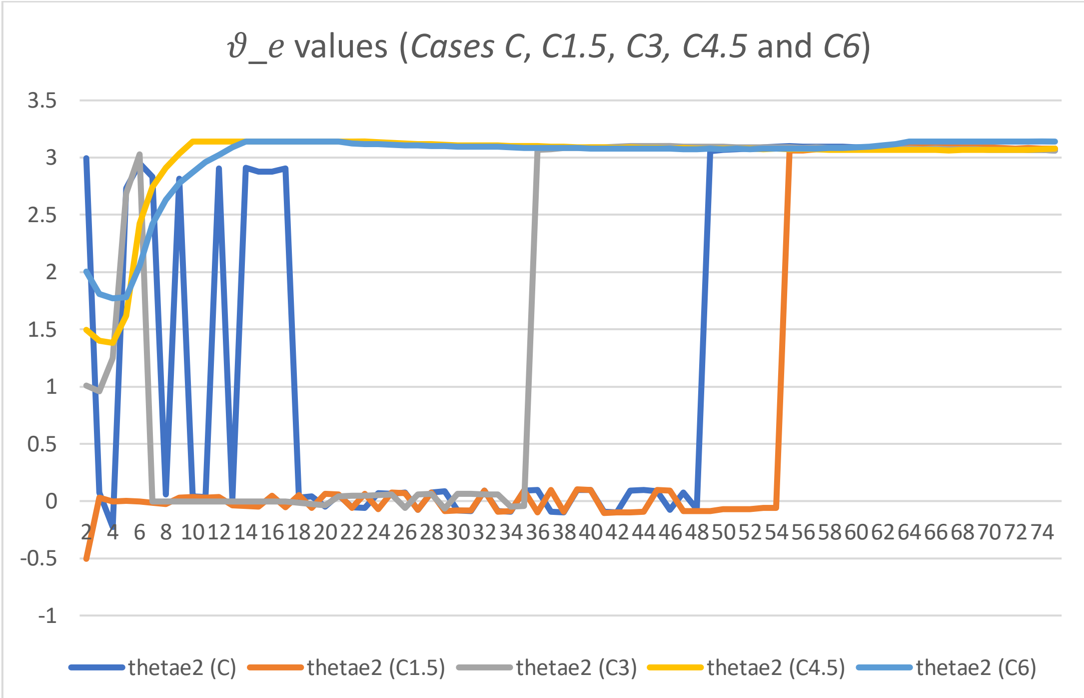

Figure 170. ϑ_e values comparison with Ω=π⁄2 rad – Aphelion

Despite the fluctuating results even for *case C* in the first section and the transition at the end of *C1.5* the occurs after that of *C*, *cases* with $i \geq 3°$ show the best results in terms of accuracy compared to the counterparts with different Ω values. In fact, C3 has the ϑ_e transition from 0 to π at asteroid #37, including almost 50% of the asteroids of the set in the optimal solution (no other cases with $i = 3°$ does that), and *C4.5* has an almost identical trend to *C6*, keeping ϑ_e in a range of the optimal solution for nearly all 75 asteroids. The fact that case C4.5 also managed to have this trend and this response is certainly due to the contribution of the quadrature which, together with an adequate inclination value (but still small to adhere to Edelbaum's approximation [6,7]), has improved the overall response of the algorithm at the cost of a few more kilos of fuel consumed.

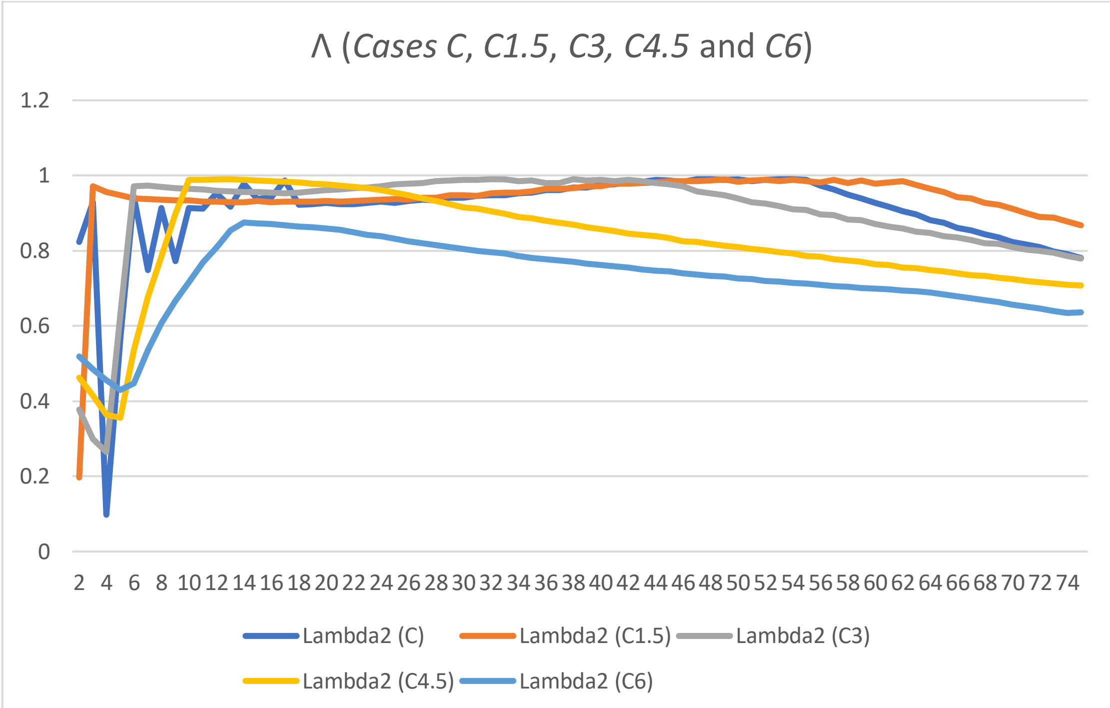

Figure 171. Λ values comparison with Ω=π⁄2 rad – Aphelion

While *cases C*, *C1.5* and *C3* have globally very high Λ values and do not improve the situation with respect to their counterparts, *cases C4.5* and above all case *C6* have slightly lower values. In detail, the peak value of C6 trend is equal to 0,87516 (while the peak values of the other cases almost touch 1) and at asteroid #76 one has $\Lambda = 0{,}63582$ which is not a very high value with respect to the average.

CONCLUSIONS

An analytical method for the fast and accurate estimation of orbital trajectories to NEAs [2], based on Edelbaum's approximation, has been employed in this paper to find out how much the required changes of some orbital parameters affect the output results in perihelion and aphelion maneuvers.

The orbital elements whose variations have heavily influenced the solutions and the costs are the inclination and the right ascension of ascending node (RAAN). As it is clear from the first cases studied in this work, there are essentially two possible solutions among which the algorithm can choose: the optimal solution is the one actually foreseen by the theory and it is obviously the best in terms of accuracy, while another solution is almost always present and does not strictly respect the relations that govern the method. However, even with this last answer, perihelion and aphelion maneuvers are in any case symmetrical as well as the burning arcs, consequently it is considered a suboptimal solution which offer a similar performance with respect to the optimal one (no strange variations in consumption are detected) and in which the in-plane thrust angle α and the reference right ascension ϑ_e appear discontinuous and not centered in the theoretically correct point.

A first revelation comes out of the analysis of the cases with variable inclination. In fact, with $i = (1/8)e$, both in perihelion and aphelion there are two sections in the trends of the fundamental parameters of the method: the first one, that includes a significant number of asteroids, where there is the suboptimal solution and then, following a transition, the final one with the farthest asteroids from Earth that present the optimal solution. It almost seems that within a certain distance from Earth the algorithm is led to choose something unexpected, but still acceptable, while after this distance it reaches the theoretical answer. One must note that even in this first cases the transition is anticipated for cases where $\Omega \neq 0$, hence cases with the ascending node not coincident to the perihelion has more asteroids with the optimal solution both in perihelion and aphelion. Furthermore, the very first asteroids of the set always (both in perihelion and aphelion, and with any value of inclination and/or RAAN) show chaotic, fluctuating, and unclear responses in the graphs. Probably the short distance that separates these asteroids from the Earth still influences the results, bringing the possible solutions very close and preventing the algorithm from obtaining a stable and clear response. In the future, this phenomenon should be investigated to strengthen the method and allow it to evaluate transfers also for real asteroids and close to our planet.

Setting the inclination leads, particularly for cases with $i \geq 3°$, to better results in terms of optimal solution together with an obvious increase in consumption. In fact, despite cases with $i = 1.5°$ have no global improvements since this inclination value is higher than that of the very first asteroids but equally lower than that of the farthest ones, the imposed values higher than this ($3°$, $4.5°$ and $6°$) tend to lead faster the algorithm to the expected solution, as evidently shown both in perihelion and aphelion by the graphs of the fundamental parameters of the method, ϑ_e and $\alpha_{iniz} - \alpha_{fin}$ above all. In perihelion maneuver ϑ_e and $\alpha_{iniz} - \alpha_{fin}$ trends are indeed almost identical for cases with the three highest inclinations values, and this may be explained by the fact that the maneuver here is easier to handle since the thrust verse is taken for granted and it is concurrent with the direction of advancement and so it is not difficult to frame the optimal answer. The two possible solutions indeed offer similar performances, since for the first asteroids $\vartheta_e \cong \pi$ decreases the parameters' variations and shortens the burning arcs. Aphelion maneuver is instead more complex (and this can be seen in the various patterns) since the vehicle at this point can also brake, so there are two possible thrust verses and the optimal solution can be found only in the graphs, observing where ϑ_e and α are centered, that is also the point in which the maneuver must be centered. In aphelion, the two possible solutions ($verse = 1$ and $\vartheta_e \cong 0$, $verse = -1$ and $\vartheta_e \cong \pi$) are even closer to each other and the algorithm finds one or the other, without the regularity present in the perihelion maneuver. Despite this phenomenon, however, the aphelion maneuver remains almost perfectly symmetrical to the perihelion maneuver, hence the output results are still accurate. Together with the inclination, Ω too gives a huge contribution to widening the range of the expected solution almost in each case dealt with. It seems that, with small-to-null eccentricity and inclination values, spacing out the line of apsides and the line of nodes increases the overall accuracy of the method at the cost of an expected but limited rise of the consumption, since the thrust is provided at the perihelion and not at the ascending node. From these considerations, the results with the highest level of accuracy among all the cases studied come from the cases with $\Omega \neq 0$ and $i \geq 3°$. In fact, in aphelion the first case to extend the optimal solution to almost all the 75 asteroids is C4.5 ($\Omega = \pi/4$ and $i = 4.5°$), where $verse = -1$ throughout the set, while cases with $i = 6°$ all present identical trends, also accurate and predicted by the theory. The only parameter that, especially in aphelion, has values a bit counter trend is Λ, with the trends that in perihelion are penalized by the increases in inclination while in aphelion it seems to improve with them and with $\Omega \neq 0$. Despite this, the results still remain generally accurate since ϑ_e and α are perfectly fit with the optimal solution as inclination increases, even if Λ should be subject of study to understand the reasons of these high values.

Lastly, as one can now guess, the estimation method completely embraces the solution foreseen by the theory when the inclination is significantly raised (but not too much to still adhere to Edelbaum's approximation [6,7]) and the perihelion does not coincide with the ascending node, that is, non-zero RAAN, with these relevant changes that lead to a slight increase in the cost of the mission. These consumption estimations are sufficiently precise since if the variation increase, the costs increase as well [2], hence there are no particular strange cases. The results generally follow the theoretical expectations with $i \neq 0$ and $\Omega \neq 0$. New studies and analyses may be focused on improving the accuracy of the solution in the planar problem, i.e., with null inclination, in which the perihelion and the ascending node are coincident, that is, $\Omega = 0$.

REFERENCES

[1] A. Mantani, *La propulsione spaziale – sparare razzi in orbita*, www.missionescienza.it, 2020.

[2] L. Mascolo, A. De Iuliis, L. Casalino, *Fast and Accurate Estimation of Fuel-Optimal Trajectories to Near-Earth Asteroids*, Acta Astronautica 188 (2021) 49-56.

[3] G. Romeo, R. Marsilio, *Configurazione dei propulsori elettrici per uso spaziale: la propulsion ionica*, DIMEAS – Politecnico di Torino, 2018, pp. 9-10.

[4] J.S. Lewis, *Mining the Sky: Untold Riches from the Asteroids, Comets, and Planets*, msur, 1996.

[5] N. Anthony, M. R. Emami, *Asteroid Engineering: the state-of-the-art of Near-Earth Asteroids science and technology*, Prog. Aerosp. Sci. 100 (2018) 1-17.

[6] T. N. Edelbaum, Propulsion requirements for controllable satellites, ARS J. 31 (8) (1961) 1079-1089.

[7] N. Stronati, L. Casalino, *Ottimizzazione di traiettorie orbitali per satelliti in LEO sotto l'influenza di* J_2, DIMEAS – Politecnico di Torino, 2020, pp. 18-19.

[8] J. McAdams, D. Dunham, L. Mosher, J. Ray, P. Antreasian, C. Helfrich, J. Miller, *Maneuver History for the NEAR Mission Launch through Eros Orbit Insertion*, paper AIAA 2000-4141, AIAA, 2000.

[9] L. Casalino, L. Mascolo, A. Bosa, *Fast Estimation Method for Trajectories to Near-Earth Asteroids*, AAS 19-761, in: Advances in the Astronautical Science Series, vol. 171, ISBN: 978-0-87703-666-1, 2019, pp. 3089-3100.

[10] R. A. Egler, Orbital Elements and Astronomical Terms, Dept. of Physics – North Carolina State University, https://web.archive.org/web/20070403095234/http://www.physics.ncsu.edu/courses/astron/orbits.html, 2001.

[11] J. B Tatum, *Celestial Mechanics*, paper, Physics Topics, chapter 10, pp. 1-3.